MODELLING THE IMPACTS OF CLIMATE CHANGE ON WATER SUPPLY AND DEMAND BALANCE OF BÜYÜK MENDERES BASIN

by

Zülküf İbrahim Erkol

B.Sc. in Civil Engineering, Boğaziçi University, 2017

Submitted to the Institute of Environmental Sciences
in partial fulfilment of the requirements for the degree of
Master of Science
in
Environmental Sciences

Boğaziçi University
2020

ACKNOWLEDGEMENTS

I would like to express my sincere appreciation to my advisor Asst. Prof. İrem Daloğlu Çetinkaya for the convenient guidance, remarks and encouragement through the learning process of this thesis. I am grateful that Asst. Prof. Çetinkaya has taught me how to generate a structured thesis from intricate content. I would also like to thank my self-sacrificing darling Helin Nur Güler, my friend Kamil Çöllü, and my lovely brother Fatih Erkol for the helps and supports they provided throughout the challenging moments that I have experienced during the formation process of this thesis.

ABSTRACT

MODELLING THE IMPACTS OF CLIMATE CHANGE ON WATER SUPPLY AND DEMAND BALANCE OF BÜYÜK MENDERES BASIN

With impacts of climate change and increasing agricultural water requirement rates due to irrigated land area expansion, freshwater demand in Büyük Menderes Basin (BMB), Turkey increases. Besides, usage of low-efficiency irrigation systems exacerbates the water demand and supply balance in BMB. Hence, enhanced water management practices are crucial to achieve sustainable freshwater management in BMB under climate change. In this study, Water Evaluation and Planning Systems (WEAP) modeling program, as an Integrated Water Resources Management (IWRM) tool, is utilized to model the effects of climate change and agricultural changes (i.e., irrigation system changes, irrigated land expansion) on water demand and supply balance by 2100. The model has different agricultural management and climate change scenarios. The climate change scenarios are based on the outputs of CNRM-CM5.1 and MPI-ESM-MR global circulation models (GCMs), agricultural management scenarios investigate the impacts of changes in irrigation systems and irrigated land area. According to CNRM-CM5.1, unmet agricultural water demand increases under all simulated scenarios in BMB between 2019 and 2100. However, according to results of MPI-ESM-MR, total unmet agricultural water demand is significantly lower compared to that of CNRM-CM5.1. Regional differences of climate change impacts on reservoir storage volumes are also critical. Under CNRM-CM5.1 results, reservoirs in Aydın show declining storage volume rates compared to their average baseline rates and reservoirs in Denizli indicate increasing storage volume rates. Under MPI-ESM-MR results, average storage volume rates increase in reservoirs located in Aydın and Denizli. This study demonstrates the role of GCMs and their inherent uncertainties in coupled modeling systems for freshwater ecosystems.

ÖZET

BÜYÜK MENDERES HAVZASI SU ARZ TALEP DENGESİNE İKLİM DEĞİŞİKLİĞİ ETKİLERİNİN MODELLENMESİ

İklim değişikliğinin etkileri ve sulanan alanların genişlemesi nedeniyle artan tarımsal su ihtiyacı yüzünden Büyük Menderes Havzası'nda (BMH) su talebi artmaktadır. Ayrıca, düşük verimli sulama sistemlerinin kullanılmaya devam etmesi de BMH'deki su arz ve talep ve arz dengesini daha da bozmaktadır. Bu nedenle, iklim değişikliği etkileri altında olan BMH'de sürdürülebilir su yönetimi sağlamak için geliştirilmiş su yönetimi uygulamaları çok önemlidir. Bu çalışmada, Entegre Su Kaynakları Yönetimi (IWRM) aracı olarak Su Değerlendirme ve Planlama Sistemleri (WEAP) modelleme programı, iklim değişikliği ve tarımsal değişikliklerin (yani sulama sistemi değişiklikleri, sulanan arazi genişlemesi) 21. yüzyıl sonuna dek havzanın su arz ve talep dengesi üzerindeki etkilerini modellemek için kullanılmıştır. Model, farklı tarımsal yönetim metotları ve iklim değişikliği senaryolarına sahiptir. İklim değişikliği senaryoları, CNRM-CM5.1 ve MPI-ESM-MR küresel dolaşım modellerinin (GCM'ler) çıktılarına dayanmaktadır. Tarımsal yönetim senaryoları ise sulama sistemlerindeki ve sulanan arazi alanındaki değişikliklerin etkilerini araştırmaktadır. CNRM-CM5.1'e göre, BMH'de 2019 ve 2100 yılları arası dönem için simüle edilen tüm senaryolarda karşılanmamış tarımsal su talebinin arttığı gözlemlenmektedir. Bununla birlikte, MPI-ESM-MR sonuçlarına göre, toplam karşılanmamış tarımsal su talebinin CNRM'ye kıyasla önemli ölçüde daha düşük olduğu gözlemlenmektedir. Ayrıca, iklim değişikliğinin rezervuar depolama hacimleri üzerindeki bölgesel farklılıkları da kritiktir. CNRM-CM5.1 sonuçlarına göre, Aydın'daki rezervuarlar tarihsel ortalamalarına göre daha düşük depolama hacim oranları gösterirken, Denizli'deki rezervuarlar artan depolama hacmi oranlarını göstermektedir. MPI-ESM-MR sonuçlarına göre, Aydın ve Denizli'de bulunan rezervuarlarda ortalama depolama hacim oranları artmaktadır. Bu çalışma, tatlı su ekosistemleri için bağlantılı modelleme sistemlerinde GCM'lerin rolünü ve bunların doğasında var olan belirsizliklerini göstermektedir.

TABLE OF CONTENTS

LIST OF FIGURES

LIST OF TABLES

LIST OF ABBREVIATIONS

Abbreviation	Explanation
BAU	Business as Usual
BMB	Büyük Menderes Basin
CNRM-CM5.1	National Centre of Meteorological Research- Coupled Global Climate Model, version 5
DSI	State Hydraulic Works
ET	Reference Evapotranspiration
ET_C	Crop Evapotranspiration
ET_0	Reference Crop Evapotranspiration
ESA	European Space Agency
GCM	Global Circulation Models
GIS	Geographic Information Systems
HADGEM2-ES	Hadley Centre Global Environment Model version 2
HE-HLUC	High Efficiency with High Land Change
HE-NLUC	High Efficiency with No Land Change
IE	Irrigation Efficiency
IPCC	Intergovernmental Panel on Climate Change
IWR	Irrigation Water Requirement
IWRM	Integrated Water Resources Management
Kc	Crop Coefficiency
LE-HLUC	Low Efficiency and High Land Change
MENA	Middle East and North Africa
MGM	General Directorate of Meteorology

MPI-ESM-MR	Max Planck Institute for Meteorology Earth System Model
NSE	Nash-Sutcliffe Efficiency
OAT	One-at-a-Time
PBIAS	Percent Bias
Pe	Effective Precipitation
R^2	The Coefficient of Determination
RCP	Representative Concentration Pathways
RM	Recent-Modern
SCM	Rainfall Runoff Method
TAGEM	Head Office of Agricultural Research and Policies
TUİK	Turkish Statistics Institute
WEAP	Water Evaluation and Planning Programme
WUE	Water Use Efficiency

1. INTRODUCTION

Water has already been a limited resource in many regions throughout history and even the word "rival" comes from the word "rivus" which means individuals using the same stream (Wictionary, 2020). Therefore, even modern language carries the traces of historical conflicts that have sprung from the vital role of water in daily life to date. We can realize from this simple knowledge how critical the water issue is regardless of the era people live in. Today's high water demand for increasing production levels and climate change negatively affect water supply levels in many watersheds and exacerbate these already existent water conflicts. The significance of water supplies and downward spiral nature of water scarcity that human beings currently face necessitate inclusive studies that cover all major causes and symptoms of the problem. Two of the major components of water shortage problem which are also central to this study are absolute scarcity and the differential impact of this scarcity experienced by different socioeconomics groups of society, such as farmers, industrial producers. By absolute scarcity concept, enforcement of general scarcity by nature is expressed (Daly, 1991). In our case, this enforcement is devoted to the impacts of climate change. So, it should not be confused with abrupt natural disasters that causes absolute scarcity. The term explains the aspect of scarcity imposed on all stakeholders and a common suffering shared by all no matter what their status and/or socioeconomic background are.

On the other hand, the adaptive capacity[1] of communities and watersheds are not uniform, therefore the climate change impacts experienced differently depending on the geographic, socio-economic and institutional differences. At this point, adaptive capacity term soundly helps reveal "status quo of different communities and groups in terms of their distinctive vulnerabilities and strengths in times of crisis (Smith et al., 2003). Besides, adaptive capacity concept qualitatively and quantitatively shows us courses of how to improve this capacity within different segments of society. Therefore, it helps us understand the drivers of water shortage and its varying effects and its solutions simultaneously. In this regard, it is an invaluable means through which the disproportionately increasing (with respect to socioeconomic power of people) negative impacts of climate change related problems, such as water scarcity, can be mitigated.

[1] Adaptive capacity: the ability of a system to adjust to including extreme climatic events and climate variability to come with climate change, recognizing the difference in adaptive capacity level of different regions becomes more critical to decide which regions are more threatened and to act accordingly (IPCC, 2018).

One of the regions that water scarcity problem is expected to compound in the following years is Büyük Menderes Basin (BMB). The basin is vulnerable against climate change impacts due to its geographical and socioeconomic situation. In the BMB approximately 80% of total water use is dedicated to agricultural purposes (TUBITAK, 2010) and 44% of the basin is used for agricultural purposes and agricultural production is inherently sensitive to weather conditions (Çakmak and Baran, 2015). On top of the dependency on water, streamflow rates of BMB decreases 20% in the next thirty years (Tarım ve Orman Bakanlığı, 2007). A number of studies indicate that the basin experiences significant changes in climatic parameters. Goubanova and Li (2007) state that higher maximum temperature values are observed, and average precipitations decrease especially in winter and summer in Mediterranean region. These results are compatible with Giorgi (2017) which indicate that long lasting drought periods that follows from warmer seasons is expected in the following years in southern regions of the Mediterranean. In Aegean region specifically, Giorgi (2017) projects a temperature increase around 3 to 4 Celsius degrees in all seasons which is significant considering the already threatened condition of BMB.

On the other hand, a basin conservation report prepared by the Ministry of Forestry and Agriculture (2018) reveals that BMB is a profitable homeland for crops with net revenue margins up to two billion TL. Among these profitable crops, industrial crops like corn and cotton stand out the most. Besides, these crops are highly water dependent. For example, the report of Ministry of Forestry and Agriculture (2018) reveals that growing one hectare of corn requires (one of the most prominent crops of the region) more than 5500 m^3 of water in a typical production period. Besides, the amount of agricultural area allocated to production of corn in BMB is approximately 40000 hectares. Multiplying the irrigation water requirement (IWR) of one hectare of corn and total land used for corn production gives us an annual water demand exceeding 200 million m^3 per year solely for corn growth in the basin. As the long term average annual total water budget of BMB is 2 hm^3 (Yıldız et al., 2007), 200 million m^3 of water used for corn production comprises approximately 10% of the total water budget of the basin. These Figures indicate that agricultural production depends heavily on the supply of water budget and is the largest shareholder on demand side. Given the economic benefits that agriculture sector provides for the region, agriculture’s inherent fragile structure for climatic parameters, and agriculture’s natural dependency on water resources, it is more evident that urgent and viable adaptation solutions must be implemented in the following years.

For these reasons, in my thesis study, I chose BMB as the study area. Since agriculture is the most common livelihood and the largest water shareholder, my thesis study mainly concentrates on agricultural water use in the area. Firstly, I evaluate the current water budget of BMB demonstrating the current status in the basin and representing it as the baseline scenario in the models that I construct for the observation period between 2005 and 2018. Afterward, using basin scale models, I explore the potential impacts of high-efficiency irrigation systems and land use changes in the entire basin considering the different climate change scenarios. That is, I concentrate on applying different methods and scenarios to improve irrigation water efficiency rates in the basin and concentrate on analyzing the potential impacts of each method and consequent scenarios. At this point, investigating thoroughly the baseline condition, along with its future situation aid in exploring the degree to which BMB get affected by climate change impacts. Consequently, based on the results of this scrutinization, plausible adaptive capacity improvement strategies can be put forward before the expected crises hit the basin. Climate scenarios are based on downscaled results of RCP4.5 and RCP8.5 (Representative Concentration Pathways) while management scenarios focus on irrigation efficiency improvement and irrigated land expansion.

In this study, Water and Evaluation Planning (WEAP) tool is used to simulate the impact of different future scenarios such as downscaled climate change scenarios, increased irrigation efficiency and land use change scenarios. Therefore, this thesis aims at contributing feasible solutions to future water scarcity problems of BMB at the watershed scale.

2. LITERATURE REVIEW

Irregular precipitation patterns, increasing temperature averages and changes in wind patterns and evaporation rates are some of the most salient indicators of climate change that we increasingly observe over the last few decades (NASA, 2020). These irregularities brought by the impacts of climate change has significant impacts on every aspect of our lives, i.e. our economic activities, natural resource management, and consequently water security. The irregularity in climatic parameters enforces us to think of potential effects of these aspects on our daily lives and to improve our existing projection capabilities, along with advancing our technological infrastructures so that we can minimize the expected damages due to climate change. On the other hand, intensifying impacts of climate change remarkably decreases our ability to project the variations observed in climatic parameters (Stocker et al., 2013). This increasing uncertainty in predicting the future climatic conditions clearly shows the significance of the steps towards advancing climate projection methods. The advancements in climate projection studies are critical in two senses. Firstly, they show possible future climatic conditions in advance. Secondly, success rate of climate projections has a direct and critical impact on projection studies utilizing from them for different purposes, such as river discharge projections. At this point, modeling tools have been proved to be useful. There are sound and solid examples in which models have been utilized so far in many types of projection studies for different purposes such as determination of possible future water budget. The range of applications which we take advantage of are broad and one of the application realms that grab the attention of many researchers around the world is water security and budget. Water security is, by a broad definition, a community's accessibility to sufficient amount of water having predefined quality standards for sustaining human and ecosystem health, and a community's protection capacity against water-related hazards such as floods and droughts (Water Aid, 2012). As to questions of how water security is achieved in and how the improvements regarding water security can be investigated, two central concepts must be incorporated into analysis. The first one is irrigation efficiency (IE) which is classically defined as the ratio between the water applied to fields and the water used by crops (Brouwer et al., 1991). However, irrigation systems comprise of multiple components. Therefore, various definitions focusing different aspects of the system have emerged over time in addition to classical one. These definitions are handled in Section 2.3. The second central concept is the tool through which necessary analysis is performed. WEAP (Water Evaluation and Planning) is one of the viable tools used in the literature. It is a water resource planning tool and allows us to keep water demand and supply information, and to simulate water demand, supply, flows, and storage based on different climate and management scenarios (Sieber and Purkey, 2015). Thus, it is a suitable tool to examine water security of a region and its applications, along with its features are discussed in detail in Section 2.4.

Water security is heavily dependent on conjecture of climate change, societal transformations and current economic systems. Therefore, it is a multi-layered issue requiring extensive and integrated approaches. For taking these approaches and applying to problems which vary spatially and involve different dimension of water security related problems, WEAP is helpful. This is because it allows us to involve “seemingly” disconnected sides of the issue and allow us to make more sound and reliable projections, which is one of the most pivotal actions towards accomplishing water securities. WEAP allows its users to integrate different water demand shareholders (household, farmers, industrial users) into same modeling environment with the water supply sites. WEAP also provides the opportunity to place preferential order among supply and demand sites, allowing to simulate competition for the existing water resources.

There is extensive literature on investigating water security issues around the globe. This literature review particularly focuses on the definition water security studies in general and probe the impacts of climate change and irrigation efficient and land use changes on water security. The specific focus of the literature review is on studies that used WEAP modeling tool to investigate the water security of the basins. The literature on Büyük Menderes Basin is rather limited, however this review analyzes basin specific studies as well.

2.1. Downscaled Climate Change Projections

BMB is a watershed of 25000 km^2 area and located in Aegean Region of Turkey (Çakmak and Baran, 2015). According to Demircan and colleagues (2017), the annual mean temperature in the Aegean Region is expected to increase around 3°C and annual precipitation rates projected by Global Circulation Models (GCM) model GFDL-ESM2M used in the study are expected to decline around 10% by the end of 21st century. This indicates that BMB is under a serious threat of climate change. Temperature and precipitation changes in BMB due to climate change are particularly critical given that approximately half of BMB is utilized for agricultural purposes (Büke et al., 2013).

Turkish Ministry of Forestry and Agriculture (formerly Ministry of Forestry and Water) is the institution which so far has carried out the most extensive and reliable studies on local climate change impacts on BMB. In this report, three GCMs, HadGEM2-ES, MPI-ESM-MR and CNRM-CM5.1 are used for RCP 4.5 and RCP 8.5 scenarios. GCMs are the models used to simulate atmospheric circulation patterns (Hannah, 2014). CNRM-CM5.1, HadGEM2-ES, MPI-ESM-MR models are among the most commonly used GCMs in the literature and presented as well in IPCC's "The Physical Science Basis Report" (Randall et al., 2007, Ning and Bradley, 2015, Almutairi et al., 2019). As to question of why three GCMs are used in numerous studies for assessment of climate change effects, firstly it is important to note that climate change projections inherently involve uncertainties. Utilizing from more than one GCM helps reduce uncertainties and obtain more reliable findings (Hannah, 2020). Therefore, projection results from GCMs are critical in evaluating climate change impacts on our study areas and parameters of our interest. Here, in Figure 2.1 and in Figure 2.2, projected temperature changes in BMB are displayed. Based on the projections of HadGEM2-ES model for RCP 4.5 scenario, a temperature increase around 3°C degrees by the end of 21st century (Orman ve Su İşleri Bakanlığı, 2016). This projection constitutes the worst case scenario compared to findings of the other two GCM. This is because MPI-ESM-MR model expects a 2°C temperature increase and the other one expects a 2.5°C temperature increase by the end of the century. Similarly, the projection of HadGEM2-ES performed based on RCP 8.5 scenario indicates worst case scenario compared to other two GCM. It projects an approximately 5°C temperature rise by 2100. On the other hand, MPI-ESM-MR and CNRM-CM5.1 GCMs expect a temperature increase around 4°C. From these projections, we can conclude that BMB is under a serious threat since temperatures are inevitably rising and this has the same effect on other climatic parameters such as evapotranspiration (Sun et al., 2016). This type of a change in the basin becomes particularly more critical given that approximately half of the basin area is utilized for agricultural purposes and that some of the main agricultural products of BMB are highly water dependent crops, such as cotton and corn (Büke et al., 2013).

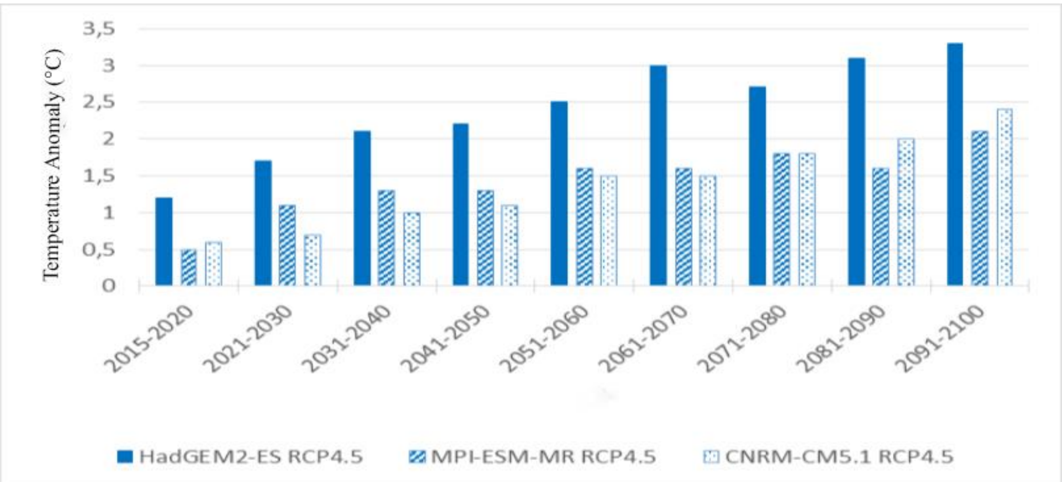

Figure 2.1. Temperature changes modelled by HadGEM2-ES, MPI-ESM-MR and CNRM-CM5.1 under RCP 4.5 scenario in BMB (Orman ve Su İşleri Bakanlığı, 2016).

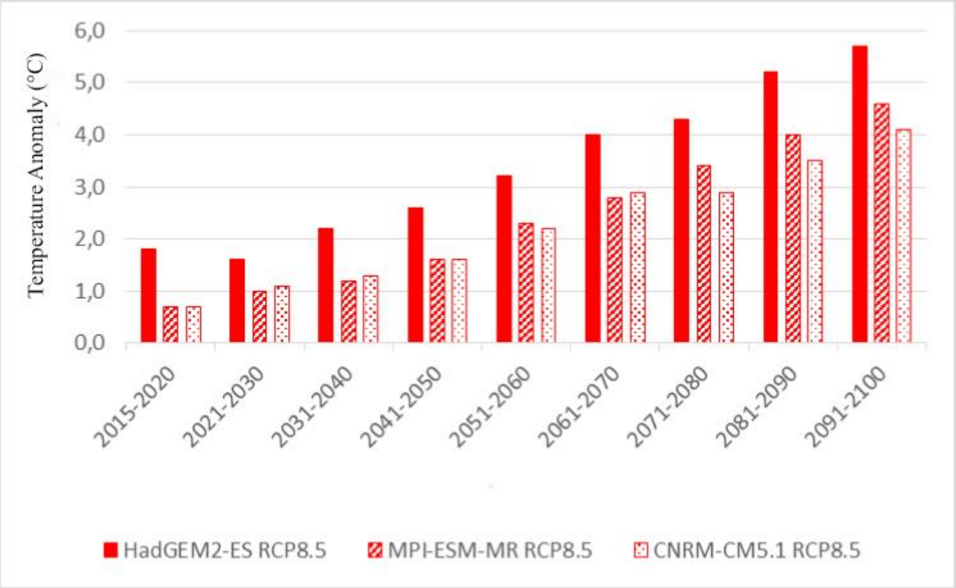

Figure 2.2. Temperature changes modelled by HadGEM2-ES, MPI-ESM-MR and CNRM-CM5.1 under RCP 8.5 scenario in BMB (Orman ve Su İşleri Bakanlığı, 2016).

According to Ministry of Forestry and Water (2016), not all GCM indicate the projections regarding precipitation changes in BMB as monotonic as in the case of temperature predictions. That is, projections performed for precipitation rate changes do not show a linear decrease or increase throughout 21st century. Under RCP 4.5 scenario, HadGEM2-ES model expects around 30 and 600 mm increase in annual average precipitation rates between 2015-2030 and 2041-2050 simulation periods respectively. However, the same model projects barely any decline between 2031 and 2040 while average reduction is projected to be 50 mm between 2051 and 2099. On the other hand, MPI-ESM-MR projects rather monotonic decreases in annual precipitation changes although the rate of anomalies in rates considerably vary in different simulation periods. Conversely, CNRM-CM5.1 model does not display a significant decline in precipitation rates compared to projections of other two downscaled GCMs.

As of projections executed under RCP 8.5 scenario, findings are naturally much more drastic. MPI-ESM-MR model expects a linear decrease of 130 mm in precipitation rates on average between 2051 and 2100 simulation period. Projection of HadGEM2-ES model shows around a 100 mm decrease for the same period and does not vary considerably much for each decade from 2051 to 2100. However, projections carried out for simulation period of 2015-2050 demonstrates some irregularities in terms of expected precipitation anomalies. For example, HadGEM2-ES model anticipates a 50 mm decrease in the simulation period between 2015-2020 while for 2021-2030 period, it shows a 50 mm increase. These findings are not aligned with other two other downscaled GCM projections. Nevertheless, all GCMs project “less” negative changes in precipitation rates between 2015 and 2050 period. As seen for different models, different projections are drawn for precipitation anomalies. According to MPI-ESM-MR model, the declines projected for RCP 4.5 based scenarios is around 60 mm per year and RCP 8.5 scenario results indicate a 100 mm reduction in annual precipitation rates. On the contrary, HadGEM2-ES model projects a 20 mm decline for annual precipitation rates under RCP 4.5 based scenario and CNRM-CM5.1 model projects hardly any decline. Under RCP 8.5 scenario, HadGEM2-ES simulates a 100 mm decline on average between 2015 and 2100 period while CNRM-CM5.1 simulates a rather monotonic 50 mm decline on average for the same simulation period. Lastly, MPI-ESM-MR model simulates a 100 mm decline in precipitation rates on average as in HadGEM2-ES. However, it is important to note here that between 2021 and 2040, HadGEM2-ES and MPI-ESM-MR models simulate antagonistic results, which is highly influential in assessing climate change impacts during different time periods.

All in all, it is an obvious fact that significant differences exist between the findings of three models. These differences may result from resolution of the models and downscaling methods used to create GCMs (Le Treut et al., 2007, Lupo and Kininmonth, 2009). Here, resolution of the models represents basically how fine the earth is gridded (higher resolution is smaller grids) while downscaling is to estimate local scale climate variables from relatively larger scale models. Figure 2.5 summarizes decadal average projected streamflow rates simulated with datasets obtained from previously mentioned GCMs under RCP 4.5 and RCP 8.5 scenarios (Orman ve Su İşleri Bakanlığı, 2016).

The term of "*precipitation elasticity of streamflow*" introduced by Schaake (1990) can have a great use for us to visualize what these precipitation reductions mean to the budget of entire basin. Schaake (1990) defines the term as the ratio between proportional change in annual mean streamflow and the proportional change in annual mean precipitation. For example, if 1% reduction in annual mean precipitation rate causes a 3% reduction in annual mean streamflow rate this means that "*precipitation elasticity of streamflow*" is 3 in the region of interest. The value for the elasticity coefficient ranges from 1 to 3.

According to the elasticity formulation, we can make a rough estimation here regarding the impact of changes of precipitation rates on streamflow and consequently on water budget of BMB. In the best case scenario if we assume precipitation elasticity of streamflow value for BMB is equal to 1, we can make two different estimations here. Based on RCP 4.5 scenario outcomes, the proportional change in precipitation of BMB amounts to around 9%. This ratio is around 15% if we take the projections of RCP 8.5. Supposing elasticity value is 1, these proportional changes result in

9% and 15% changes in annual mean streamflow rates, based on the results of respectively RCP 4.5 and RCP 8.5. The report of Ministry of Forestry and Water (2016) states that annual mean streamflow of BMB is 3 billion m^3. Taking the 9% and 15% of this average value, we end up with a streamflow reduction between 270 million and 450 million m^3. These rough estimations calculated with a simple formulation shows the detrimental impacts of climate change on water budget of BMB. In the projections conducted by Ministry of Forestry and Water, average annual streamflow reductions for the next 100 years are between 30-35%. This result shows that projections regarding streamflow declines are higher than our best case assumption.

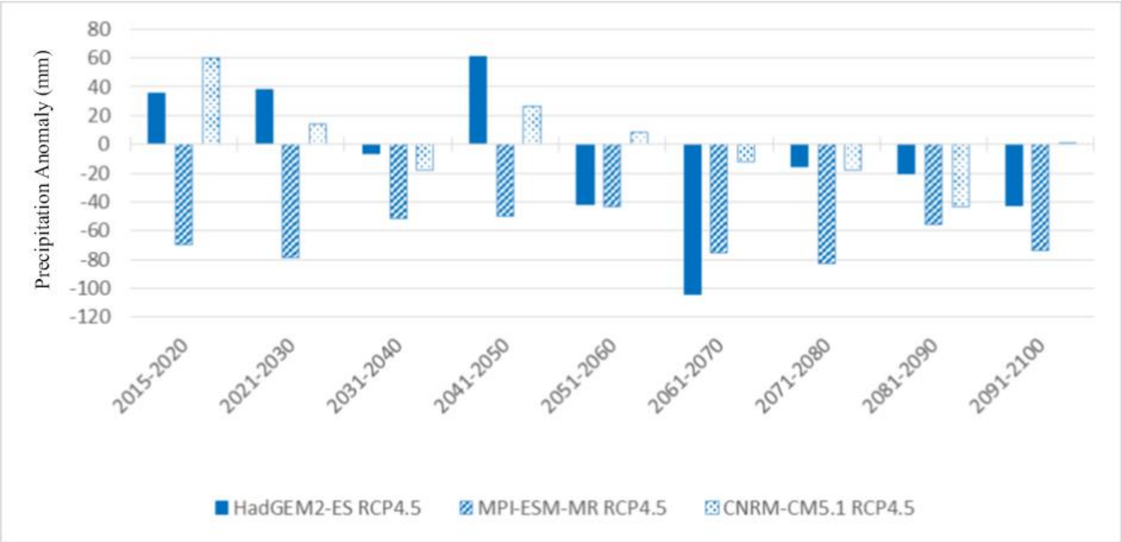

Figure 2.3. Precipitation changes modelled by HadGEM2-ES, MPI-ESM-MR and CNRM-CM5.1 under RCP 8.5 scenario in BMB (Orman ve Su İşleri Bakanlığı, 2016).

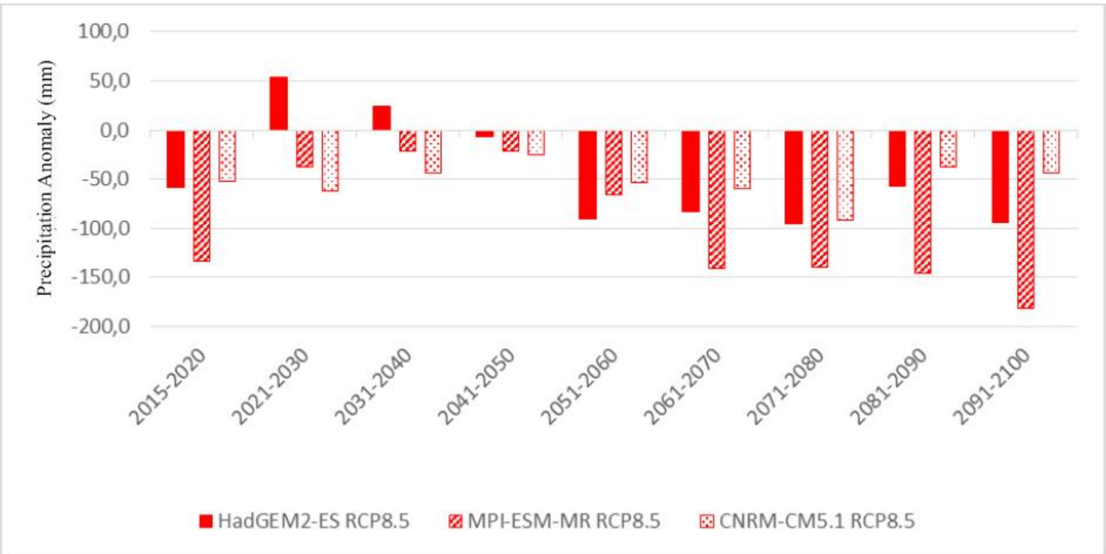

Figure 2.4. Precipitation changes modelled by HadGEM2-ES, MPI-ESM-MR and CNRM-CM5.1 under RCP 8.5 scenario in BMB (Orman ve Su İşleri Bakanlığı, 2016).

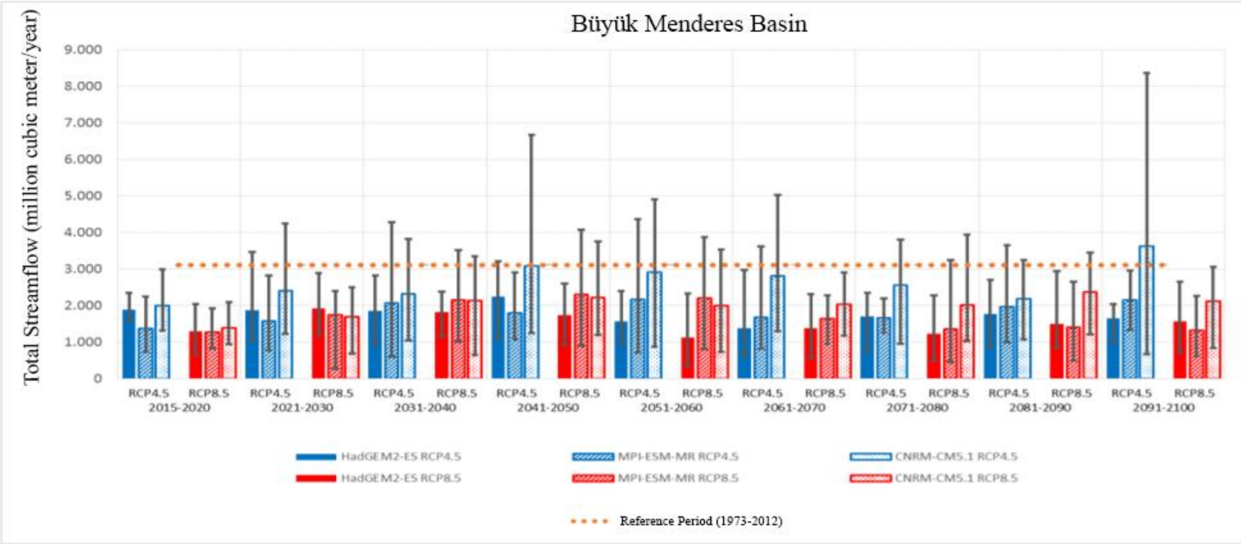

Figure 2.5. Average decadal streamflow projections conducted based on Büyük Menderes Basin Climate Change Projections (Orman ve Su İşleri Bakanlığı, 2016).

These results attained through different GCM tools indicate clearly that using the same conventional methods such as flooded irrigation and inefficient infrastructures to meet water requirement of BMB create a considerable burden on water budget of the basin and likely cause larger gaps in the budget (especially based on the projections of MPI-ESM-MR). The results that Ozkul (2009) obtained in his study concerning the impact of climate change in BMB also support the findings of MPI-ESM-MR model. Ozkul (2009) states that, by the end of 2030, the decrease in runoff in selected portions of the basin reach up to 20% and this ratio rise up to 50% by the end of the century.

On the other hand, according to Durdu (2010) the effects of climate change on the BMB is already evident as statistically analyzing the temperature, precipitation and streamflow changes observed between 1963 and 2007. Based on the results of Durdu's study, during observation period, annual mean temperature has already risen 1 °C. However, the study does not show any significant change in annual mean precipitation rates. The only change observed regarding precipitation rates is that spatial and temporal distributions of precipitation have become more skewed over the observation period (Durdu, 2010). Precipitation patterns becoming more erratic over time implies severe differences and irregularities in streamflow rates in the basin. This fact is what precipitation elasticity of streamflow concept basically points at in terms of situation of our future water security.

All these existing projection studies indicate the serious threat under which BMB is due to climate change effects and the degree of severity compounds considering water dependency of BMB and high water demand crops grown in the region. The next section presents studies regarding water security and its assessment studies.

2.2. Water Security

It goes without saying that water is the most essential component among those that makes life possible on earth. Water security, by definition, is the access to enough water of acceptable quality levels for health, livelihoods and assorted economic activities (Grey and Sadoff, 2007). At the same time, water security is to "climate-proof" the existing water demand (Zeitoun et al., 2013). However, it is critical to note that climate proofing must be valid for each demand site utilizing from water resources, namely environmental, social and economic. Each demand site with water security in the center is illustrated in Figure 2.6 for more clarification of various components water security concept (Asian Development Bank, 2013). As depicted in Figure 2.6, assuring water security is a multi-faceted task while simultaneous taking the pressing threat of climate change. However, it is not straightforward especially considering inter-competition between branches of water security. For example, from sectoral point of view, both agricultural water security and environmental water security have water needs which can be problematical to satisfy with scarce water resources.

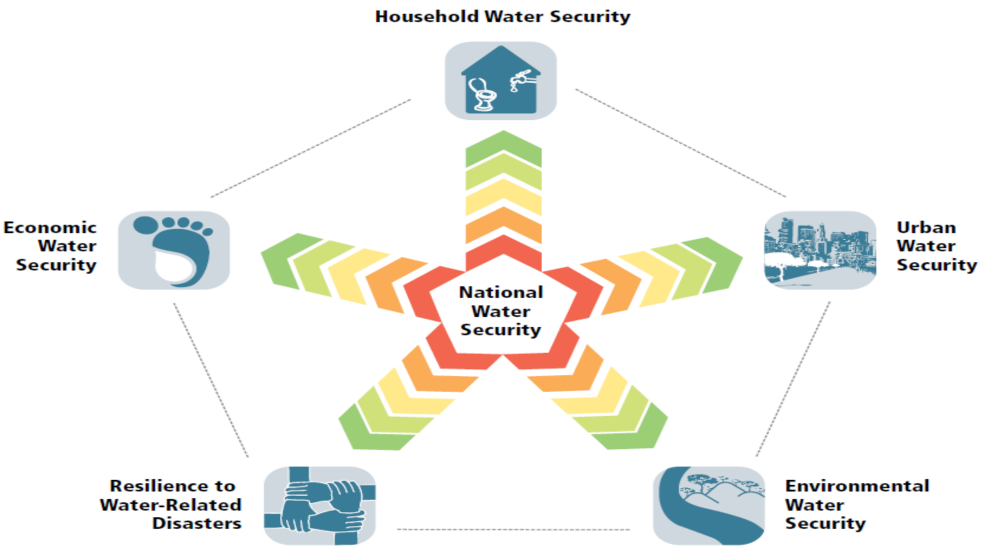

Figure 2.6. Branches of water security presented by Asian Development Bank (Source: Asian Water Development Outlook, 2013).

As the Figure 2.6 shows, requirements of accomplishing water security are different for each stakeholder within the branches. In the context of agricultural water security, farmers of highly salt-tolerant crops in their field, they probably need water resources satisfying predefined quality standards for their crops. Therefore, attempts to fulfill water security for all parties require various actions to be implemented. These actions are shortly listed as below (Schultz and Uhlenbrook, 2008).

- Conservation of water systems
- Sustainable utilization of water systems
- Precaution against extreme weather events
- Protection of the services provided water systems for both environment and human beings

The significance of each of these actions that we must take for securitization of water becomes more prominent as the impacts of climate change appear to be more significant and visible on water security. For example, water security report of NATO states that the world in 2007 alone, has experienced record-breaking floods of China and Sudan followed by multi-year droughts in East Africa and Australia (Jones et al., 2009). Besides, taking a glance at national scale of extreme cases, US has been through consecutive flood events since the beginning of 21st century (Mallakpour and Villarini, 2015). On the other hand, the drought map prepared by National Drought Mitigation Center (2020) presents another extreme fact that the percentage of US lands experiencing more severe drought periods is increasing over the last twenty years. The climate change is increasing the frequency of extreme events on both ends of the water cycle, both floods and droughts. In the local context, BMB is experiencing similar irregularities and extreme events at the basin scale. Each of these catastrophes with increasing frequencies due to climate change imply that achieving water security becomes a more challenging task each day and there must be more conclusive and cohesive steps for solving it.

Defining water security, its importance and climate change's obstructing role in ensuring it, leads to the crucial discussion on how to achieve water security. In order to secure water accessibility in predetermined quality standards, firstly, we need to grasp multi-layered and interconnected structure of water security issue. Water security consists of ecological, societal and economic aspects and it must be assured in a way that all these three aspects can survive and continue their existence simultaneously while competing for existing water resources (Spring and Brauch, 2009). Therefore, the needs of each component must be regarded, together with the interdependence of individual demands on each other. However, in addition to competition among the components, there is cooperation as well. Tickner and Acreman (2013) exemplify the cooperation component by stating the pivotal role of ecological water security as societal and economic aspects depend on the ecological water security. Nature based solutions also can be shown as an exemplary approach focusing on cooperation part of the subject. Nature based solutions are steps toward protecting, managing and restoring natural resources in a way that provide well-being and benefit for both humans and ecosystems (Cohen-Schacham et al., 2016). Conservation of a forest is an example of nature based and cooperative solutions to water security problems. Forests provide vital ecosystem services with their role in water cycle (water regulation through absorption and infiltration to groundwater resources and prevention of excessive runoff/floods in urban settings) (Nagabhatla et al., 2018). Unfortunately, water conflict between different parties also exist as in various cases all around the world. The number of conflicts has been steadily increasing from 177 in 20th century to 466 in the last decade (World Water, 2020). This increase is strongly linked to climate change and increasing water demand. Flörke and colleagues (2018) states that based on their projections for 482 water resources of the largest cities of the world, compounding the effects of increasing urban water demand and climate change is expected to cause a surface-water shortage between 1,3 and 6,7 billion m^3. According to study, this deficit takes place in approximately 30% of these cities (Flörke et al., 2018). At this point, sound solutions to overcome conflict of interest issue between water users are needed. An example can be reducing the water demand of users as an applicable solution and since agriculture is the largest water shareholder, focusing on agricultural water demand is crucial (FAO, 2015). The issue is two-folded as agricultural production is both dependent on water security and at the same time challenging water security from quality and quantity perspectives.

The impacts of climate change on water resources continue to escalate and agricultural production depends on precipitation or irrigation. Hence, the effect of irrigation on water security and the effect of climate change on agriculture's water security deserve attention. In order to visualize the dependence and effect of agriculture on water resources, FAO's (2015) global and continental water withdraw ratios presented in Figure 2.7 should be of great help. The Figure 2.7 demonstrates that around 70% of water resources are dedicated to agricultural purposes. There are two sides of this problem. Firstly, any rate of change in water resources has a great impact on agricultural activities. Elliott and colleagues (2013) reveal that 20 to 60 Mha cropland may have to be converted from irrigated to rain-fed management system in global scale due to climate change. Given that current irrigated land size is 324 million hectares, a conversion of 20 to 60 Mha means an around 6% to 18% change in global irrigated land size (FAO, 2014). This conversion definitely has got a huge impact on overall agricultural activities. Besides, projection of Döll's (2002) study, regarding the effect of climate change on irrigation water requirements (IR), shows a global 3-5% increase by 2020s, and a 5–8% increase by 2070 in overall IR. Therefore, the impacts of climate change on water security of agricultural activities intensify in the following years.

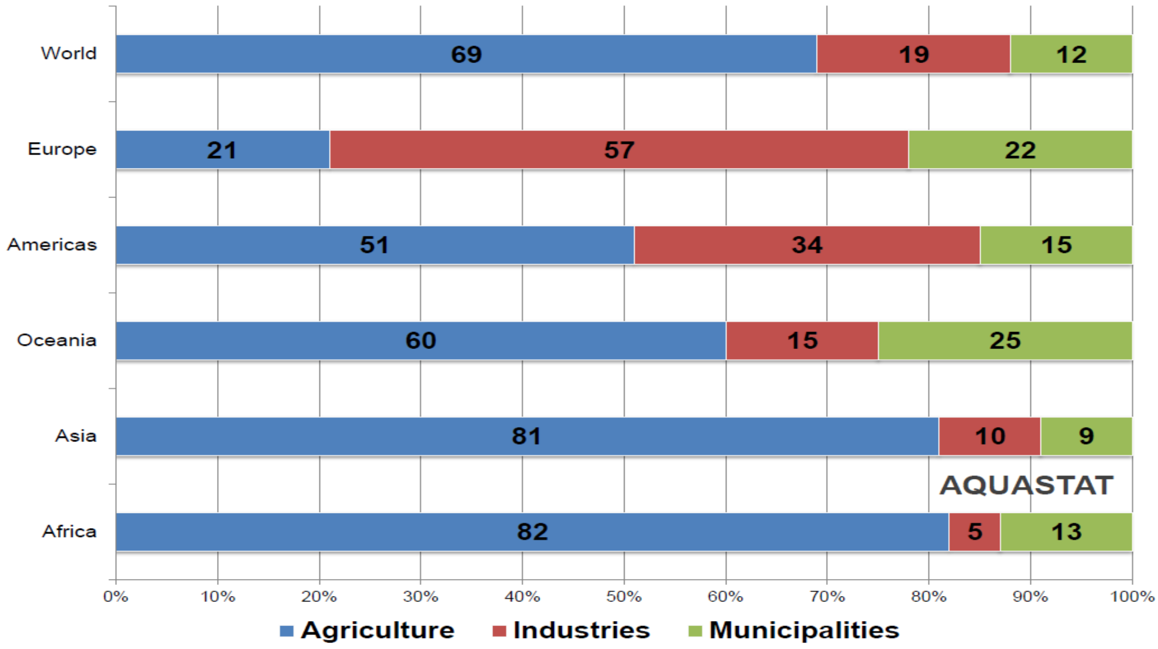

Figure 2.7. Global and continental water withdrawal ratios presented by FAO (Source: fao.org/aquastat/en/overview/methodology/water-use, 2015).

Secondly, magnitude of agricultural water demand poses a great threat for other water demand shareholders in terms of water security due to the competition for existing resources. Water conflicts happening all around the world such as in Gavkhouni Watershed India, in an Inter-Andean Watershed Peru, and in Nile River Basin Egypt, among different players of water security is illustrative cases for this point (Ravar et al., 2020, Guevara-Gil, 2012). At this point, irrigation efficiency (IE) improvement comes into play as a viable solution because it allows farmers to produce the same or even more yield by using the same amount of water (Jensen, 2007). This implies a relief for other water users while not threating agricultural water security. As to how IE can be accomplished, there are effective methods such as irrigation system change, improvement of water retention capacity of soil. Initiating a transition to high-efficiency drip irrigation systems for dominant crops as in many countries such as India is a good example for application of this systemic change (Bell et al., 2020). The details of efficiency improvement methods, their applications, and key concepts regarding IE are thoroughly discussed in the following section.

2.3. Irrigation Efficiency Improvement

Agricultural irrigation represents approximately 70% of the total water demand worldwide and this ratio reaches up to 80% in continents such as Africa and Asia (FAO, 2015). Therefore, any improvement in irrigation has an immense potential to contribute to water security related problems. Irrigation efficiency (IE) concept comes into play right at this point. IE indicates, by a broad definition, how much of the applied water to fields reaches to root zone of crops (Hillel, 2008). Naturally, a certain gap due to conveyance, field conditions, and climatic parameters takes place between the water applied to crops and the water used efficiently by them. Various approaches for increasing IE have emerged. For example, for economic reasons, farmers are curious to investigate their yield produced per m^3 of water which is also defined as "how much crop per drop" (Grafton, 2018). Another important definition is *conveyance efficiency* which indicates the ratio between the water delivered to fields from the sources and the water reaching out to farms/fields (Howell, 2003). Therefore, different definitions and formulations for IE have been developed so far by different approaches. The Table 2.1. presents a list of efficiency types prevalently used in the literature (Howell, 2003, Heerman et al., 1992). Depending upon the purpose of research and data availability, any of these efficiency source can be adapted. Researchers can also assume predefined IE values for different irrigation systems and utilize from these values directly for different purposes, such as evaluating the impact of system changes on water use. These values are presented in Figure 2.8.

Table 2.1. Definition and formulations of different efficiency types (Source: Howell, 2003, Heerman et al.,1992).

Efficiency Type	Definition	Formulation
Conveyance Efficiency	V_f is the volume of water that reaches the farm or field (m^3), and V_t is the volume of water diverted (m^3) from the source	100*Vf/Vt
Application Efficiency	Vs is the irrigation needed by the crop (m^3), and V_f is the water delivered to the field or farm (m^3)	100*Vs/Vf
Seasonal Efficiency	V_b is the water volume beneficially used by the crop (m^3). V_f is the water delivered to the field or farm (m^3).	100*Vb/Vf
Water Use Efficiency (WUE)	Y_g is the economic yield (g/m^2), and ET is the crop water use (mm).	WUE= Y_g/ET

IE is mainly dependent on how much water crops require to fully grow, and this water requirement is quantified by "crop evapotranspiration" (ET_c). ET_c is the combination of evaporation and transpiration. Evapotranspiration in agricultural sense represents the sum of the water loss through soil evaporation plus transpiration which is evaporation by various plant issues such as stomata (Hirschi et al., 2020). Therefore, ET_c is dependent upon internal factors such as properties of crops and external factors such as soil moisture, temperature and rainfall. In order to take both exogenous and endogenous components into account while finding out ET values, FAO approach is frequently used (Ramirez and Harmsen, 2014). ET_0 is reference crop evapotranspiration and represents evaporational side of evapotranspiration. Kc is crop coefficient through which crop properties can be incorporated into ET_c (2014). There are two dominantly used methods to find out ET_0. One of them is to use Penman- Monteith equation (Reicosky and Wilts, 2004). The other method is to directly measure ET_0 value by pan method. Chen and colleagues (2005) explain that pans are filled with water and the decrease in water depth inside the pans gives ET_0. Pans help us represent various weather events affecting ET_0 value, such as of radiation, wind, temperature and humidity (Chen et al., 2005).

So, there are many factors that affect water requirement of crops (ET_c) and therefore its values considerably vary from crop to crop and from region to region. For example, TAGEM (Head Office of Agricultural Research and Policies) and DSI (Hydraulic Services of State) (2016) state in their report that for a melon grown in Muğla ET value is around 600 mm and for maize it is 450 mm. Given that 1 mm irrigation amounts to 10 m^3 water per hectare, the ET difference between maize and melon gives us an additional irrigation of 1500 m^3 per hectare per season. Naturally, this difference becomes much larger as the area size goes up. Besides, even for the same crop, ET value changes remarkably as in the case of melon that its ET value calculated in Izmir's conditions is approximately 560 mm while it is calculated as 600 mm in Muğla (TAGEM and DSI, 2016). ET_c is the part that forms the crop water requirement part of efficiency formulations presented in Table 2.1. The irrigation systems employed in the fields greatly impact IE as well (Figure 2.8)

Table 2.2. Efficiency values for different irrigation systems (Source: Irmak et al., 2011).

Irrigation System	*"Potential" Application Efficiency (%)*
Sprinkler Irrigation Systems	
LEPA	80-90
Linear move	75-85
Centre move	75-85
Travelling gun	65-75
Side roll	65-85
Hand move	65-85
Solid Set	70-85
Surface Irrigation Systems	
Furrow (conventional)	45-65
Furrow (surge)	55-75
Furrow (with tailwater reuse)	60-80
Basin (with or without furrow)	60-75
Basin (paddy)	40-60
Precision level basin	65-80
Micro irrigation Systems	
Bubbler (low head)	80-90
Micro spray	85-90
Micro-point source	85-90
Micro-line source	85-90
Subsurface drip	> 95
Surface drip	85-95

There are significant differences among various irrigation methods. TAGEM and DSI's (2016) report suggests that one hectare of melon requires theoretically around 6000 m^3 of water. As incorporating IE values of different methods displayed in the Figure 2.8, for a field having surface drip irrigation, this (IR) rises up to 9000 m^3 per hectare. One of the most important factors resulting in the difference between conventional and drip irrigation water requirement is that drip irrigation reduces soaked soil surface area (Evett et al., 2005). Consequently, less water is lost through ET due to relatively smaller wetted soil area. A study conducted in Albacete Spain reveals parallel results in this regard. The study finds out a reduction of approximately 20% in ET rates (Valentin et al., 2019).

Another important fact is that drip irrigation system reduces soil salinization (Hanson and May, 2011). This is because drip irrigation obstructs excessive water entrance into soil, and this stops too much mineral to be accumulated in soil. Conventionally, soil leaching/washing has been a prevalent manner to alleviate excessive soil salinization (Balyuk et al., 2018). This is another reason that increases water loss as conventional irrigation systems are employed. According to an important study conducted in BMB, soil washing applications due to high salinization in soil are prevalent in Söke and Sarayköy which are the two important districts of BMB (Girgin and Kayam, 2002). Therefore, transition to drip irrigation has a great potential to achieve considerable water savings in two important manners. Firstly, through reducing evapotranspiration rates, it reduces overall IWR. Secondly, by avoiding high saline conditions in soils requiring to apply large amounts of water, drip irrigation reduces again overall water need in fields.

Another important phenomenon affecting water security is land use change by impacting both total water supply and water demand. The following section scrutinizes historical/baseline and future trends in land use change. Besides, it delves also into the question how these trends affect water supply and demand in global, national, and local scales.

2.4. Land Use Change

Land-use is shaped by the different types of economic and social activities (FAO, 2005). Therefore, land-use of a region represents the way of living in that region and shows the effects of general societal activities on land cover of the area. Being different than land-use, land cover is used to characterize the cover over the lands which may be biological, physical and/or human-made (Liang and Wang, 2020). On the other hand, land-use change, by definition, displays the anthropogenic changes that result in drastic alterations in different environmental settings (Dellasala, 2018). Since the beginning of industrial revolution, the magnitude of human inducing land-use change is utterly high given that total converted area from forests and grasslands to cropland exceeds 10 million km^2 (Ramankutty and Foley, 1999). Besides, the “Land and Water Resources for Food and Agriculture” report of FAO (2012) reveals that global irrigated agricultural area has increased from 2 million km^2 to 2,5 million km2 between 1990 and 2008. Extracting land cover datasets for Europe, Turkey, and BMB from CORINE Land Cover datasets, increasing trends are obtained as well regarding changes in “permanently irrigated land” area. In Europe, total irrigated land has risen from approximately 88.494 km^2 to 110.000 km^2 between 2006 and 2018. In the same time period, total irrigated area has risen from about 57.000 km^2 to 69.000 km^2 in Turkey. Lastly, in BMB, total irrigated area has increased from approximately 2790 km^2 to 2890 km^2 between 2012 and 2018 (Copernicus, 2019). On the other hand, the increase of global urban area follows a similar trend to cropland expansion both globally and locally. Based on the results of Goldewjivk and colleagues (2010), between 1800 and 1950, global urban area has increased tenfold. Moreover, He and colleagues (2019) puts forward that an increase about 130% in total urban area worldwide has taken place between 1992 and 2016. In other words, overall urban land has increased from 275.000 km^2 to 621.000 km^2 and this rapid increase has occurred within just 24 years. The land-use changes realizing at these rates should warn us about two serious issues. The first important issue is functioning of geochemical cycles and the second one is over-consumption of natural resources. Both topics are reviewed in terms of their potential impacts on water security and water budget.

Firstly, it is a well-known fact that overall functioning of geochemical cycles is strongly related to the land-use changes. Therefore, increasing extent of land-use changes at a planetary scale clearly indicates that larger disturbances of land-use change related consequences are becoming more salient on geochemical cycles. For instance, a recent study regarding the origin and fate of atmospheric moisture states that Rio de La Plata basin depends on the evaporation originated from the Amazon forest for 70% of its water resources (Ent et al., 2010). Rio de La Plata is the second biggest basin in South America and its boundaries include Paraguay, South Bolivia, and North Argentina, and Southern and Central Brazil (Guerrero et al., 1997). Given the disturbingly high rates of deforestation in Amazon forests, it is not difficult to state that water security of both the basin itself and the countries located inside the basin's boundaries get highly pressured in the following years. Another example of land-use effect on water cycles is from Liu and colleagues (2017). In their study, the effect of farmlands on runoff of Taoer River in Northeast China is found to be negative while the impact of woodland is expressed as positive on runoff. These results are not surprising considering that forests act as sponges and feed nearby water bodies such as groundwater aquifers which later feed surface water bodies (Peña-Arancibia et al., 2019).

On the other hand, there are also other studies revealing that surface runoff and river discharge increase in the wake of deforestation. Costa and colleagues (2003) find out that 25% increase has occurred in in Tocantins River Brazil's discharge between 1960 and 1995 when there is no significant fluctuations in precipitations rates and when forests are cleared for intensifying agricultural activities. Another study revealing similar trends belongs to Lopez-Moreno and colleagues (2014). Their study is carried out in Upper Aragon River Spain and finds out that increments in forest cover leads to a 16% decrease in annual streamflow in the basin. Another study conducted in Palas basin Turkey also demonstrates that runoff rates have increased 40% between 1987 and 2011 due to increase in agricultural areas (Azgın and Çelik, 2020). Nevertheless, in this study, contrasting results regarding the effects of land-use changes on runoff rates is attributed to the fact that bare soil area has been replaced with agricultural lands in the meantime.

Secondly, land-use changes such as irrigated land expansion leads to an increase in total water demand. Siebert and colleagues (2014) show in their historical study that total irrigated area has almost tripled between 1950 and 2005 from 111 Mha to 306 Mha globally. Additionally, FAO (2014) states that worldwide irrigated area has reached up to approximately 324 Mha. Another study reviewing global irrigated land expansion between 1964 and 1999 reveals the 1.68-fold increase in worldwide irrigated land (Tilman, 1999). Although time intervals of both studies are not the same, their findings show parallel trends for global irrigated land expansion.

Water budget and irrigated land area expansion are closely related as agriculture constitutes 70% of global water use, this rate might be even higher in developing countries such as Turkey with agricultural water share of 73% (FAO, 2017, World Bank, 2014). The relationship between water budget and the irrigated land signals their important role on water security. Increases in irrigated land area basically necessitate an increase in overall irrigation water use. According to estimates carried out by Siebert and Doell (2007), between 1950 and 1955, global irrigational water withdrawal has increased from 1080 km^3 water per year to 2504 km^3 water per year. This more than two-fold increase proves the strong correlation between total agricultural water consumption rise and increasing irrigated land expansion of which global and nation scale changes are presented above. Here, it can be concluded that the effect of agricultural land increase on global irrigational water use is salient. Therefore, its critical role on global water use rates must not be omitted and further attention is needed to grasp impacts of its future trend.

There are a host of threats such as climate change and socioeconomical changes (i.e. increasing agricultural production, overfishing) posing upon global, national, and local scale water security (Vörösmarty et al., 2010, Allan et al., 2013). Each of these threats are powerful enough to enlarge the disparity between water supply and demand given the high rates of land-use changes. Reviewing the studies which focus on projection of future water security situation, a number of studies find out an increase in global water demand based on the assumption that total irrigated area increases in the following decades. Huang and colleagues (2019) estimate an increase of about 11% for global irrigated land and the impact of this expansion on global blue water and green water withdrawal is presented in Figure 2.9 and 2.10. Here blue water is defined as the ET resulting from irrigation while green water is described as the ET resulting from rainfall (Schyns et al., 2019). In other words, blue water represents total withdrawal abstracted from groundwater resources, rivers, and reservoirs. On the other hand, green water is illustrated as the ET from soil moisture which is gained through rainfall in agricultural lands (Rockström et al., 2009).

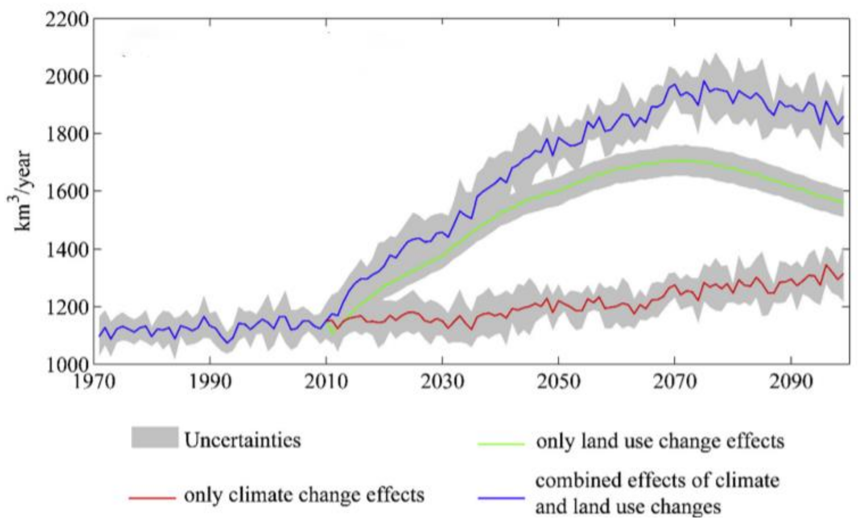

Figure 2.8. Global crop blue water consumption (Huang et al., 2019).

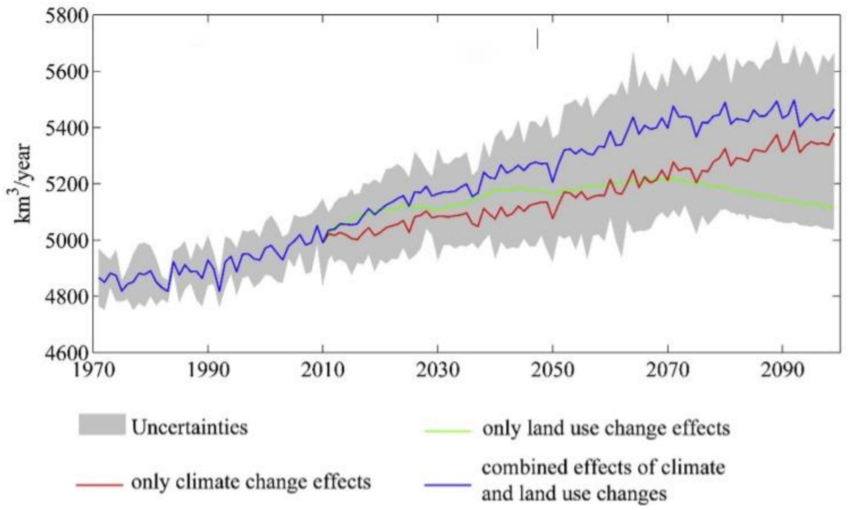

Figure 2.9. Global crop blue water consumption (Huang et al., 2019).

There are also numerous local scale studies modeling the future trends of land-use changes under different scenarios. In these studies, strict interrelation between land-use changes, water demand and are quantified.

A study carried out in Sao Francisco Basin Brazil analyzes the impact of A2 and B1 scenarios on future water supply and water demand. According to IPCC's (2000) special report on emission scenarios, A2 scenario presumes a less globalized world where economic development is low, population growth is high and environmental awareness is low. On the other hand, B1 scenario assumes a more globalized world where population growth is low, economic development and environmental awareness is high. In the study, based on the assumptions of A2 scenario, it is estimated that irrigated cropland area rises from 4.4 Mha to 9.3 Mha between 2005 and 2035 while natural vegetation areas drops from 26.6 million Mha to 20.7 million Mha (Koch et al., 2015). As to the assumptions of B1 scenario, no cropland expansion is observed even though crop patterns change. As a result of the difference between two scenarios, simulated future irrigation water demand is higher in A2 scenario. Mean annual irrigation demand is approximately 15 billion m^3 for A2 scenario while it is 8.5 billion m^3 for B1 scenario.

Similarly, another study carried out in California's Central Coast assumes a decrease in annual crop lands and an increase for perennial land in its BAU scenario conditions (Wilson et al., 2020). Besides, Wilson and colleagues (2020) set another scenario which is recent-modern (RM) scenario. In RM scenario, they assume a slightly higher annual cropland decline and approximately 35% more increase in perennial land compared to BAU scenario. Projected land-use changes are shown in Figure 2.11 while their aggregate impact on total water demand is presented in Figure 2.12. In projected water demand Figure, by the end of 21st century, BAU scenario reveals an increase about 220 million m^3 in water demand while RM scenario approximately 360 million m^3 rise.

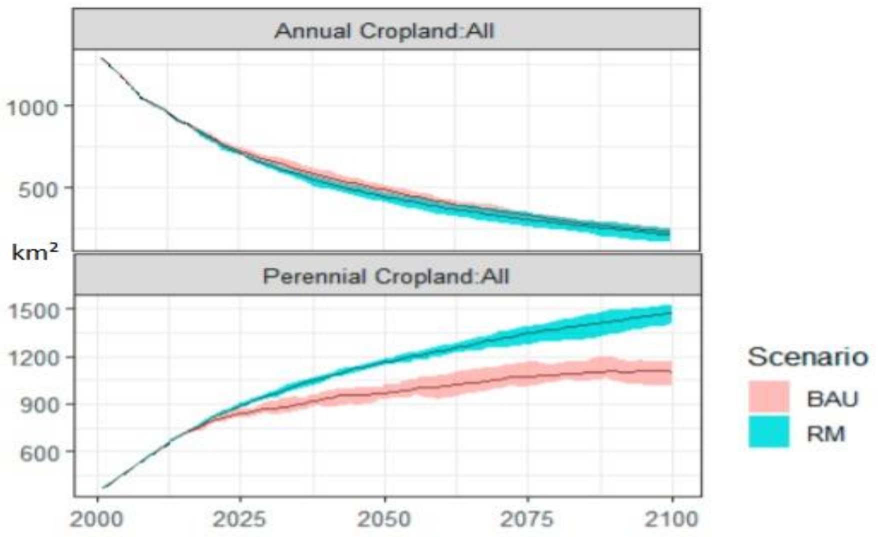

Figure 2.10. Annual and perennial cropland change projection in km^2 by 2100 (Wilson et al., 2020).

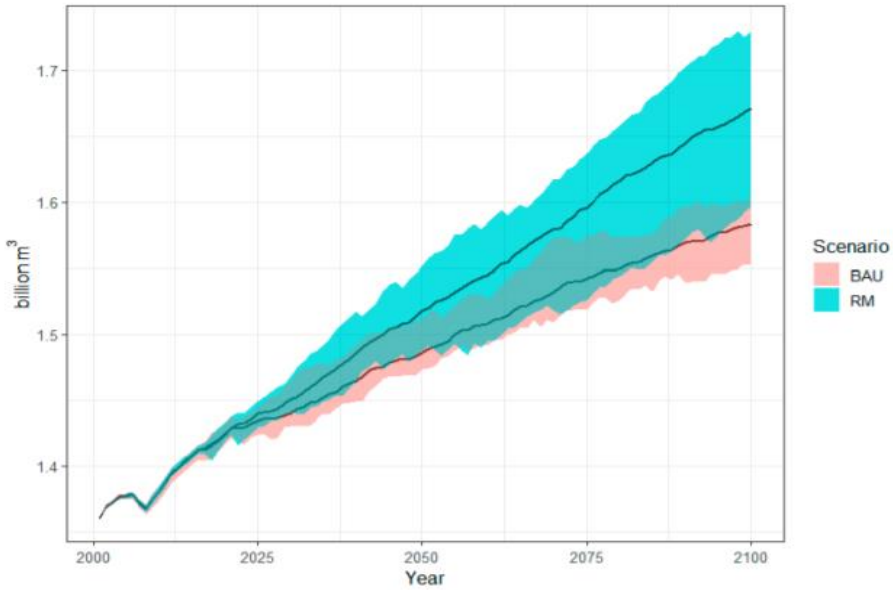

Figure 2.11. Projected land-use change related water demand in billions of m^3 (Wilson et al., 2020).

Deducing from the global and local scale studies presented above, being the largest water use shareholder, any change in agriculture has an immense effect on total water consumption both locally and globally. Land-use change in favor of increase of irrigated land size is one of the most central changes in today's world. Therefore, there are multitude of studies concerned with both historical change of total irrigated land and with its possible future trajectories so that they can quantify the impact of irrigated land change on overall water demand trend. Besides, cropping patterns in irrigated lands is also proven to be critical in affecting overall water demand. Thus, researchers need to analyze both quantity and quality of irrigated lands within the areas of interest so that more thorough and inclusive findings can be obtained.

In the following section 2.5, I focus on one of the most important modeling tools used to quantify the effects of different parameters (i.e. land-use change, climatic conditions) on variables such as river runoff and reservoir storage volumes. The modeling tool being reviewed is WEAP and throughout section I discuss the applications of WEAP utilized in different areas of the world for various purposes, such as future discharge and water demand estimation.

2.5. WEAP and Its Applications

Water management is described as the sum of activities carried out to analyze and monitor water resources along with measures developed and implemented to keep the resources within a desirable condition (Pahl-Wostl, 2009). On the other hand, Integrated Water Resource Management (IWRM) is a relatively new concept developed to enlarge the scope of classical water management notion. It is defined as the type of water management that involves a wide range of factors effective in management process, such as water allocation related modifications, environmental management enhancement, and community and stakeholder engagement (Page et al., 2020). WEAP is one of the most effective tools used to have a comprehensive approach to water resource planning and management and therefore it serves for practicing IWRM applications (SEI US, 2020). It helps planners in various manners. For example, WEAP keeps demand and supply information in the role of database. That is, in a broader sense, it works as a water accounting book. Additionally, it works as a projection and policy analysis tool. As a projection tool, WEAP performs various simulations on parameters, such as discharge rates, water demand, storage, runoff and evapotranspiration. Besides, being a policy tool, it assists in evaluating the impacts of assorted water management related decisions. These decisions considerably vary from new infrastructure projects (stormwater management projects) to economic activity changes (i.e. rapid industrialization) and to water user behavior alterations (Sieber and Purkey, 2015). In using WEAP, the assessments of different management decisions are performed through scenario analysis. During scenario analysis process, WEAP provides users with a platform and interface on which they can change certain factors affecting the course of water resource management in an area (Yang et al., 2020).

After explaining the services that WEAP can provide for its users, it is now the time to elaborate on how WEAP can operate the tasks mentioned above. To begin with, WEAP calculates water supply based on the amount of water which falls on a typical watershed (Yates et al., 2005). After completing the water supply part of watersheds, WEAP forms the demand side of the relation between water resources and users by including firstly evapotranspiration (Mahmood and Hubbard, 2002). Remaining water inside the watershed right after evapotranspiration process, according to the algorithm of WEAP, is the water available to the use of environmental and human water needs. For supply side, WEAP allows to pick up elements such as reservoirs, wastewater treatment facilities, groundwater resources, and rivers. On the other side, for demand side, household, irrigation and industrial units are the options to choose. Catchment and supply demand elements of WEAP are presented through a graphical interface. In the Figure 2.13, there is an example of WEAP's graphical interface.

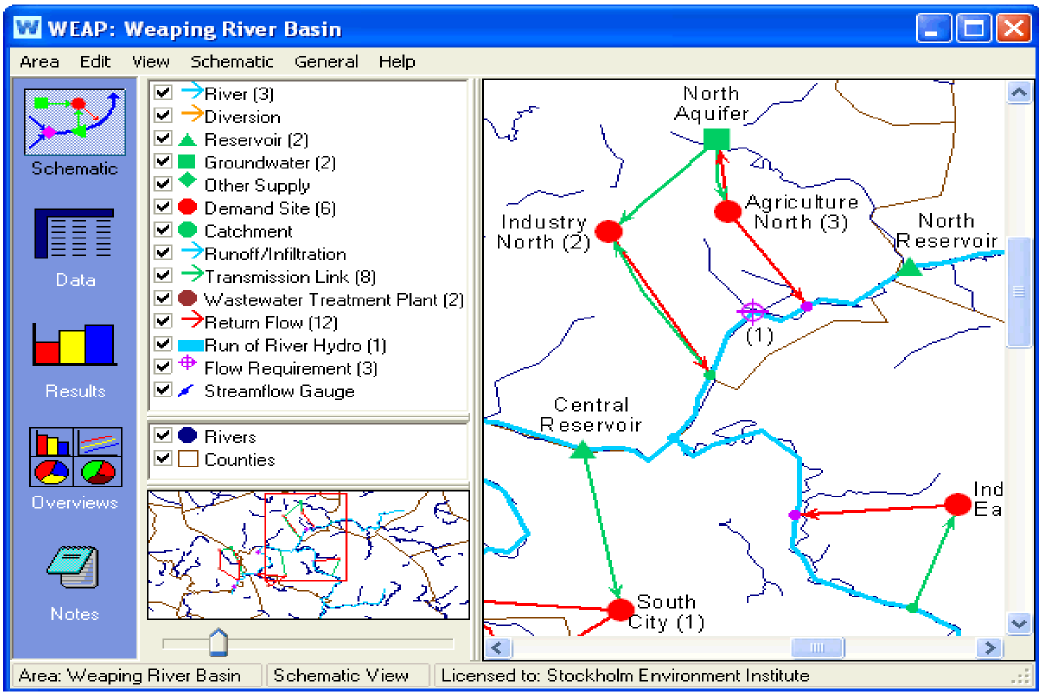

Figure 2.12. Graphical interface of WEAP schematics (Source:WEAP21).

The interface seen in Figure 2.13 enables to visualize the positions of the supply and demand elements within the catchment (McCartney and Arranz, 2009). After defining supply and demand components of the catchment, WEAP carries out simulations whose period can extend from one to 100 years. During simulation processes, WEAP simulates these hydrological processes under different climate and management scenarios and provides sound outcomes regarding the potential impact of these scenarios (Yates et al., 2005).

Capabilities and potential contributions of WEAP become more outstanding given the future of water security problems intensified due to climate change, as explained in Water Security section. Integrated water management strategies can bring solutions to water security problems considering the economic and hydrological processes (Grantham et al., 2012). WEAP is one of the most viable tools that are in accordance with this purpose. In the following paragraphs, we analyse the applications of WEAP and their findings. The WEAP applications discussed below are regarding household and agricultural water security related problems.

In China, Yang and colleagues (2020) conduct an evaluation study on the effects of policies on the balance between water supply and demand. Since WEAP provides a sound and effective ground for assessing the potential impacts of the integrated parameters (such as hydrological and social ones) in water management processes, they utilize from WEAP as a tool. Simulation period of the study is between 2019 and 2035. For the 16 years under consideration, Yang and colleagues (2020) examine the impacts of population growth, crop planting area and irrigation water use on the water budget of Beijing. Their results indicate that population growth is the most powerful factor affecting water budget in the area compared to two other parameters in question. The study states that a population growth restriction can diminish overall water demand by more than 3 million m^3 and that even a successful population growth regulation does not end unmet water demand, which means various implementations must be jointly performed in (Yang et al., 2020). This study demonstrates some of the applications which WEAP permits its users to have. It also shows how researchers can get policy regulations and hydrological factors involved in their assessment studies and therefore how they can take an integrated approach while tackling with water budget related problems.

Another study is conducted in Israel which is famous for being the world's one of the most water-stressed countries (Maddocks et al., 2019). In Sade and colleagues (2016), they focus on agricultural water security of Lake Kinneret Watershed and simulates the trend of unmet demand between 1996 and 2005 for different scenarios. Main purpose of the study is to identify vulnerable partial areas inside the watershed in terms of water availability during 1996 and 2005. In doing so, Sade and colleagues (2016) define "coverage" as a proxy for water availability in the catchments inside Lake Kinneret Watershed. Coverage is the ratio between the water demand and water supply and shows the severity level of drought in various subregions in the area. It is important to note that agriculture comprises of the water demand in the area. After defining coverage, researchers of the study determine their scenarios based on the changes in precipitation distributions and patterns, along with ET values. They attempt at finding out the degree to which drought level is affected by changing precipitation and ET values. At the end of the study, Sade and colleagues (2016) conclude that coverage (the ratio between demand and supply) increases towards the end of simulation period. Their findings display the continuously deteriorating impacts of precipitation and ET values on the watershed.

In Sacramento Valley, another agricultural water security-based study is conducted with the help of WEAP. Purkey and colleagues (2007) explore the hydrological responses of Sacramento River Basin to possible adaptation strategies and climate change scenarios. Firstly, findings of the study reveal that reservoir inflows diminish due to increasing temperatures and decreasing precipitation regardless of whether any adaptation strategies are taken. Purkey and colleagues (2007) define this effect as "absolute" and suggests that possible adaptation strategies can have an important role in mitigating the impacts of this impact on agricultural water security in the area. The adaptation strategies which researchers observe in this study are irrigation efficiency improvement and increasing land fallowing practices in the area. These strategies serve as tools which help reduce overall irrigation demand in the basin. Consequently, these strategies help reduce vulnerability of local farmers against detrimental effects of climate change because a higher proportion of their irrigation requirements can be achieved thanks to lower water need per unit area. Another finding of study is also worth evaluating that projections performed between 2005 and 2100 shows no significant change in groundwater levels. Purkey and colleagues (2007) postulate two possible reasons for this projection. To begin with, despite overall irrigation water requirement in the area, declining precipitation and increasing temperatures offset possible increases in groundwater reservoirs. Secondly, water savings achieved through reduction in agricultural water demand are transferred to satisfy water demand of urban users and environmental components. As seen here, the integrated structure of WEAP enables practitioners to observe the interdependence of different water users and shows how water security of different users can be simultaneously achieved through various adaptation strategies.

Gediz Basin is also one of the study areas where WEAP is employed to observe. Main purpose of the study is to find out the impact of climate change on water budget of the basin, especially during drought periods (Yilmaz and Harmancioglu, 2010). As the previous two examples of WEAP applications, this research focuses as well on agricultural water use and deficit in the basin because agricultural lands occupy half of the basin and they consist 80% of overall water demand in the area (Çevre ve Şehircilik Bakanlığı, 2015). In their study, Yilmaz and Harmancioglu (2010) assign three different hydrological scenarios for the basin which are Business as Usual (BAU), Pessimistic, and Optimistic scenarios. For BAU scenario, researchers assume that the monthly stream flow data observed between 1977 and 2003 are repeated for the simulation period starting from 2003 to 2030. On the other hand, as to pessimistic scenario, they use the findings of Ozkul's (2009) study projecting that 23% decline is expected for runoff by 2030. Lastly, optimistic scenario foresees a 23% increase for stream flow by the end of simulation period. After defining three distinct hydrological scenarios, Yilmaz and Harmancioglu (2010) proposes four different adaptation strategies and combination of these four strategies to reduce IWR and evaluates their potential effects on future water budget of Gediz basin. These strategies are maintenance of irrigation canals, crop pattern change, transition to drip irrigation, installation of pressurized irrigation systems and combination of these four main strategies. At the end of the study, it is concluded that transition to drip irrigation reduces irrigation water deficit most significantly for both BAU and optimistic scenario while joint application of crop pattern changes and drip irrigation transition work best for pessimistic scenario.

As seen in the applications of WEAP, this model helps its users consider different components of water management processes. This feature of WEAP makes it a useful means for the purposes

IWRM which has been developed to take broader approaches for water management related problems. As seen in the applications, numerous researchers utilize from WEAP for different purposes, including climate change and adaptation impact analyses.

3. METHODOLOGY

This thesis study utilizes WEAP modeling tool to evaluate the future water budget of BMB under different land use, irrigation methods, and climate scenarios for the time interval between 2005 and 2100.

WEAP is a useful tool allowing its users to model water budget of a basin. In doing so, WEAP requires datasets to create the basin's water budget using existing water supply and demand in the study area. In Figure 3.1, the flowchart of how a typical modeling study is carried out using WEAP is demonstrated.

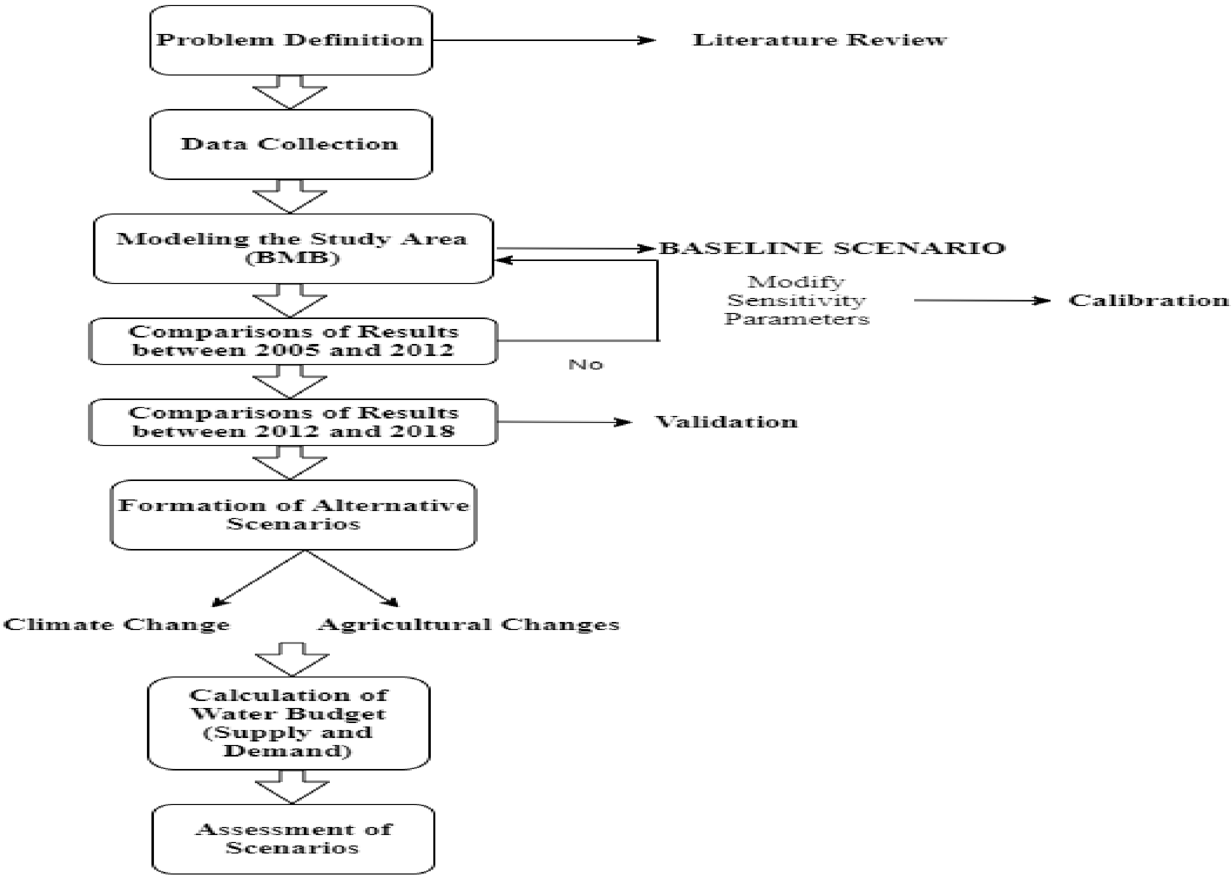

Figure 3.1. WEAP flowchart.

3.1. Study Area

BMB is the 8th largest basin of Turkey and occupies an area of about 25000 km^2 (DSI, 2010). Aydin, Denizli, Muğla and Uşak consists of around 90% of the total basin area (Çevre ve Şehircilik Bakanlığı, 2016). Among these four cities, Aydin, Denizli, together with Muğla host the most important reservoirs of BMB. The storage capacities, initial storage values, and irrigation areas of these significant reservoirs are shown Table 3.1 (Tübitak, 2010). There are also several other relatively small reservoirs in the area. However, within the scope of this thesis study, the focus is merely on the reservoirs displayed in the Table 3.1. and the agricultural areas irrigated by these reservoirs.

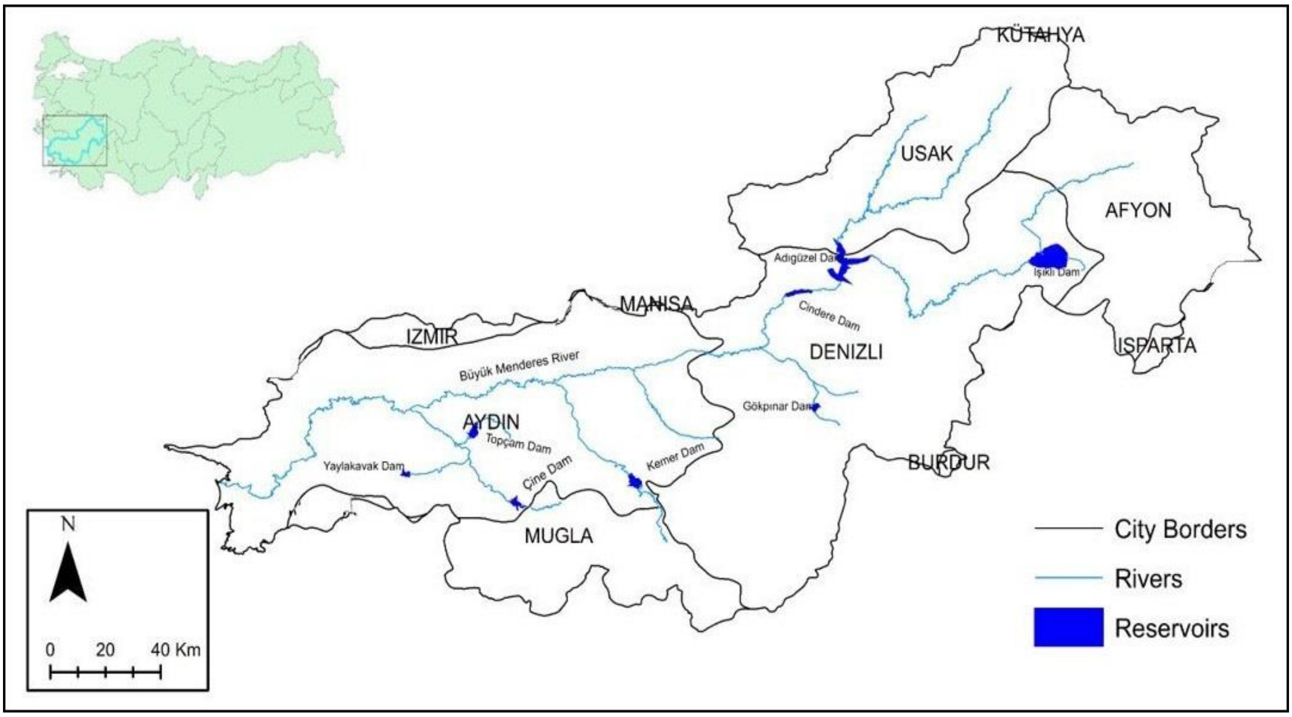

Figure 3.2. Map of BMB with water supplies and city borders.

The first reason why BMB is chosen as study area is that approximately 85% of total IWR is satisfied through surface water resources in BMB. The second main reason is that reservoirs among the surface water resources outstands as one of the most broadly used resources. On the other hand, Büke and colleagues (2013) demonstrate that agricultural lands comprise of 44% of the entire basin and total agricultural land consumes around 80% of total water supply mainly stored in the reservoirs shown in Figure 3.1. That is, agricultural water use is the most dominant water use shareholder in BMB, and reservoirs are the main supplier in the area. As to the most commonly crops which require irrigation grown in BMB, cotton, maize, sunflower, and assorted fruits consist of the majority. The average distribution of each major crop grown is shown in Figure 3.3 (TUIK, 2019).

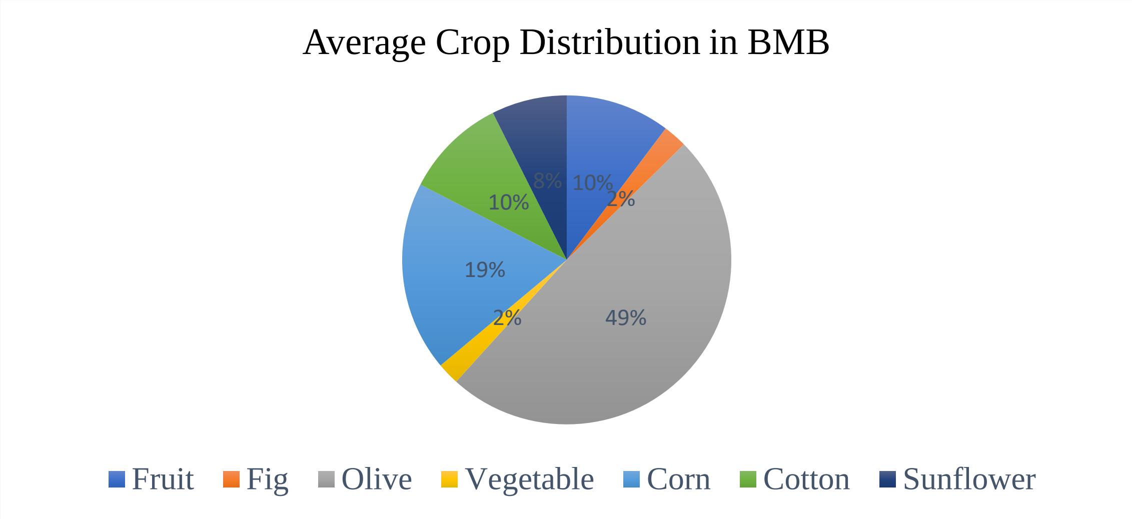

Figure 3.3. Average crop distribution in BMB (Source: TUIK, 2020).

According to Ministry of Forestry and Hydraulics Works (2016), currently the Ministry of Agriculture and Forestry, total surface water reserve of BMB is approximately 3 billion m^3 annually and total agricultural area inside watershed borders is around 11000 km^2. Taking a quick look at the water reserve stored by the reservoirs and the size of area irrigated through them tells that this thesis study chooses to observe one third of the irrigated land in BMB and again observe one third of total surface water reserve flowing through the watershed per annum.

Table 3.1. Water reservoirs in BMB (Data accessed on 28.07.2020)

Reservoirs	Reservoir Capacity (million m^3)	Initial Storage at the year of establishment (million m^3)	Planned Irrigation Area (ha)	Year of Establishment
Kemer	419,170	123,847	58930	1958
Yaylakavak	31,420	3,294	3348	1997
Topçam	97,740	25,986	4983	1985
Çine	350,000	221,814	22358	2010
Karacasu	17,200	9,342	2814	2012
İkizdere	194,960	83,131	3625	2009
Adıgüzel	1076,000	477,526	78060	1990
Işıklı	237,800	72,335	50486	1953
Gökpınar	27,720	12,219	5824	2002
Cindere	84,270	59,249	78060	2008
Tavas	65,000	51,135	3304	2010
Bayır	7,170	1,919	1050	2008
Total	2608,450	1141,797	312842	

On the other hand, it is important to note that, under BAU scenario (with no change in IE), this already high IWR is expected to increase even more in the following years due to rising temperature levels (increasing evapotranspiration rates) in the area while runoff values are projected to diminish for the changes expected in precipitation and temperature figures (Ozkul, 2009). Besides, based on the findings of Atmaca's (2010) study, population of the basin is expected to go up between 27% and 35% varying based on the assumptions made for each different population scenario for BMB. Adding increasing population's household water requirement to anticipated increases in IWR indicates water security related problems of BMB deteriorate over time because of changing climatic conditions and social changes.

Reservoirs presented in the Table 3.1 convey the required water to fields through irrigation channels and most of the agricultural land is irrigated by flood irrigation method. At the beginning of the second half of 2020's, number of reservoirs in the basin considerably increased and continue to increase with recently completed projects such as Akbaş reservoir in Denizli province which started serving in 2018 (Denizli Çevre ve Şehircilik Müdürlüğü, 2017). The main purpose of new reservoir projects is to expand irrigated land in the entire area and consequently increase overall agricultural production.

3.2. WEAP Modelling Tool

WEAP is a physical modeling tool used to estimate water budget of watersheds under altering hydrological conditions and policy scenarios. WEAP provides a sound basis to evaluate possible impacts of changes in policies and hydrological circumstances on water budget of the areas of interest. That WEAP allows its users to input different components of water budget calculation makes it a perfect tool for implementation of IWRM concepts in various parts of the world. So far, WEAP has been used as a strong model which helps create water budget of watershed by incorporating both climatic and social conditions.

To assess how BMB gets affected by climate change until end of the century, I build a water budget model using WEAP software. As being a water budget model tool, WEAP requires datasets of both water supply and demand for the area of researchers' interest. With these datasets in background, WEAP creates a water account in that income part consists of water supply from different resources (i.e. aquifers and reservoirs) and in that expenditure part is comprised of water demand of various agents/users such as municipalities, households and agricultures. In addition to keeping water accounts inside, WEAP is used also for forecasting purposes (Yates et al., 2015). That is to say that future water budget estimations can be realized with the help of the software and these estimations can be carried out based on different scenarios and assumptions regarding future climatic conditions, demographic conditions, water use policies and infrastructures (Yates et al., 2015).

Typical models created using WEAP consist of supply and demand nodes and transmission links connect them to each other (Sieber and Purkey, 2015). Supply nodes generally comprise of reservoirs, groundwater resources, and rivers while demand nodes consist of household, industrial, and agricultural water demand units. Users can give different priorities for each demand node and can predetermine certain flow requirements while constructing their models (Yates et al., 2005). For example, researchers can apply an upper limit for maximum withdrawal from a certain reservoir and can also prioritize meeting of a particular demand (i.e. household water need) over other kinds of water demands.

The most important novelty which WEAP brings with itself is that it helps reveal the bilateral relationship between water resources and social conditions. Through constructing various scenarios created using a reference one, its users can obtain results regarding the individual or compounded effect of different components of water budget (Khalil et al., 2018). Scenarios can be created using various changes in both water supply and demand nodes and pre-requirements for satisfaction of different conditions. From supply side, these changes can be decreasing inflow rates due to climate change. Moreover, these amendments can be decisions made in favor of environmental water need satisfaction, that is alleviating more water to environment and restricting agricultural and/or industrial water use. On the other hand, from demand side, the modifications which we can represent through different scenarios can be increases/decreases in overall water demand due to many reasons, such as efficiency improvement projects and irrigated land expansion.

Another important feature of WEAP is that users can view their study area in five different ways through the graphical interface provided by WEAP (Sieber et al., 2015). Schematic view shows the spatial and physical representation of watersheds with supply and demand nodes. The second view sort is data view and it is where physical properties and datasets regarding supply and demand nodes can be input. Users can input data such as climatic parameters, area sizes, reservoir properties and population changes over time. Thirdly, results view demonstrates the final output which your model gives based on the inputs entered. The range of results which WEAP provide is considerably broad and varies from inflow to reservoirs to net evaporation values on watershed scale. Nevertheless, although it may change depending on the purpose of research, the most important output which WEAP yields is unmet water demand of each node (if it exists at all). Export and/or import of file types such as Word, HTML, CSV, together with Excel is another advantage of employing WEAP as an IWRM tool (Sieber et al., 2015). Another useful function of WEAP is its capability to integrate the outputs from other modeling environments. The data can easily be imported from or exported to file formats such as Excel and CSV. (Sieber et al., 2015).

3.2.1. Data Requirements

WEAP requires a number of datasets in order to calculate water budget of hydrological systems such as watersheds. Since water budget consists of water supply and demand sides, each particular component comprising overall supply and demand has to be entered into WEAP so that it can carry out necessary calculations.

Depending on the method choice on WEAP, different datasets necessitate. There are five methods in WEAP. These methods are Irrigation Demands Only Method (Simplified Coefficient Method), Rainfall Runoff Method (Simplified Coefficient Method), Rainfall Runoff Method (Soil Moisture Method), MABIA Method and Plant Growth Model (Sieber et al., 2015). For example, MABIA method require datasets regarding plant physiology and daily Et values while Soil moisture method requires physical properties of soil. The preferable method for this thesis study is Rainfall Runoff Method (SCM) and the datasets required for this method is shown in Table 3.2.

In WEAP model, demand nodes generally represent municipal, household, and agricultural demands. However, in this thesis study, the model contains only agricultural demand nodes. WEAP calculates agricultural demands as the multiplication of annual activity level (irrigated land size in this case) with water use rate (water demand per hectare), and monthly variation of water demand. On the other side, the calculation of monthly inflow is somewhat more complicated and shown in below equation 3.1. As the formulation below indicates, among many climatic parameters, SCM requires only precipitation, reference evapotranspiration (ETref), and crop coefficient (Kc) rates on a monthly basis. Here, ETref is dependent on temperature, humidity, solar radiation and wind speed. It gives evapotranspiration rates particular to different land classes and crops as multiplying by Kc (Allen et al., 2004).

Table 3.2. Data requirements of WEAP simulating water budget through Rainfall Runoff Method

	DATA REQUIREMENTS	UNIT	TIME FRAME	SOURCE
Water Demand	Annual activity level	ha	2005-2018	State Hydraulic Works (DSI)
	Water use rate (agricultural)	m^3/ha	2005-2018	State Hydraulic Works (DSI)
	Monthly Variation (of water use)	percent (%)	2005-2018	State Hydraulic Works (DSI)
Water Supply	Storage Capacity	m^3	2005-2018	State Hydraulic Works (DSI)
	Monthly Storage Volume	m^3	2005-2018	State Hydraulic Works (DSI)
	Buffer Zone Storage Capacity	m^3	2005-2018	State Hydraulic Works (DSI)
	Top of Conservation Storage Capacity	m^3	2005-2018	State Hydraulic Works (DSI)
	Volume-Elevation curve	m^3/m	2005-2018	State Hydraulic Works (DSI)
Catchment Hydrology (Land Use)	Land Cover	percent (%)	2005-2018	European Space Agency (ESA)
	Crop Coefficient	Unitless	Consistent	SacWAM Documentation. 5-16–Draft, September 2016
	Effective Precipitation	Unitless	Consistent	Calculated using Smith (1992) method
	Catchment Area	m^2	2005-2018	State Hydraulic Works (DSI)
Catchment Hydrology (Climate)	Evapotranspiration	mm	2005-2018	Global Land Evaporation Amsterdam Model (GLEAM)
	Precipitation	mm	2005-2018	General Directorate of Meteorology (MGM)

Crop coefficient or Kc represents specific properties of certain land types and/or crops in terms of their evaporativity rates in different growth stages (Hillel, 2008). On the other hand, according to SCM Algorithm of WEAP, Effective precipitation (Pe) is defined as the ratio of overall precipitation available for evapotranspiration (Sieber et al., 2015). It should also be added that among the variables used for calculating inflow rates of reservoirs are Pe and crop coefficient which are mainly dependent upon land classes. Therefore, it is highly critical to determine land class types to be used in models. In this study, agriculture, forest, grassland, and urban areas are included in the model. In SCM, the inflow calculated using Kc, ETref, and Precipitation can be determined as river head flow and/or the source of the water inside catchments. Since the obtained river flow datasets are not reliable enough for the purposes of this study, river head flows are not chosen as the inflow sources of reservoirs, instead, catchment nodes are storing water. Besides, it should be added that inflow calculation is not adequate as it comes to reservoir modeling in WEAP because storage capacity, volume-elevation curve, buffer zone and top of conversation storage volumes are necessary for the model to construct the structure of reservoirs. These constructions are particularly critical as analyzing the correlation between storage volume and reservoir height and as determining the behavior of reservoir depending on the current storage volume inside reservoirs.

$$\text{Inflow} = (\text{Precipitation-ETref*Kc*Pe}) \text{ *Catchment Area} \tag{3.1}$$

3.2.2. Baseline Scenario

Before delving into further steps such as calibration, validation, and scenario analysis, it is necessary to create a baseline scenario which shows the current situation BMB in hydrological and socioeconomic manners. The purpose of this study is to model water budget of BMB. In doing so, WEAP serves as a modeling tool which makes use of various inputs to calculate BMB's water supply and demand under certain conditions. The list of inputs which WEAP uses is given in Section 3.2.1.

For constructing the basic structure of watersheds, WEAP requires Geographical Information Systems (GIS) layers. These layers show the physical properties of watersheds in Schematic View explained in section 3.2. Through GIS layers with land cover datasets downloaded from the database of European Space Agency (ESA), WEAP shows land cover distribution within the borders of watersheds, elevation bands, and calculates flow direction in the basins (Sieber et al., 2015).

After creating BMB with the help of GIS layers and land use datasets, supply and demand nodes can be inserted onto the watershed of interest. As stated previously, in this thesis study, demand nodes consist primarily of agricultural water demands and supply nodes are composed of reservoirs and catchment nodes which store the water coming from precipitation. In this study, the water sources of reservoirs are catchments. Catchments feed reservoir through runoff links. Later, reservoirs transfer water to demand nodes, that is to fields, through transmission links whose efficiency, loss rates, limitations are adjustable.

In this study, each catchment serves to one reservoir and each reservoir serves to merely one single district's agricultural demand site. However, there are two exceptions here. Firstly, Çine district is irrigated by both Çine and Topçam reservoirs. Secondly, Işıklı reservoir irrigates both Çivril and Baklan districts. For the purpose of simplification, in this study, I assign single agricultural demand node for both Baklan and Çivril because there is no available information as to how much area of each district's irrigated by Işıklı reservoir. Besides, I assign two different demand nodes for district of Çine because the two areas and reservoirs are not connected to one another. Therefore, supply preference is not integrated in this model. For the question of which reservoir is responsible for meeting which demand site's irrigation need, the answer is obtained from each district's directorate of agriculture. Besides, the question of which surface water surfaces reservoirs are built onto, this information is also gathered from each district's directorate of agriculture. Finally, Table 3.3 is created by being utilized from the incoming information.

Table 3.3. The list of reservoirs, districts, and surface water sources.

Sources	**Reservoirs**	**Provinces**
İkizdere Stream	İkizdere	Aydın
Dandalaz Stream	Karacasu	Karacasu
Akçay River	Kemer	Bozdoğan
Çine River, Madran Stream	Çine, Topçam	Çine
Kocaçay Stream	Yaylakavak	karpuzlu
Çine River	Çine	Koçarlı
Yenidere River	Yenidere	Tavas
BMB River	Işıklı	Baklan, Çivril
BMB River	Adıgüzel	Sarayköy
Sırainler Stream	Bayır	Yatağan
BMB River	Cindere	Buldan
Gökpınar Stream	Gökpınar	Pamukkale

As shown in Table 3.3, there are 12 reservoirs in our model which depicts the general picture of BMB. All the reservoirs, demand nodes, along with supply nodes are presented in the schematic view of WEAP. Schematic view of this study's area is shown in Figure 3.2.

Figure 3.4. Schematic view of the WEAP Model.

After inserting demand and supply and constructing catchment hydrology, "*key assumptions*" feature of WEAP comes into play. It is a practical tool which allows users to change certain variables/parameters at once, therefore researchers do not have to conduct modifications individually for each demand. As to this study's model, key assumptions regarding Pe are crop coefficient, annual water use rate per hectare, annual activity level (total area of agricultural lands), and loss from system.

3.2.2.1. Water Supply. All the water supply nodes are reservoirs in this model. All reservoirs feed on different catchments in which they are located. Each reservoir has varying catchment size and climatic conditions and these differences affect inflow rate for reservoirs. Data requirements for reservoirs are net evaporation, inflow, storage, buffer zone, and top of conservation zone capacity, along with volume-elevation curve. In WEAP modeling tool, inflow of reservoirs mainly come from either rivers or catchments. In this study, inflow source of reservoirs are catchments. With evapotranspiration, precipitation, Pe, and crop coefficient datasets for catchments' areas, along with their area sizes, WEAP calculates inflow rates of catchments. Consequently, through runoff link from catchments to reservoirs, the captured water inside catchments transfer to reservoirs.

One of the user-friendly features of WEAP is that users can compare observed and simulated values of reservoir storage volumes on the interface of the tool. This is particularly helpful in calibration and validation processes. The storage volume of reservoirs that are included in this study is given in Figure 3.3. Time interval for reservoir storage volumes is between 2005 and 2018, yet since not all reservoirs start serving at the years, some portion of interval is empty for a few reservoirs.

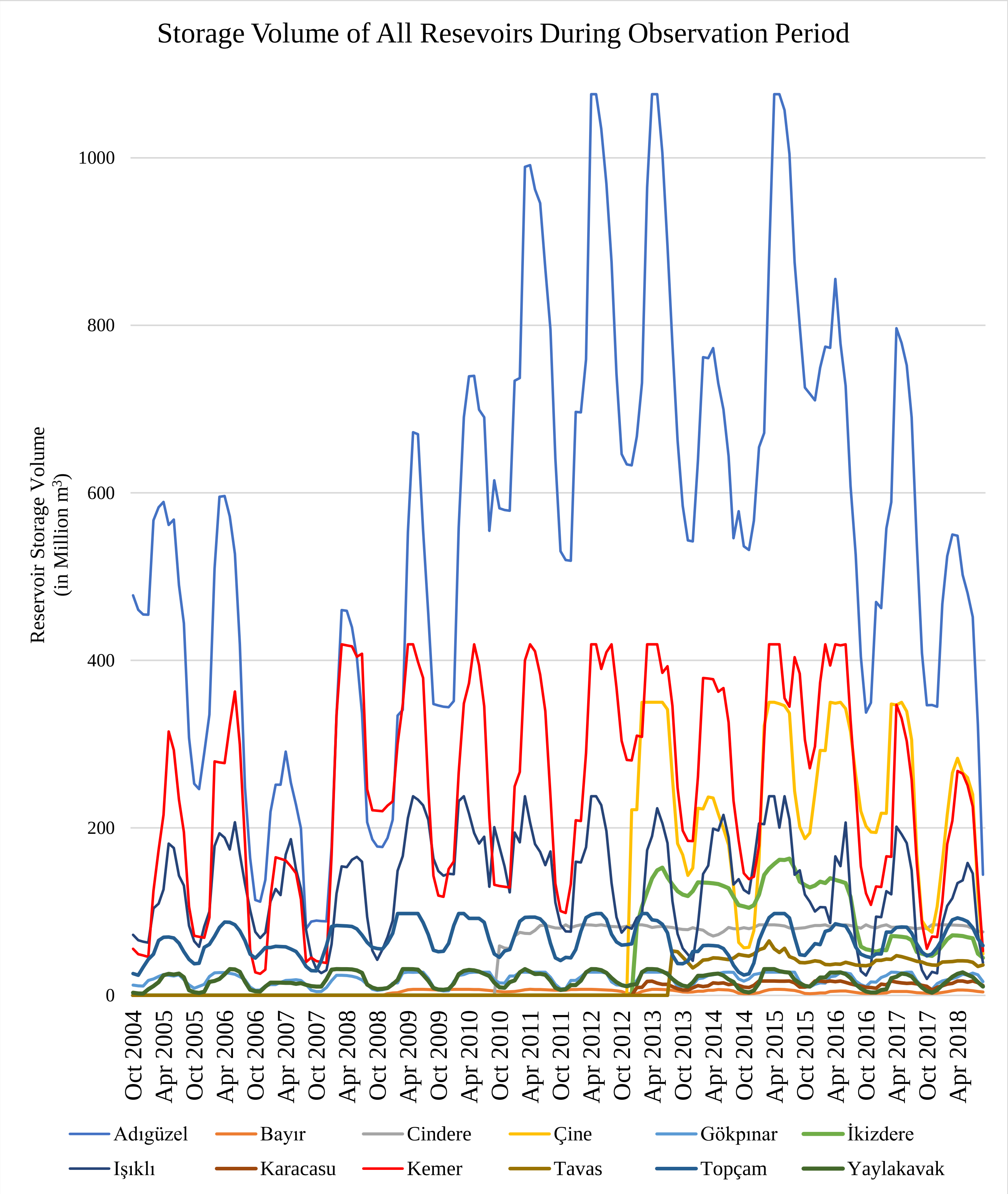

Figure 3.5. Observed storage volumes of reservoirs in BMB between 2005 and 2018.

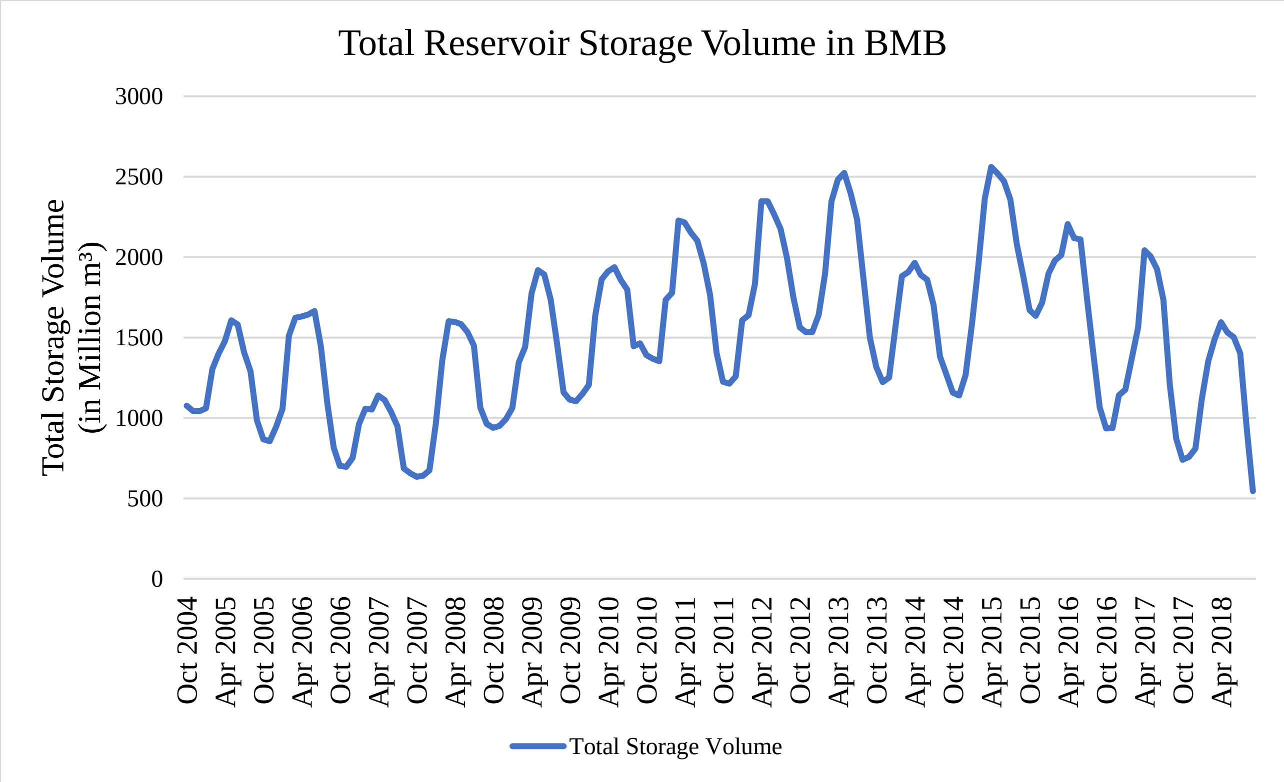

Figure 3.6. Total reservoir storage volume during 2005-2018 observation period.

3.2.2.2. Water Demand. There is only one type of demand node in this model and that is agricultural water node. Therefore, each demand node displayed in Figure 3.2. represents basically field scale water demands for different agricultural areas. Compared to calculation of inflow of reservoirs, demand calculation algorithm of WEAP is somewhat more straightforward. There are three parameters regarding demand nodes which WEAP requires to calculate water demand of different nodes. These parameters are annual activity level, annual water use rate, along with monthly variation. Regardless of what water demand type is demand nodes (that is agricultural, household, and industrial), calculation procedure is the same in WEAP modelling tool. The procedure is simply the multiplication of annual activity level, annual water use rate, and monthly variation of annual demand.

In this study, annual activity level represents agricultural water demand nodes and its unit is in hectare. Annual water use rate is, on the other hand, the water demand required per hectare and lastly monthly variation shows the distribution of annual water demand.

3.2.3. Calibration and Validation

Calibration is defined as a procedure carried out with the purpose that model results, such as storage volumes in this study, can match better to observed results (Singh and Frevert, 2002). Additionally, calibration is classified as the sum of practices aiming at better parametrizing a model to a given set of local conditions, thereby reducing the prediction uncertainty (Arnold et al., 2012). By conducting calibration process in modelling, model output and measured data are compared and the fitness of the two is observed. On the other hand, validation is defined as a process of running the model using parameters that were determined during the calibration process and comparing the predictions to observed data not used in the calibration (Arnold et al., 2012). In general, data is split into two groups and either of the groups is used for calibration while the other group is used for validation whose explanation is given below (Brath et al., 2006).

In this study, current year is defined as 2005 and therefore calibration period starts at 2005. The latest dataset available is from 2018, therefore the modeling period is divided into two with calibration period being between 2005 and 2012 and validation period being between 2013 and 2018. However, since some reservoirs are not active since 2005, their calibration and validation periods are adjusted accordingly. Calibration and validation periods of each reservoir are displayed in Table 3.4.

Monthly reservoir storage volume rates simulated by WEAP are used for calibration and validation. Compare and contrast process get conducted using observed volume rates obtained from DSI for the time period between 2005 and 2018.

Table 3.4. Calibration and validation periods of reservoirs.

Reservoirs	**Calibration Period**	**Validation Period**
Adıgüzel	2005-2012	2013-2018
Bayır	2008-2013	2014-2018
Cindere	2010-2014	2015-2018
Çine	2013-2015	2016-2018
Gökpınar	2005-2012	2013-2018
İkizdere	2013-2015	2016-2018
Işıklı	2005-2012	2013-2018
Karacasu	2013-2015	2016-2018
Kemer	2005-2012	2013-2018
Tavas	2013-2015	2016-2018
Topçam	2005-2012	2013-2018
Yaylakavak	2005-2012	2013-2018

There are well-defined statistical coefficients used in the literature for quantification of calibration and validation success of this model (i.e., quantifying overall fitness of model), such as Pearson's correlation coefficient ($R^{2)}$, Nash-Sutcliffe efficiency (NSE), and Percent bias (PBIAS). These three coefficients are commonly utilized in hydrology literature (Ndulue et al., 2015, Babar and Ramesh, 2015). R^2 reveals the linear relationship between simulated and observed data and its range varies from -1 to 1 (Moriasi et al., 2007). Therefore, it is used to show prediction capacity of models for future periods and consequently shows fitness of models. Besides, NSE reveals how fit the graph of observed versus simulated results is to y=x or 1:1 line (Nash and Sutcliffe, 1970). Its range varies from $-\infty$ to 1 yet typical NSE values are between 0 and 1, plus the values between 0.5 and 1 are acceptable for hydrological models (Moriasi et al., 2007). Lastly, PBIAS quantifies the average inclination of whether simulated flows are bigger or smaller than their observed correspondences (Liew et al., 2005). Formulation of all three coefficients are as below.

$$\text{PBIAS} = \frac{\sum_{i=1}^{n}(Y_i^{obs} - Y_i^{sim})*100}{\sum_{i=1}^{n}(Y_i^{obs})} \qquad (3.2)$$

$$\text{NSE} = \frac{\sum_{i=1}^{n}(Y_i^{obs} - Y_i^{sim})^2}{(Y_i^{obs} - Y^{mean})^2} \tag{3.3}$$

$$R^2 = \frac{\sum_{i=1}^{n}(Y_i^{sim} - Y_i^{mean})^2}{\sum_{i=1}^{n}(Y_i^{sim} - Y_i^{mean})^2 + \sum_{i=1}^{n}(Y_i^{obs} - Y_i^{mean})^2} \tag{3.4}$$

In the formulations of the coefficients above, Y_i^{obs} denotes the ith observation for the parameter evaluated which is storage volume of reservoir and Y_i^{sim} and Y_i^{mean} is the ith simulated value and the mean of observed data respectively. Besides, n represents the total number of observations which are repeated on a monthly basis in this study.

3.2.3.1. Sensitivity Analysis. Sensitivity analysis is performed for two purposes in general. The first goal is to improve models in terms of their robustness. The way sensitivity analysis promotes improvement of models is that it shows to what parameters model is sensitive (Devak and Dhanya, 2017). This way researchers can adjust the most influential parameters until they calibrate their models as sound as possible. The second purpose is to grasp the nature of interrelation between different parameters (Pushpalatha et al., 2011). For example, through sensitivity analysis, we can understand the individual effect of precipitation on reservoir storage volume and can see the combined impact of different parameters such as precipitation and temperature on reservoir volume.

In this study, sensitivity analysis is utilized for the purpose of improving model's strength so it can work more efficiently. While researchers can choose numerous sensitivity analysis methods such as derivative-based and variance-based methods, this study employs "One-at-a-time" (OAT) method (Griewank and Walther, 2008, Tarantola et al., 2007). In OAT method, impact of each single independent variable on dependent variable is observed and quantified by changing solely one parameter at a time (Pianosi et al., 2016). The same procedure is implemented for different parameters varying according to models of interest.

During sensitivity analysis of this study, OAT is carried out to quantify the impact of precipitation, ET, Pe, Kc and loss from system. Each of these parameters are increased and decreased incrementally and the impacts of these changes on reservoir storage volume (dependent variable) are observed. According to results of the analysis, sensitivity degree of the model is highest for precipitation, ET, and irrigated land expansion parameters. So, this study utilizes from these three parameters for scenario analysis. Besides, our model is also sensitive to parameters of Pe, Kc, and loss from system. Therefore, they are used as sensitivity parameters during calibration process. Figure 4.13 that is in section 4.1.1 of results chapter displays results of sensitivity analysis and show how sensitive this model is to different parameters of interest.

Formulation of sensitivity analysis is as in the below equations 3.5 and 3.6. These equations calculate output (reservoir storage volume) deviation as a 10 % percent change (multiplier) takes place in the certain input parameters.

Input variation = $\frac{I-I_{bc}}{I_{bc}} * 100$ (3.5)

Output variation = $\frac{O-O_{bc}}{O_{bc}} * 100$ (3.6)

In the equations above, I and O represent the values of the input and output variables respectively. Besides, I_{bc} and O_{bc} are the values of the output variables respectively for baseline scenario.

3.3. Scenario Analysis

Scenario analysis is defined as a method to help researchers and planners visualize future situation of a study area based upon various decisions (Dong et al. 2013). In hydrological studies particularly, scenario analysis is a useful method employed to project the changes in hydrological processes as a response to circumstances such as climate change and land use/cover change (Li et al., 2015). Thus far, scenario analysis has also been used to evaluate the assorted impacts of future developments in a region, such as urbanization, infrastructure services (Ahmadi et al., 2018).

In this study, once the model is calibrated and validated successfully, next step is scenario analysis. This analysis starts at 2019 and continues by the end of 21st century. Scenario analysis of this study consists of three distinct elements which are climate change, land use, and infrastructural change. The scenario based on climate change is created to assess particularly the impact of different climate change projections on water quantity in the BMB. The model is re-run with climate projections of CNRM-CM5.1 and MPI-ESM-MR GCMs under RCP 4.5 and RCP 8.5 scenarios.

Afterwards, reservoir storage volume between 2019 and 2100, obtained with the help of two GCMs above, are compared with baseline scenario's reservoir storages. Secondly, a scenario based on an assumption that irrigated land increase takes place in BMB is created for the simulation period. Lastly, as the third scenario, the impacts of improvement in irrigation infrastructures on overall water demand is demonstrated. In this scenario, irrigation system efficiency rates are changed employed throughout the region to quantify the impact of efficiency improvements on water budget of BMB. According to Irmak and colleagues (2011), average efficiency rate for surface drip irrigation is 90% and average efficiency rate for conventional furrow irrigation that is prevalently employed in BMB is 55%. Therefore, in calculating water demand rates under infrastructural change scenarios, I utilize from these two average efficiency rates and I carry out the necessary calculations accordingly.

Therefore, scenario analysis of this study is based on climate projections, land use changes, and technological/infrastructural development in BMB. The possible combinations of scenarios performed based on the results of two GCMs (CNRM-CM5.1 and MPI-ESM-MR) are displayed in Table 3.5.

Table 3.5. Alternative future scenarios for BMB.

Feasible Scenarios	Properties
Business as Usual (BAU)	Current technological and land-use conditions are expected to continue
High Efficiency No Land Use Change (HE-NLUC)	Low Irrigation Water requirement due to improvements in irrigation systems and no change in irrigated land size
High Efficiency Increased Irrigated Land Size (HE-IILS)	Low Irrigation Water requirement due to improvements in irrigation systems and increase in irrigated land size
Low Efficiency Increased Irrigated Land Size (LE-IILS)	High Irrigation Water requirement due to lack of technological improvements in irrigation systems and increase in irrigated land size

3.3.1. Climate Change Projections

Possible climate trajectories which the earth is expected to take in the following years are represented by RCPs. They consist of four possible GHG concentration scenarios covering a broad range of plausible anthropogenic climate forcing varying from 2.6 W m^{-2} and 4.5 to 6 and 8.5 W m^{-2}

till 2100 (van Vuuren et al., 2011). 2.6, 4.5, 6, and 8.5 W m^{-2} are the expected radiative forcing values, defined as the difference between incoming energy from sunlight and the outgoing energy sent back to outer space (Myhre et al., 2013). So, higher radiative forcing means higher heat energy is trapped in the earth which in turn contributes more to global warming in the following years.

In this study, RCP4.5 and RCP8.5 scenarios of MPI-ESM-MR, and CNRM-CM5.1 GCMs are utilized for climate change scenarios. In this study, SCM is used to simulate the hydrology of the area. Therefore, precipitation and ET rates are requirements of WEAP so that it can perform necessary calculations for projections. Figure 3.4, 3.5, and 3.6 represent ET and precipitation rates for BMB between 2005 and 2099. For the results of CNRM-CM5.1, data source is ESGF (Earth System Grid Federation) database while data source of MPI-ESM-MR model's results is Boğaziçi University Climate Change and Politics Application and Research Center. Climate projections are created based on both RCP4.5 and RCP8.5. Figure 3.5 shows precipitation and ET values simulated by CNRM-CM5.1 and Figure 3.6. presents precipitation and ET values simulated by MPI-ESM-MR. Besides, Appendix B displays decadal average differences of climatic conditions in Aydın, Denizli, Muğla, and Uşak so that differential impacts of climate change on different parts of BMB can be observed.

On the other hand, for changes in water demand between 2019 and 2100, findings of Gorguner and Kavvas's (2020) study are utilized for all reservoirs due to crop pattern similarity, geographical proximity, and similar climatic conditions between BMB and Gediz basin. Changes in IWR projections based on RCP4.5 and RCP8.5 climate change scenarios are given in Table 3.6. Changes are calculated as the percentage deviation of IWR from historical average IWR rate obtained between 1995-2003 period. In this study, IWR changes are displayed under RCP4.5 CNRM-CM5.1 and RCP4.5 MPI-ESM-MR scenarios. Similarly, IWR changes are also displayed under RCP8.5 CNRM-CM5.1 and RCP8.5 MPI-ESM-MR scenarios.

Table 3.6. Percentage changes in average IWR rates for RCP4.5 and RCP8.5 scenarios in Gediz Watershed (Source: Gorguner and Kavvas, 2020)

	2019-2044	2045-2072	2073-2099
RCP4.5	-3%	3%	4%
RCP8.5	-3%	8%	9%

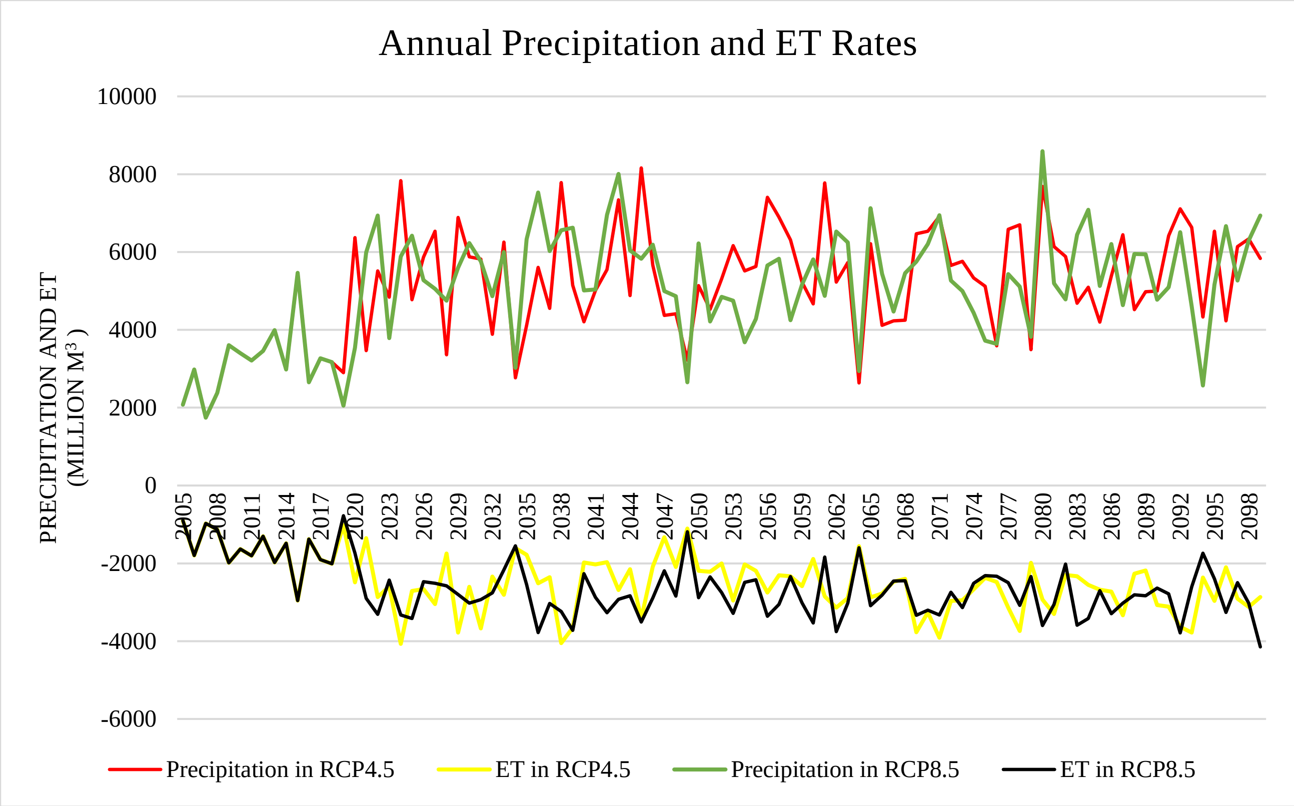

Figure 3.7. Historical and projected precipitation-evapotranspiration rates based on the results of CNRM-CM5 Model under RCP 4.5 and RCP 8.5 (million m^3 per annum).

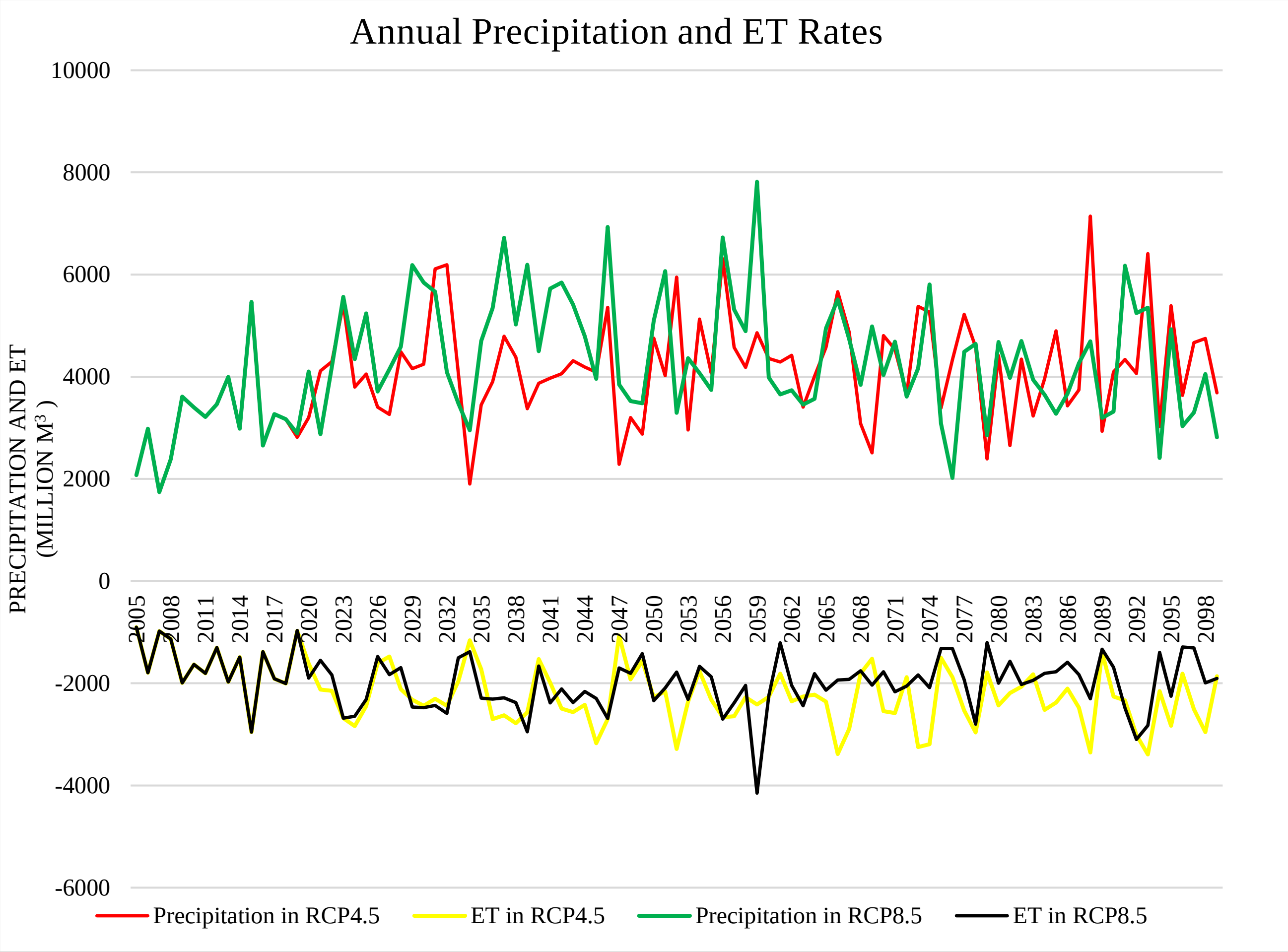

Figure 3.8. Historical and projected precipitation-evapotranspiration rates based on the results of MPI-ESM-MR Model under RCP 4.5 and RCP 8.5 (million m^3 per annum).

3.3.2. Land Use Change Projections

Land use change specified as irrigated land expansion in this study is one of the most influential parameters which affect overall reservoir storage volume in our model. Strength of the effect of land expansion is also shown in sensitivity analysis section. In WEAP modelling tool, irrigated land areas are represented by annual activity level and necessary data regarding total irrigated area in BMB is already obtained from DSI.

In land use change projection, there are two assumptions regarding land expansion. The first assumption is BAU, that is there is no change in irrigated land size. The second assumption is that irrigated land expansion is projected based on historical land expansion rate and maximum arable land size in each city. Consequently, based on reservoirs' percentage weight (determined by their current land size irrigated by each), total annual irrigated land increase is shared between reservoirs. For Aydın, maximum arable land is 36.097 ha. Historical irrigated land change data shows an average annual 5720 ha irrigated land size increase (Aydın Çevre ve Şehircilik İl Müdürlüğü, 2007, 2014, 2018). This average annual land increase is calculated taking the average land size change between 2007 and 2018. Therefore, this study assumes 5720 ha irrigated land expansion for reservoirs located within borders of Aydın (Kemer, Çine, Ikizdere, Yaylakavak, Topçam, Karacasu reservoirs). Besides, for Denizli, maximum arable land is 31.881 ha. Historical land size change shows an average annual 4706 ha irrigated land expansion (Denizli Çevre ve Şehircilik İl Müdürlüğü, 2015, 2017, 2019). This average value is calculated as in the case of Aydın city. Consequently, yearly land expansion is shared between Adıgüzel, Işıklı, Gökpınar, and Tavas reservoirs based on based on reservoirs' percentage weight. In doing so, WEAP provides its users with a predefined formula called *"growth"* so it can calculate the upcoming irrigated area sizes depending on the rate of increase being entered. Secondly, based on BAU assumption, there is no change in irrigated land size. Both land use change scenarios are implemented for CNRM-CM5 and MPI-ESM-MR models under RCP4.5 and RCP8.5 climate projections.

3.3.3. Technological Change Projections

One of the biggest problems regarding agricultural water use and/or requirements in BMB is that most of the basin is irrigated through low efficient methods, such as furrow and flooding irrigation. In the irrigation efficiency literature, irrigation methods as such are proved to have, on average, 55% efficiency rates (Irmak et al., 2011). On the other hand, efficiency rates of irrigation systems such as surface and subsurface irrigation exceed 90% in many cases.

In technological change projections, there are three possible scenarios regarding irrigation system change in BMB. The first scenario assumes full transition towards high-efficiency systems taking place all irrigated lands located in BMB. The second scenario assumes full transition to high-efficiency systems and during this transition, average irrigation efficiency rate increases from 55% to 90%. The reason why these BAU efficiency rate is chosen as 55% is that furrow irrigation is the most prevailing irrigation system in BMB. In Figure 2.8 displayed in section 2.3, average efficiency rate for furrow irrigation is 55%. Secondly, in this study, the assumption regarding efficiency improvement scenario is that transition to surface drip irrigation takes place. In Figure 2.8, average efficiency rate for surface drip irrigation is 90%. Lastly, the third scenario is based on BAU conditions with no change in irrigation efficiency.

Finally, our model has 16 different scenarios. Four of these scenarios include solely irrigated land expansion assumption while four of the scenarios include only technological changes. Six scenarios contain both irrigated land expansion and technological change presumptions while the last four scenarios contain assumption of no land expansion and no technological change. That is, the last four scenarios are based on BAU scenario.

*2 (Land use change projection) * 2 (Climate Change Scenario) * 2(GCMs) = 8*

*2 (Technological Change Scenario) * 2 (Climate Change Scenario) * 2(GCMs)= 8*

4. RESULTS

4.1. Calibration and Validation Results

Model results for the calibration and validation period have satisfactory values of NSE, R2, RSR, and PBIAS (Table 4.1, Table 4.2). The results are accepted as satisfactorily if NSE ≥ 0.5, R2 ≥ 0.5, RSR ≤ 0.7 and PBIAS ± 0.25 % for streamflow (Moriasi et al., 2007). While the optimum value is 0.0 for PBIAS, positive values imply underestimation bias and negative values imply overestimation bias (Moriasi et al., 2007). The graphs of comparison between simulated reservoir volume and observed reservoir volume for the simulation period is also helpful to analyze the results and calibrate the model for the better fitness (Figure 4.1, Figure 4.2). As these graphs and the model evaluation parameters indicate, the model behaves satisfactorily and is ready to be used in future scenario simulations.

Table 4.1. Assessment parameters of model Results (R^2, NSE, PBIAS) for calibration period (2005-2011).

	Adıgüzel	Gökpınar	Işıklı	Kemer	Topçam	Yaylakavak
R^2	0,85	0,78	0,68	0,69	0,77	0,85
NSE	0,791	0,614	0.536	0.549	0.601	0.783
PBIAS	-13,41%	-10,15%	-11,30%	-17,30%	-22,30%	-17%

Table 4.2. Assessment parameters of model results (R^2, NSE, PBIAS) for calibration period (2013-2015).

	Çine	İkizdere	Tavas	Karacasu
R^2	0,90	0,84	0,80	0,71
NSE	0.845	0,519	0.774	0.586
PBIAS	-4,86%	-10,50%	1,57%	-6,31%

Table 4.3. Assessment parameters of model results (R^2, NSE, PBIAS) for calibration period (2009-2013).

	Bayır
R^2	0,72
NSE	0.597
PBIAS	0,80%

Table 4.4. Assessment parameters of model results (R^2, NSE, PBIAS) for calibration period (2011-2014).

	Cindere
R^2	0,68
NSE	0.557
PBIAS	0,06%

Table 4.5. Assessment parameters of model results (R^2, NSE, PBIAS) for validation period (2012-2018).

	Adıgüzel	Gökpınar	Işıklı	Kemer	Topçam	Yaylakavak
R^2	0,77	0,72	0,72	0,73	0,85	0,78
NSE	0,670	0.625	0.656	0.616	0.834	0.775
PBIAS	-6,80%	-10,35%	-4%	-12,20%	3,90%	-0,60%

Table 4.6. Assessment parameters of model results (R^2, NSE, PBIAS) for validation period (2016-2018)

	Çine	İkizdere	Tavas	Karacasu
R^2	0,86	0,95	0,44	0,75
NSE	0.618	0.805	-0.215	0.604
PBIAS	-11%	1,23%	4,86%	-0,81%

Table 4.7. Assessment parameters of model results (R^2, NSE, PBIAS) for validation period (2014-2018).

	Bayır
R^2	0,77
NSE	0.588
PBIAS	2,80%

Table 4.8. Assessment parameters of model results (R^2, NSE, PBIAS) for validation period (2015-2018).

	Cindere
R^2	0,31
NSE	-0.203
PBIAS	0,04%

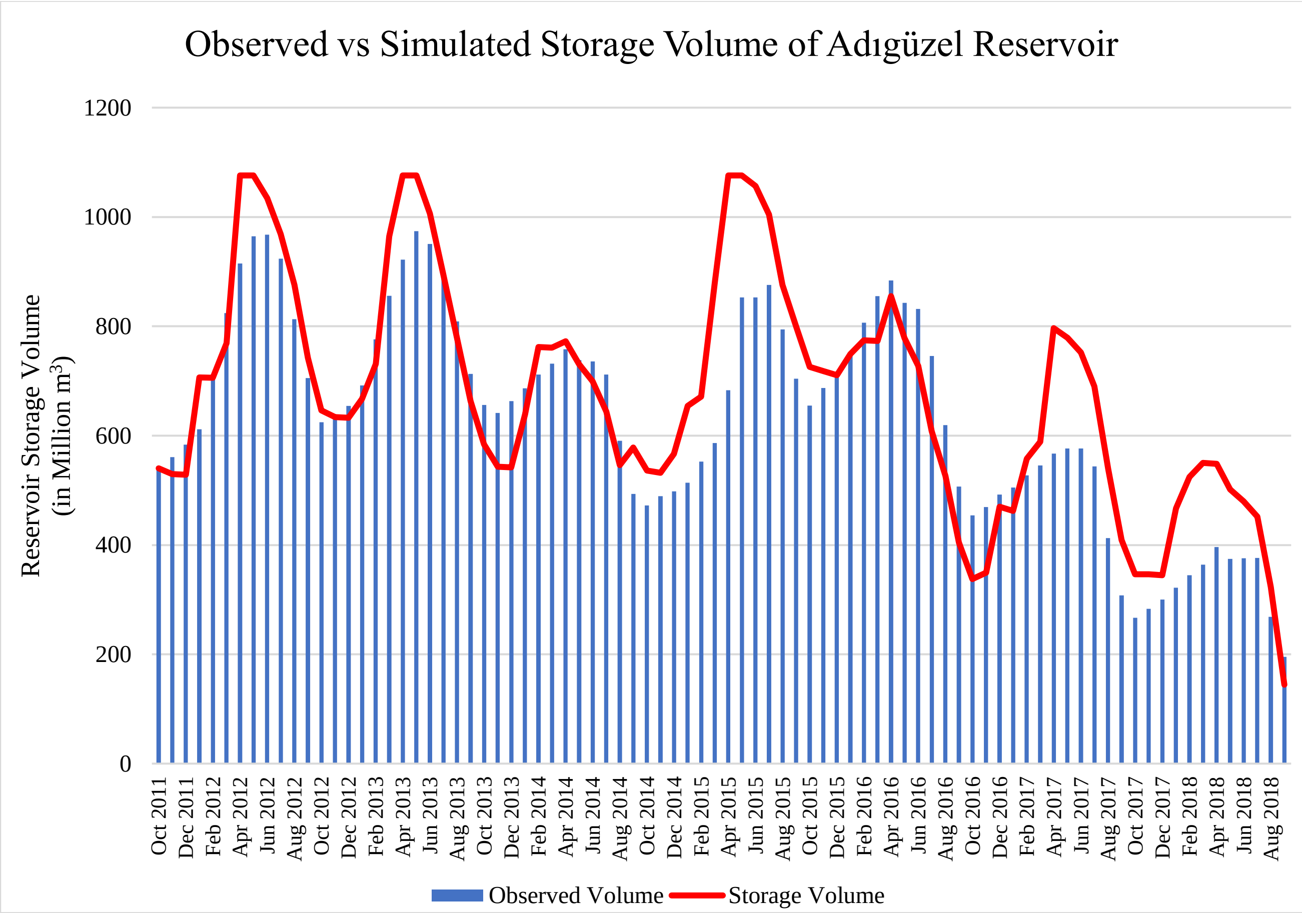

Figure 4.1. Comparison of observed and simulated storage for Adıgüzel Reservoir (Validation Period 2012-2018).

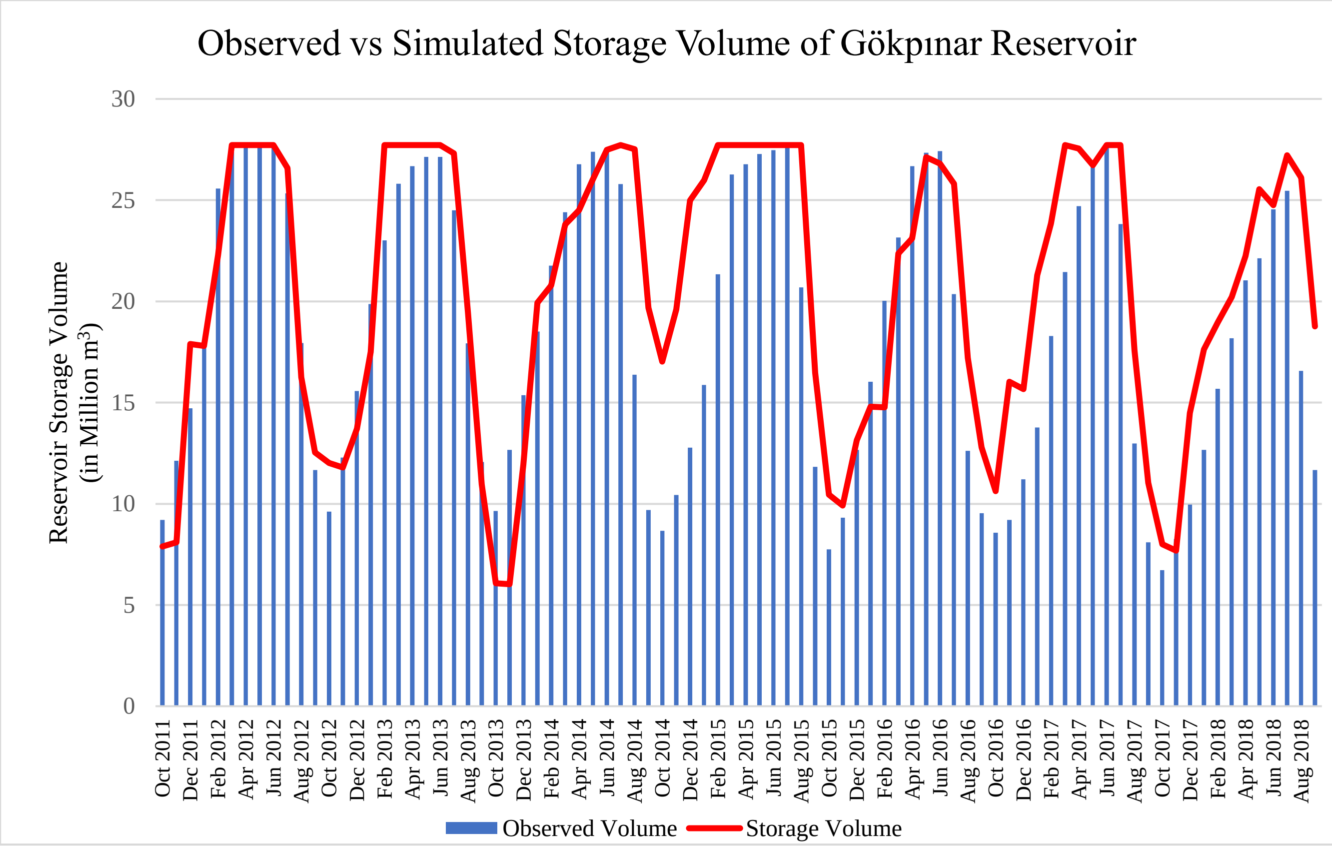

Figure 4.2. Comparison of observed and simulated storage for Gökpınar Reservoir (Validation Period 2012-2018).

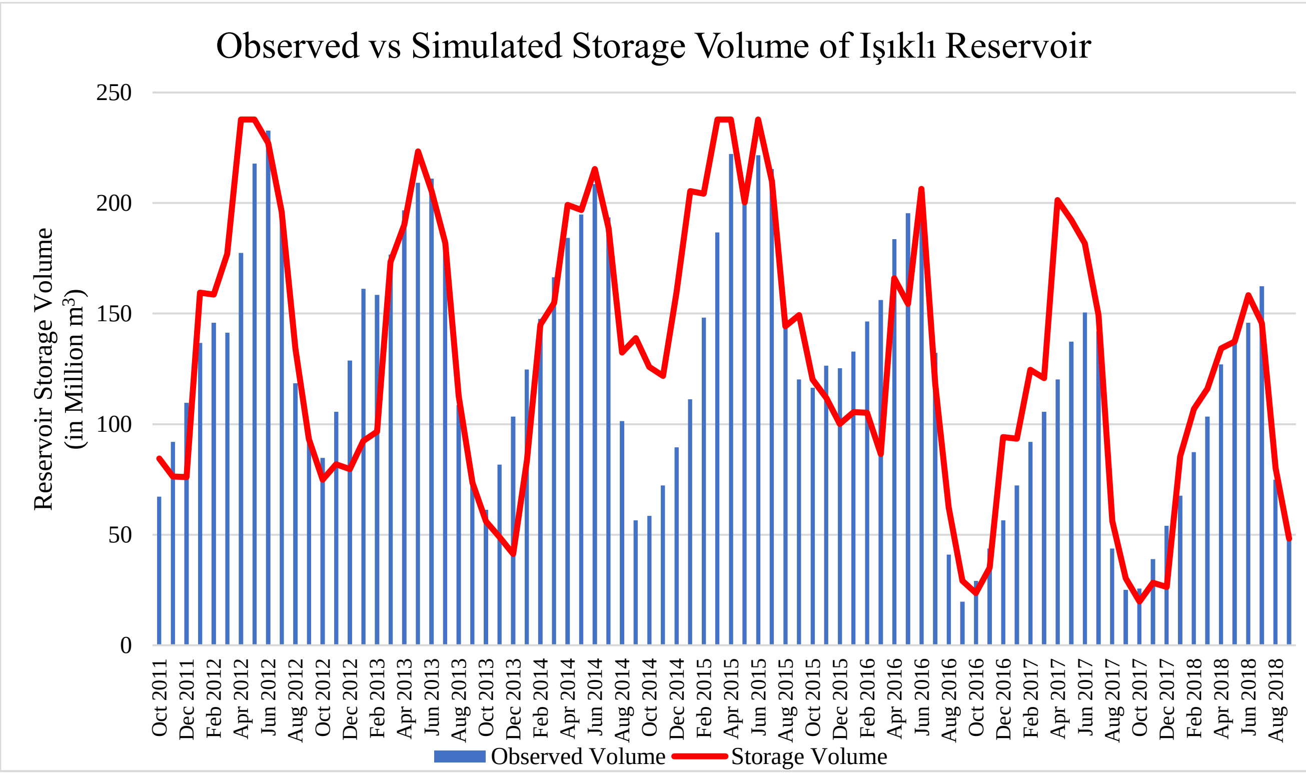

Figure 4.3. Comparison of observed and simulated storage for Işıklı Reservoir (Validation Period 2012-2018).

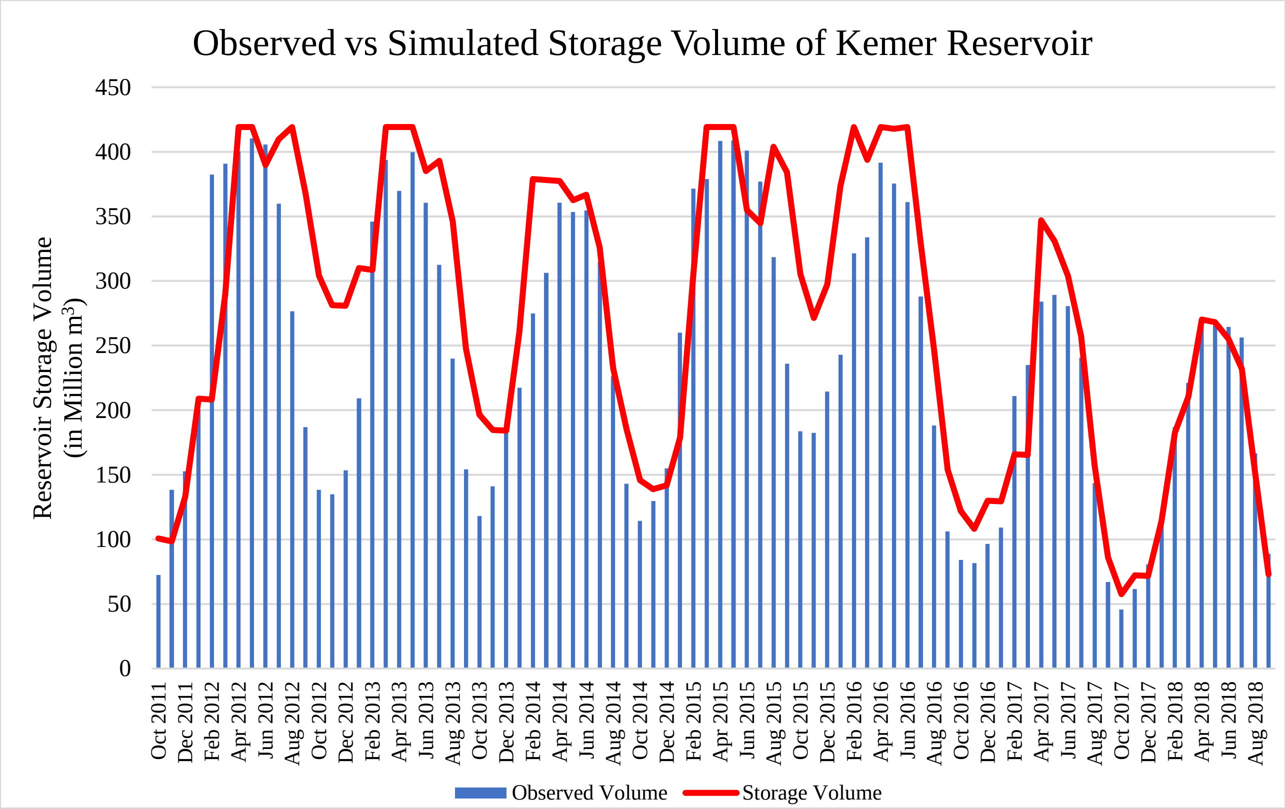

Figure 4.4. Comparison of observed and simulated storage for Kemer Reservoir (Validation Period 2012-2018).

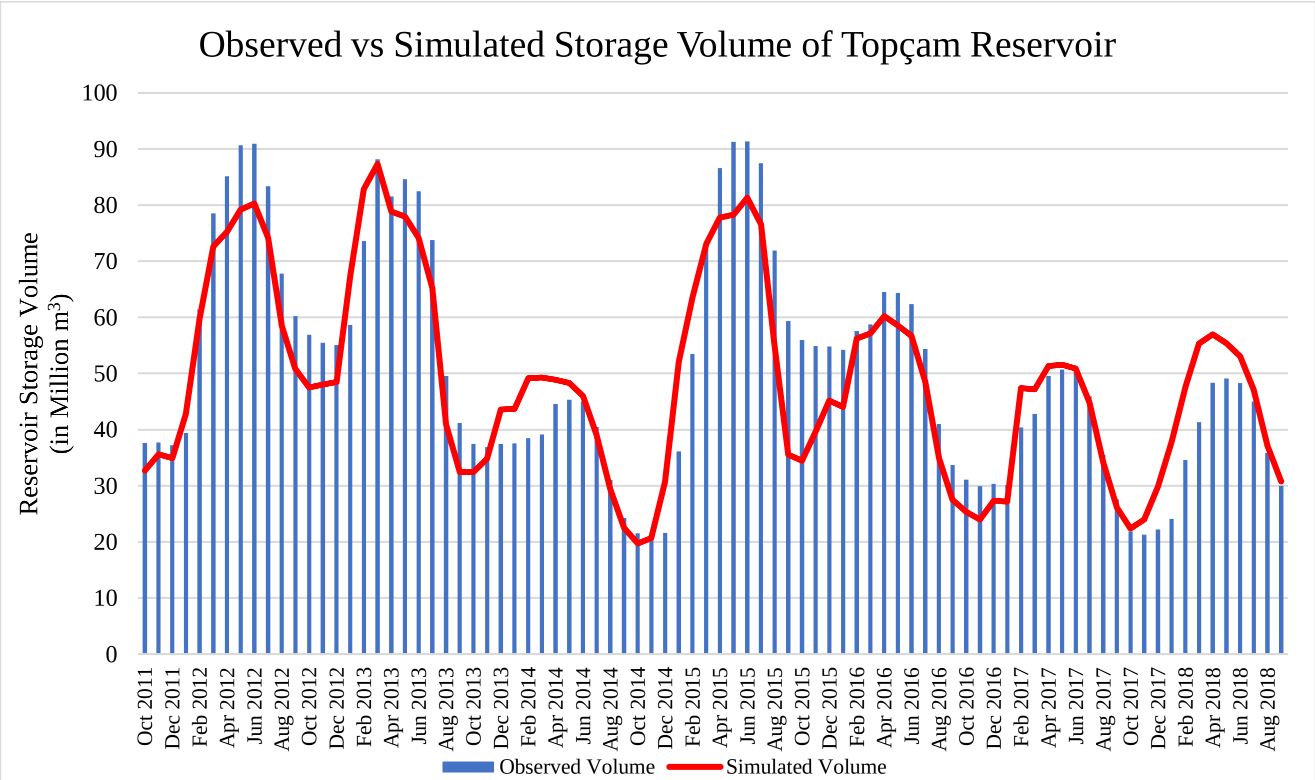

Figure 4.5. Comparison of observed and simulated storage for Topçam Reservoir (Validation Period 2012-2018).

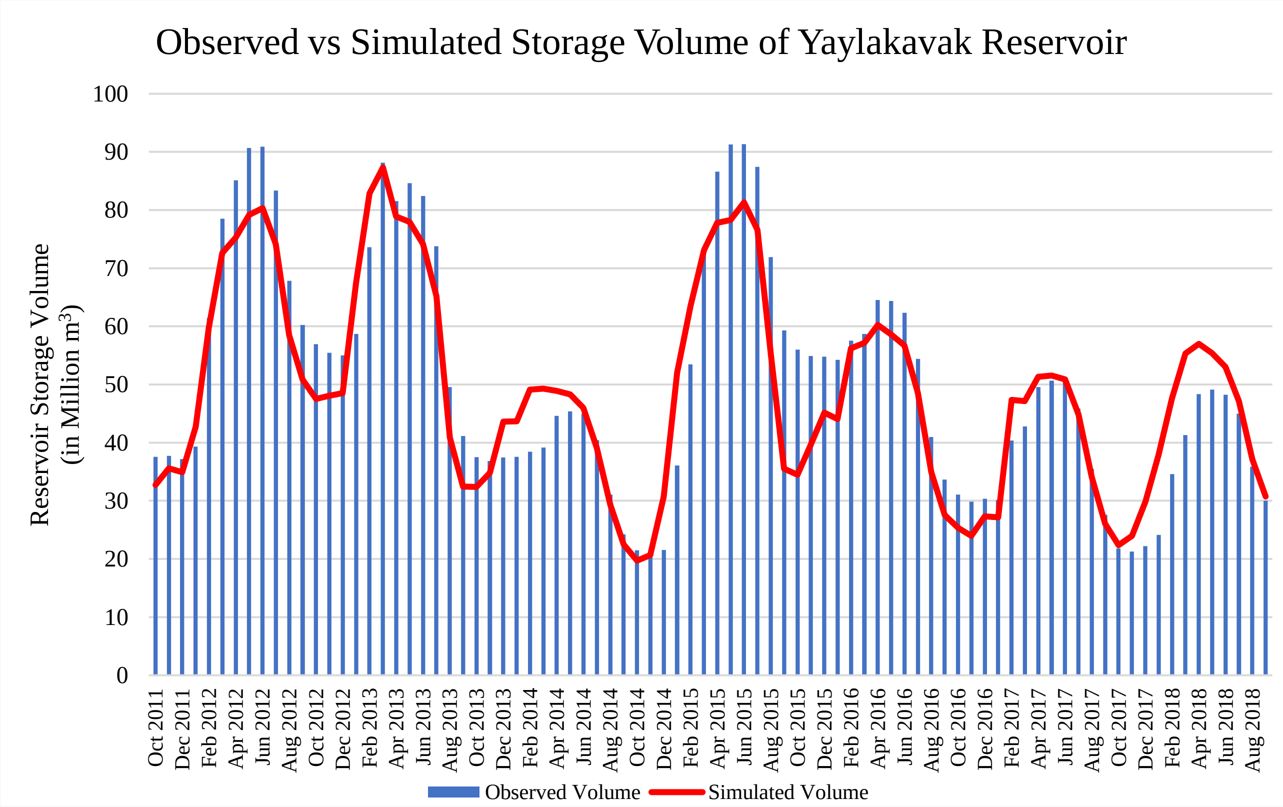

Figure 4.6. Comparison of observed and simulated storage for Yaylakavak Reservoir (Validation Period 2012-2018).

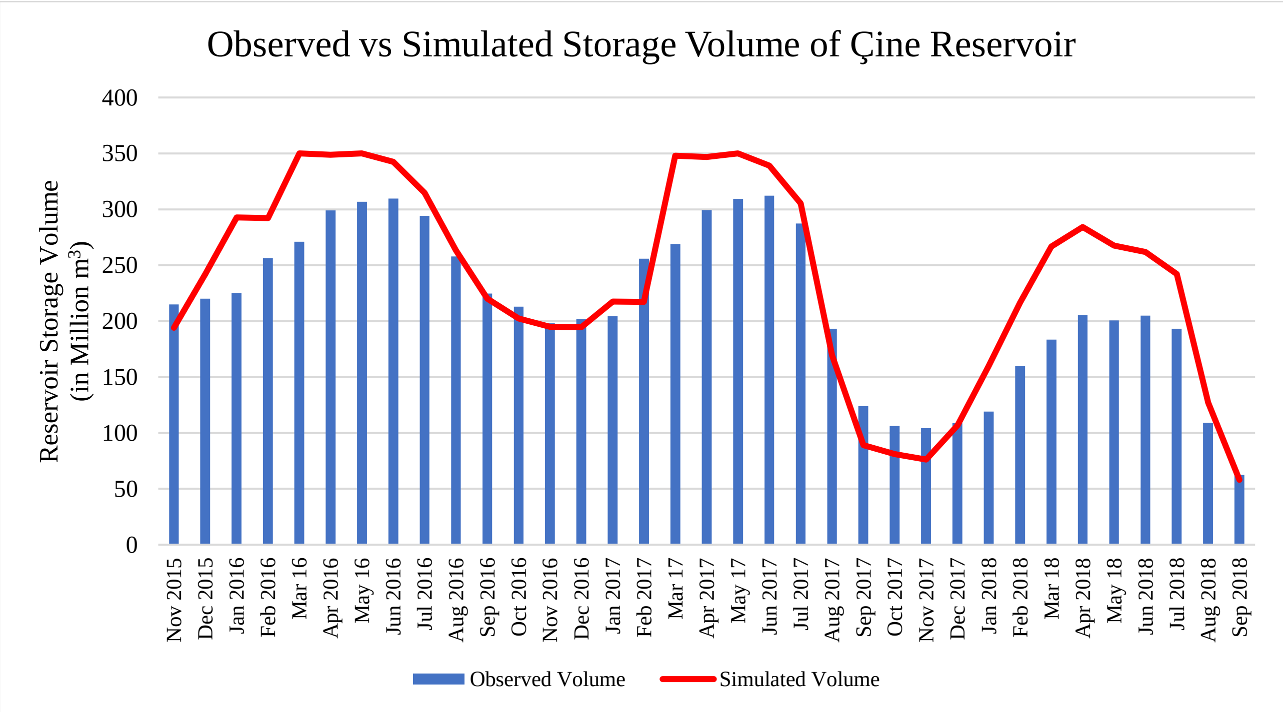

Figure 4.7. Comparison of observed and simulated storage for Çine Reservoir (Validation Period 2016-2018).

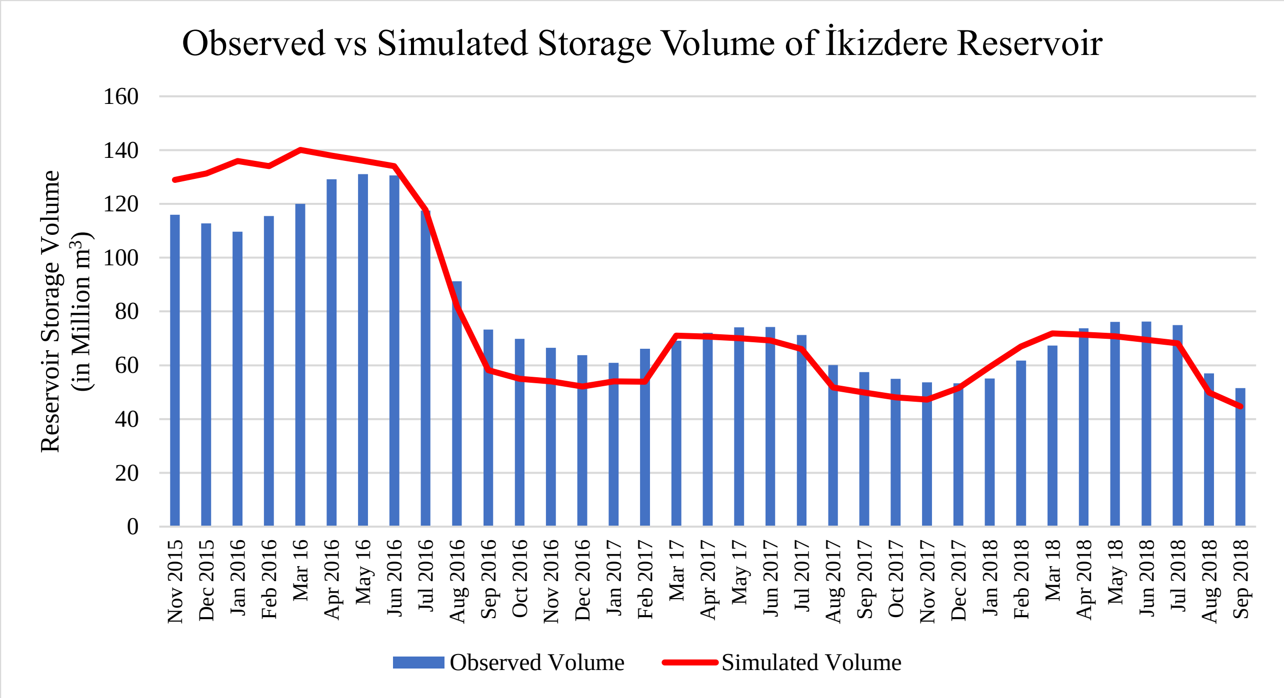

Figure 4.8. Comparison of observed and simulated storage for İkizdere Reservoir (Validation Period 2016-2018).

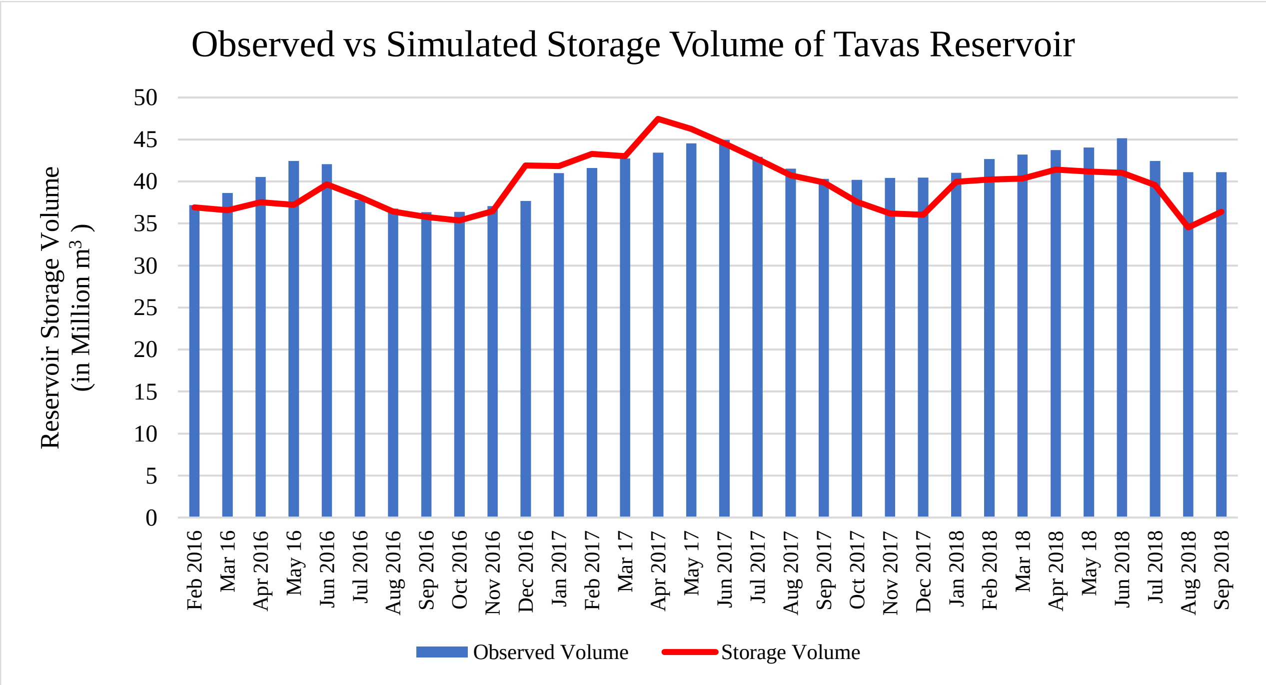

Figure 4.9. Comparison of observed and simulated storage for Tavas Reservoir (Validation Period 2016-2018).

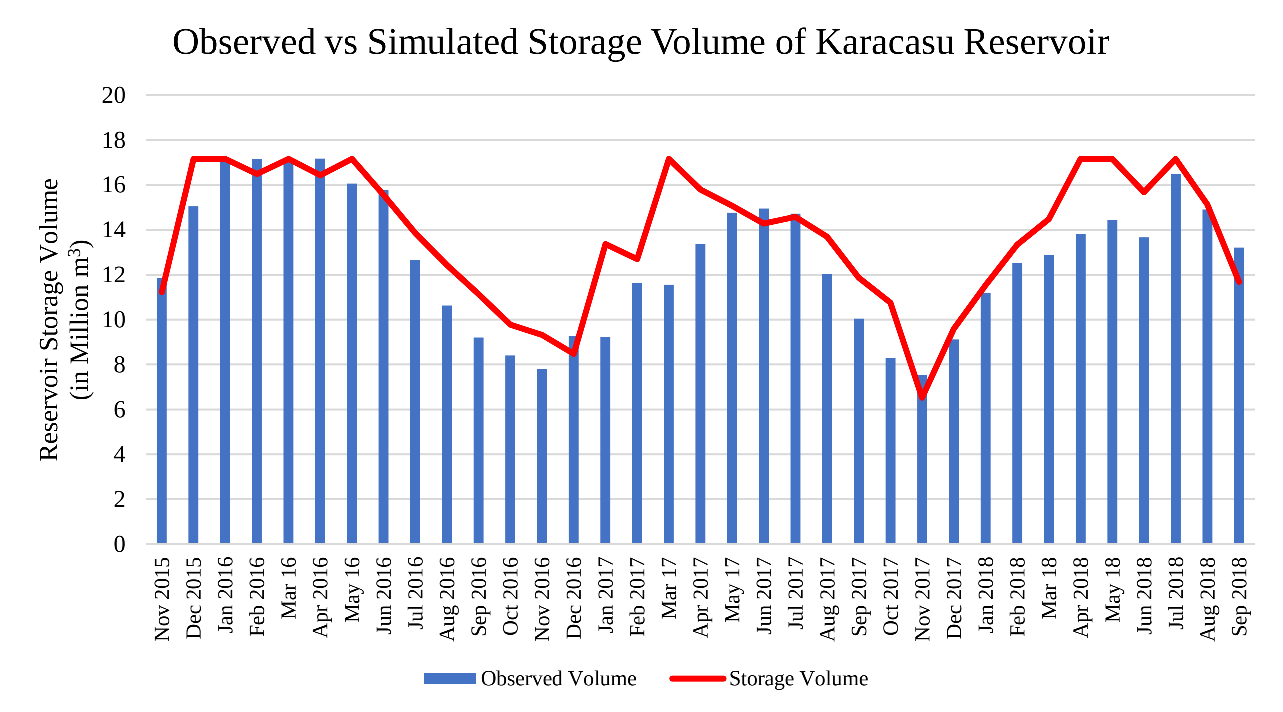

Figure 4.10. Comparison of observed and simulated storage for Karacasu Reservoir (Validation Period 2016-2018).

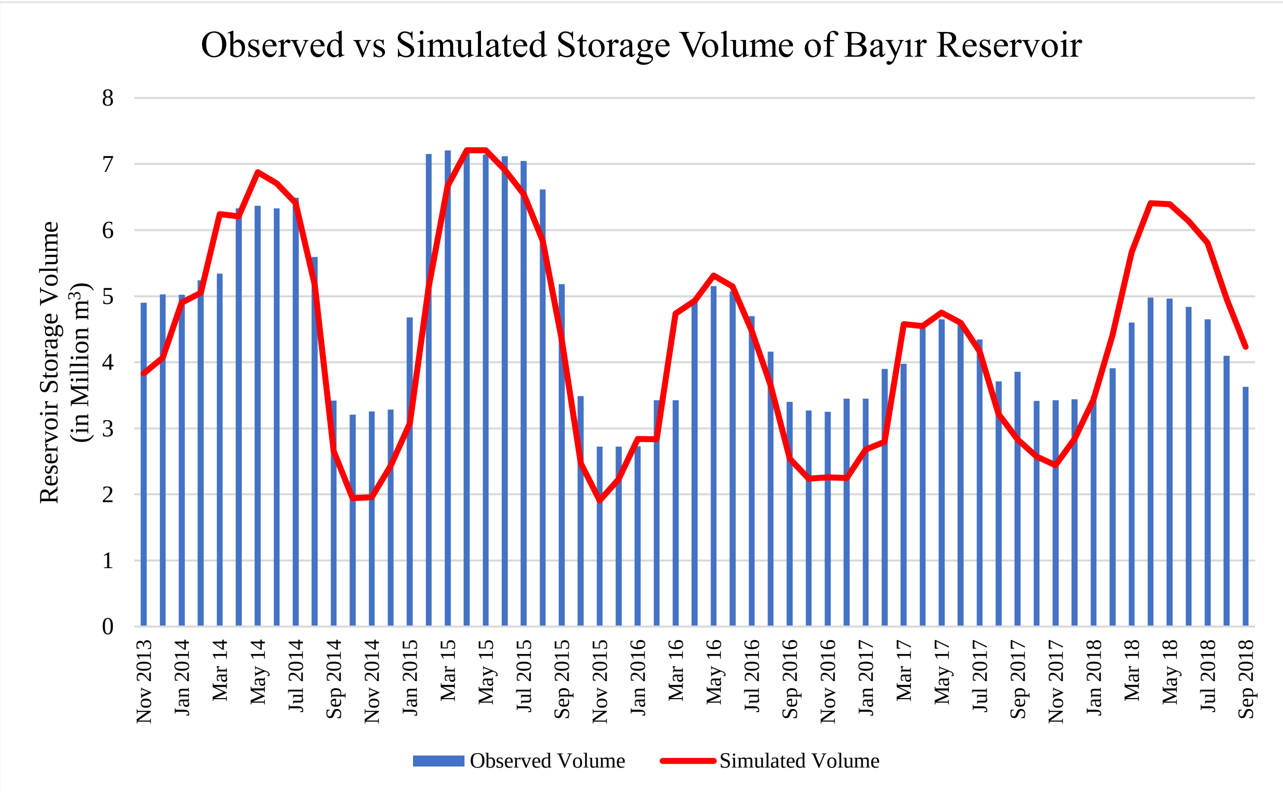

Figure 4.11. Comparison of observed and simulated storage for Bayır Reservoir (Validation Period 2016-2018).

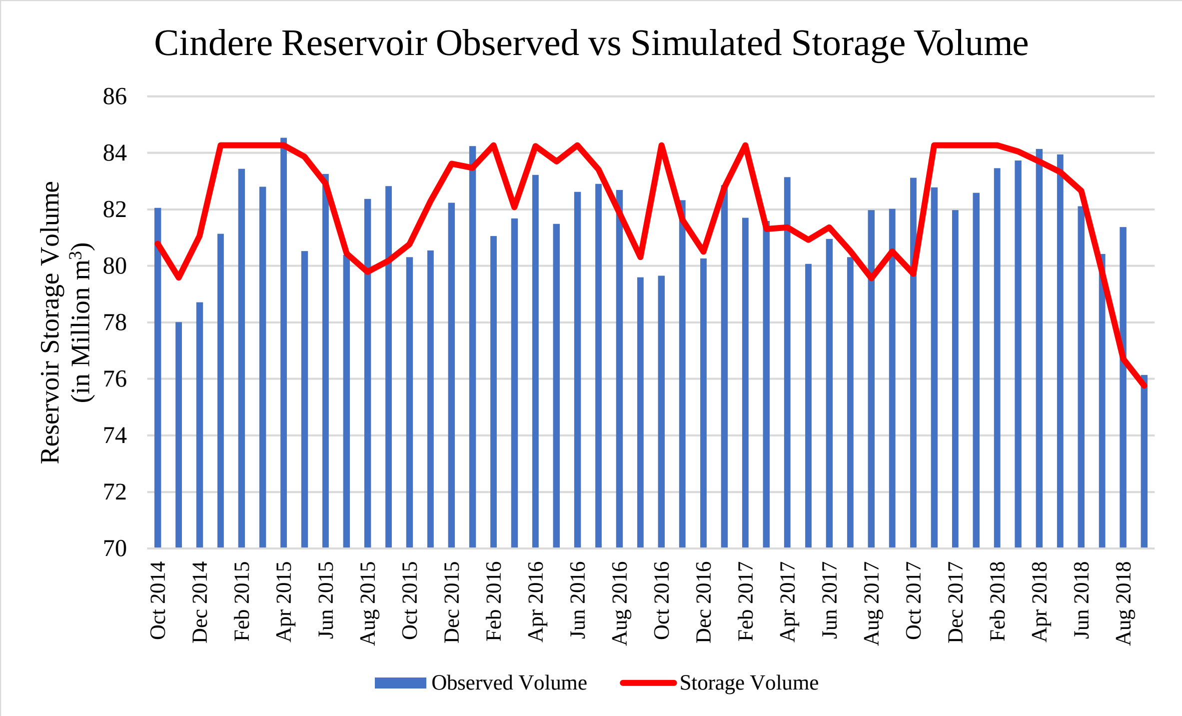

Figure 4.12. Comparison of observed and simulated storage for Cindere Reservoir (Validation Period 2015-2018).

4.1.1. Sensitivity Analysis

In this study, sensitivity analysis is utilized for the purpose of improving model's strength so it can work more efficiently. While researchers can choose numerous parameters to use in sensitivity analysis process depending on their goals, in this study chooses Pe, Kc, and loss from system to be its sensitivity parameters during calibration process. Besides, sensitivity of the model to ET, precipitation, and irrigated land expansion are studied as well so that it can be found out whether they can be potential parameters to be influential enough to use during scenario analysis process.

Table 4.9 shows that the sensitivity degree of the model is very high to precipitation, evapotranspiration, and irrigated land size change. Furthermore, the sensitivity degree is high, medium, and low for the parameters of loss from system, Pe, and Kc, respectively. However, these sensitivity results depict a general situation regarding the sensitivity rates of the model to each parameter. On the other side, Figure 4.16 and Figure 4.17 demonstrate that sensitivity rates of the model vary. In Figure 4.16, for Kc values between 0.5 and 1, the sensitivity of the model to Kc is low, yet the sensitivity rate significantly increases between 1 and 1.5. Similarly, for Pe, the sensitivity rate of the model to Pe is medium for the values between 0% and 30%. Afterwards, the sensitivity of the model to Pe rises between the values of 30% and 50% of Pe.

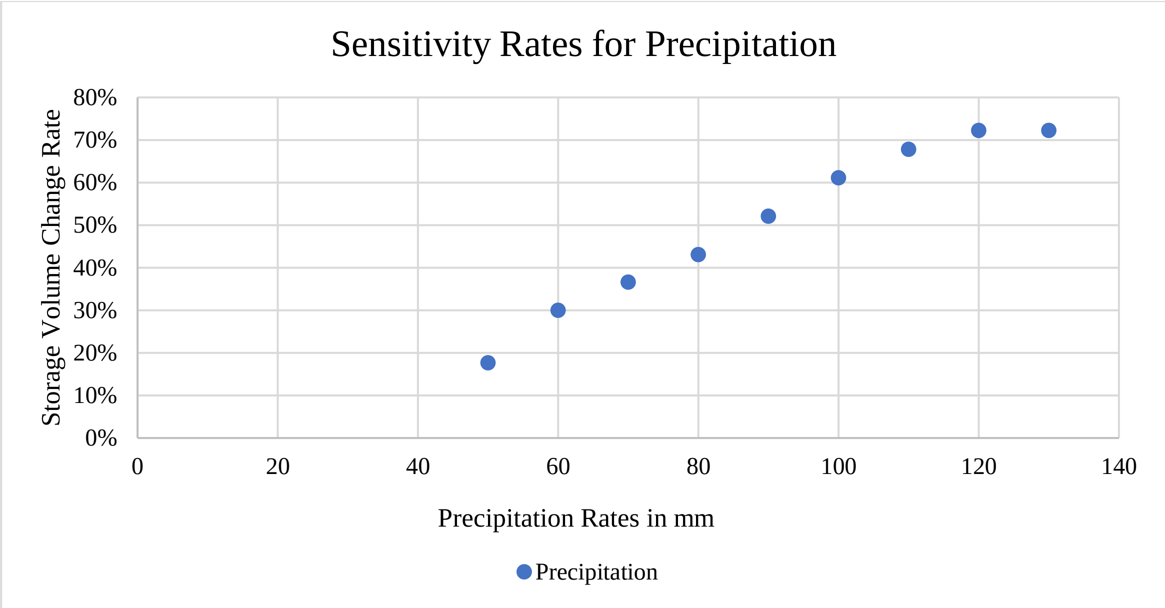

Figure 4.13. Rate of change of storage volume with changes in precipitation.

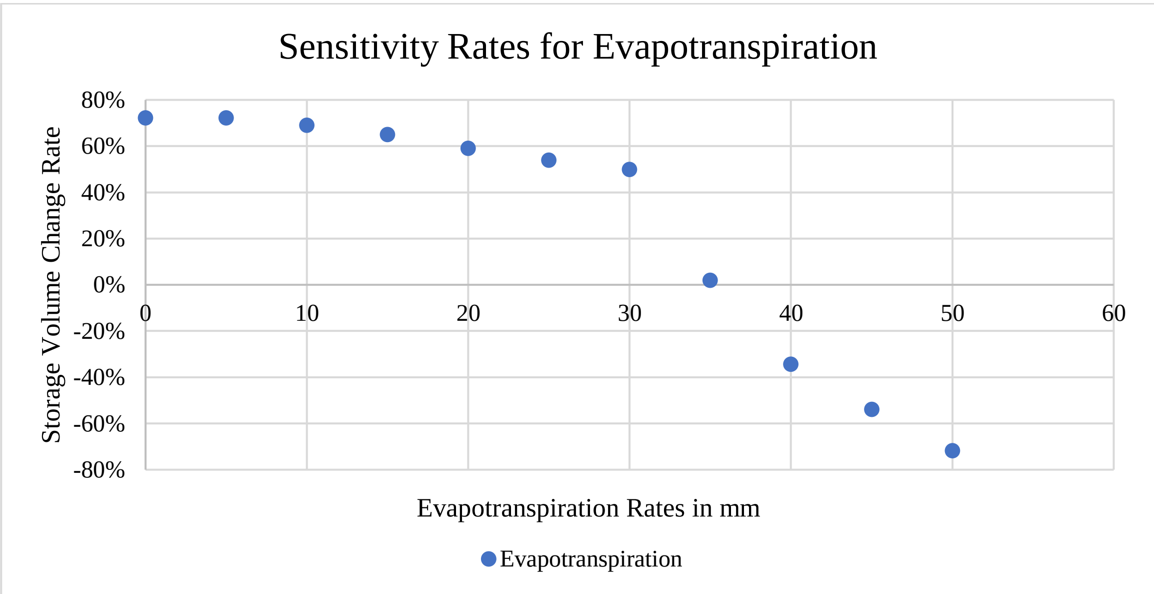

Figure 4.14. Rate of change of storage volume with changes in evapotranspiration.

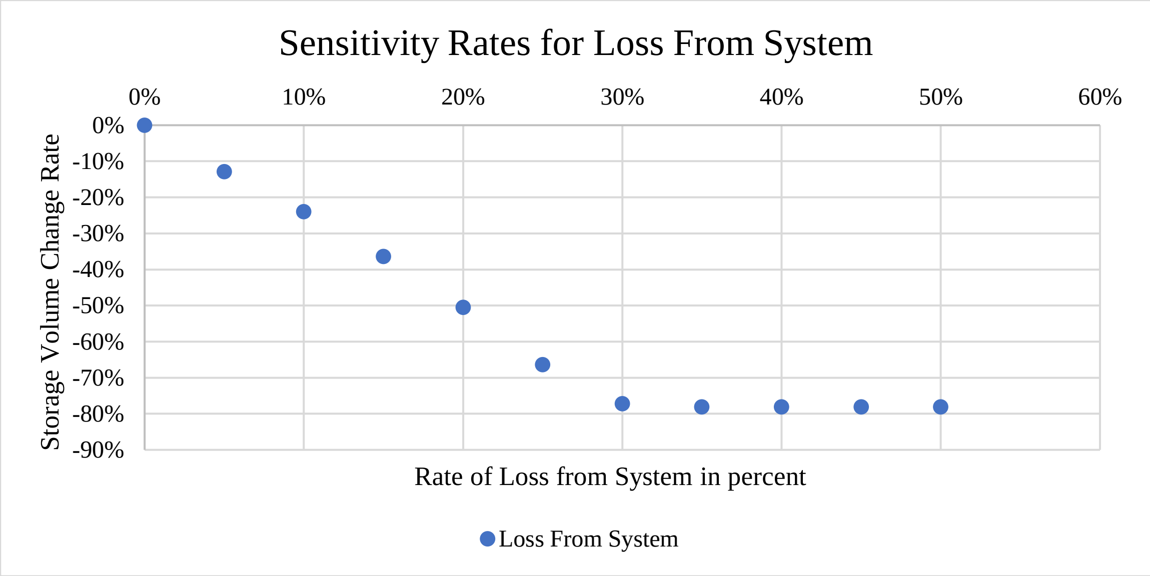

Figure 4.15. Rate of change of storage volume with changes in rates of loss from system.

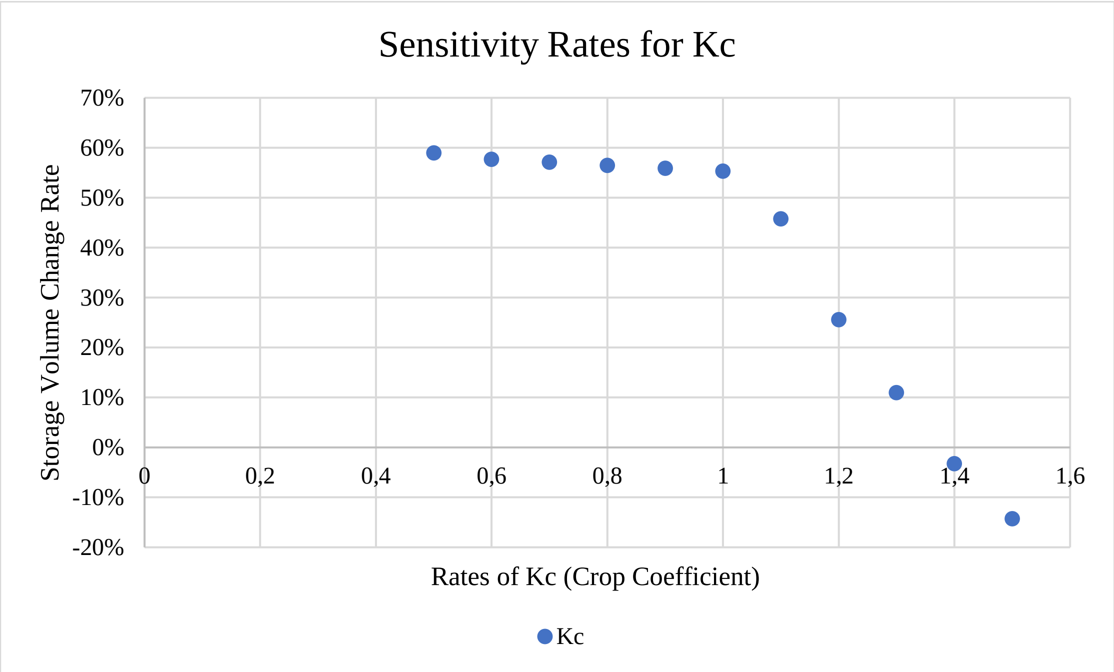

Figure 4.16. Rate of change of storage volume with changes in rates of Kc.

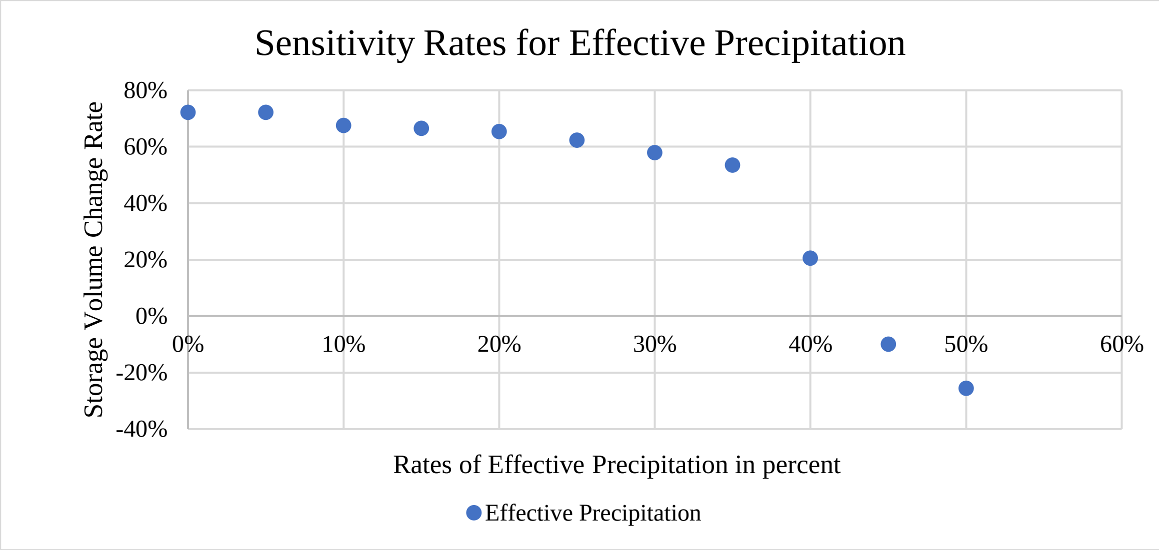

Figure 4.17. Rate of change of storage volume with changes in rates of effective precipitation.

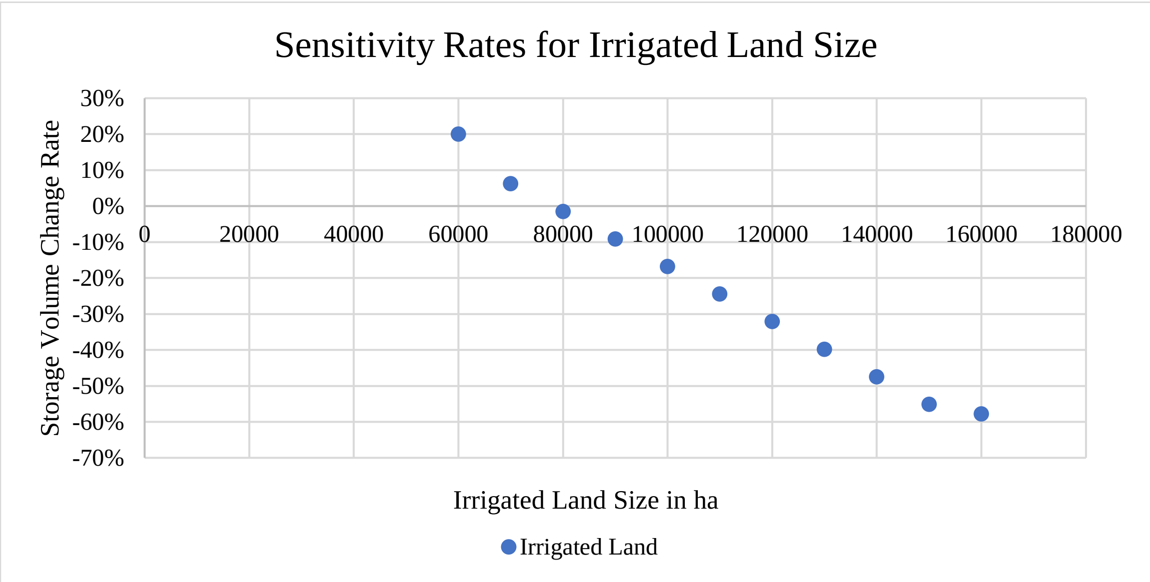

Figure 4.18. Rate of change of storage volume with changes in rates of irrigated land.

Table 4.9. Classification of sensitivity parameters.

Parameter	***Sensitivity Class***
Precipitation	Very High
Evapotranspiration	Very High
Irrigated Land	Very High
Loss from System	High
Effective Precipitation	Medium
Kc	Low

4.2. Total Water Demand Under Different Scenarios

Water demand is examined for four main scenarios. Model results indicate that water demand is sensitive to changes in both technology and land use changes (Figure 4.13). The results also show monthly water demand distribution and the impacts of three scenarios on this distribution, Business as Usual (BAU) as the status quo scenario, High Efficiency-No Land Use Change (HE-NLUC) as the best case scenario creating lowest water demand rates, Low Efficiency-Increased Irrigated Land Size (LE-IILS) as the worst case scenarios creating highest water demand, and High Efficiency-Increased Irrigated Land Size (HE-IILS) scenario (Table 3.5).

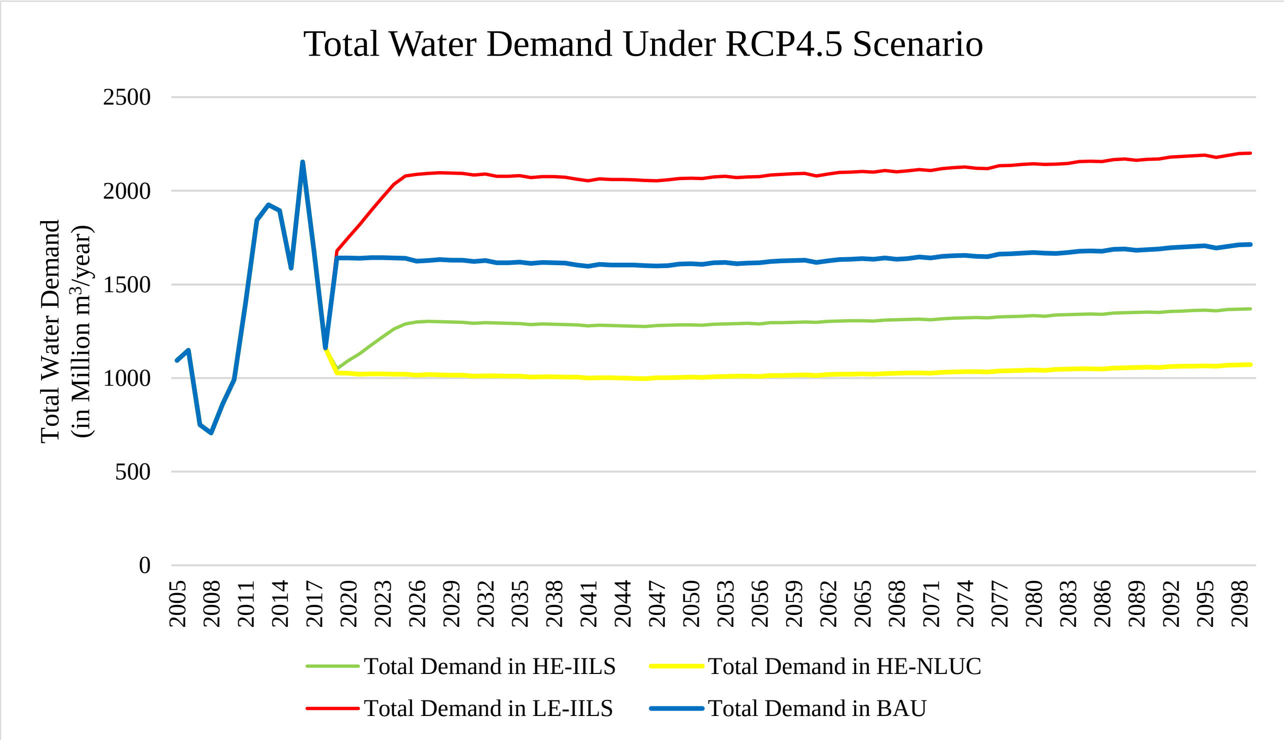

Figure 4.19. Total water demand under different scenarios for the climate scenario RCP4.5.

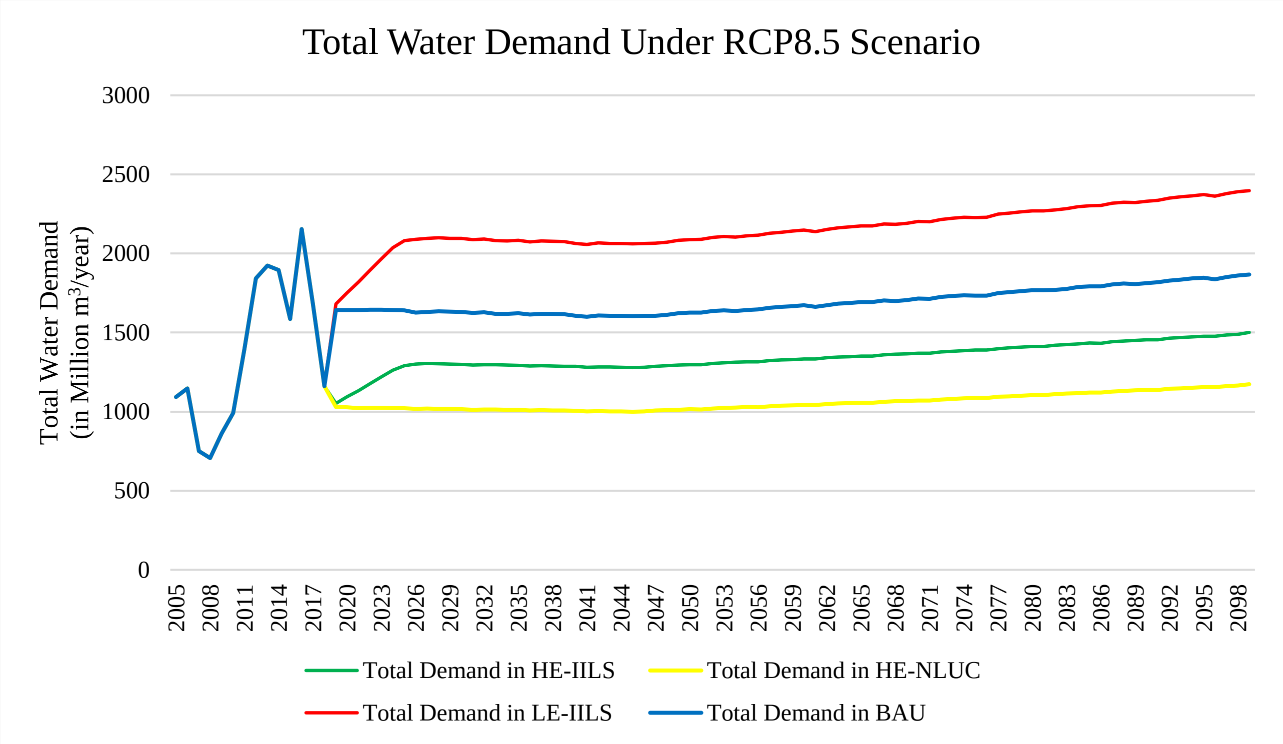

Figure 4.20. Total water demand under different scenarios and RCP8.5 scenario.

The distribution of water demand under different scenarios differs in regard to months. The highest water demand rates occur in June, July, August, and September. This is because this study assigns solely agricultural areas as water demand nodes and most of the agricultural activities are carried out during summer season in BMB. As illustrated in Figure 4.16 and 4.17, monthly demand rates are slightly higher in RCP8.5 compared to RCP4.5.

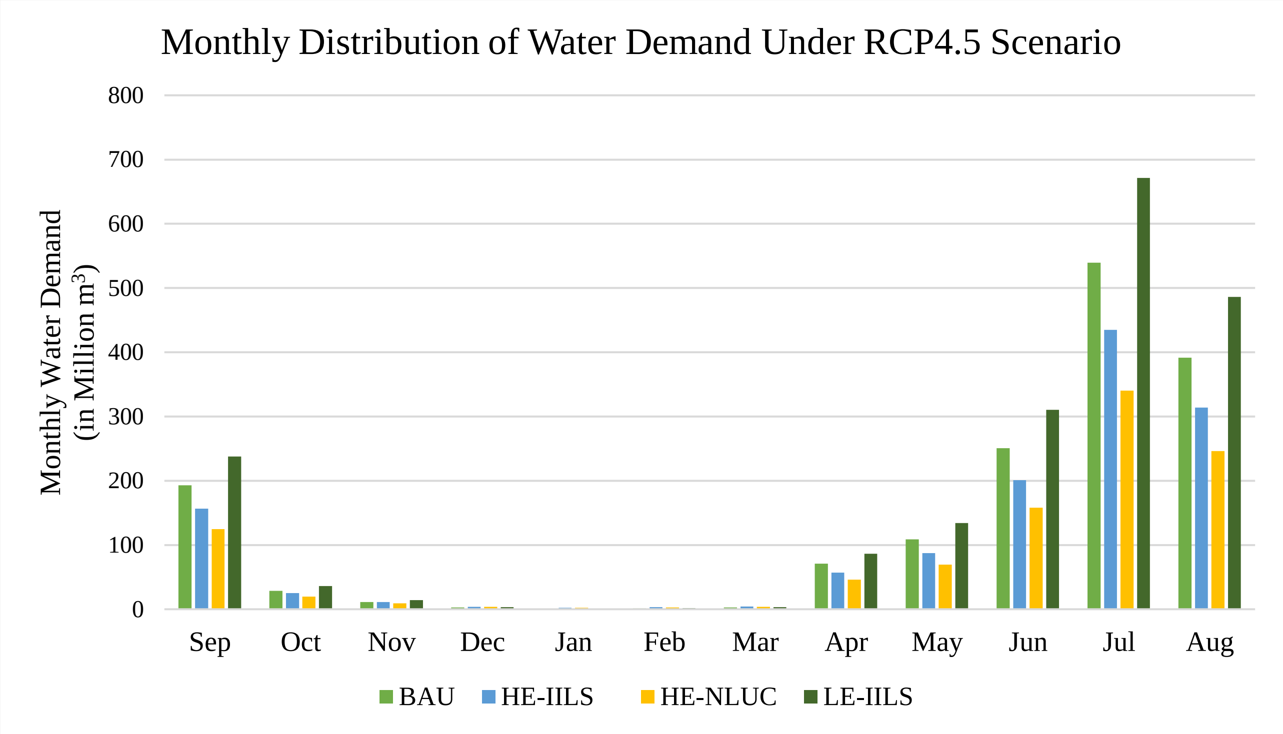

Figure 4.21. Monthly water demand distribution under different scenarios and RCP4.5 scenario.

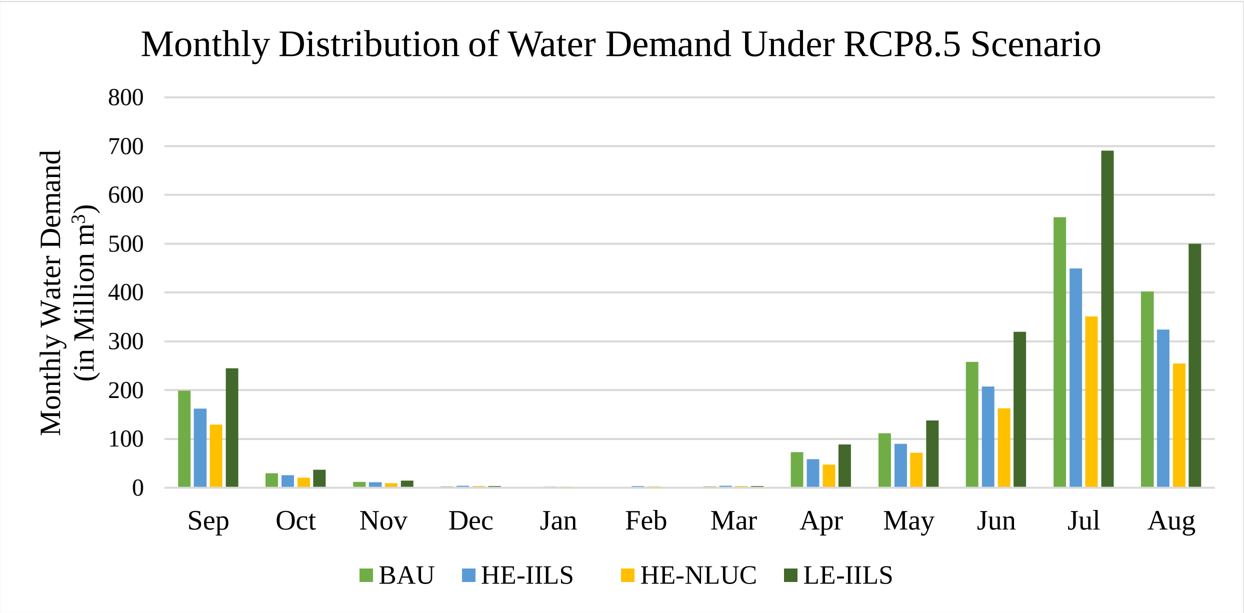

Figure 4.17. Monthly water demand distribution under different scenarios and RCP8.5 conditions.

In the best-case scenario HE-NLUC which results in lowest IWR among all four scenarios, and under RCP4.5 conditions, annual average water demand rate is 1026 million m^3 and for the worst-case scenario LE-IILS which results in highest IWR annual average rate is 2094 million m^3 for entire simulation period. On the other hand, under the same climate change scenario, HE-IILS scenario shows an annual water demand rate of 1302 million m^3 and BAU scenario shows 1642 million m^3

per year. Figure 4.19 displays annual variations of all annual water demand rates under RCP4.5 conditions.

Under RCP8.5 and best-case scenario, annual average water demand rate is 1060 million m^3 for simulation period 2019-2099. For the same time period, LE-IILS scenario shows an annual average water demand of 2165 million m^3. On the other side, for HE-IILS scenario, annual average water demand is 1347 million m^3 and for BAU scenario it is 1697 million m^3. Figure 4.20 displays annual variations of all annual water demand rates under RCP4.5 conditions.

Comparing the results of annual average water demand rates for each scenario, it is seen that the impact of efficiency change on annual water demand is slightly higher than that of land use change. Efficiency change causes a decline of 35% in average water demand rate compared to baseline scenario while land use change or irrigated land expansion results in 27% increase in average water demand rate.

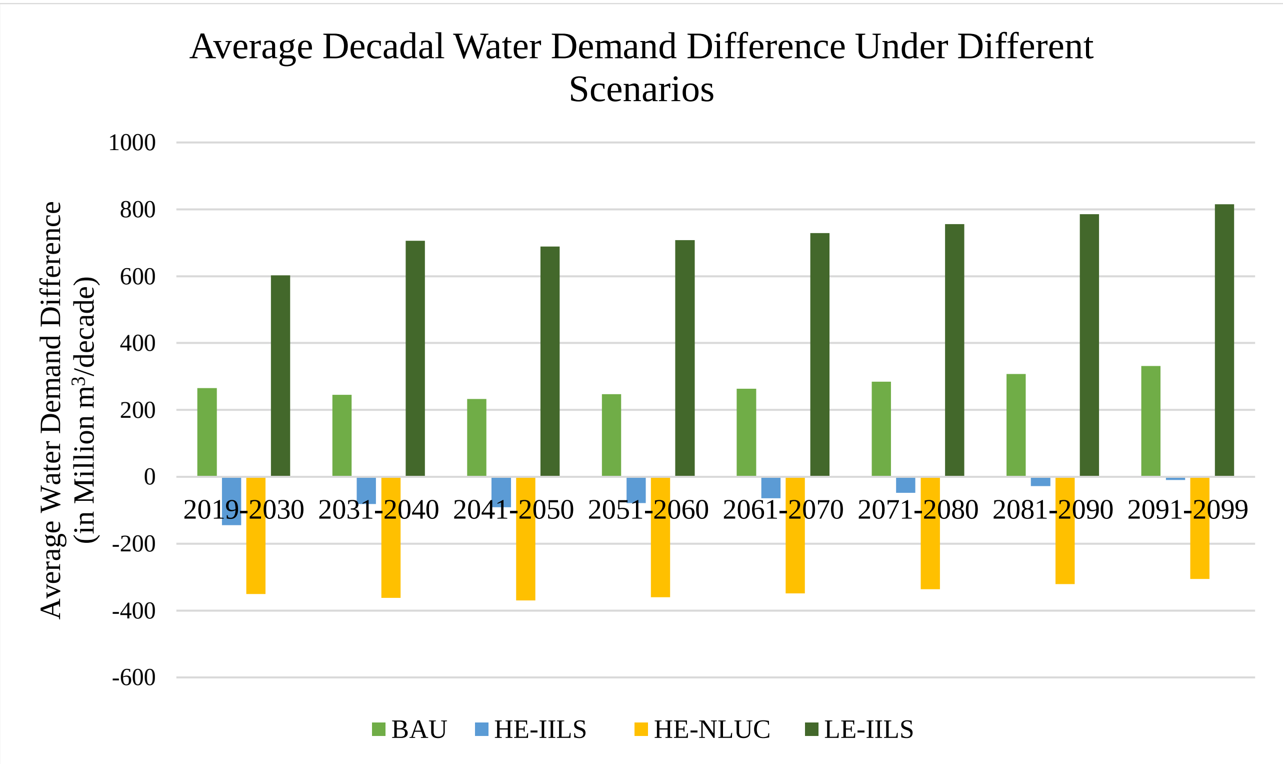

Figure 4.22. Average decadal water demand difference with respect to average demand rate of baseline scenario under RCP4.5 climate change scenario.

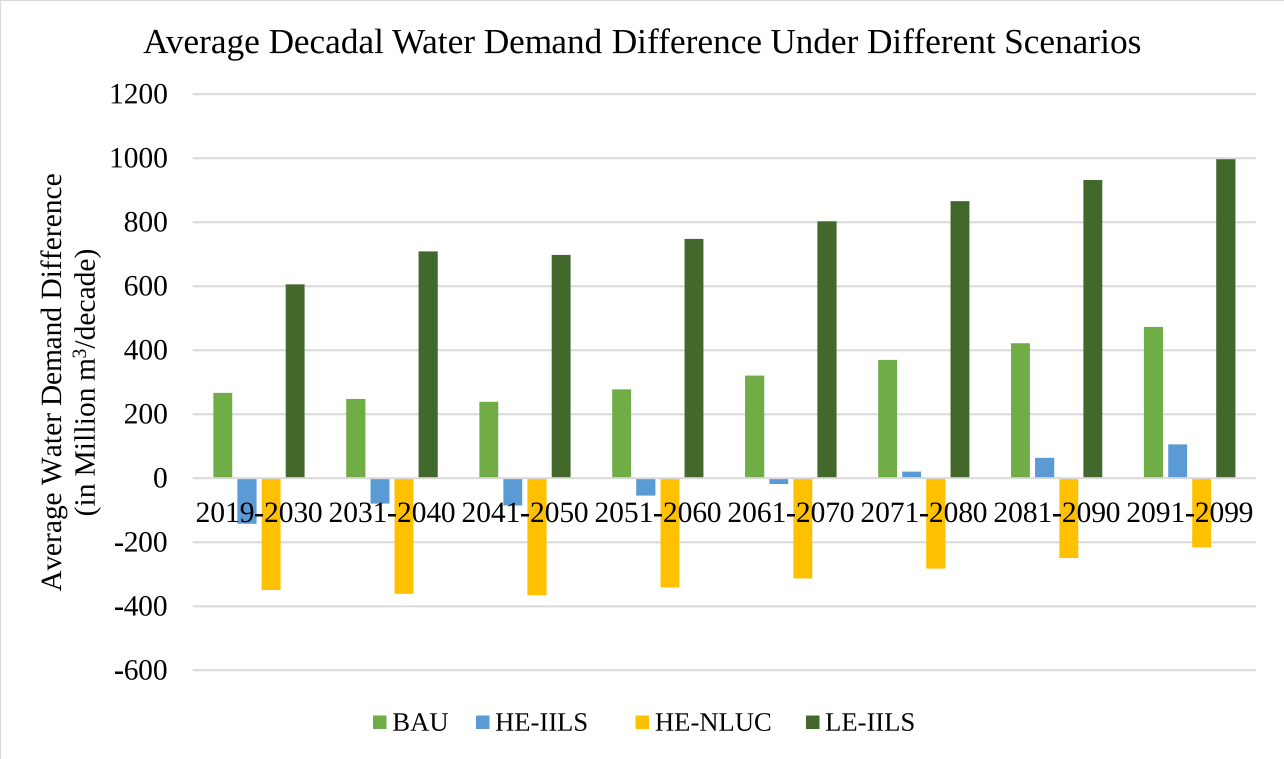

Figure 4.23. Average decadal water demand difference with respect to average demand rate of baseline scenario under RCP8.5 climate change scenario.

4.3. Total Unmet Water Demand Under Different Scenarios

In order to grasp how water budget of BMB is affected by changes in climatic conditions, technological improvements and land use change, the listed plausible scenarios in Section 3.3 are simulated. In this section, I analyse the variations in the gap between water demand and supply. This gap is called as unmet water demand. Firstly, there is no unmet water demand observed between 2005-2018 period. Therefore, all the cases in which unmet water demand occurs presented in this section belong to the simulation period taking place between 2019 and 2099. The results represent average decadal, annual, and monthly average unmet water demand rates observed during this timeline.

The widening gap between water supply and water demand is a serious threat in BMB given the decadal and annual variations represented in Figure 4.24 to Figure 4.31. According to results of model simulations for BAU and RCP4.5 scenarios, as seen in Figure 4.28, CNRM-CM5.1 model shows an average 345 million m^3 unmet water demand rate for entire simulation period. On the other hand, under the same conditions, annual total water demand in BMB is approximately 1640 million m^3 as shown in Figure 4.19. These two results demonstrate that 20% of total annual water demand is not met. Given the size of agricultural output grown annually in the watershed, this result has obviously detrimental effects on livelihoods of local farmers. Besides, as a consequence of relatively lower surface runoff rates in BMB between 2019 and 2070, the percentage of overall water demand being unmet rises up to 23%. According to results of CNRM-CM5.1 under BAU and RCP8.5 conditions, as in the Figure 4.28, the average unmet water demand rate for entire simulation period is 355 million m^3. Under the same conditions, as seen in Figure 4.20, average overall water demand is approximately 1700 million m^3. From these two results, we can conclude that the percentage of total water demand being unmet is equal to 21% on average for all simulation period. Besides, this unmet demand ratio increases between 2019 and 2070 and reaches up to 26%. Therefore, according to results of CNRM-CM5.1 model, water supply in BMB cannot meet a considerable portion of increasing IWR rates and the gap between water supply and water demand increase between 2019 and 2070 under both RCP4.5 and RCP8.5. In the following decades, unmet demand rates drop under both climate change scenarios. However, a remarkable portion of overall water demand continue to be under-supplied.

Reviewing the results of MPI-ESM-MR model under RCP4.5 and BAU conditions, results show considerably lower unmet water demand rates. Therefore, results of this model are more optimistic in terms of future water budget of BMB. As seen in Figure 4.28, the average unmet water demand rate is 77 million m^3 during all simulation period. Moreover, as seen in Figure 4.19, overall water demand is 1640 million m^3 under the same conditions. These two results indicate that solely 5% of total water demand is unmet in the area. This ratio is equal to 20% based on the results achieved through CNRM-CM5.1 under the same conditions. During simulation period, as seen in Figure 4.28, results of MPI-ESM-MR show that unmet water demand rates follow a decreasing trend in all decades except 2081-2090 period. This means that the average 5% overall unmet demand ratio in total water demand decreases even more and the gap in between water supply and demand becomes even smaller. For instance, during 2071 and 2080 period, the ratio of unmet demand ratio in overall water demand drops down to 3%. Under RCP8.5 and BAU conditions, according to results of MPI-ESM-MR, as seen in Figure 4.28 , average decadal unmet water demand rate is equal to 60 million m^3. As shown in Figure 4.20, average annual overall water demand is 1700 million m^3. We can conclude that 3,5% of total water demand is unmet on average during entire simulation period while this ratio is equal to 21% based on the results of CNRM-CM5.1. According to results of MPI-ESM-MR under RCP8.5 and BAU conditions, for all decades in simulation period except the period between 2071 and 2080, unmet demand rates follow a decreasing trend. During 2041 and 2050 period, the average rate drops down 9 million m^3.

Moreover, reviewing the decadal variations of unmet water demand rate under CNRM-CM5.1 RCP4.5 and BAU scenario, as seen in Figure 4.28, a 5% increase occurs between 2019 and 2061 in decadal unmet water demand rate. In the following decades, a 28% drop is observed in decadal average unmet water rate, from 377 to 258 million m^3. On the other hand, according to results of MPI-ESM-MR model, decadal average unmet water demand rates sharply decrease in approximately 50% between 2019 and 208. As shown in Figure 4.28, a big leap occurs between 2081 and 2090 and decadal average unmet demand jumps to 137 million m^3 and in the following decade unmet water demand decreases to 70 million m^3.

Under BAU and RCP8.5 scenarios, as seen in Figure 4.28, CNRM-CM5.1 model shows slightly larger unmet water demand rates while MPI-ESM-MR shows remarkably smaller unmet water demand rates. According to results of CNRM-CM5.1, decadal average rates rises up to 14% on average. Between 2061 and 2099, a slow but steady decrease is observed from 377 million m^3 to 357 million m^3. On the other hand, based on the results of MPI-ESM-MR displayed in Figure 4.28, average unmet demand rates show approximately 90% decline between 2019 and 2060. After 2051-2060 period, unmet demand rates show an increasing trend and rise fivefold.

For HE-IILS and RCP4.5 conditions, as seen in Figure 4.29, CNRM-CM5.1 model outcomes demonstrate an average 245 million m^3 unmet water demand rate for the entire simulation period. Under the same conditions, as seen in Figure 4.19, average annual water demand rate is 1300 million m^3. These two rates demonstrate that approximately 18% of overall water demand is not met on average under HE-IILS and RCP4.5 conditions. Between 2019 and 2080 time period, the percentage of water demand being unmet increases up to 22%. Compared with the results achieved under BAU scenario, we see that ratio of overall water demand being unmet here is slightly lower compared to that of BAU scenario. Besides, under HE-IILS and RCP8.5 conditions, CNRM-CM5.1 model outcomes demonstrate an average 263 million m^3 unmet water demand rate for the entire simulation period as in Figure 4.25. Besides, as seen in Figure 4.20, average overall water demand is 1347 million m^3 annually. Therefore, 19% of overall water demand is unmet in BMB annually under HE-IILS and RCP8.5 conditions. As in RCP4.5 conditions, during 2019 and 2080, average unmet water demand rates also increase under RCP8.5. The portion of overall water demand being unmet reaches up to 25% between 2051 and 2060.

According to results of MPI-ESM-MR, under HE-IILS and RCP8.5 conditions, as seen in Figure 4.25, average unmet water demand rate is 30 million m^3. Besides, as seen in Figure 4.19, average overall water demand is 1347 million m^3. These two results show that approximately 2% of total water demand is unmet. Here, we see once again the huge difference between the results of CNRM-CM5.1 and MPI-ESM-MR GCMs. Except the time period between 2081 and 2090, there is a decreasing trend for unmet water demand rate based on the results of MPI-ESM-MR. Therefore, there are time periods in which overall water demand being unmet is even lower than average 2% level, i.e. 2041 and 2050 period. On the other hand, under RCP8.5 conditions, results of MPI-ESM-MR in Figure 4.29 show an average 16 million m^3 unmet water demand rate. This rate is 50% lower than the average unmet water demand rate obtained under RCP4.5 conditions and average portion of overall water demand being unmet here is approximately 1%. This ratio drops as the unmet demand rates decrease for all simulation period based on the results of MPI-ESM-MR.

According to CNRM-CM5.1 under RCP4.5 and HE-IILS conditions, as seen in Figure 4.29, there is a continuous increase around 40% for average unmet water demand rate between 2019 and 2091, from 202 to 283 million m^3. In the last decade of simulation period, the average rate drops down to 163 million m^3. On the other side, according to outcomes of MPI-ESM-MR model, the average unmet demand rate is 30 million m^3 as seen in Figure 4.29. The only remarkable deviations from the average is observed during periods of 2081-2090 and 2041-2050. Between 2081 and 2090, the average rate is 59 million m^3 while it is 12 million m^3 between 2041 and 2050.

For HE-IILS and RCP8.5 conditions, average unmet water demand rate under RCP8.5 is 7% higher compared to that of RCP4.5. As seen in Figure 4.29, the average unmet water demand rate increases from 228 to 333 million m^3 between 2019 and 2060. During 2061 and 2070, the average rate drops down to 280 million m^3 and in the following decades, it rises up to 360 million m^3. On the other hand, outcomes of MPI-ESM-MR model depicts a decreasing trend for unmet water demand rates from 38 to 12 million m^3 between 2019 and 2090. However, in the last decade of simulation period, the average unmet water demand rate rises up to 23 million m^3. The average unmet water demand rate, based on the results of MPI-ESM-MR, is 50% lower under RCP8.5 conditions compared to RCP4.5 results.

Under HE-NLUC and RCP4.5 climate change scenario, as seen in Figure 4.30, CNRM-CM5.1 shows an average 115 million m^3 unmet water demand rate for all simulation period. On the other hand, as shown in Figure 4.19, overall water demand under the same conditions is approximately 1025 million m^3. Therefore, percentage of total water demand being unmet is 11% on average for the entire simulation period. Under HE-IILS and BAU scenarios and RCP4.5 climate change conditions, this unmet water demand ratio is 20% and 18% respectively. Therefore, HE-NLUC is the scenario in which the smallest gap takes place between water supply and water demand. Besides, between 2019 and 2080, average unmet water demand ratio increases and consequently portion of total water demand being unmet rises as well. During 2071 and 2080 period, this ratio reaches up to 14%. Under

HE-NLUC and RCP8.5 conditions, as seen in Figure 4.30, average unmet water demand rate for all simulation period is 123 million m^3. Besides, as seen in Figure 4.20, overall water demand under the same conditions is approximately 1060 million m^3. Therefore, percentage of total water demand being unmet is 12% on average. Since there is an increasing trend in average unmet water demand rates between 2019 and 2060, as seen in Figure 4.26, unmet water demand ratio increases as well. Between 2051 and 2060, this ratio reaches up to 18%.

As seen in Figure 4.30, according to results of CNRM-CM5.1 under RCP4.5 and HE-NLUC conditions, between 2019 and 2080, decadal unmet water demand rate increases from 101 to 149 million m^3. In the following decades the average rate drops down to 44 million m^3. On the other side, according to MPI-ESM-MR for the same conditions, solely 2019-2030 period shows considerable unmet water demand rates. During this period, the average rate is approximately 28 million m^3 and in the following decades unmet demand is hardly observed.

Under RCP8.5 and HE-NLUC conditions, as seen in Figure 4.30, there are considerable increases in average unmet demand rates based on the results of CNRM-CM5.1. For results of MPI-ESM-MR, similar to RCP4.5 outcomes, solely 2019-2030 time period shows a remarkable unmet demand rate, which is 33 million m^3 and corresponds to a 15% increase compared to RCP4.5. In the following decades, unmet demand is barely observed.

Under LE-IILS and RCP4.5, higher average unmet water demand rates take place compared to other scenarios mentioned so far. As seen in Figure 4.31, CNRM-CM5.1 shows an average 568 million m^3 unmet water demand rate for all simulation period. On the other hand, as shown in Figure 4.19, overall water demand under the same conditions is approximately 2095 million m^3. Therefore, percentage of total water demand being unmet is 27% on average for the entire simulation period. Besides, between 2019 and 2080, as seen in Figure 4.31, average unmet water demand ratio increases and consequently portion of total water demand being unmet rises as well. During 2071 and 2080 period, this ratio reaches up to 29%. Under LE-IILS and RCP8.5 conditions, as seen in Figure 4.31, average unmet water demand rate for all simulation period is 580 million m^3. This unmet water demand rate is highest unmet rate among all scenarios presented in this study. Besides, as seen in Figure 4.20, overall water demand under the same conditions is approximately 2165 million m^3. Therefore, percentage of total water demand being unmet is 27% on average. Since there is an increasing trend in average unmet water demand rates between 2019 and 2060, as seen in Figure 4.31, unmet demand ratio increases as well. Between 2051 and 2060, this ratio reaches up to 31%.

According to results of MPI-ESM-MR under LE-IILS and RCP4.5 conditions, as seen in Figure 4.31, the average unmet water demand rate is 283 million m^3 for all simulation period. On the other hand, as shown in Figure 4.19, overall water demand under the same conditions is approximately 2095 million m^3. Therefore, percentage of total water demand being unmet is approximately 13% on average for the entire simulation period. Besides, between 2019 and 2050, as seen in Figure 4.27, average unmet demand ratio increases and consequently portion of total water demand being unmet rises as well. During 2041 and 2050 period, this ratio reaches up to 16%.

Reviewing the decadal variations under LE-IILS and RCP4.5 conditions, as shown in Figure 4.31, CNRM-CM5.1 shows the average unmet water demand rate increases from 535 to 606 million m^3 between 2019 and 2070. Therefore, there is a 12% increase in average unmet demand rates in the meantime. In the following decades, the average unmet water demand rate drops down to 491 million m^3. Under the same conditions, MPI-ESM-MR demonstrates that the average unmet water demand rate increases by 36% between 2019 and 2050 from 212 to 333 million m^3 while fluctuating trends prevail in the following decades.

Under RCP8.5 and LE-IILS conditions, as seen in Figure 4.31, results of CNRM-CM5.1 indicate that average unmet demand rate increases from 546 to 661 million m^3. That is, there is a 21% increase in average unmet water demand rate. In the following decades, the average rate drops by 11%. On the other hand, for MPI-ESM-MR model, the average unmet water demand rate increases by 35% between 2019 and 2040 from 124 to 167 million m^3. During 2041-2050 period, the average rate sharply drops down to 73 million m^3. In the following decades, the average unmet water demand rate rises up to 435 million m^3.

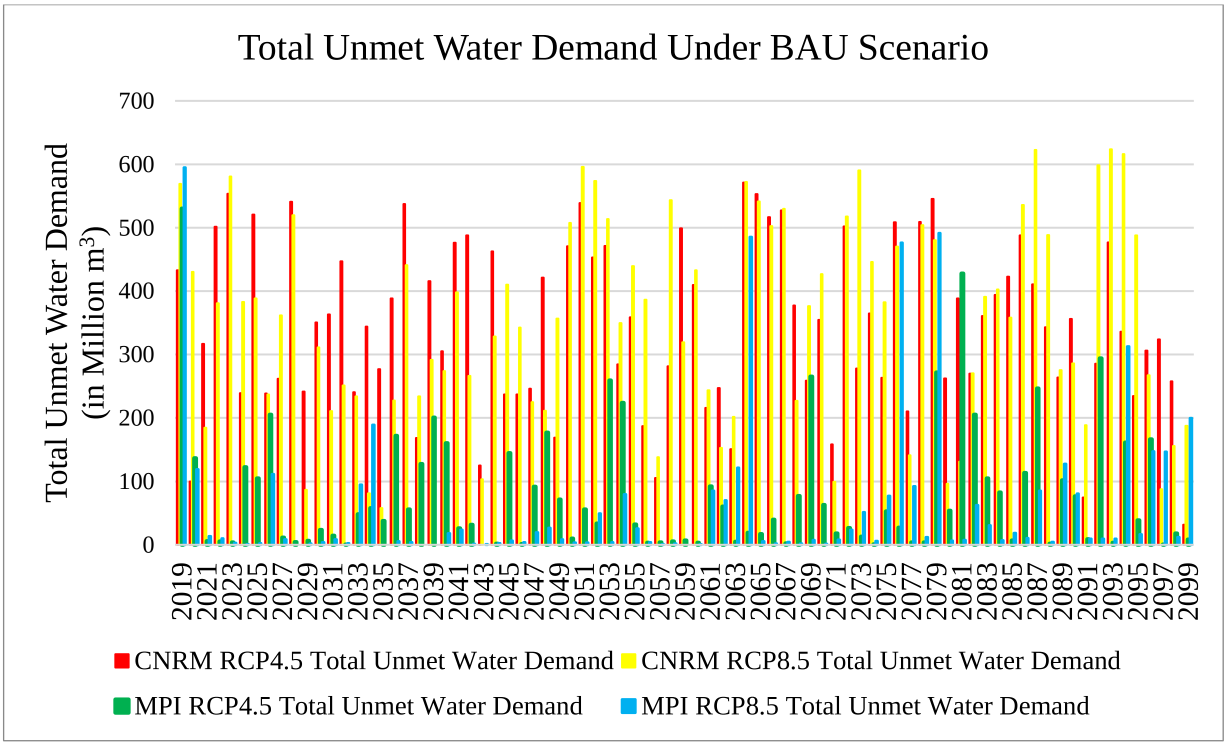

Figure 4.24. Total unmet water demand under BAU scenario with CNRM RCP4.5, RCP8.5 and MPI RCP4.5, RCP8.5 climate change scenarios.

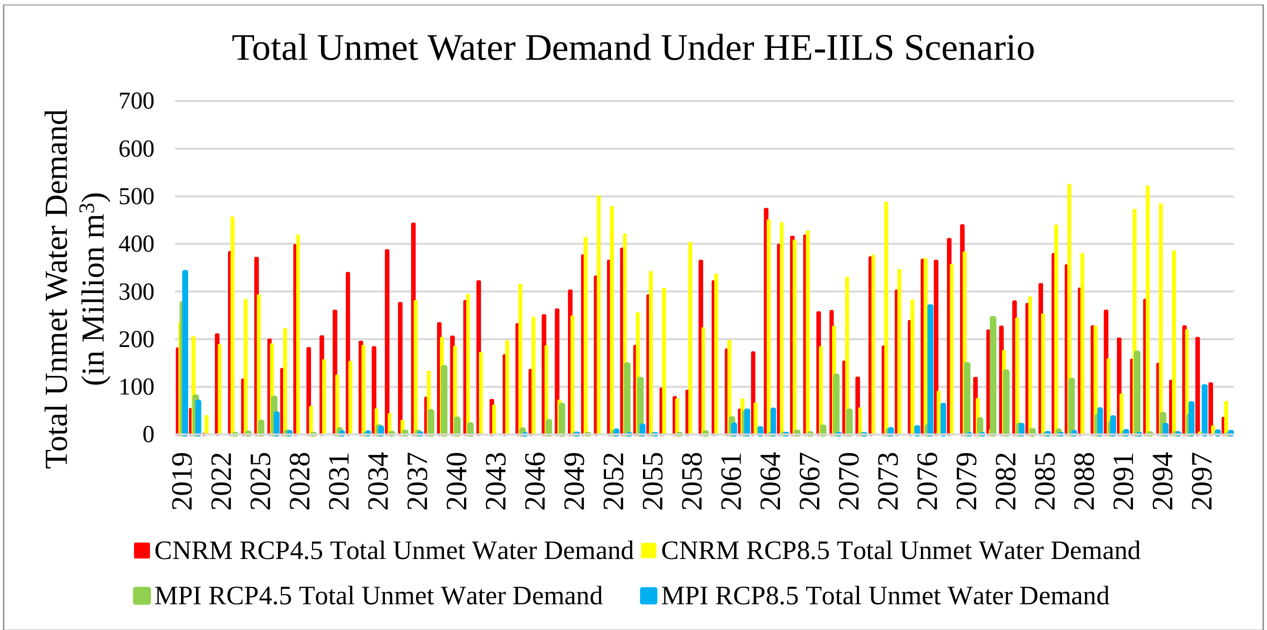

Figure 4.25. Total unmet water demand under HE-IILS scenario with CNRM RCP4.5, RCP8.5 and MPI RCP4.5, RCP8.5 climate change scenarios.

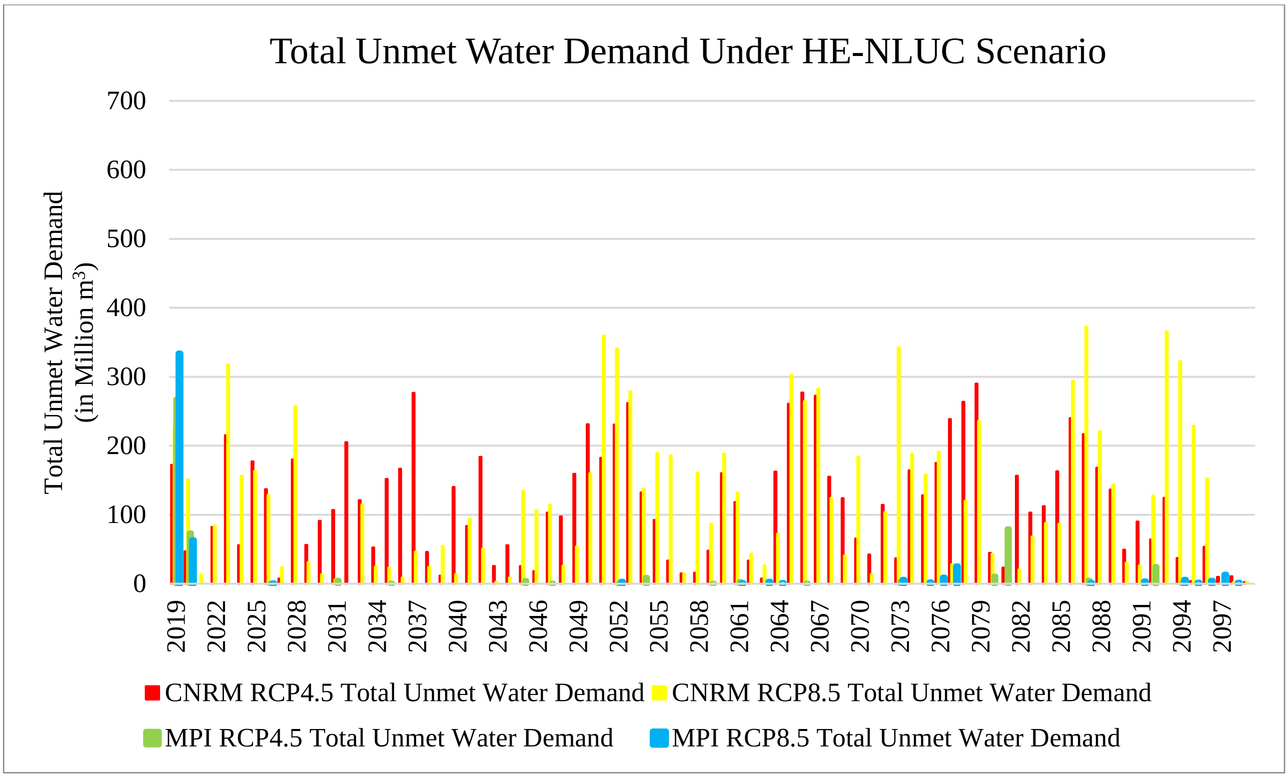

Figure 4.26. Total unmet water demand under HE-NLUC scenario with CNRM RCP4.5, RCP8.5 and MPI RCP4.5, RCP8.5 climate change scenarios.

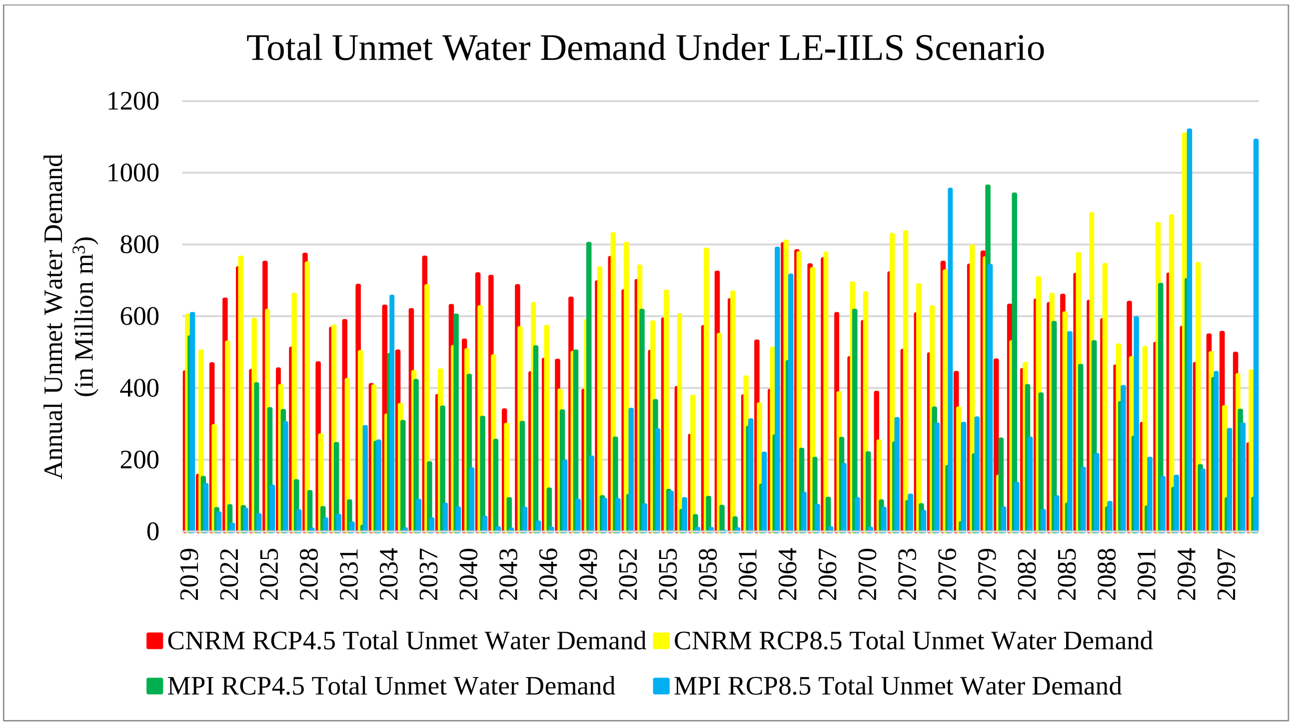

Figure 4.27. Total unmet water demand under LE-IILS scenario with CNRM RCP4.5, RCP8.5 and MPI RCP4.5, RCP8.5 climate change scenarios.

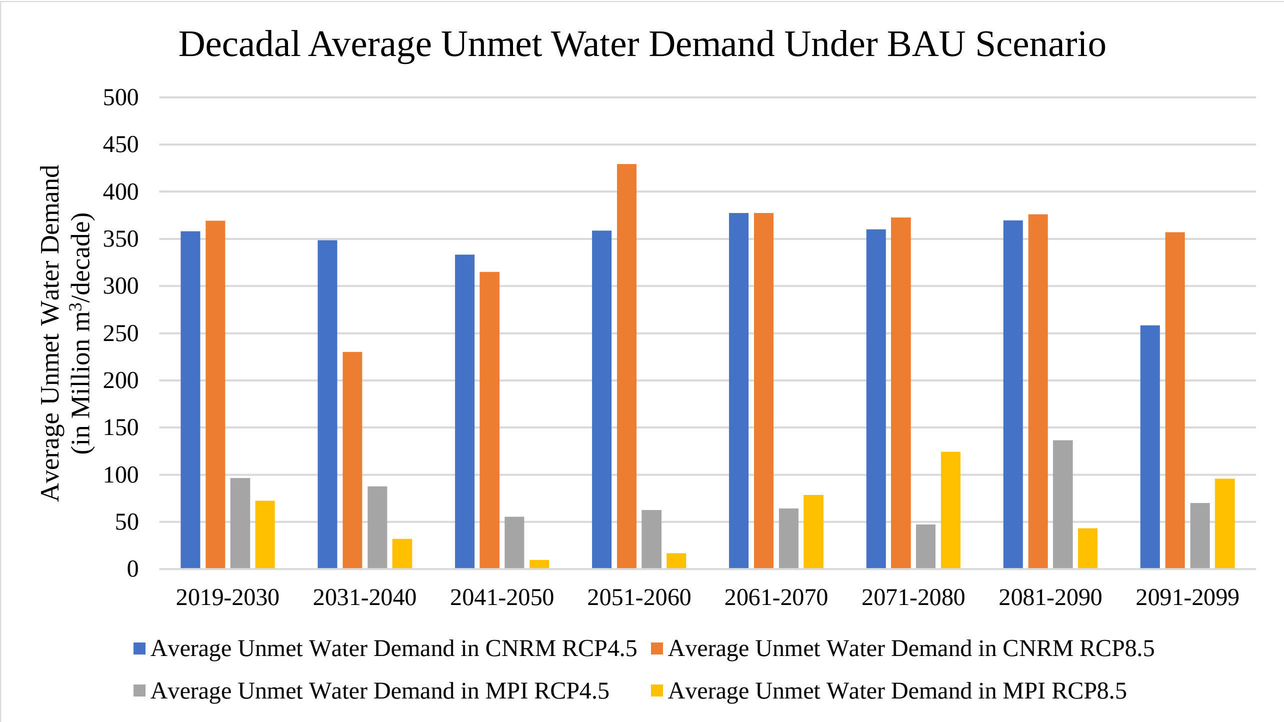

Figure 4.28. Total unmet water demand under BAU scenario with CNRM RCP4.5, RCP8.5 and MPI RCP4.5, RCP8.5 climate change scenarios.

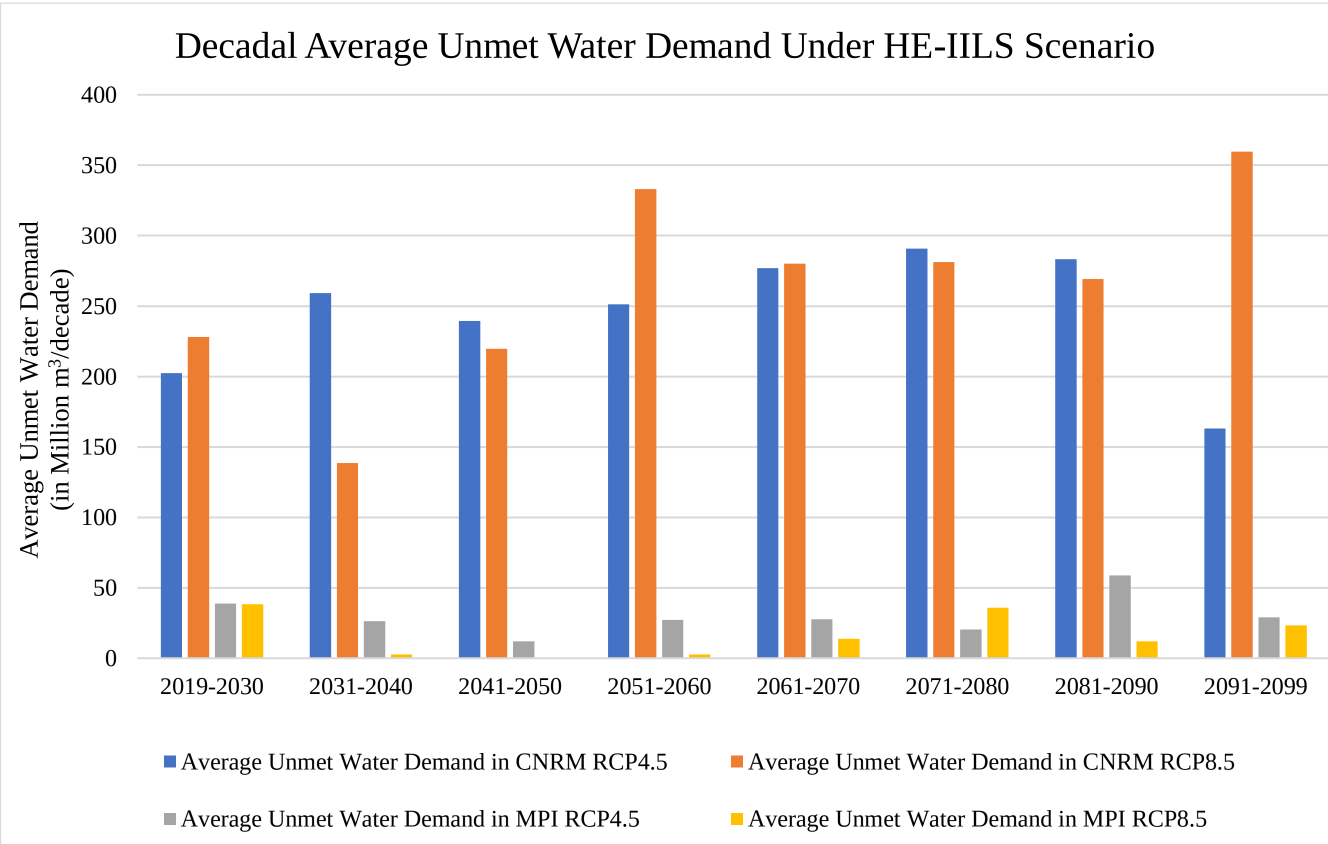

Figure 4.29. Decadal average unmet water demand under HE-IILS scenario with CNRM RCP4.5, RCP8.5 and MPI RCP4.5, RCP8.5 climate change scenarios.

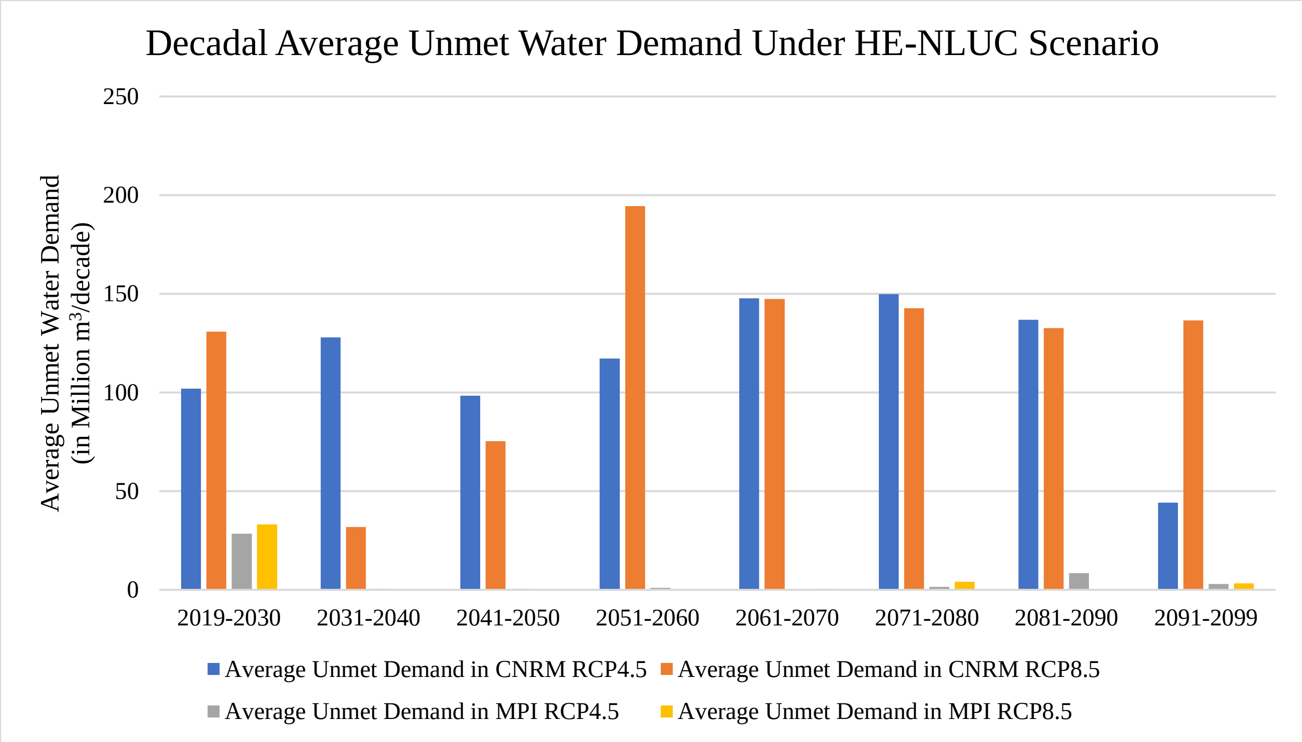

Figure 4.30. Decadal average unmet water demand under HE-NLUC scenario with CNRM RCP4.5, RCP8.5 and MPI RCP4.5, RCP8.5 climate change scenarios.

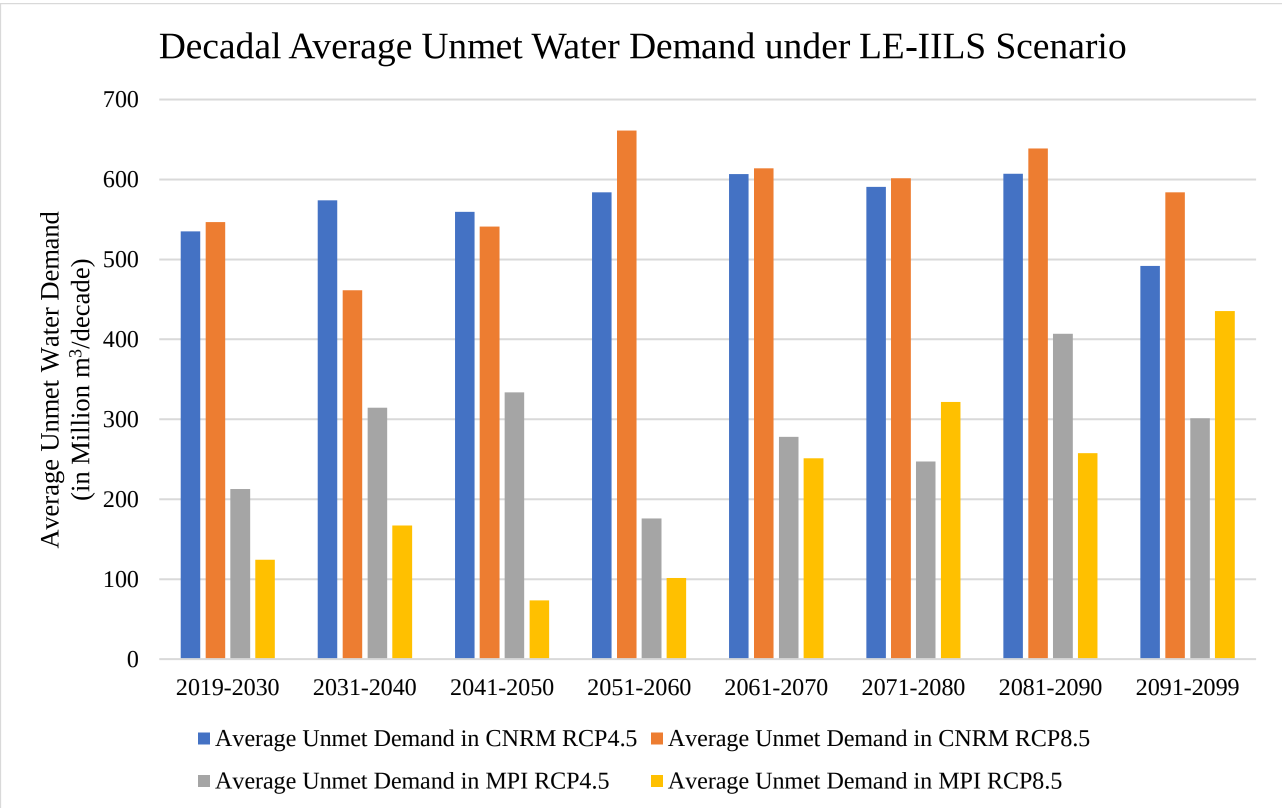

Figure 4.31. Decadal average unmet water demand under LE-IILS scenario with CNRM RCP4.5, RCP8.5 and MPI RCP4.5, RCP8.5 climate change scenarios.

The distribution of unmet water demand under different scenarios differs with regard to months. The highest unmet water demand takes place in June, July, August, and September. The main reason here is that this thesis study chooses singly agricultural areas as water demand nodes and agricultural activities are mostly conducted during summer season in BMB.

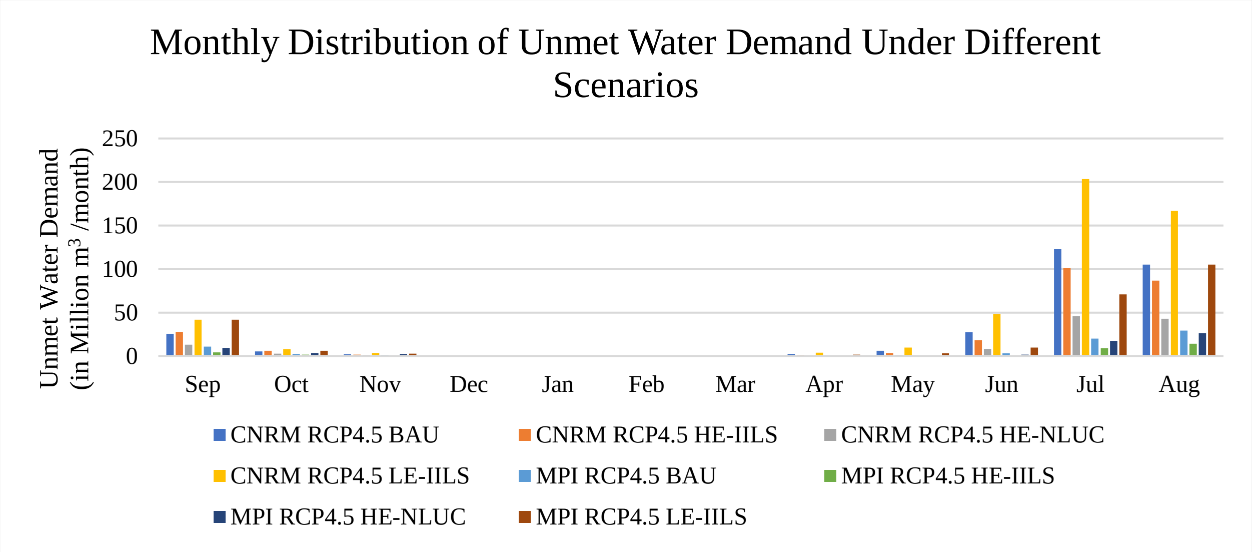

Figure 4.32. Monthly distribution of unmet water demand under different scenarios with CNRM RCP4.5 and MPI RCP4.5 climate change scenarios.

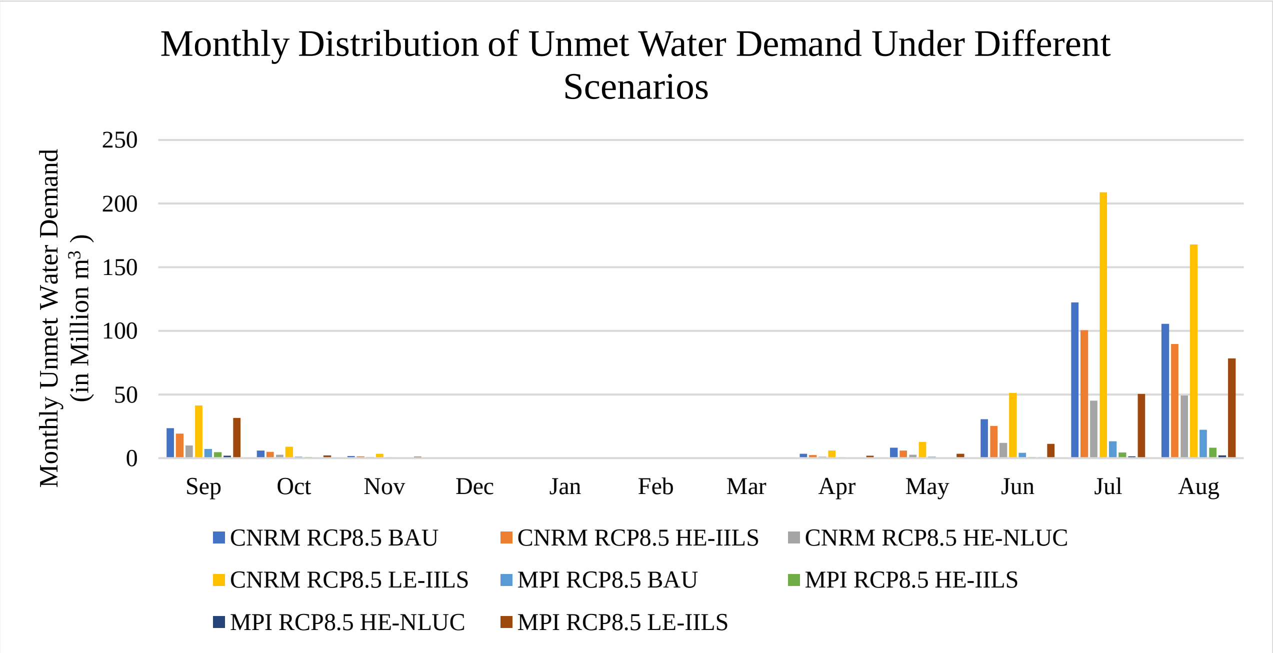

Figure 4.33. Monthly distribution of unmet water demand under different scenarios with CNRM RCP8.5 and MPI RCP8.5 climate change scenarios.

Moreover, the model employs SCM method. By SCM method, the model calculates surface runoff solely as the subtraction of precipitation from ET. Surface runoff rates under different climate change are displayed in Figure 4.34 and 4.35 Besides, Figure 4.36 shows decadal average difference in surface runoff rates with respect to 2005-2018 time period.

As seen in Figure 4.34 and Figure 4.35, average surface runoff rate is approximately 1500 million m^3. As shown in Figure 4.35, under RCP4.5 and CNRM-CM5.1, the average surface runoff rate is around 2600 million m^3 during simulation period. Under RCP 4.5 and MPI-ESM-MR, simulation period demonstrates an average surface runoff rate of 1850 million m^3. These results indicate that average surface runoff rate increases by 74% and 22% under the results of CNRM-CM5.1 and MPI-ESM-MR respectively.

Under RCP8.5, Figure 4.35 demonstrates that average surface runoff rate of CNRM-CM5.1 is lower compared to that of RCP4.5. The average surface runoff rate is around 2400 million m^3. That is, the average surface runoff rate is 8% lower under RCP8.5 conditions. On the other hand, Figure 4.35 shows the average surface runoff is approximately 2200 million m^3 during simulation period under MPI-ESM-MR results. That is, according to results of MPI-ESM-MR, the average surface runoff rate is 18% higher under RCP8.5 conditions compared to that of RCP4.5.

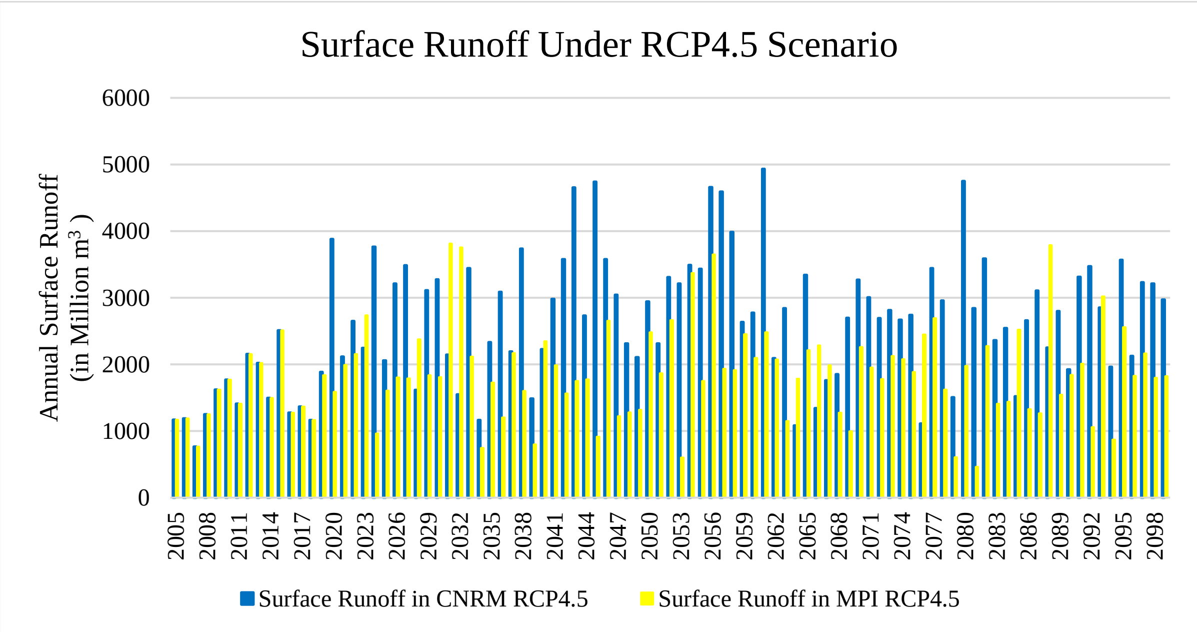

Figure 4.34. Surface runoff rates under CNRM RCP4.5 and MPI RCP4.5 climate change scenarios.

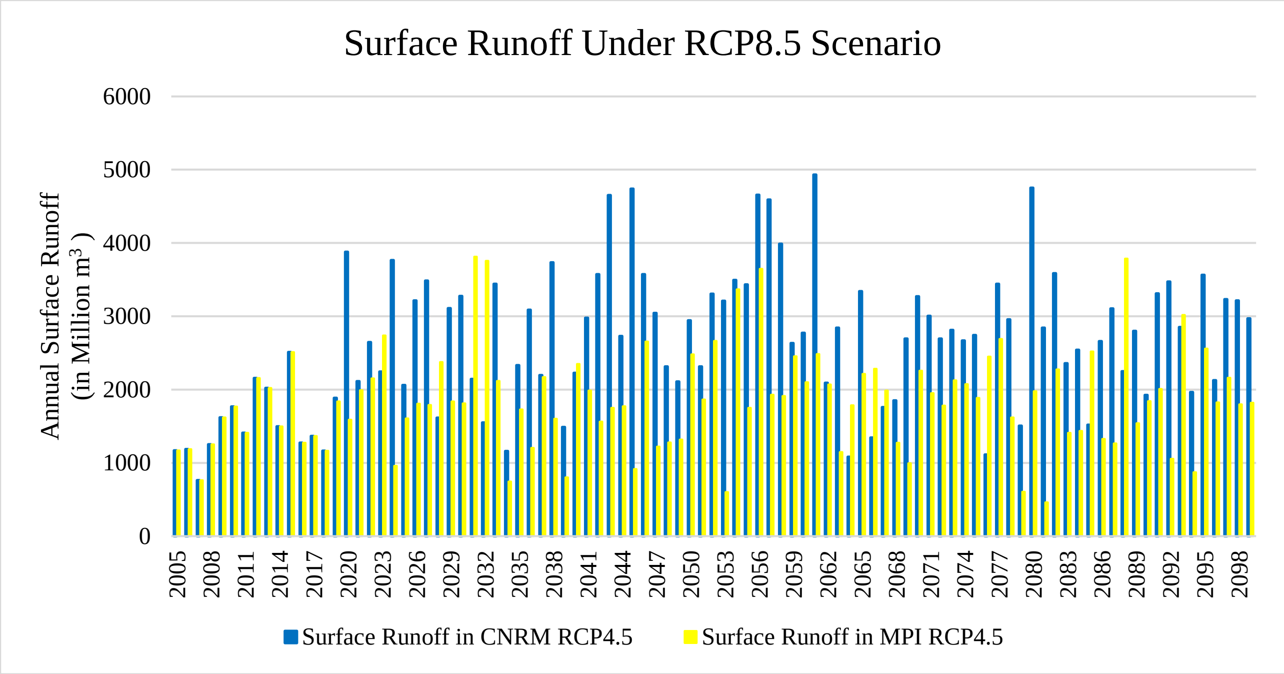

Figure 4.35. Surface runoff rates under CNRM RCP8.5 and MPI RCP8.5 climate change scenarios.

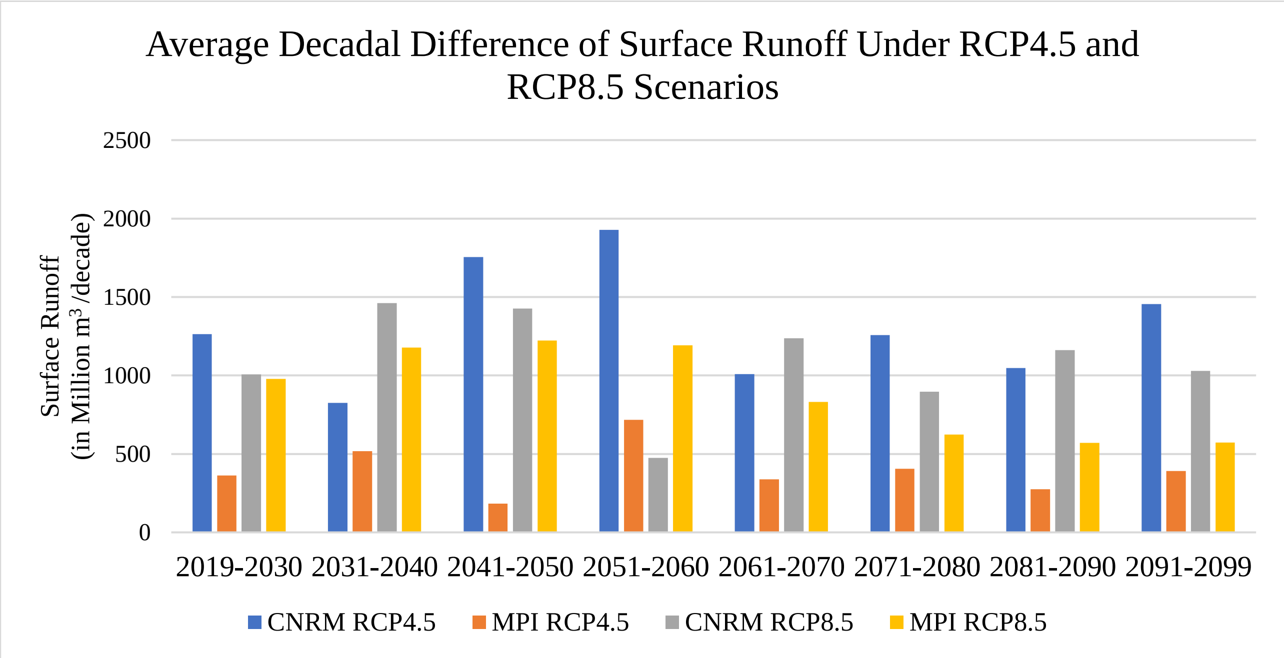

Figure 4.36. Decadal average difference of surface runoff rates with respect to 2005-2018 period under CNRM RCP4.5, RCP8.5 and MPI RCP4.5 RCP8.5 climate scenarios.

4.4. Reservoir Storage Volumes Under BAU

This section presents changes in storage volume of reservoirs under BAU scenario. Based on the assumption of BAU, there is no infrastructural change or land use change in BMB. The only difference is regarding climatic conditions which are already embedded in results of CNRM-CM5.1 and MPI-ESM-MR models.

According to results of CNRM-CM5.1 under RCP4.5, as seen in Figure 4.38, rates of average decadal reservoir volume follow generally an increasing trend throughout simulation period with respect to baseline average rates. As displayed in Figure 3.6 shown in section 3.2.2, baseline average rate for total reservoir volume is 1500 million m^3. Based on the results of CNRM-CM5.1 under RCP4.5, as shown in Figure 4.38, average total reservoir volume rate increases by 120 million m^3 during simulation period. These two average rates show that total average reservoir volume increases by 8% between 2019 and 2099. As to decadal variations of average volume rate, Figure 4.38 presents that the decadal difference increases from 78 to 183 million m^3 between 2019 and 2060. Until 2081-2090 period, the difference drops down to 100 million m^3 until and rises to 155 million m^3 in the last decade of simulation period. On the other hand, under RCP8.5 conditions, results of CNRM-CM5.1 represent relatively lower average total storage volume rates compared to that of RCP4.5. Average total reservoir storage volume, as shown in Figure 4.38, is around 75 million m^3 higher than average baseline rate. This rate corresponds to a 5% increase of average total reservoir volume with respect to baseline scenario. Under RCP4.5 and the same model's results, the rate of increase is equal to 8%.

On the other hand, as shown in Figure 4.38, results of MPI-ESM-MR under RCP4.5 conditions show that average reservoir volume rate is approximately 250 million m^3 lower than average baseline rate. Given that average baseline total reservoir volume rate is 1500 million m^3, the 250 million m^3 decline under RCP4.5 conditions correspond to a 16% increase. According to results of CNRM-CM5.1, the rates of increase with respect to baseline rate are 8% and 5% under RCP4.5 and RCP8.5 respectively. As to decadal variations of average volume rate under RCP4.5 and MPI-ESM-MR results, Figure 4.38 presents that the average decadal difference decreases from 215 to 175 million m^3 between 2019 and 2050. After the abrupt increase of decadal difference up to 480 million m^3, in the following decades, the average decadal difference rate drops down to 310 million m^3. Besides,

Figure 4.38 shows that the average increase of average total reservoir volume with respect to baseline rate is approximately 430 million m^3. This average rate corresponds to an 28% increase while the rate of increase is 16% based on the results of MPI-ESM-MR under RCP8.5 conditions. As to decadal variations of average volume rate under RCP8.5 and MPI-ESM-MR results, Figure 4.38 presents that the average decadal difference decreases from 415 to 635 million m^3 between 2019 and 2050. In the following decades, the average decadal difference rate drops down to 260 million m^3.

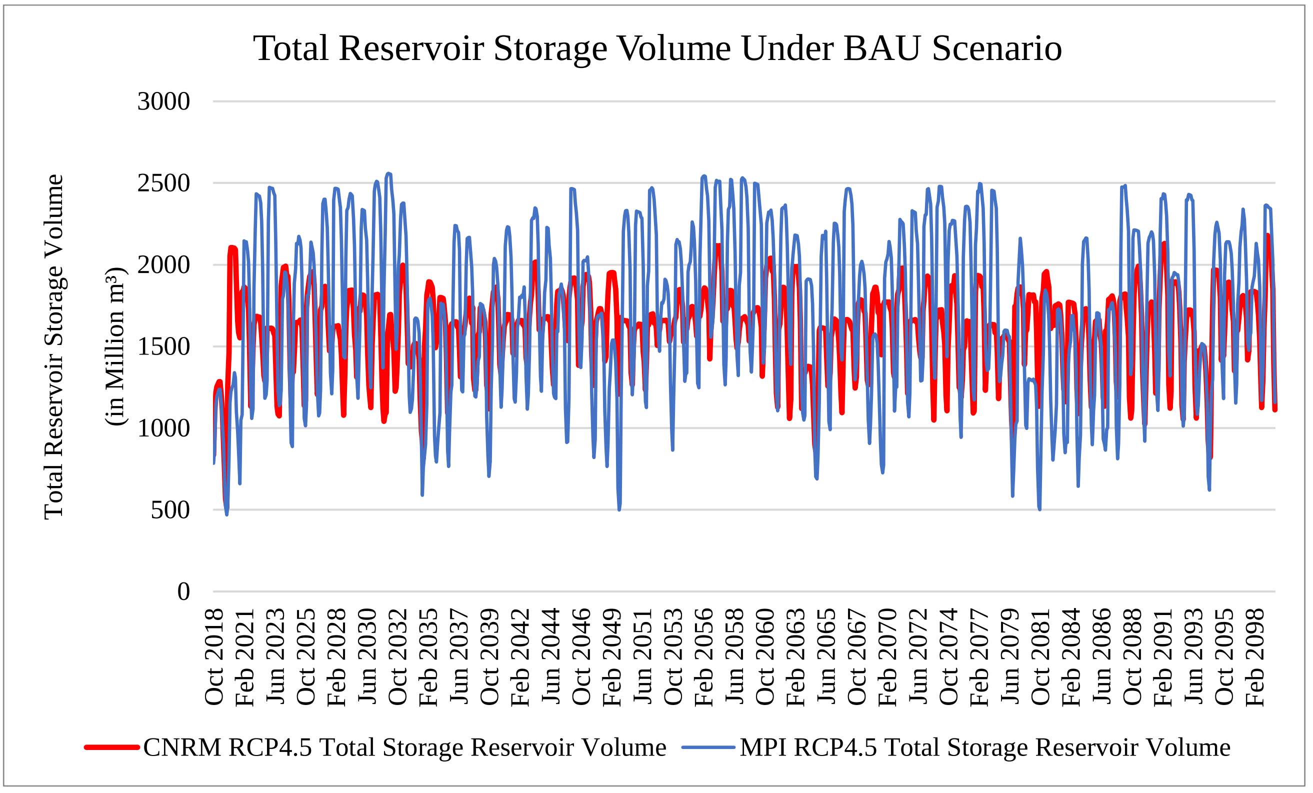

Figure 4.37. Total storage volume under BAU scenario with CNRM RCP4.5 and MPI RCP4.5 climate change scenarios.

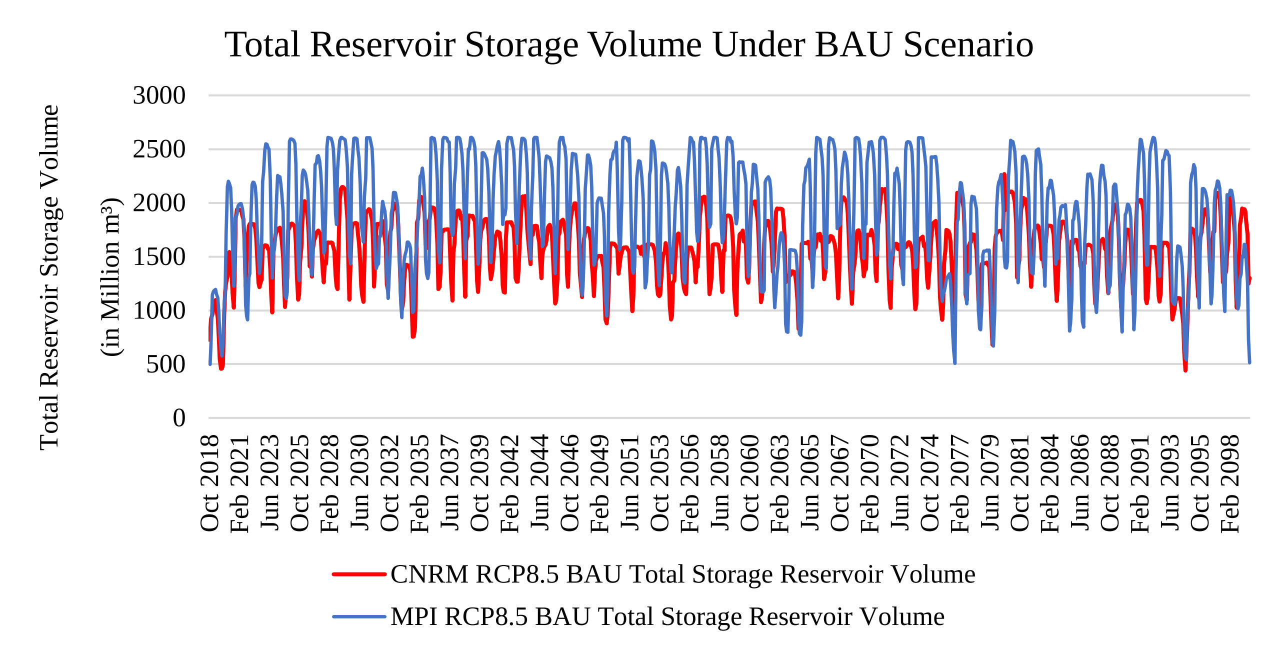

Figure 4.38. Total reservoir storage volume under BAU scenario with CNRM RCP8.5 and MPI RCP8.5 climate change scenarios.

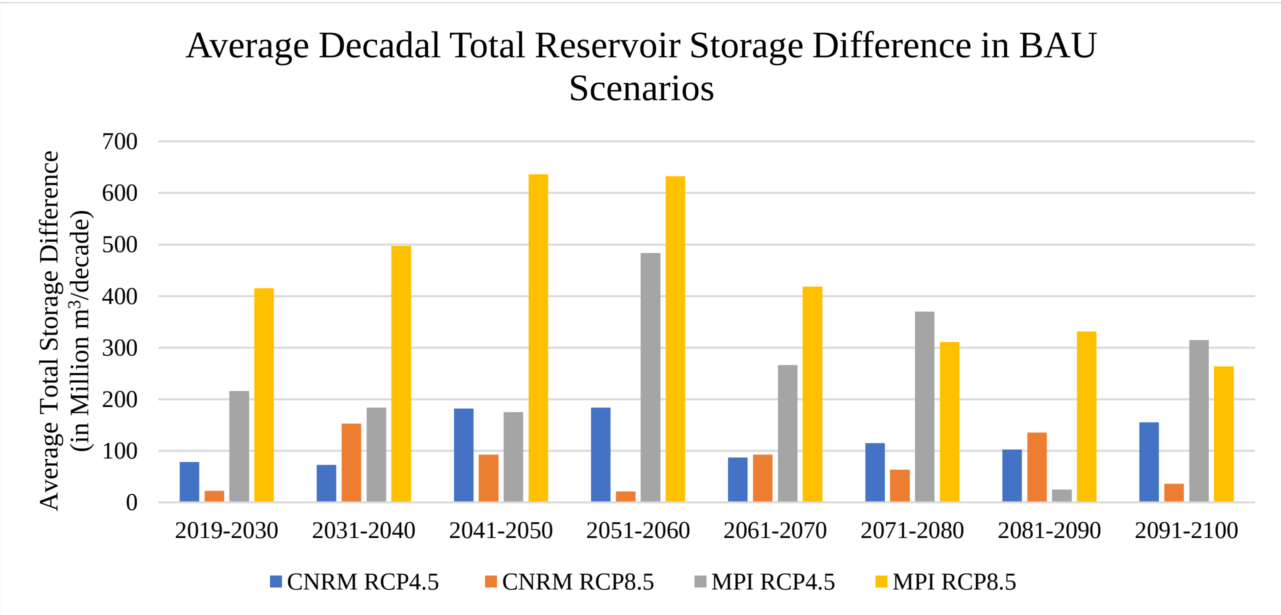

Figure 4.39. Decadal average difference of total reservoir storage volume with respect to 2005-2018 period under CNRM RCP4.5, RCP8.5 and MPI RCP4.5 RCP8.5 climate change scenarios.

As to impacts of climatic conditions on each reservoir separately under BAU scenario, it is seen that there exist two distinct group of reservoirs. These groups are reservoirs situated within Aydın and reservoirs situated within Denizli. As displayed in Appendix C, results of CNRM-CM5.1 show that decadal average precipitation rates decline critically in Aydın under both RCP4.5 and RCP8.5. Under RCP4.5 conditions, according to results of CNRM-CM5.1, average precipitation decline for entire simulation period is 105 mm per year in Aydın. Besides, under RCP8.5 conditions, average precipitation decline is around 110 mm per year. These declines correspond to an approximately 17% decline in decadal average precipitation rates in Aydın with respect to baseline average precipitation rates provided by MGM for Aydın. The historical precipitation rates granted by MGM compasses the observation period between 2005-2018 and they are displayed in Appendix B. On the other side, as shown in Appendix C, the same model shows a 900 and 720 increase in decadal average precipitation rates for Denizli under RCP4.5 and RCP8.5 conditions respectively. These average rates correspond to 130% and 125% increases with respect to average baseline precipitation rates of Denizli. Moreover, according to results of CNRM-CM5.1 displayed in Appendix C, increases in average decadal ET rates of Aydın for the entire simulation period are 521 and 575 mm under RCP4.5 and RCP8.5 conditions respectively. On the other side, increases in rates of average decadal average ET of Denizli are 178 and 295 mm during simulation period. Therefore, surface runoff rates (that is precipitation minus ET) become much lower in reservoirs located in Aydın compared to reservoirs in Denizli. Consequently, reservoirs in Aydın demonstrate lower storage volume rates compared to their baseline storage rates between 2005 and 2018. The reservoirs located in Aydın are Çine, İkizdere, Karacasu, Kemer, Topçam, and Yaylakavak. On the other hand, due to increasing surface runoff rates, reservoirs in Denizli naturally show higher storage volume rates compared to their baseline rates. The reservoirs in Denizli are Adıgüzel, Cindere, Işıklı, Tavas, Gökpınar reservoirs. Lastly, the only reservoir excluded from these two group of reservoirs is Bayır reservoir that is located in Muğla. Similar to Aydın, as shown in Appendix C, CNRM-CM5.1 results show decreasing precipitation rates and increasing ET rates for Muğla. Therefore, reservoir storage volume rates of Bayır are also lower under both RCP4.5 and RCP8.5. Declines in average precipitation rates of Muğla are 63 and 80 mm under RCP4.5 and RCP8.5 conditions respectively. These declines correspond to approximately 6% and 7% decreases considering the average baseline precipitation rates displayed in Appendix B for Muğla.

On the other side, results of MPI-ESM-MR demonstrate increasing precipitation rates for Aydın, Denizli, and Muğla altogether. As shown in Appendix C, increases in average precipitation rates of Aydın are 256 and 330 mm under RCP4.5 and RCP8.5 conditions respectively. These average rates correspond to 40% and 50% increase in average precipitation rates with respect to average baseline rates. For Denizli, according to MPI-ESM-MR, the rates of increase in average precipitation rates are lower than that of CNRM-CM5.1 model. The increase in average precipitation rates are 52 and 71 mm under RCP4.5 and RCP8.5 conditions respectively. Therefore, given the historical average precipitation rates displayed in Appendix B, these rates correspond to 9% and 12% increases respectively for Denizli. As presented in Appendix C, for Muğla, increases in decadal average precipitation rates are 228 and 310 mm under RCP4.5 and RCP8.5 conditions respectively. These average increase rates correspond to 21% and 28% increases with respect to baseline average precipitation rates for Muğla. Additionally, according to results of MPI-ESM-MR displayed in Appendix C for Aydın, the increase in average decadal ET rate is approximately 360 mm higher under RCP4.5 compared to that of CNRM-CM5.1. Under RCP8.5, the decline in average ET rate is 413 mm compared to results of CNRM-CM5.1 achieved under RCP8.5 conditions. Hence, based on the results of MPI-ESM-MR, the surface runoff rates become higher for Aydın under RCP8.5 conditions due to declining ET rates and increasing precipitation rates compared to RCP4.5. For Denizli, according to results of MPI-ESM-MR presented in Appendix C, decadal average ET rate of all simulation period is approximately 7 mm lower than baseline average rates under RCP4.5 conditions. Under RCP8.5, the average increase in ET rate is 33 mm. Therefore, according to results of MPI-ESM-MR, surface runoff rate for Denizli is comparatively higher under RCP4.5 conditions than that of RCP8.5 due to relatively lower average ET rates.

There is an important reason why this section gives details regarding the results of ET and precipitation rates achieved through CNRM-CM5.1 and MPI-ESM-MR under RCP4.5 and RCP8.5 conditions. The reason is that BAU is the scenario in which the individual impact of climate change on reservoir storage volume in BMB can be observed most clearly because there are no other parameters being changed/manipulated in this scenario, such as efficiency rates and irrigated land area. Therefore, the impact of changes in ET and precipitation rates on storage volume rates are most visible under BAU scenario. Consequently, the scenario in which variations in reservoir storage volume rates follow most closely the changes in climatic conditions is BAU. In the following section, with the revelations regarding variations in reservoir storage volumes, this case becomes clearer and more understandable.

Firstly, as seen in Appendix A, Aydın reservoirs show falling storage volume rates with respect to baseline average volume rate under both RCP4.5 and RCP8.5 conditions according to results of CNRM-CM5.1. For instance, in Topçam reservoir, as seen in Appendix A, the declines in average storage volume rates are 58% and 60% under RCP4.5 and RCP8.5 respectively with respect to average baseline storage volume. Besides, for Yaylakavak reservoirs, based on the results of CNRM-CM5.1, the declines are 74% and 75% under RCP4.5 and RCP8.5 correspondingly. On the other side, according to results of CNRM-CM5.1, storage volume rates of reservoirs in Denizli follow an increasing trend as a result of rising surface runoff rate under both RCP4.5 and RCP8.5. As seen in Appendix A, during simulation period, average storage volume of Adıgüzel reservoir rises to 75% and 68% under RCP4.5 and RCP8.5 conditions respectively. Moreover, for Işıklı reservoir, the rates of increase are 66% and 62% under RCP4.5 and RCP8.5 conditions respectively. Being another reservoir in Denizli, average storage volume of Gökpınar reservoir also shows an increase of 29% and 25% under RCP4.5 and RCP8.5 correspondingly. Lastly, as seen in Appendix A, average storage volume of Bayır reservoir being located in Muğla also increases. The rates of increase are 18% and 13% under RCP4.5 and RCP8.5 respectively.

The main reason for big differences in declines and increases observed for each reservoir is that each reservoir differs in size. As a result of having relatively less reservoir capacities, smaller reservoirs may not always be able to keep enough water for times of over water consumption. Consequently, they are more likely to face the risk of drying out in certain time periods. Differences in annual water requirement per hectare is also critical in the sense that reservoirs get affected variously by changes in climatic conditions. For many reasons such as different crop patterns and different infrastructural conditions, annual water requirement per hectare may vary among different reservoirs. Secondly, according to results of CNRM.CM5.1, average reservoir storage volumes are relatively higher under RCP4.5 conditions. There are two main reasons for this difference in between. The first reason is lower surface runoff rates observed under RCP8.5 conditions. Besides, IWR rates are higher under RCP8.5 conditions, which in turn increases annual water demand rates.

On the other hand, according to results of MPI-ESM-MR, results are brighter for reservoirs located in Aydın with respect to baseline scenario. The variations observed in average storage volume rates of Topçam and Yaylakavak are again good examples to explain this relatively brighter situation. As displayed in Appendix A, average storage volume of Topçam reservoir increases by 34% and 65% under RCP4.5 and RCP8.5 respectively. As opposed these increasing rates, it is important to remark here that average volume of Topçam reservoir drops by 58% and 60% under the same conditions according to results of CNRM-CM5.1. Moreover, average storage volume of Yaylakavak reservoir does barely change under RCP4.5 and increases by 40% under RCP8.5 conditions. On the other side, as seen in Appendix C, surface runoff rates are relatively lower in Denizli under the results of MPI-ESM-MR compared to that of CNRM-CM5.1. Consequently, the rates of increase for reservoirs located in Denizli are comparatively lower by the results of MPI-ESM-MR. For instance, as seen in Appendix A, average storage volume of Adıgüzel reservoir increases by 40% and 29% under RCP4.5 and RCP8.5 conditions respectively. These rates are 75% and 68% under the results of CNRM-CM5.1. Besides, Işıklı reservoir follows a similar pattern to Adıgüzel reservoir. As shown in Appendix A again, average storage volume of Işıklı reservoir increases by 44% and 40% under RCP4.5 and RCP8.5 respectively. The rates of increase, according to results of CNRM-CM5.1, are 66% and 62%. Hence, reservoirs in Denizli still demonstrate increasing storage volume rates under the results of MPI-ESM-MR yet the rates are relatively lower compared to that of CNRM-CM5.1.

Regarding the results achieved through outputs of MPI-ESM-MR, it is important to note here that reservoirs in Denizli show lower increasing rates under RCP8.5 compared to RCP4.5 while that is the opposite for reservoirs in Aydın. The reason behind this disparity is differential impacts of climate change on both cities. As seen in Appendix C, according to results of MPI-ESM-MR, increases in average decadal precipitation rates of Aydın are considerably higher than that of Denizli under both RCP4.5 and RCP8.5. Besides, average ET rate of Aydın is again lower under RCP8.5 conditions compared to Denizli. Therefore, increases in surface runoff rates offset higher IWR rates under RCP8.5.

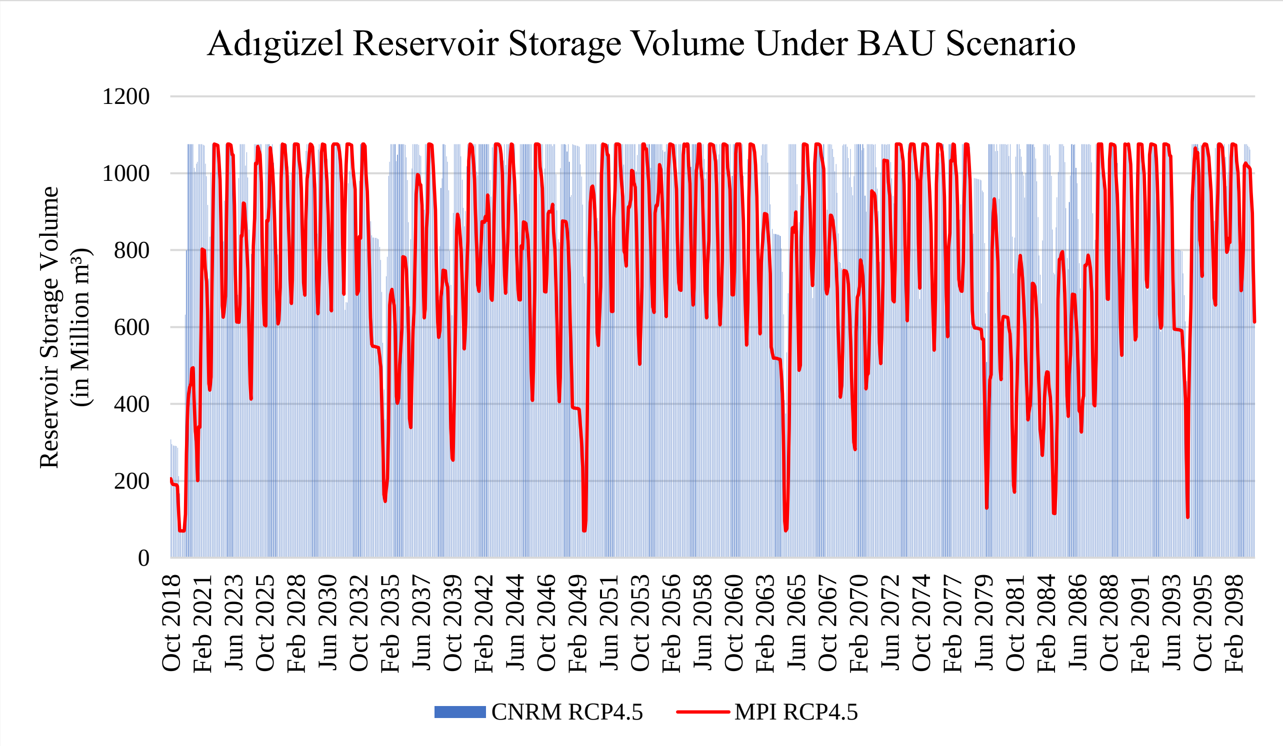

Figure 4.40. Storage volume of Adıgüzel Reservoir under BAU scenario with CNRM RCP4.5 and MPI RCP4.5 climate change scenarios.

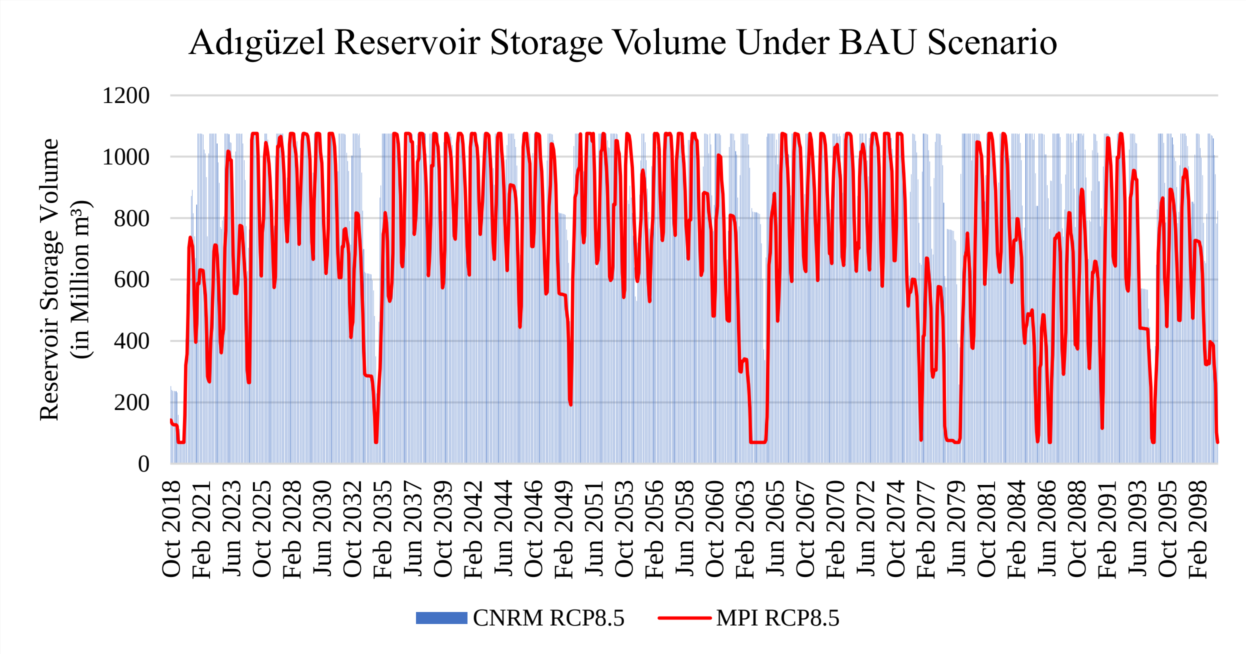

Figure 4.41. Storage volume of Adıgüzel Reservoir under BAU scenario with CNRM RCP8.5 and MPI RCP8.5 climate change scenarios.

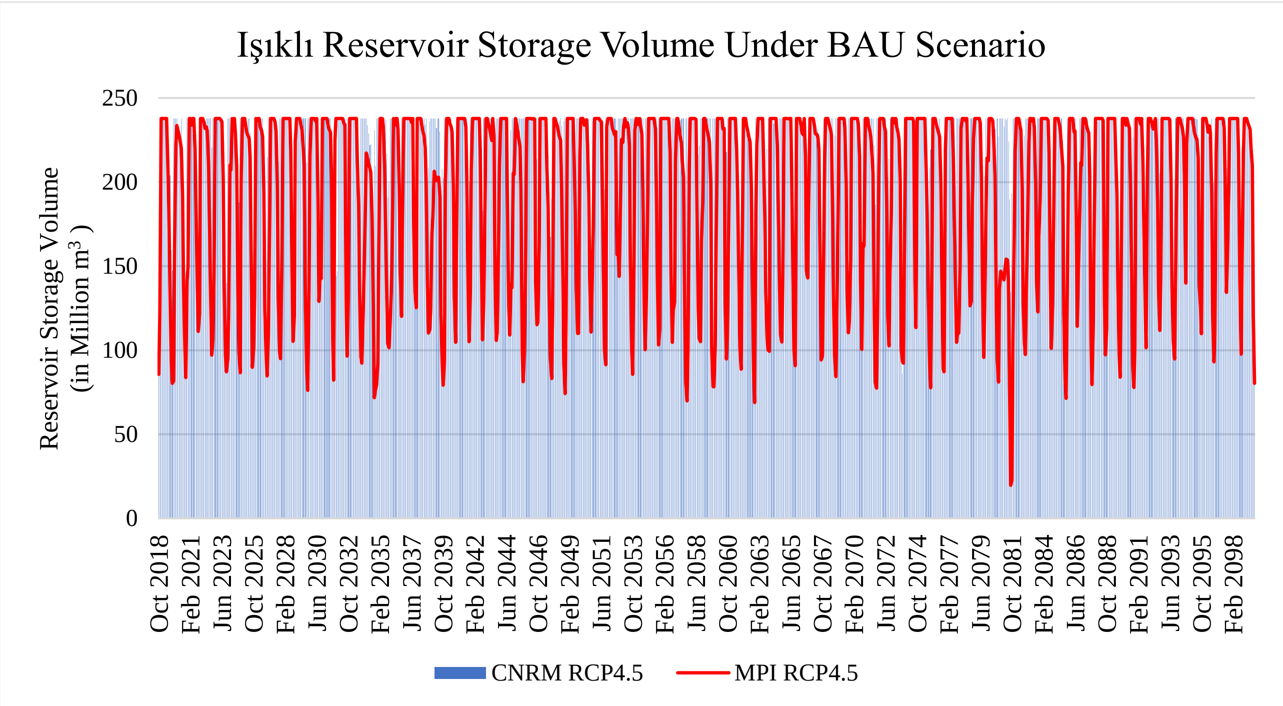

Figure 4.42. Storage volume of Işıklı Reservoir under BAU scenario with CNRM RCP4.5 and MPI RCP4.5 climate change scenarios.

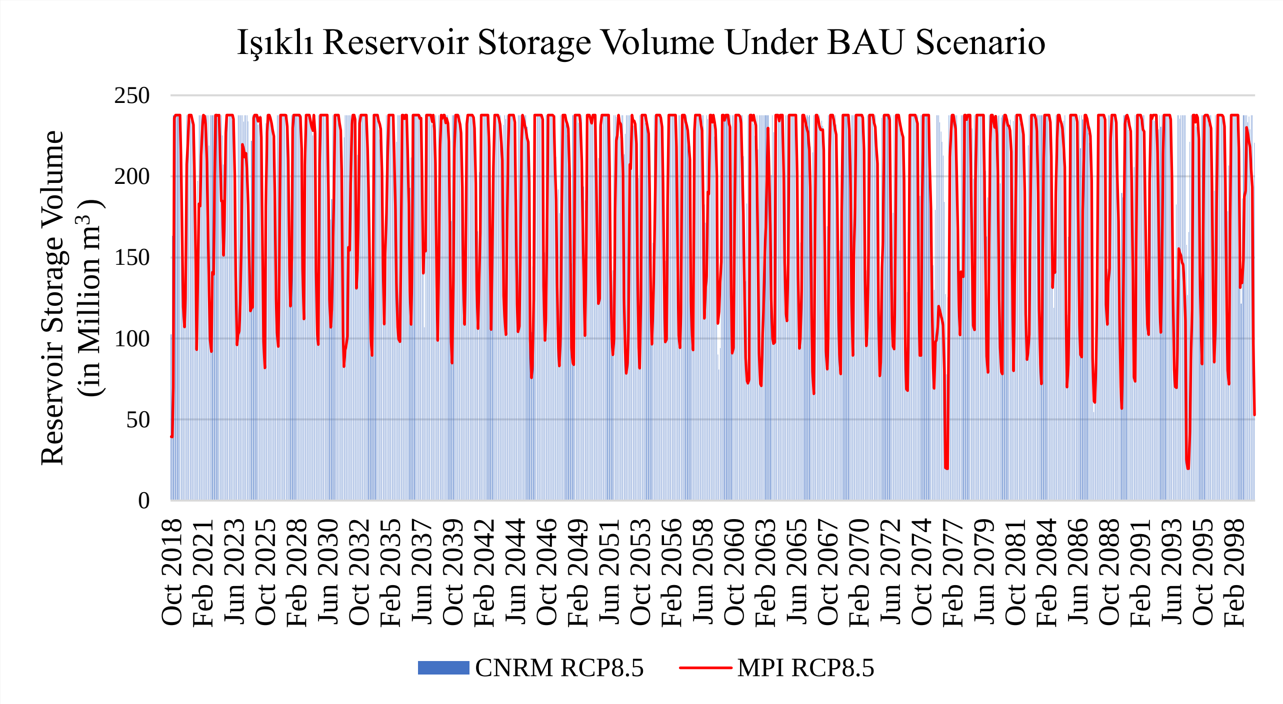

Figure 4.43. Storage volume of Işıklı Reservoir under BAU scenario with CNRM RCP8.5 and MPI RCP8.5 climate change scenarios.

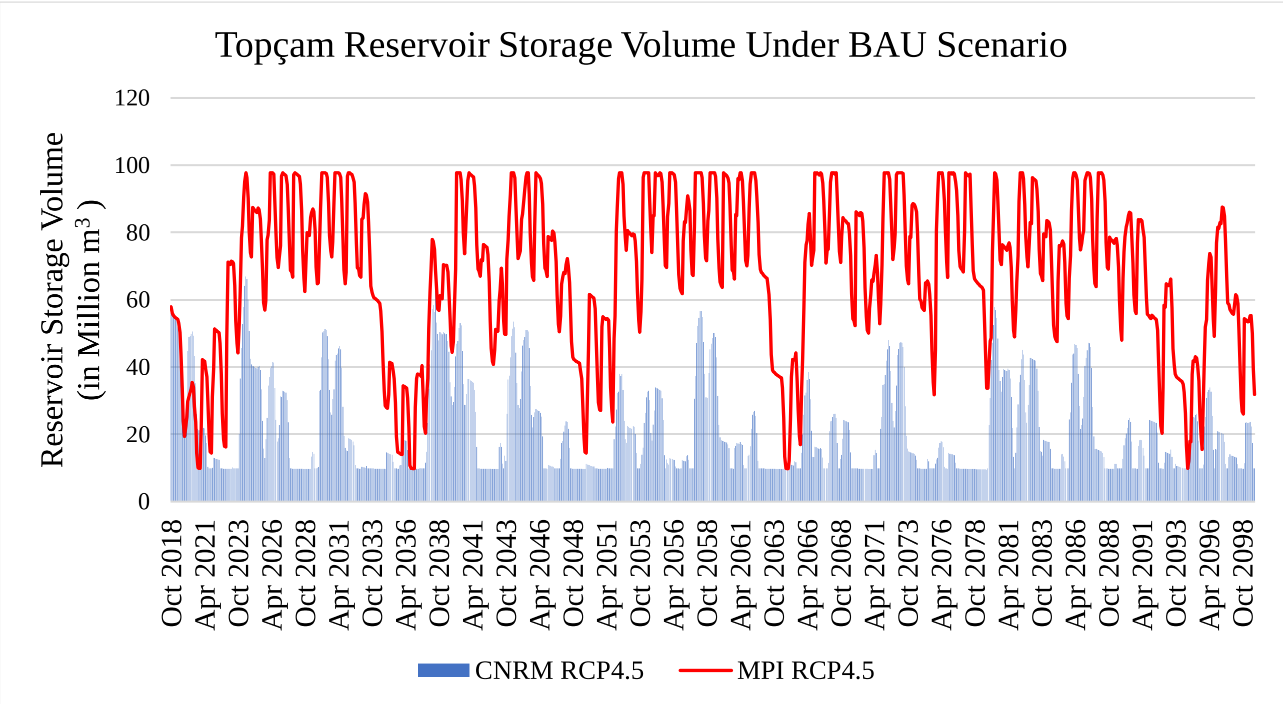

Figure 4.44. Storage volume of Topçam Reservoir under BAU scenario with CNRM RCP4.5 and MPI RCP4.5 climate change scenarios.

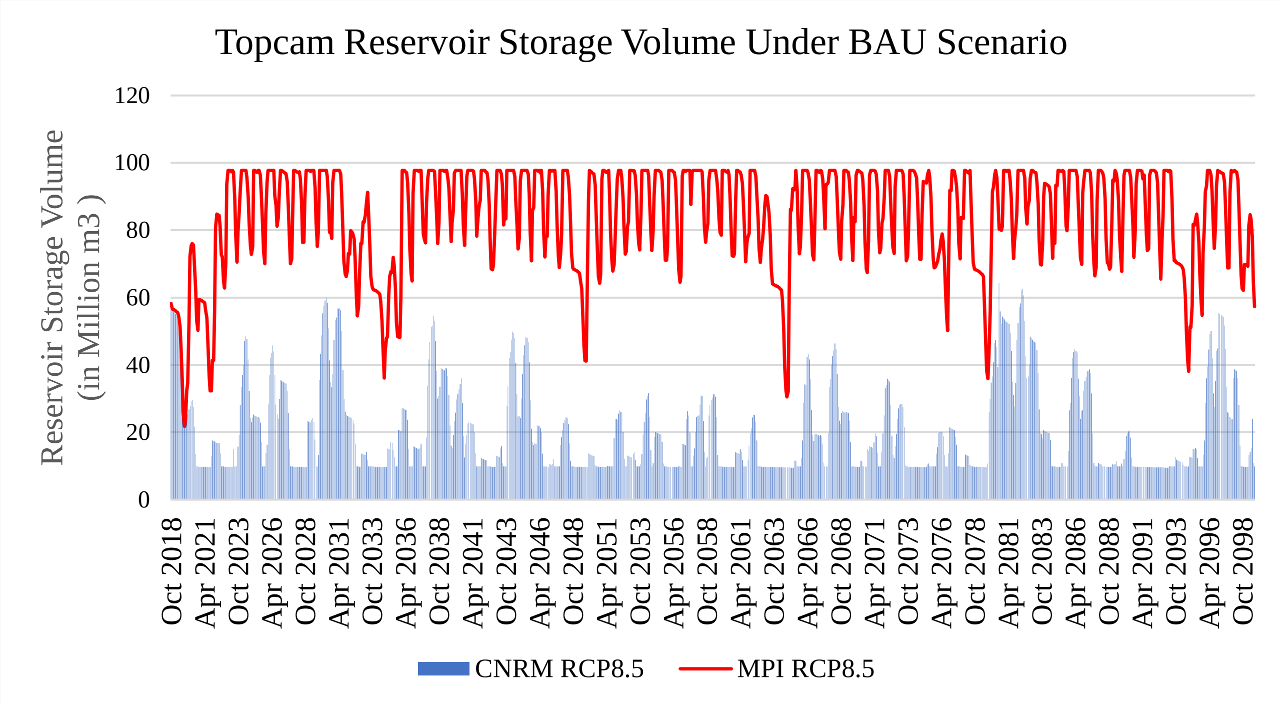

Figure 4.45. Storage volume of Topçam Reservoir under BAU scenario with CNRM RCP8.5 and MPI RCP8.5 climate change scenarios.

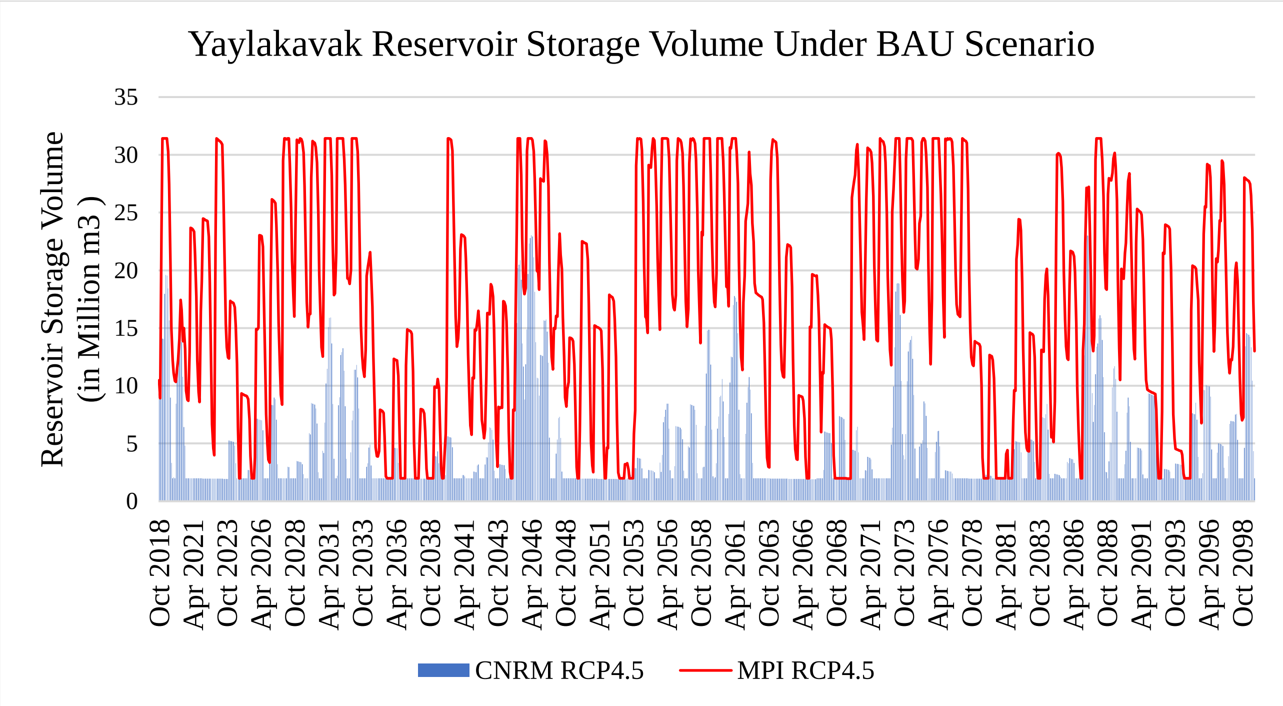

Figure 4.46. Storage volume of Yaylakavak Reservoir under BAU scenario with CNRM RCP4.5 and MPI RCP4.5 climate scenarios.

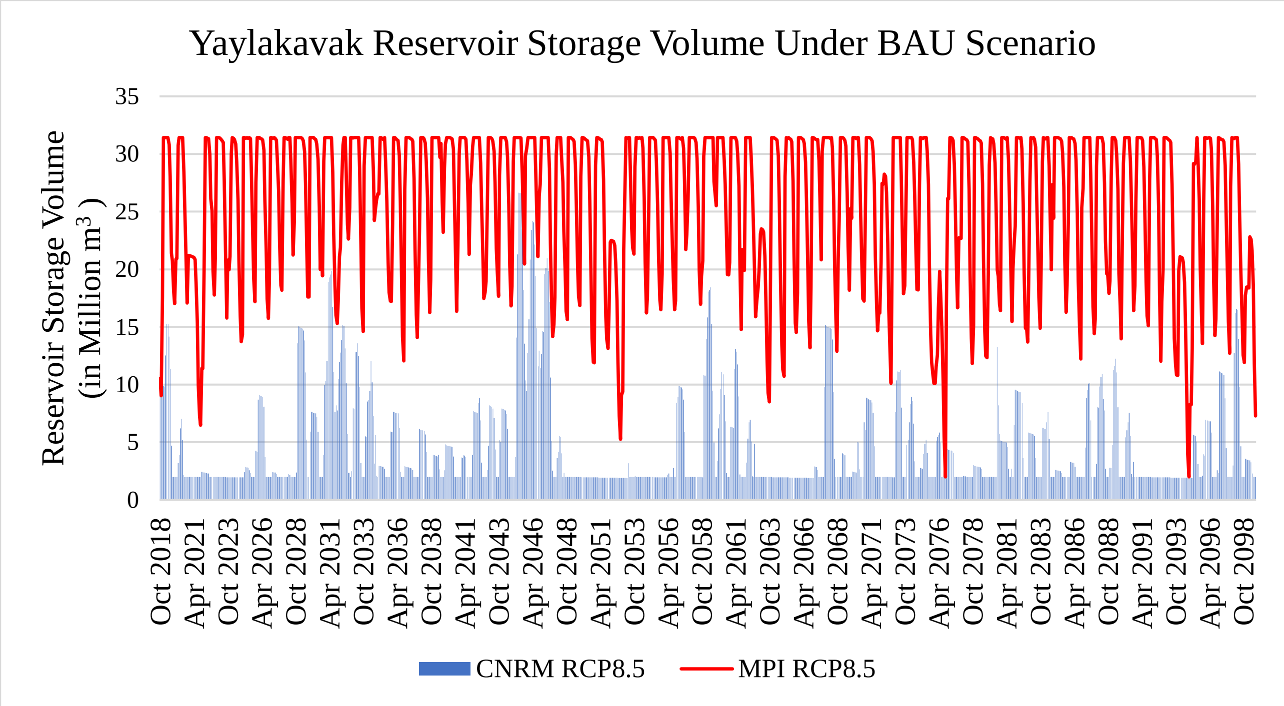

Figure 4.47. Storage volume of Yaylakavak Reservoir under BAU scenario with CNRM RCP4.5 and MPI RCP4.5 climate scenarios.

4.5. Reservoir Storage Volumes Under LE-IILS Scenario

This section displays changes in reservoir storage volumes under LE-IILS scenario, in other words worst-case scenario which results in highest IWR rates. Based on the assumption of LE-IILS, there is no infrastructural change while irrigated land size increases over time throughout all BMB. Therefore, in this section, combined effect of land use change and climate change on reservoir storage rates are observed.

According to results of CNRM-CM5.1 under RCP4.5, as seen in Figure 4.66, rates of average decadal reservoir volume follow generally an increasing trend throughout simulation period with respect to baseline average rates. As displayed in Figure 3.6 shown in section 3.2.2, baseline average rate for total reservoir volume is 1500 million m^3. Based on the results of CNRM-CM5.1 under RCP4.5, average reservoir volume rate increases by 63 million m^3 during simulation period. These two average rates show that total average reservoir volume increases by 4% between 2019 and 2099. However, as displayed in Figure 4.66, it is important to remark here that average decadal volume rate is 13 million m^3 lower than baseline scenario. On the other hand, under RCP8.5 conditions, results of CNRM-CM5.1 represent relatively lower average total storage volume rates compared to that of RCP4.5. Average volume rate of simulation period with respect to baseline scenario, as shown in

Figure 4.66, does barely change throughout simulation period. However, during periods of 2019-2030, 2051-2060, 2071-2080, and 2091-2099 periods, decadal average rates are lower compared to average baseline rate. The declines in average decadal rates for these periods are 18, 58, 22, and 47 million m^3 respectively. The disparity between decadal results and average result of simulation period indicate that fluctuations in average decadal reservoir volume rates prevail throughout simulation period under RCP8.5 conditions.

On the other hand, as shown in Figure 4.66, results of MPI-ESM-MR under RCP4.5 conditions show that average reservoir volume rate is approximately 50 million m^3 lower than average baseline rate. Given that baseline average total reservoir volume rate is 1500 million m^3, the 50 million m^3 decline under RCP4.5 conditions correspond to a 3% decrease. There are also abrupt increases during decades of 2051-2060 and 2091-2099 yet declining rates are dominant throughout simulation period. As seen in Figure 4.66, rates of increase throughout 2051-2060 and 2091-2099 decades are 277 and 64 million m^3. Besides, as a result of higher surface runoff rates observed under RCP8.5 based on the results of MPI-ESM-MR, average reservoir volume rates are relatively higher than both baseline scenario and RCP4.5 results. The average increase with respect to baseline rate is approximately 160 million m^3. This average rate corresponds to an 11% increase. However, it is important to note as well that there are fluctuations under RCP8.5 conditions. As displayed in Figure 4.66, average reservoir volume rates show lower results towards the end of simulation period. These results altogether demonstrate that average volume rates are around 210 million m^3 higher under RCP8.5 conditions compared to that RCP4.5. An increase of 210 million m^3 corresponds to 14% of average baseline reservoir volume rate.

Comparing the results of CNRM-CM5.1 and MPI-ESM-MR under both RCP4.5 and RCP8.5 conditions, it reveals that CNRM-CM5.1 shows no lower average volume rate than that of baseline scenario. However, under RCP4.5 conditions, MPI-ESM-MR indicate that total average reservoir volume is 3% lower than baseline rates. On the other hand, results of MPI-ESM-MR under RCP8.5 show that total average reservoir volume rate 11% higher than baseline rate while the average rate is almost the same based on the results of CNRM-CM5.1.

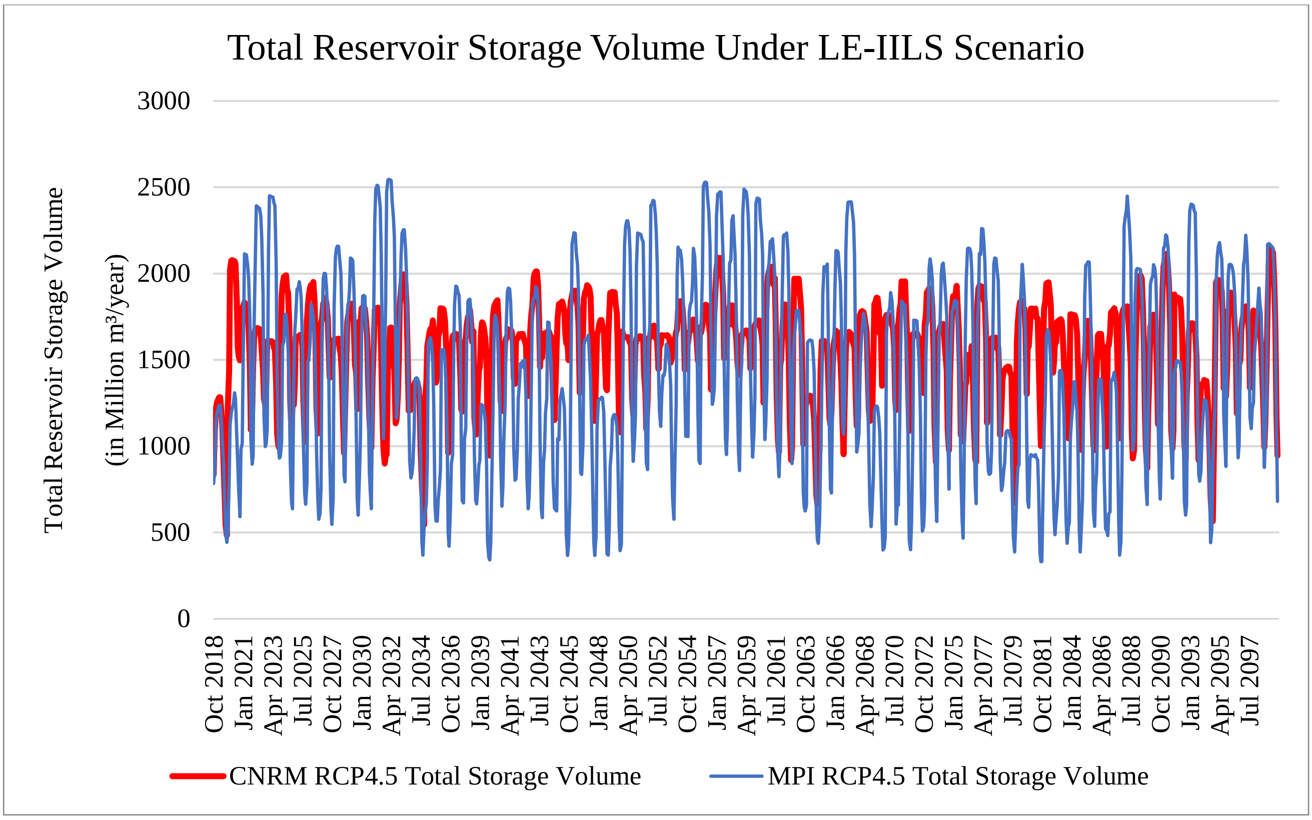

Figure 4.48. Total reservoir storage volume under LE-IILS scenario with CNRM RCP4.5 and MPI RCP4.5 climate change scenarios.

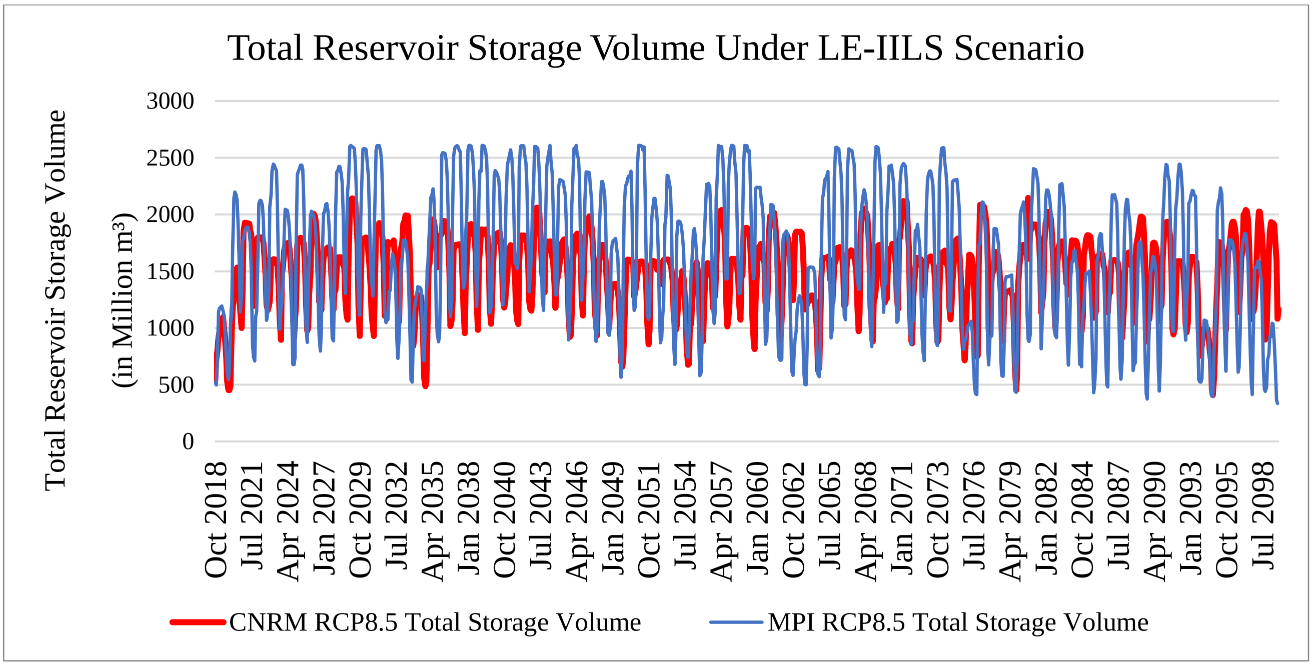

Figure 4.49. Total Storage Volume under LE-IILS scenario with CNRM RCP8.5 and MPI RCP8.5 climate change scenarios.

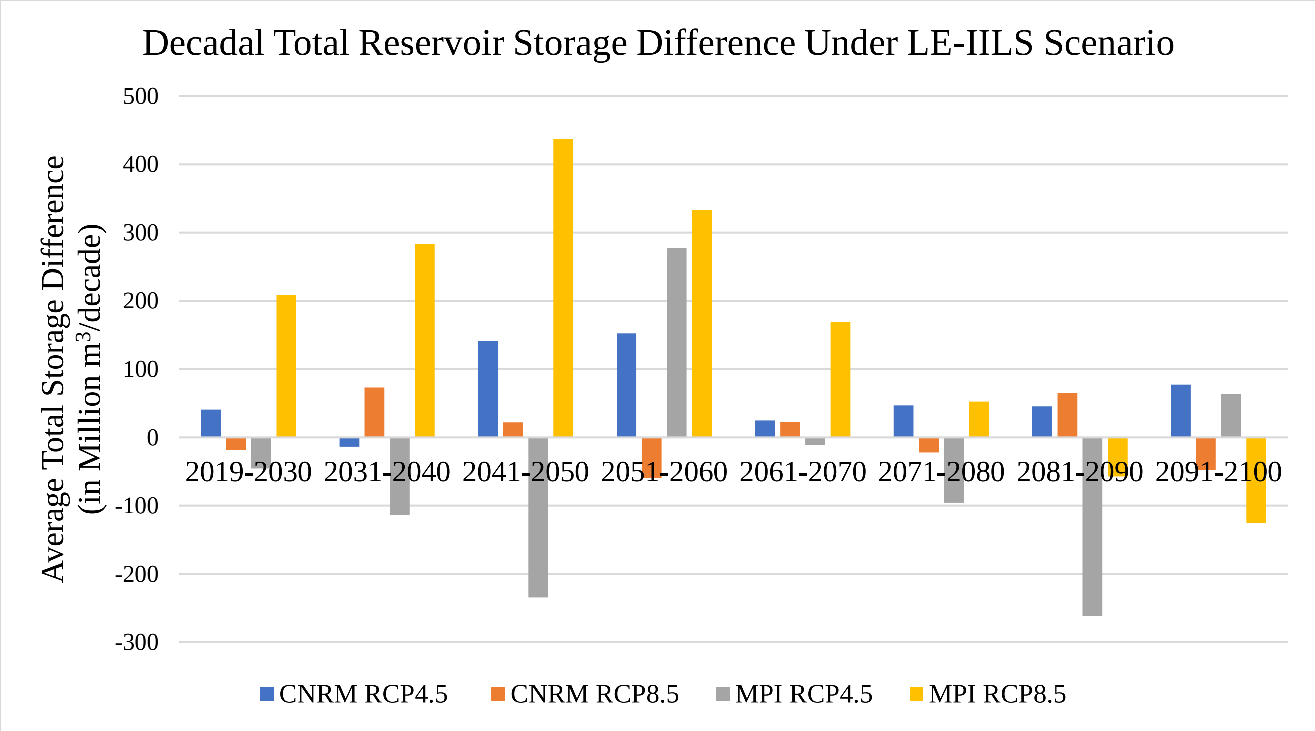

Figure 4.50. Average total reservoir storage difference with respect to baseline scenario under LE-IILS scenario with CNRM RCP4.5, RCP8.5 and MPI RCP4.5, RCP8.5 climate change scenarios.

As to impacts of land use change on each reservoir separately, firstly it is important to note that both CNRM-CM5.1 and MPI-ESM-MR model results show considerably higher surface runoff rates for reservoirs in Denizli compared to that of baseline scenario. Therefore, despite the highly increasing water demand as a result of increased irrigated land size and low efficient irrigation systems, reservoirs in Denizli mostly follow an increasing trend in their average storage volume rates under LE-IILS scenario. On the other side, as displayed in Appendix A, reservoirs in Aydın show decreasing average rates in their volumes according to results of CNRM-CM5.1 under both RCP4.5 and RCP8.5. However, based on the results of MPI-ESM-MR, average volume rates of reservoirs in Aydın increase under RCP8.5 conditions. Under RCP4.5 conditions and the results of MPI-ESM-MR, the average rates still decrease though as in the results of CNRM-CM5.1. In the following paragraph, the examples regarding variations in volume rates of individual reservoirs helps comprehend the situation more thoroughly and clearly.

Average storage volume of Adıgüzel reservoir, as seen in Appendix A, is 70% higher under RCP4.5 compared to its average baseline reservoir rates based on the results of CNRM-CM5.1. Besides, under RCP8.5, average storage volume of Adıgüzel reservoir is 60% higher compared to baseline average volume. Similar trends are observed for Işıklı reservoir as well under the results of CNRM-CM5.1. Under RCP4.5, as in Appendix A, average volume of Işıklı reservoir between 2019 and 2100 is 63% higher than its average baseline rate. Additionally, under RCP8.5, average volume rate is 57% higher for Işıklı reservoir. On the other hand, results of MPI-ESM-MR present remarkably lower increasing rates for reservoirs located in Denizli. For Adıgüzel reservoir, the rates of increase are 9% and 5% under RCP4.5 and RCP8.5 respectively. Besides, for Işıklı reservoirs, the rates of increase are 35% and 29% under the same conditions.

For average storage volume of Çine reservoir, as seen in Appendix A, the results of CNRM-CM5.1. under RCP4.5 show a 60% decline rate. Under RCP8.5 conditions, this average decline rate reaches up to 71%. Moreover, according to results of CNRM-CM5.1, the average storage volume rates of Topçam reservoir show a 64% and 65% decline under RCP4.5 and RCP8.5 respectively. On the other hand, according to results of MPI-ESM-MR, reservoirs in Aydın are relatively better off. The decline rates in average volume of Çine reservoir are 35% and 18% under RCP4.5 and RCP8.5 conditions respectively. Besides, the decline rate in average volume of Topçam reservoir is 10% under RCP4.5 and the rate of increase rate is 47% under RCP8.5 conditions.

Lastly, it is important to note that the reservoirs located in the same city show differential variations in their average storage volume rates even though climatic conditions are the same for them. There are particularly two important reasons for the differences in between under LE-IILS scenario. Firstly, LE-IILS is the scenario including irrigated land expansion and the rate of irrigated land expansion rates are not the same for all reservoirs. Land expansion rates are partitioned among reservoirs based on reservoir size. Consequently, relatively bigger reservoirs such as Adıgüzel is affected more heavily by land use change compared to other two reservoirs in Denizli. Similarly, Çine reservoir of Aydın is bigger compared to Topçam reservoir and the impact of land change is comparatively more significant on Çine. Secondly, the differences in average baseline rate of annual water requirement per hectare which varies reservoir to reservoir. The differences are especially important because increases in IWR rates are calculated based on percentages of historical average values.

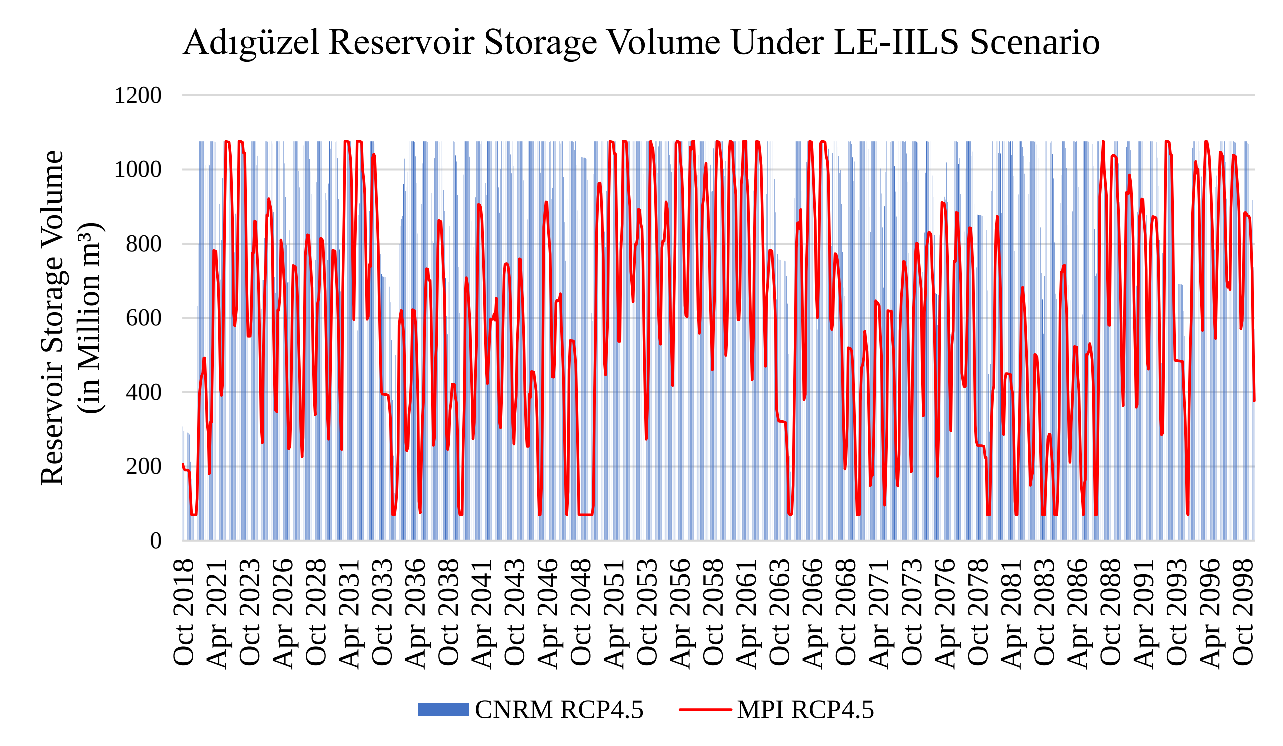

Figure 4.51. Storage volume of Adıgüzel Reservoir under LE-IILS scenario with CNRM RCP4.5 and MPI RCP4.5 climate change scenarios.

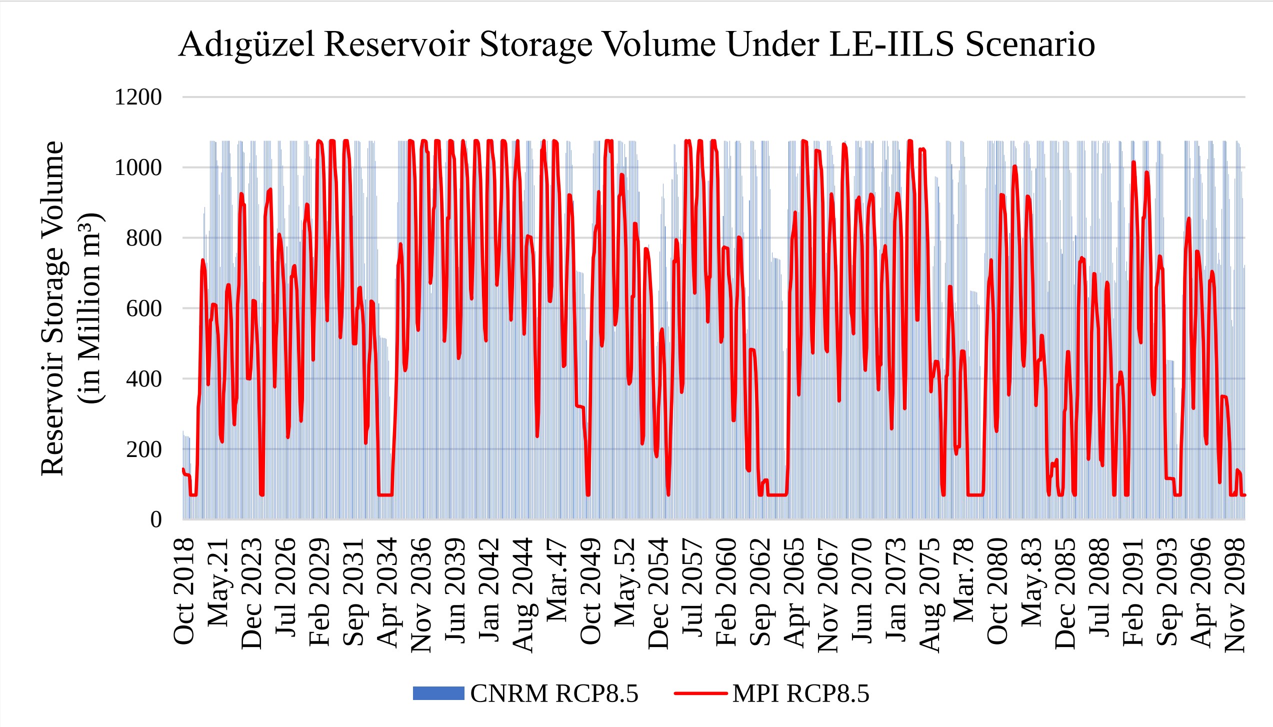

Figure 4.52. Storage volume of Adıgüzel Reservoir under LE-IILS scenario with CNRM RCP8.5 and MPI RCP8.5 climate change scenarios.

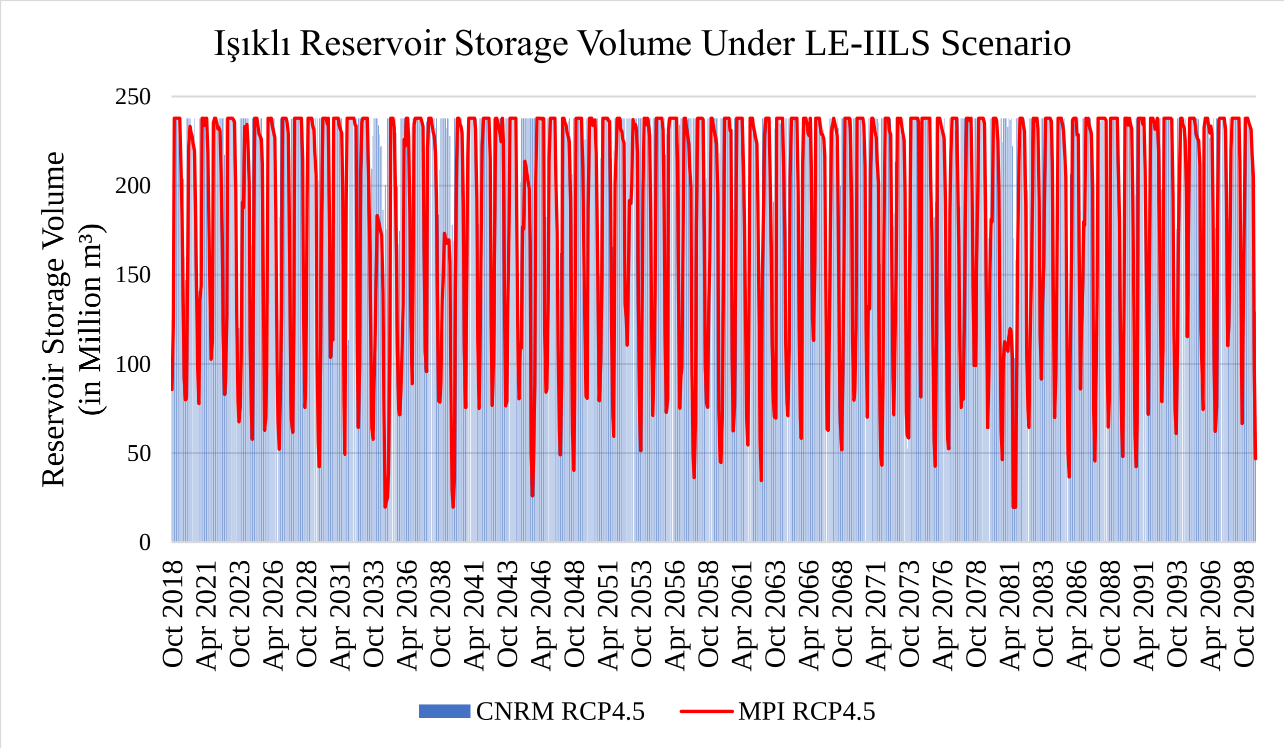

Figure 4.53. Storage volume of Işıklı Reservoir under LE-IILS scenario with CNRM RCP4.5 and MPI RCP4.5 climate change scenarios.

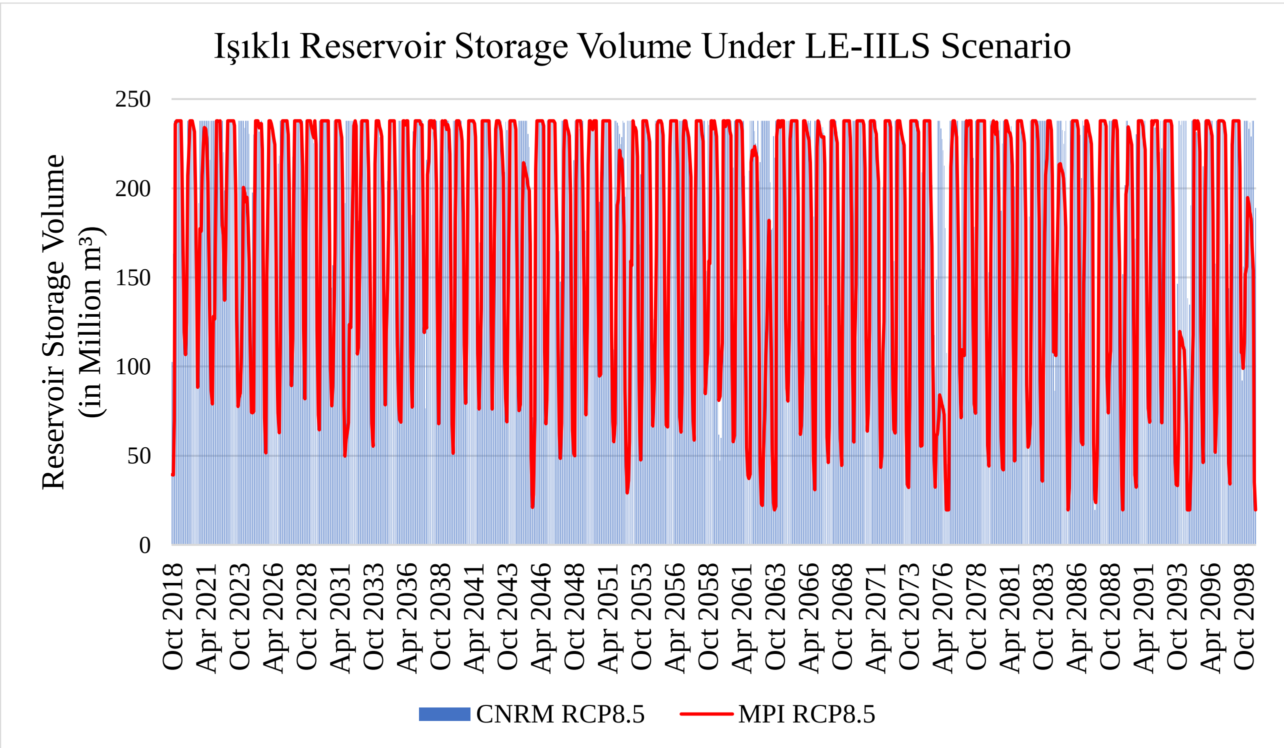

Figure 4.54. Storage volume of Işıklı Reservoir under LE-IILS scenario with CNRM RCP8.5 and MPI RCP8.5 climate change scenarios.

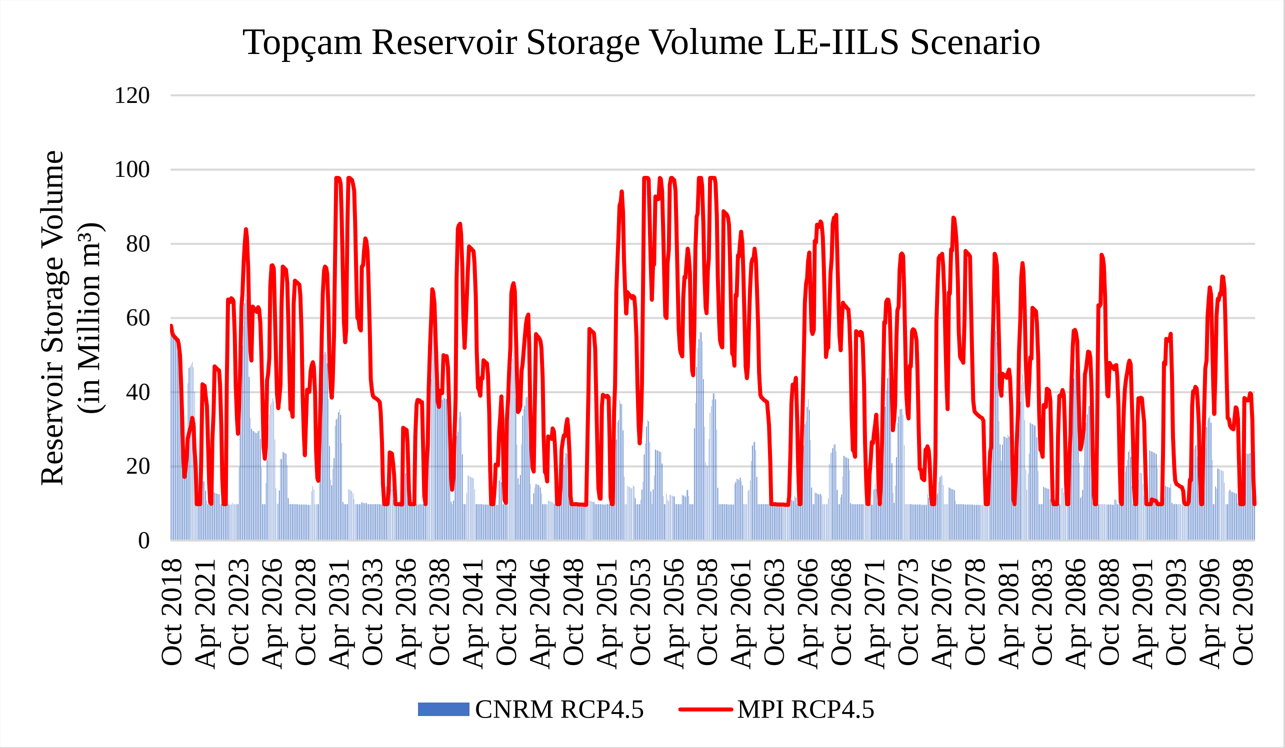

Figure 4.55. Storage volume of Topçam Reservoir under LE-IILS scenario with CNRM RCP4.5 and MPI RCP4.5 climate change scenarios.

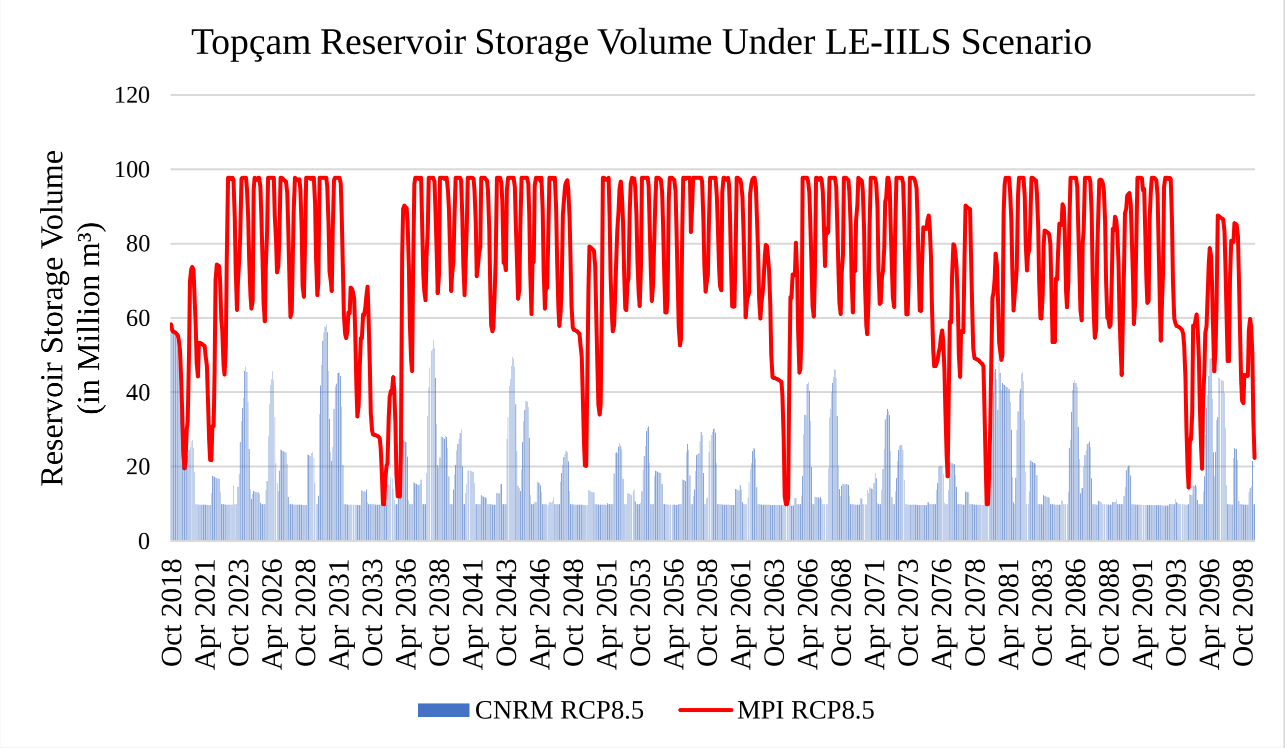

Figure 4.56. Storage volume of Topçam Reservoir under LE-IILS scenario with CNRM RCP8.5 and MPI RCP8.5 climate change scenarios.

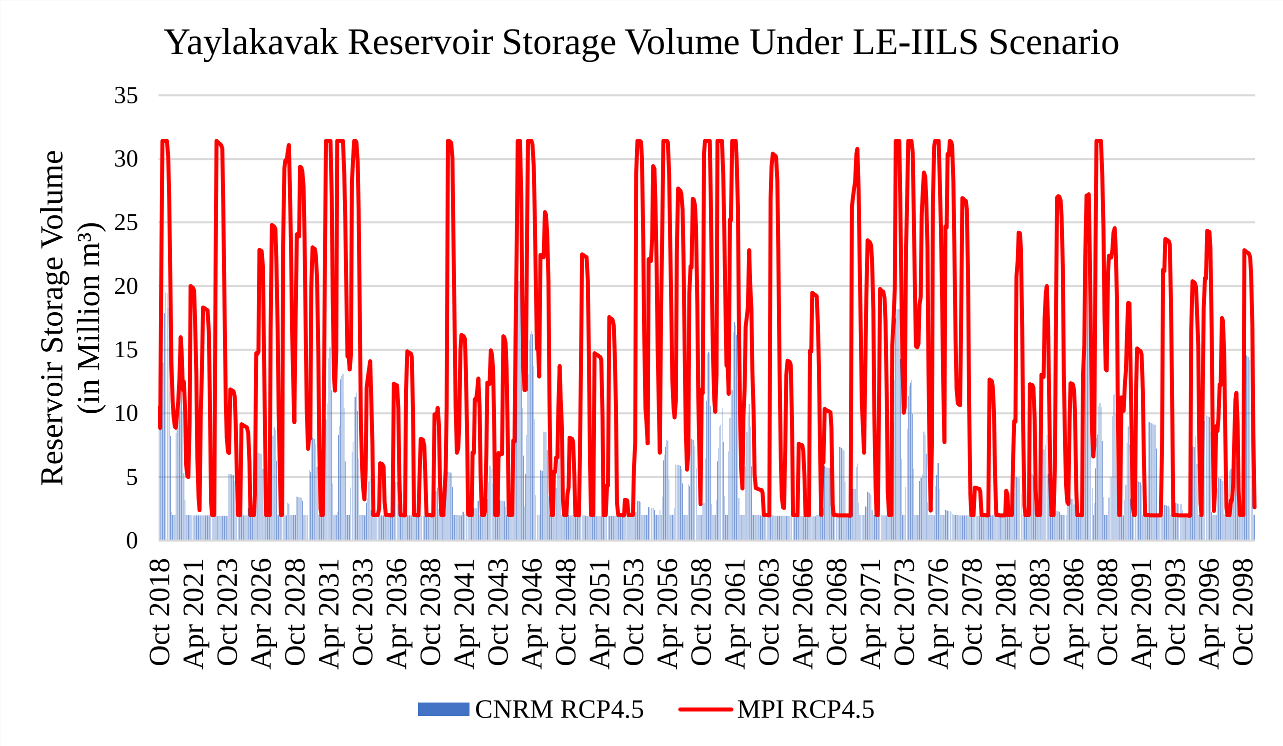

Figure 4.57. Storage volume of Yaylakavak Reservoir under LE-IILS scenario with CNRM RCP8.5 and MPI RCP8.5 climate change scenarios.

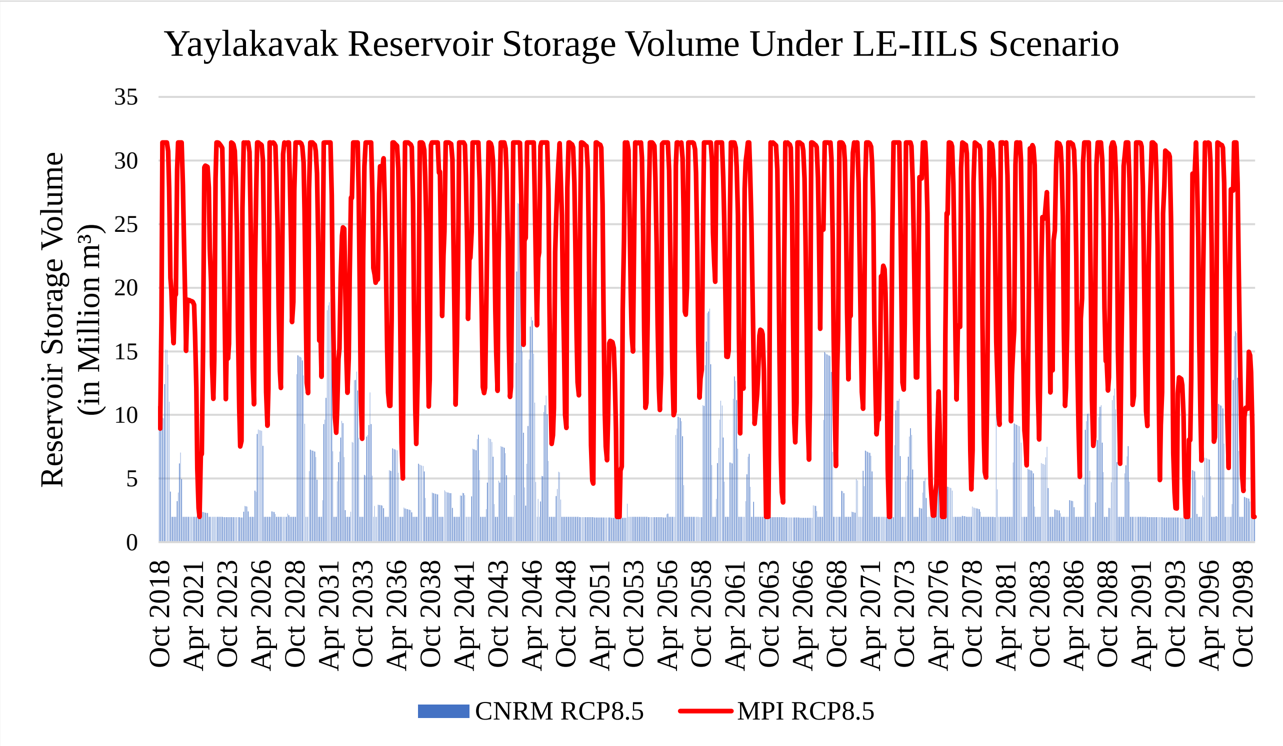

Figure 4.58. Storage volume of Yaylakavak Reservoir under LE-IILS scenario with CNRM RCP8.5 and MPI RCP8.5 climate change scenarios.

4.6. Reservoir Storage Volumes Under HE-NLUC Scenario

This section displays changes in reservoir storage volumes under HE-NLUC scenario (best-case scenario). Based on the assumption of HE-NLUC, there are infrastructural changes and full transition to high-efficiency drip irrigation system takes place while irrigated land size remains constant throughout all BMB. Therefore, in this section, combined effect of infrastructural changes and climate change on reservoir storage rates are observed.

Under RCP4.5 scenario of CNRM-CM5.1, as seen in Figure 4.93, decadal average rates of total reservoir storage volume are always higher than baseline scenario rates throughout simulation period. Average baseline rate of total reservoir storage volume is 1500 million m^3. On the other hand, as seen in Figure 4.93, the average storage volume rate is approximately 220 million m^3 higher than average baseline rate under RCP4.5 conditions and CNRM-CM5.1 results. Hence, the average storage volume rate of simulation period is 15% higher than baseline scenario. Reviewing decadal variations under RCP4.5, Figure 4.93 indicates that rates of increase in average storage volume are higher during first half of simulation period. The decadal difference of reservoir storage volume between simulation and observation period increases from 170 to 252 million m^3 between 2019 and 2050 while the difference in between drops down to 192 million m^3 towards the end of simulation period. On the other hand, as seen in Figure 4.93, CNRM-CM5.1 results under RCP8.5 conditions show the average storage volume rate is approximately 240 million m^3 higher than average baseline rate. Therefore, the average storage volume of simulation period is 16% higher than baseline scenario. This means that results under RCP8.5 conditions are slightly higher compared to that of RCP4.5. As to decadal variations of total reservoir storage volume under RCP8.5 conditions, as seen in Figure 4.93, the difference between average decadal volume and baseline rate get bigger between 2019 and 2040 from 140 to 415 million m^3. In the following decades, the difference in between declines down to 260 million m^3 towards the end of simulation period.

According to results of MPI-ESM-MR under RCP4.5, as seen in Figure 4.13, the average decadal difference of total reservoir storage volume with respect to baseline rates is approximately 630 million m^3 higher during simulation period. Given that baseline reservoir volume rate is 1500 million m^3, the 630 million m^3 difference in between shows that total reservoir volume increases by 42% on average for simulation period. According to results of CNRM-CM5.1, on the other side, the rates of increase are 15% and 16% under RCP4.5 and RCP8.5 respectively. The disparity between results is considerable once again. As to decadal variations of average total reservoir volume under RCP4.5 and MPI-ESM-MR, as shown in Figure 4.93, the decadal increase of total storage volume goes up from 457 to 757 million m^3 between 2019 and 2060. In the following decades, the decadal increase with respect to baseline rate drops down to 660 million m^3. Besides, under RCP8.5 conditions and MPI-ESM-MR results, Figure 4.93 shows that total average reservoir storage volume during simulation period is approximately 780 million m^3 higher than average baseline rate. Given that baseline reservoir volume rate is 1500 million m^3, the 780 million m^3 difference in between shows that total reservoir volume increases by 52% on average for simulation period. The rate of increase is 42% under RCP4.5 conditions and MPI-ESM-MR results. Besides, according to results of CNRM-CM5.1, the rates of increase are 15% and 16% under RCP4.5 and RCP8.5 respectively. Lastly, as to decadal variations of total storage volume rates under RCP8.5 and MPI-ESM-MR results, as shown in Figure 4.93, the average decadal difference increases from 668 to 868 million m^3 between 2019 and 2060. In the following decades, the average difference drops down to 730 million m^3.

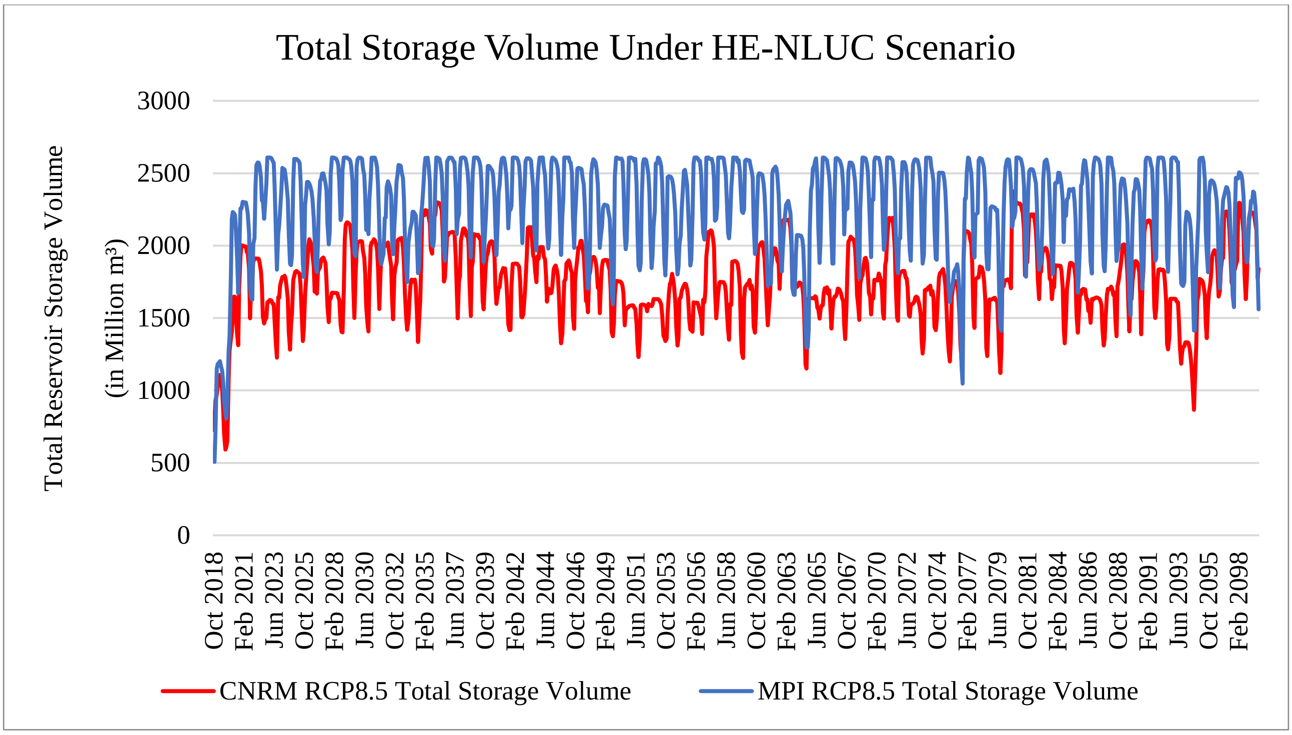

Figure 4.59. Total reservoir storage volume under HE-NLUC scenario with CNRM RCP4.5 and MPI RCP4.5 climate change scenarios.

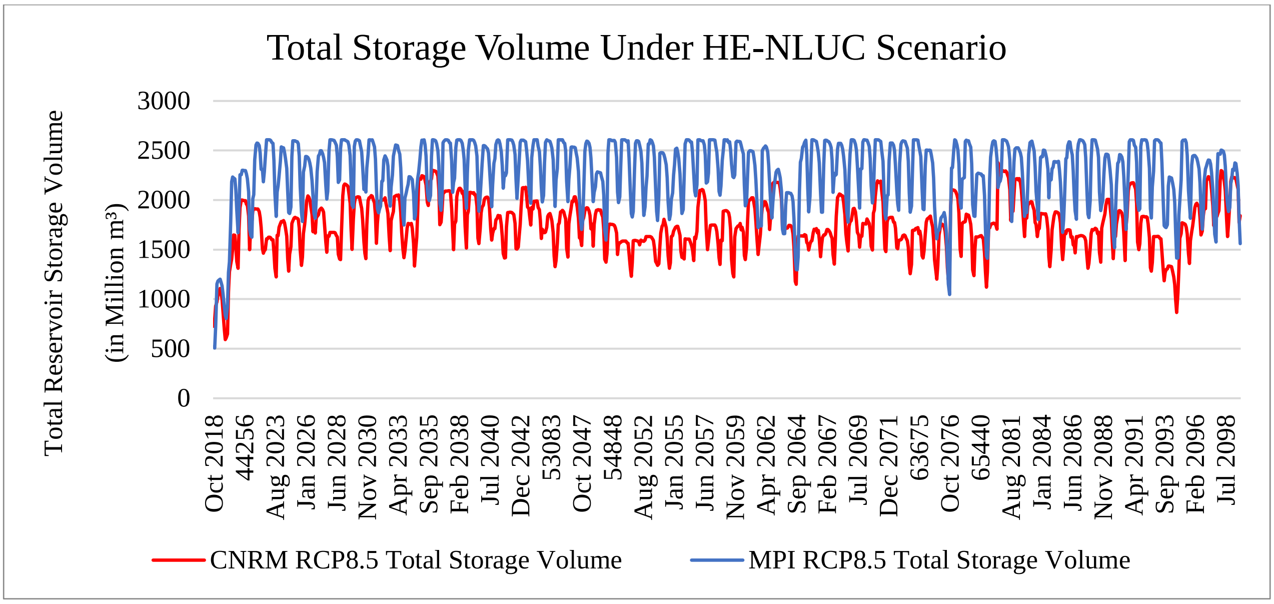

Figure 4.60. Total reservoir storage Volume under HE-NLUC scenario with CNRM RCP8.5 and MPI RCP8.5 climate change scenarios.

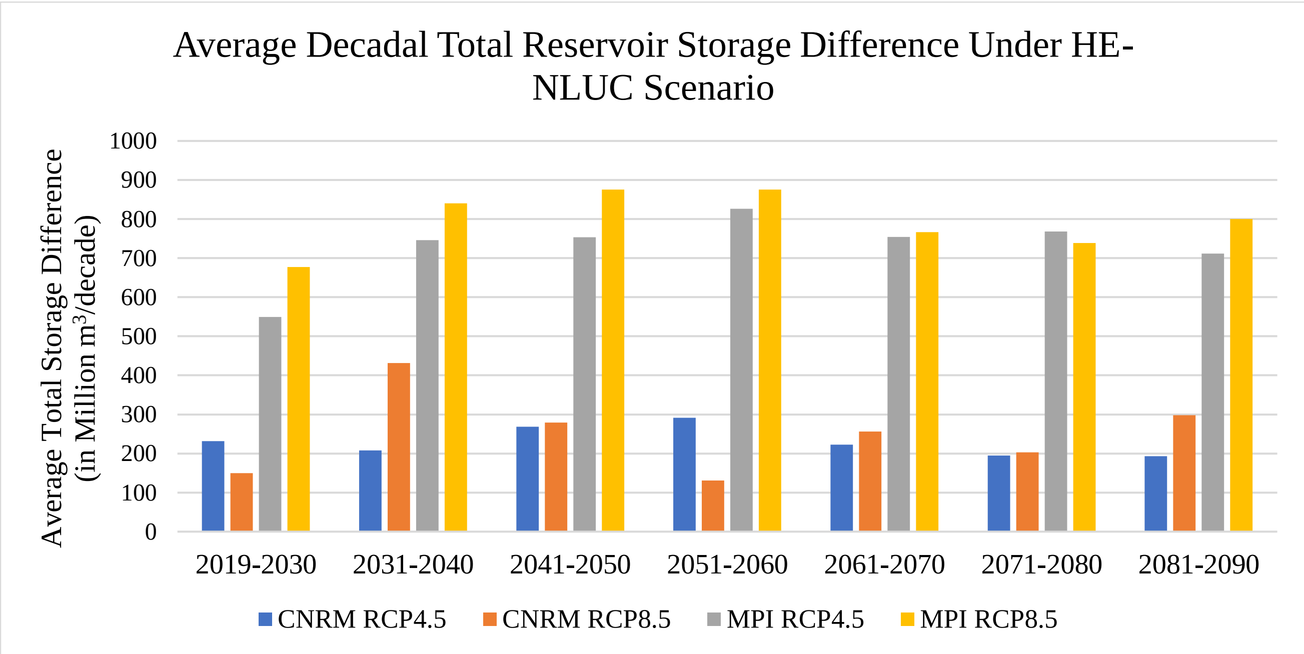

Figure 4.61. Average total reservoir storage difference with respect to baseline scenario under HE-NLUC scenario with CNRM RCP4.5, RCP8.5 and MPI RCP4.5, RCP8.5 climate change scenarios.

As to impacts of climatic conditions on each reservoir separately under HE-NLUC scenario, it is seen that there exist again two distinct group of reservoirs, namely reservoirs located in Aydın and Denizli. Since lowest water demand rates take place under HE-NLUC scenario, naturally highest reservoir storage volume rates are observed under this scenario for all reservoirs.

According to CNRM-CM5.1 results under RCP4.5, as shown in Appendix A, the average decline rates of volume of Topçam reservoir with respect to baseline scenario are 35% and 42% under RCP4.5 and RCP8.5 respectively. Besides, for Yaylakavak reservoir, the decline rates are 62% and 63% under RCP4.5 and RCP8.5 respectively. On the other hand, results of MPI-ESM-MR show that the average storage volume of Topçam reservoir is higher compared to that CNRM-CM5.1. As displayed in Appendix A, average volume of Topçam reservoir is 66% and 78% higher than baseline rate under RCP4.5 and RCP8.5 conditions respectively. Moreover, average volume of Yaylakavak reservoir is 33% and 55% higher than baseline rate under RCP4.5 and RCP8.5 conditions respectively. Therefore, MPI-ESM-MR results show increasing storage volume rates for reservoirs situated in Aydın while CNRM-CM5.1 results indicate decreasing rates for the same reservoirs.

On the other side, reservoirs in Denizli show increasing average storage volume rates under the results of both CNRM-CM5.1 and MPI-ESM-MR. As shown in Appendix A, according to results of CNRM-CM5.1, average storage volume rates of Adıgüzel reservoir are 83% and 79% higher than average baseline rate under RCP4.5 and RCP8.5 respectively. Besides, for Işıklı reservoir, the rates of increase 71% and 69% under RCP4.5 and RCP8.5 respectively. On the other hand, results of MPI-ESM-MR show that the average storage volume of Adıgüzel reservoir is lower compared to that of CNRM-CM5.1. As displayed in Appendix A, average volume of Adıgüzel reservoir is 69% and 64% higher than baseline rate under RCP4.5 and RCP8.5 conditions respectively. Moreover, average volume of Işıklı reservoir is 58% and 55% higher than baseline rate under RCP4.5 and RCP8.5 conditions respectively. These rates are 71% and 69% for Işıklı reservoir under the results of CNRM-CM5.1. Therefore, it reveals that MPI-ESM-MR results show higher increasing storage volume rates for reservoirs situated in Denizli compared to CNRM-CM5.1.

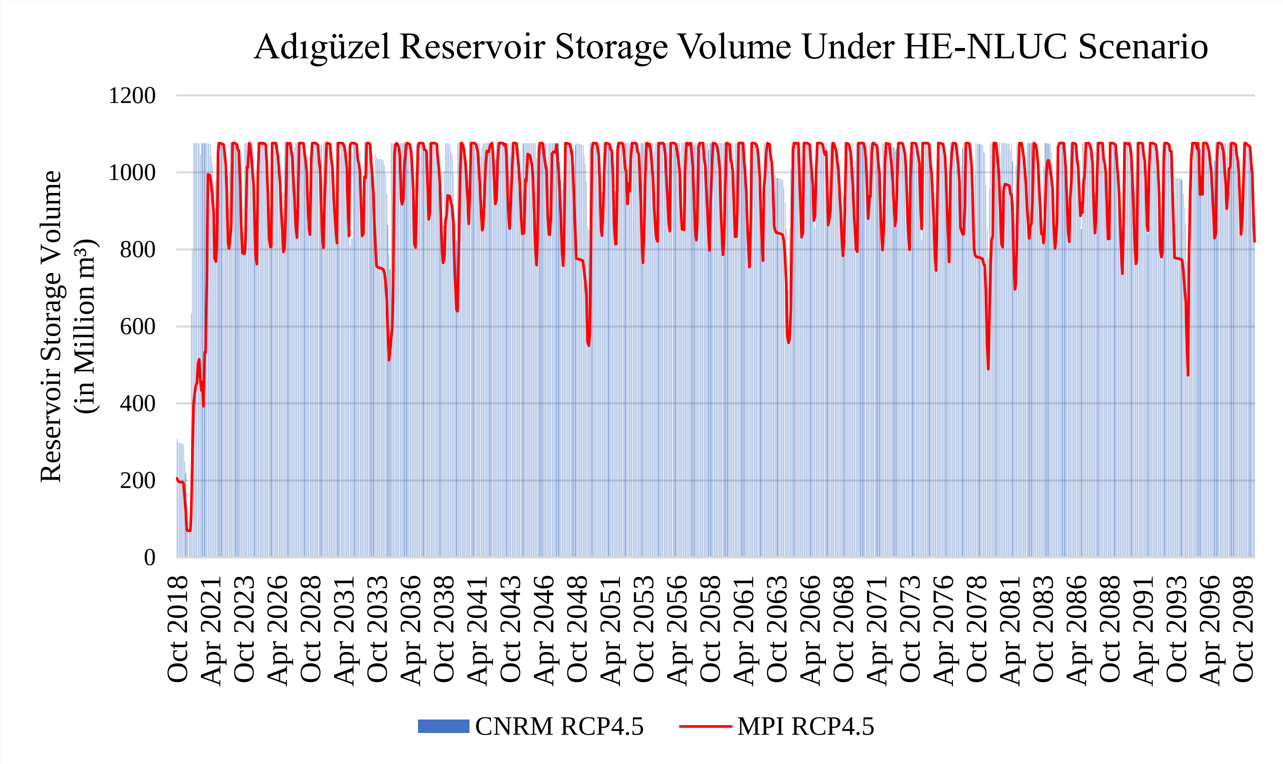

Figure 4.62. Storage volume of Adıgüzel Reservoir under HE-NLUC scenario with CNRM RCP4.5 and MPI RCP4.5 climate change scenarios.

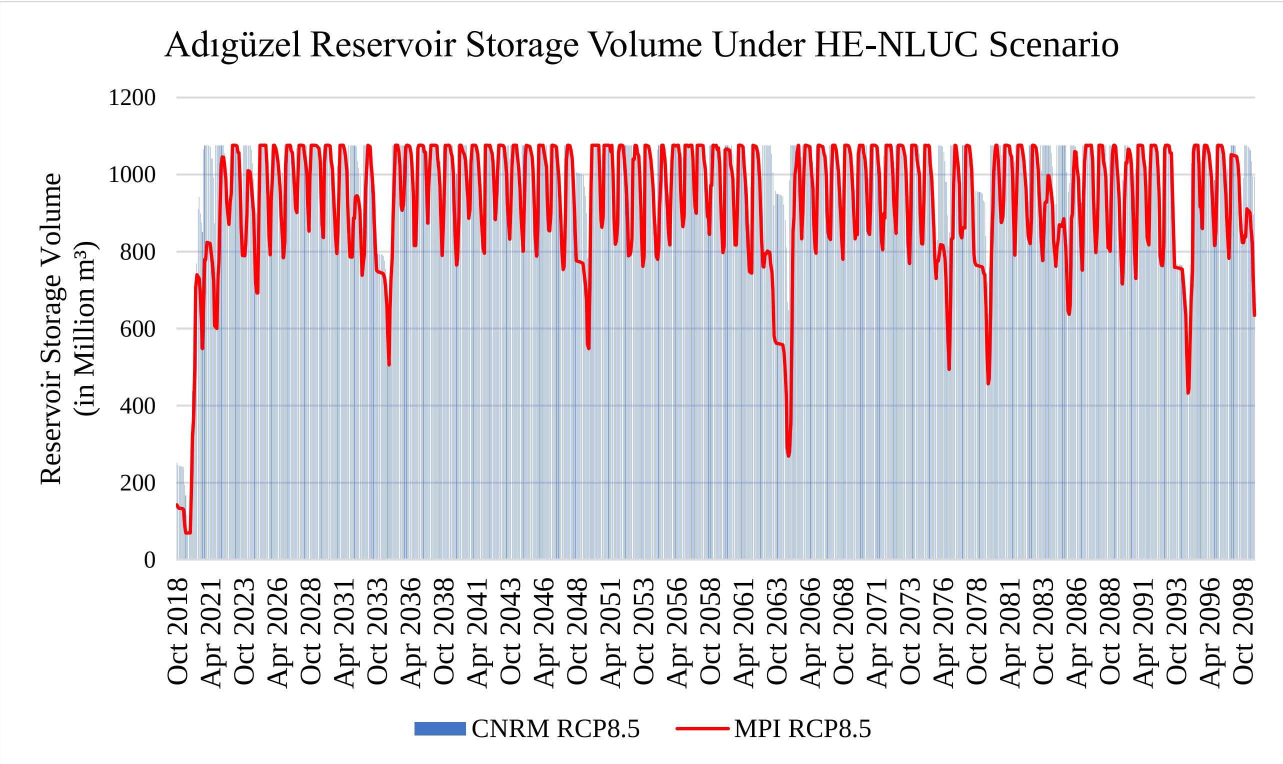

Figure 4.63. Storage volume of Adıgüzel Reservoir under HE-NLUC scenario with CNRM RCP8.5 and MPI RCP8.5 climate change scenarios.

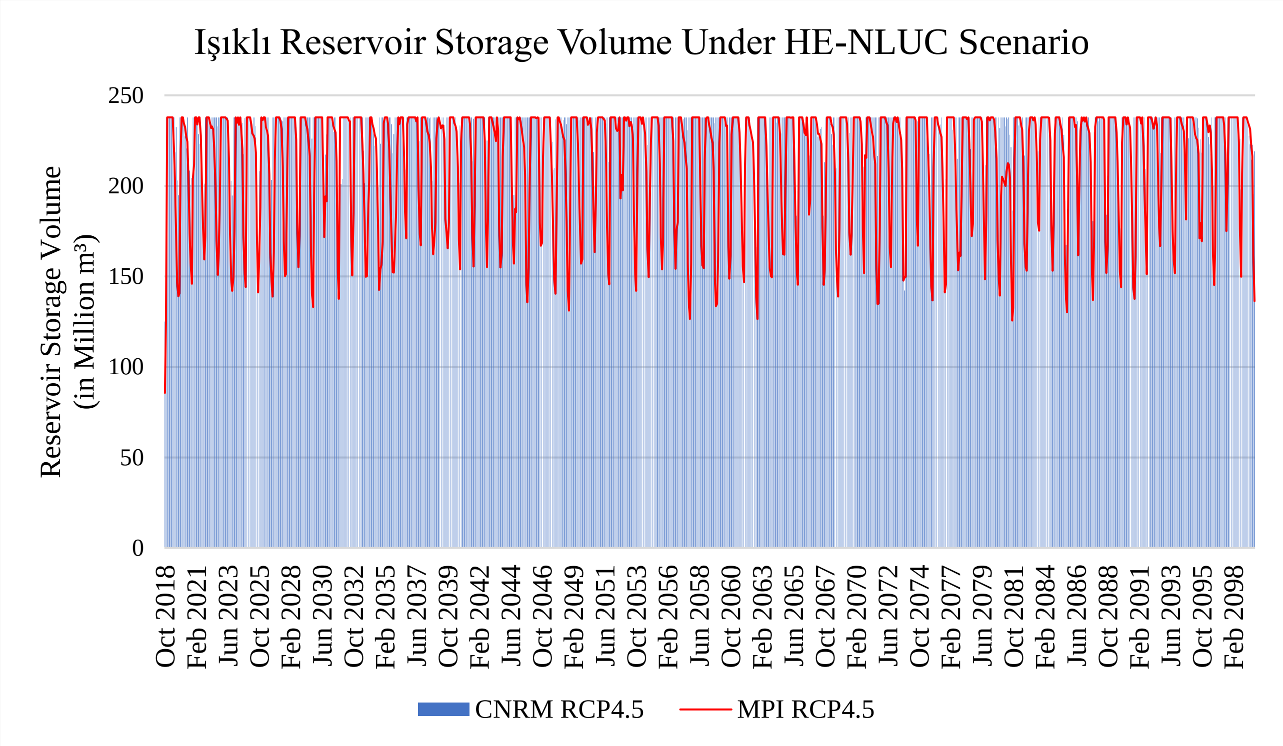

Figure 4.64. Storage volume of Işıklı Reservoir under HE-NLUC scenario with CNRM RCP4.5 and MPI RCP4.5 climate change scenarios.

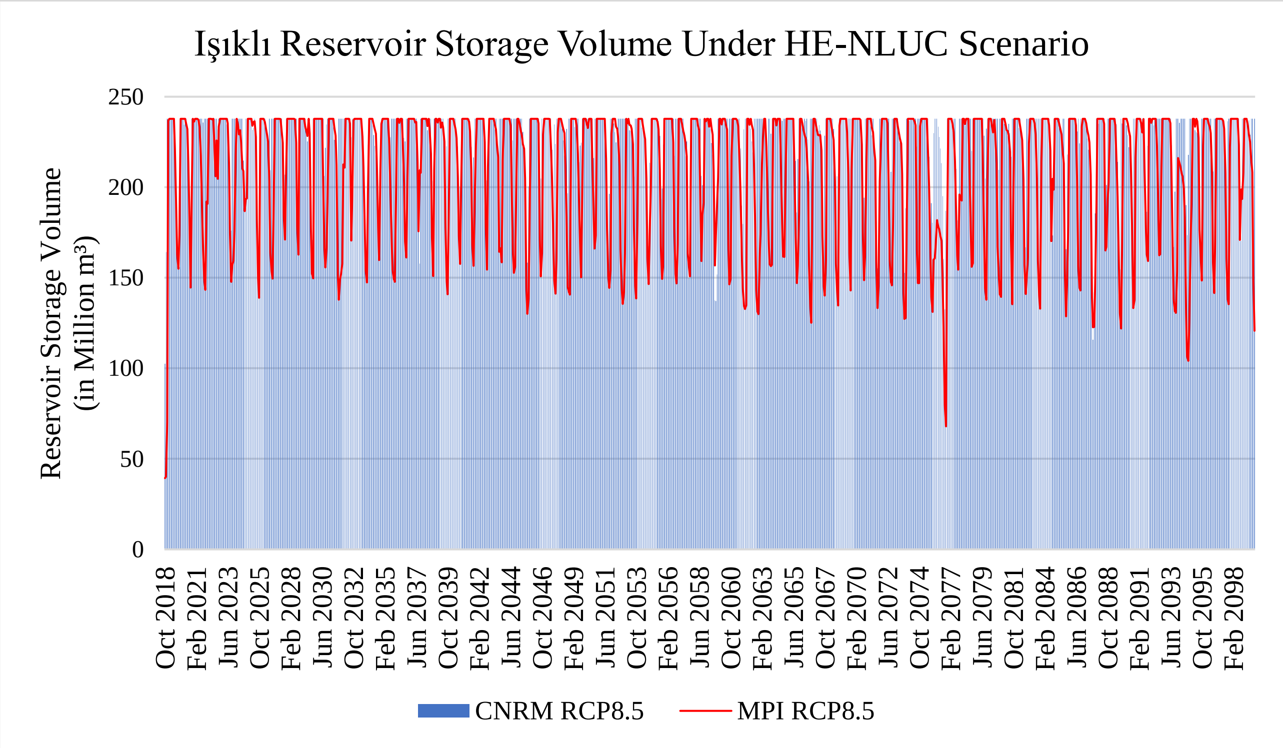

Figure 4.65. Storage volume of Işıklı Reservoir under HE-NLUC scenario with CNRM RCP8.5 and MPI RCP8.5 climate change scenarios.

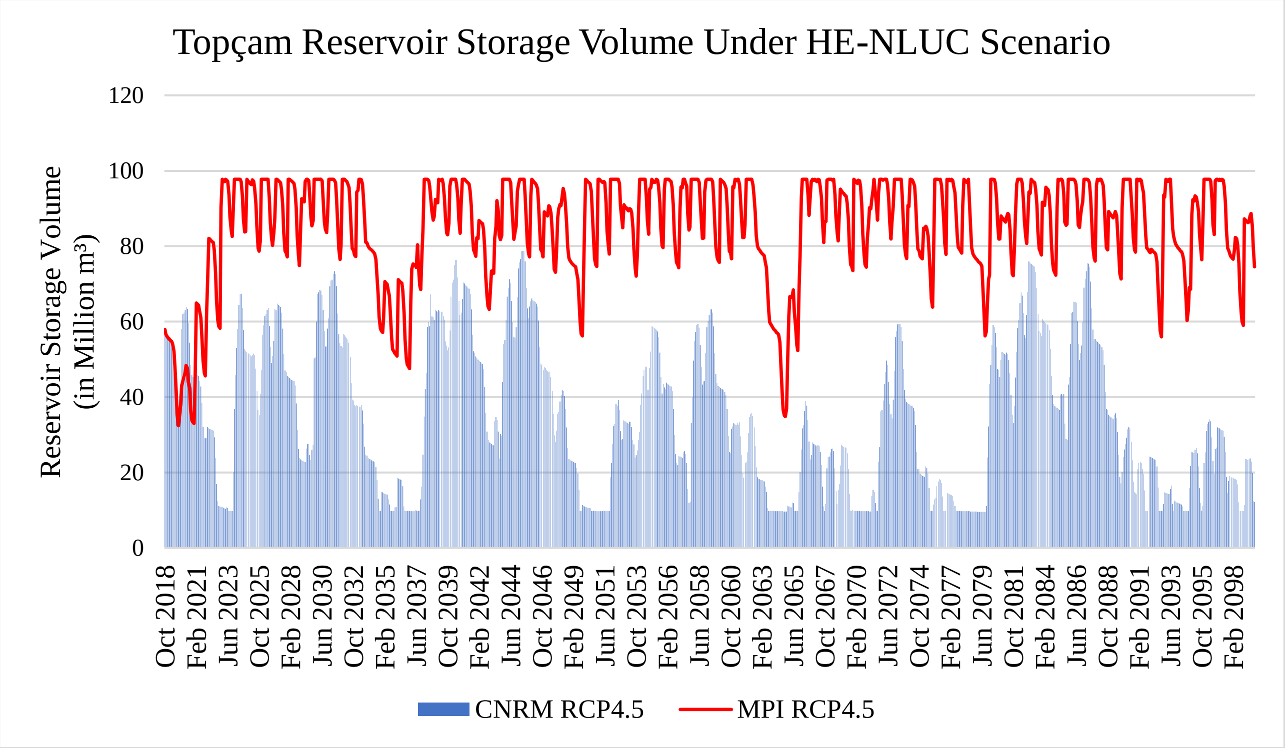

Figure 4.66. Storage volume of Topçam Reservoir under HE-NLUC scenario with CNRM RCP4.5 and MPI RCP4.5 climate change scenarios.

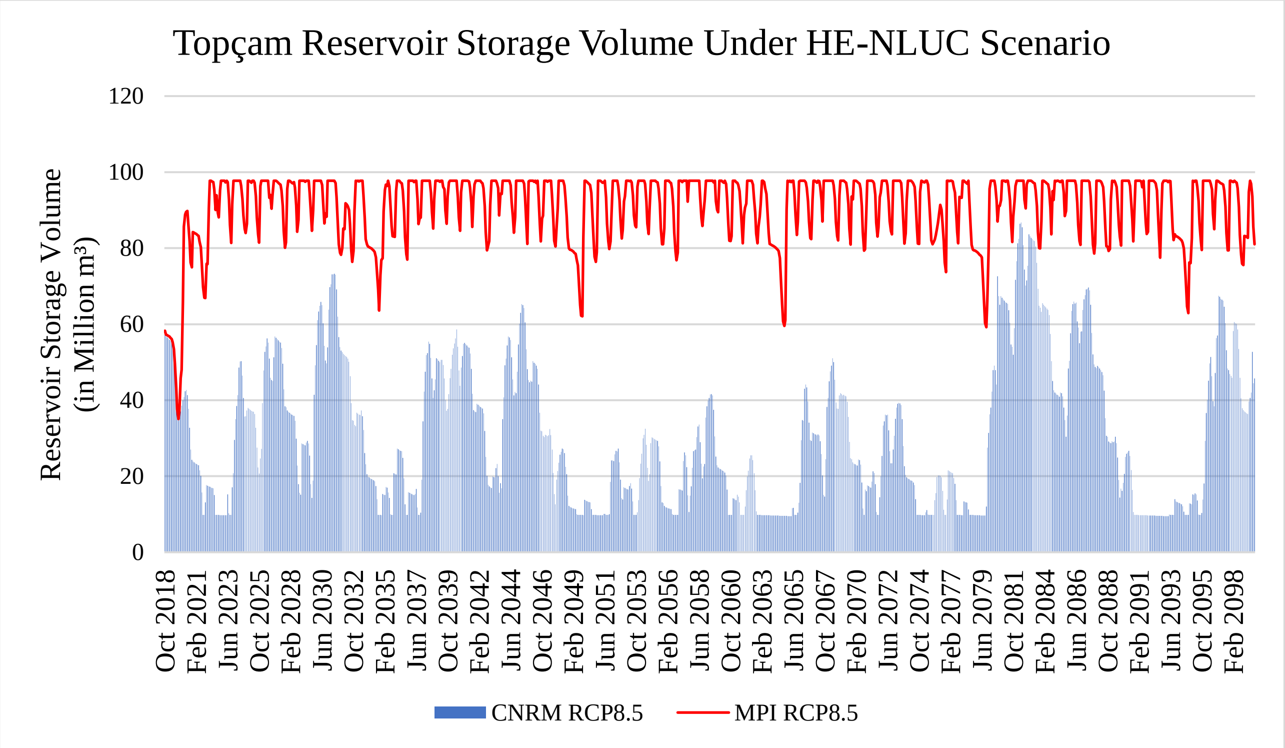

Figure 4.67. Storage volume of Topçam Reservoir under HE-NLUC scenario with CNRM RCP8.5 and MPI RCP8.5 climate change scenarios.

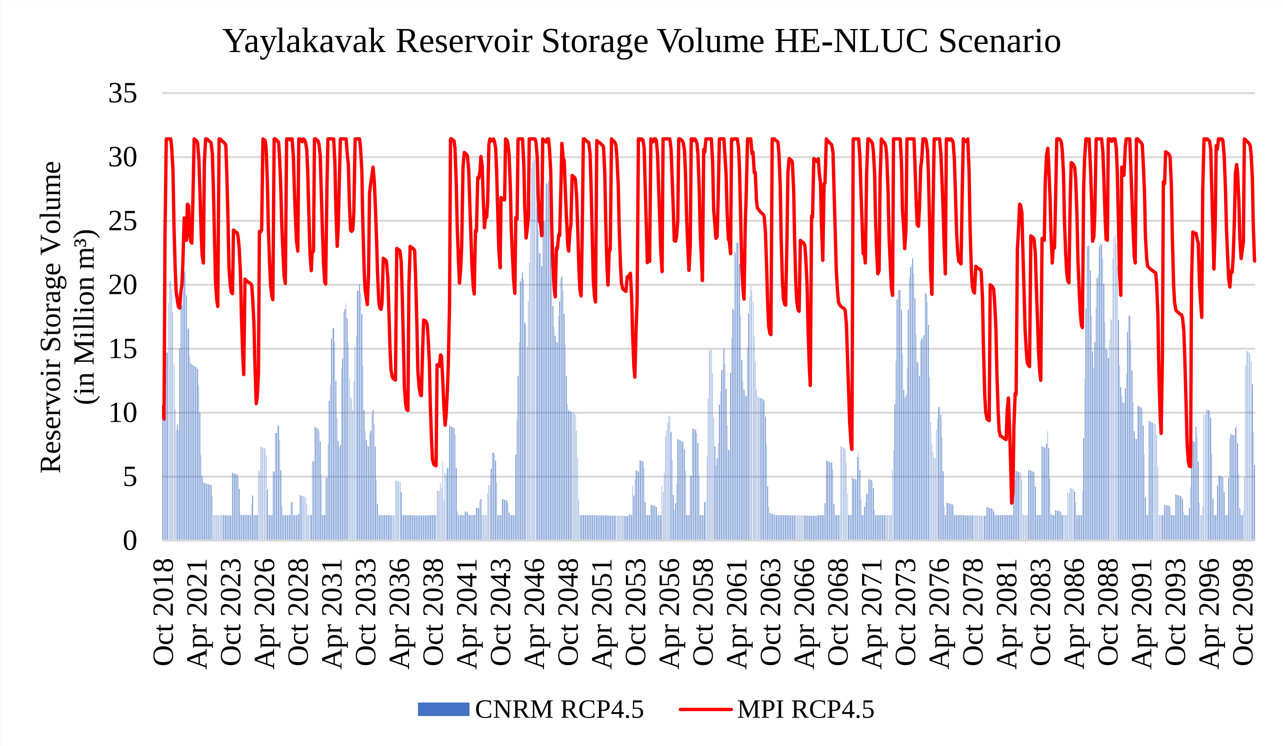

Figure 4.68. Storage volume of Yaylakavak Reservoir under HE-NLUC scenario with CNRM RCP4.5 and MPI RCP4.5 climate change scenarios.

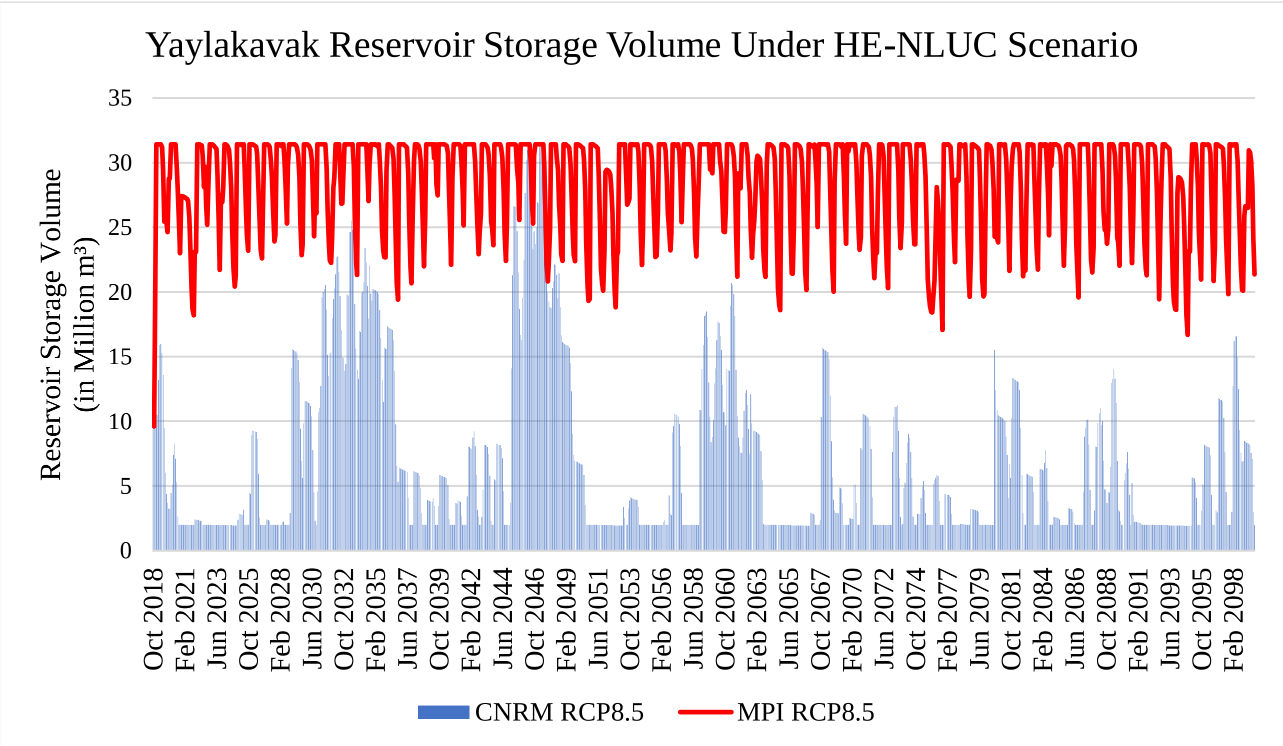

Figure 4.69. Storage volume of Yaylakavak Reservoir under HE-NLUC scenario with CNRM RCP8.5 and MPI RCP8.5 climate change scenarios.

4.7. Reservoir Storage Volumes Under HE-IILS Scenario

This section displays changes in reservoir storage volumes under HE-IILS scenario. Based on the assumption of HE-IILS, there is not only infrastructural change (full transition to high-efficiency drip irrigation system) but also there takes place irrigated land expansion throughout BMB. Therefore, in this section, combined effect of infrastructural changes, land use changes, and climate change on reservoir storage rates are observed.

Under RCP4.5 scenario of CNRM-CM5.1, as seen in Figure 4.120, decadal average rates of total reservoir storage volume are always higher than baseline scenario rates throughout simulation period. Average baseline rate of total reservoir storage volume is 1500 million m^3. On the other hand, as seen in Figure 4.120, the average storage volume rate is approximately 160 million m^3 higher than average baseline rate under RCP4.5 conditions and CNRM-CM5.1 results. Hence, the average storage volume rate of simulation period is 11% higher than baseline scenario. As to decadal variations under RCP4.5, Figure 4.120 indicates that decadal average difference of storage volume with respect to baseline scenario increases from 131 to 202 million m^3 between 2019 and 2050. Until 2081-2090 period, the difference drops down to 139 million m^3 and in the last decade rises to 200 million m^3 back again. On the other hand, as seen in Figure 4.120, CNRM-CM5.1 results under RCP8.5 conditions show the average storage volume rate is approximately 140 million m^3 higher than average baseline rate. Therefore, the average storage volume of simulation period is 9% higher than baseline scenario. This means that results under RCP8.5 conditions are slightly lower compared to that of RCP4.5. As to decadal variations of total reservoir storage volume under RCP8.5 conditions, as seen in Figure 4.120, the difference between average decadal volume and baseline rate get bigger between 2019 and 2040 from 83 to 242 million m^3. In the following decades, the difference in between declines down to 116 million m^3 towards the end of simulation period.

According to results of MPI-ESM-MR under RCP4.5, as seen in Figure 4.120, the average decadal difference of total reservoir storage volume with respect to baseline rate is approximately 460 million m^3 higher during simulation period. Given that baseline reservoir volume rate is 1500 million m^3, the 460 million m^3 difference in between shows that total reservoir volume increases by 31% on average for simulation period. According to results of CNRM-CM5.1, on the other side, the rates of increase are 11% and 9% under RCP4.5 and RCP8.5 conditions respectively. As to decadal variations of average total reservoir volume under RCP4.5 and MPI-ESM-MR, as shown in Figure 4.120, the decadal increase of total storage volume goes up from 375 to 617 million m^3 between 2019 and 2060. In the following decades, the decadal increase with respect to baseline rate drops down to 448 million m^3. Besides, under RCP8.5 conditions and MPI-ESM-MR results, Figure 4.120 shows that total average reservoir storage volume during simulation period is approximately 630 million m^3 higher than average baseline rate. Given that baseline reservoir volume rate is 1500 million m^3, the 630 million m^3 difference in between shows that total reservoir volume increases by 42% on average for simulation period. The rate of increase is 31% under RCP4.5 conditions and MPI-ESM-MR results. On the other side, according to results of CNRM-CM5.1, the rates of increase are 15% and 16% under RCP4.5 and RCP8.5 respectively. So, the highest increase for storage volume rates takes places under MPI-ESM-MR results and RCP8.5 conditions. Lastly, as to decadal variations of total storage volume rates under RCP8.5 and MPI-ESM-MR results, as shown in Figure 4.93, the average decadal difference increases from 668 to 868 million m^3 between 2019 and 2060. In the following decades, the average difference drops down to 730 million m^3.

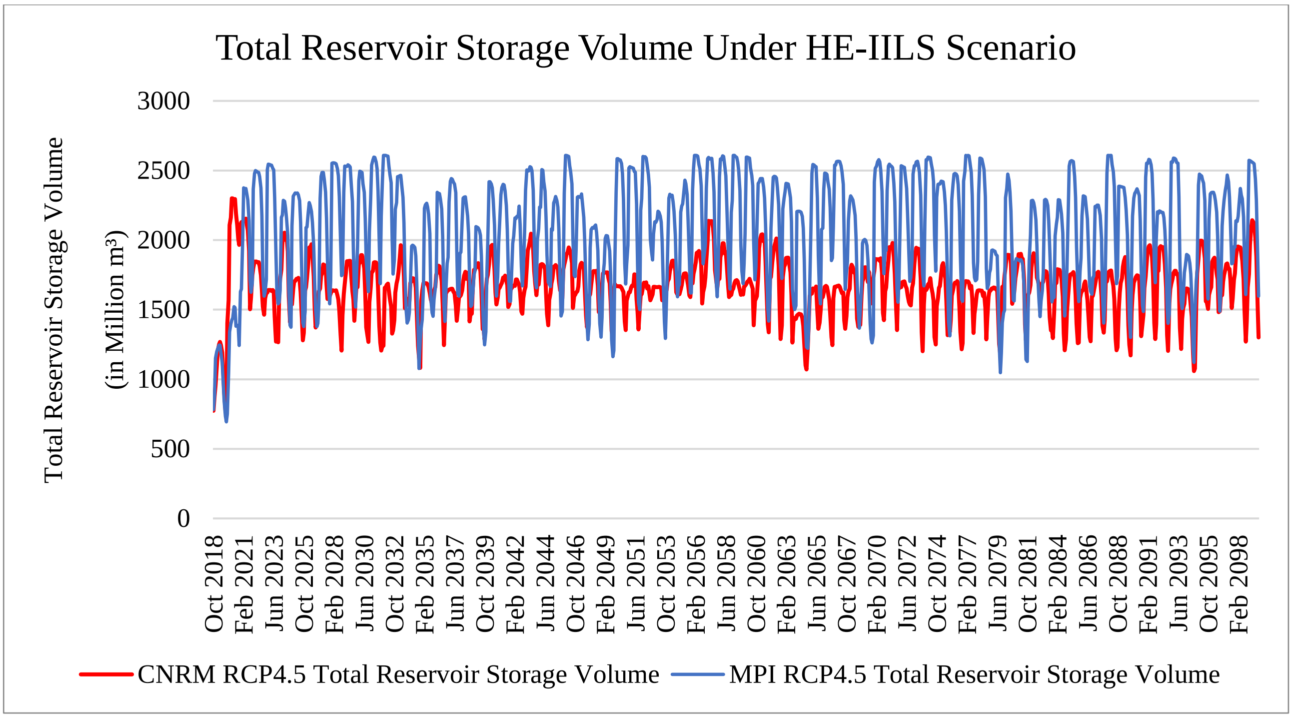

Figure 4.70. Total storage volume under HE-IILS scenario with CNRM RCP4.5 and MPI RCP4.5 climate change scenarios.

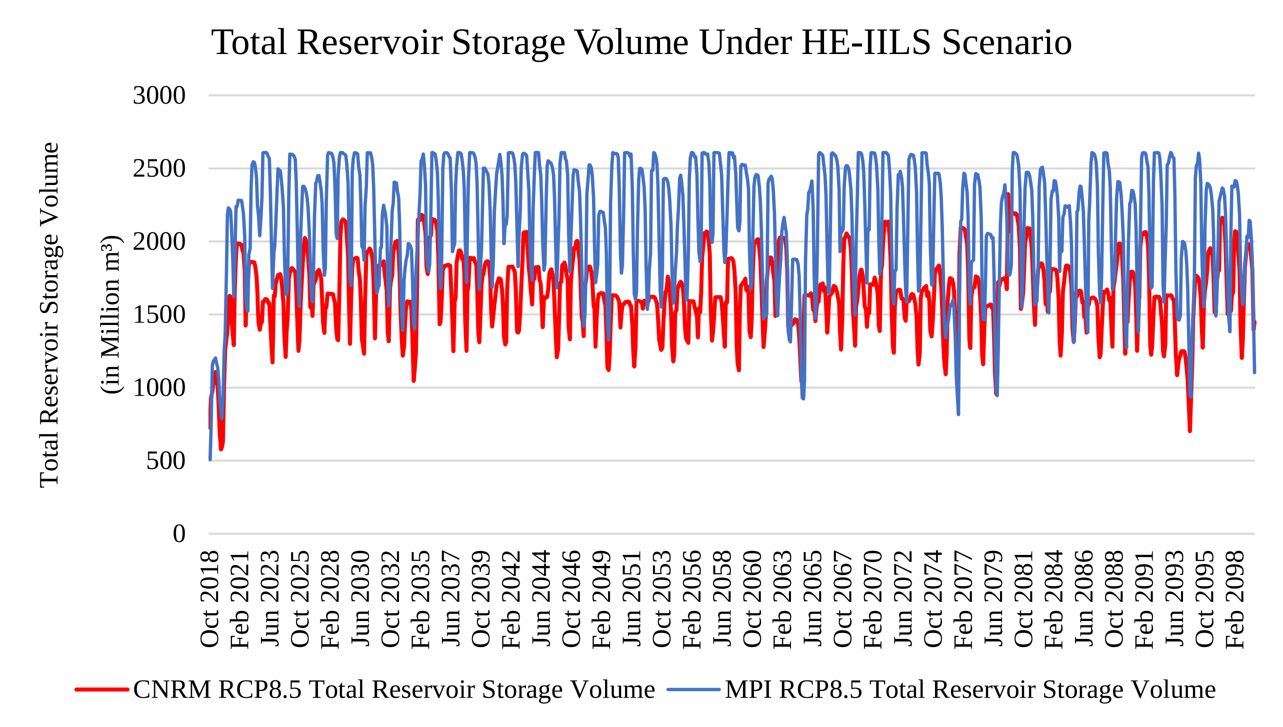

Figure 4.71. Total storage volume under HE-IILS scenario with CNRM RCP8.5 and MPI RCP8.5 climate change scenarios.

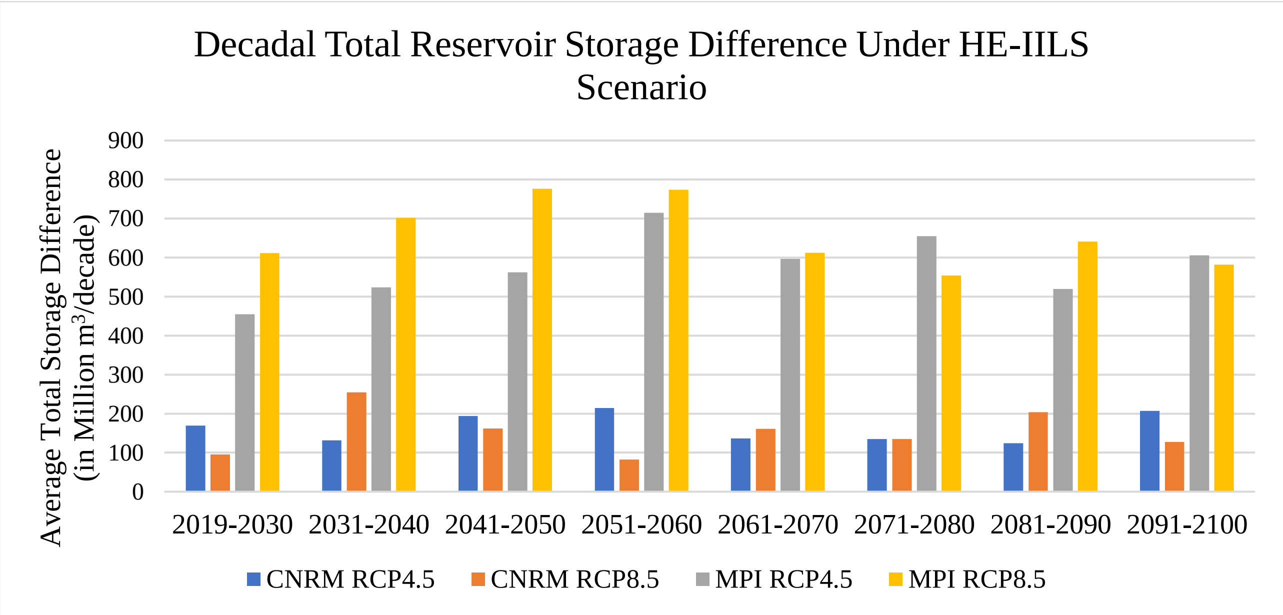

Figure 4.72. Decadal average difference of total reservoir storage volume with respect baseline scenario under CNRM RCP4.5, RCP8.5 and MPI RCP4.5 RCP8.5 climate change scenarios.

As to combined impact of land use change and efficiency improvement on each reservoir separately, according to results of both CNRM-CM5.1 and MPI-ESM-MR, reservoirs in Denizli indicate higher reservoir volume rates. However, rates of increase obtained based on the results of CNRM-CM5.1 is higher than that of MPI-ESM-MR because of higher surface runoff rates in CNRM-

CM5.1 model. On the other side, according to results of CNRM-CM5.1, reservoirs in Aydın show declining storage volume rates under both RCP4.5 and RCP8.5 conditions. However, according to results of MPI-ESM-MR, reservoirs located in Aydın generally show increasing storage volume rates as seen in Appendix A. The following paragraphs explain

According to CNRM-CM5.1 results under RCP4.5, as shown in Appendix A, the average decline rates of volume of Topçam reservoir with respect to baseline scenario are 52% and 55% under RCP4.5 and RCP8.5 respectively. Besides, for Yaylakavak reservoir, the decline rates are 13% and 14% under RCP4.5 and RCP8.5 respectively. On the other hand, results of MPI-ESM-MR show that the average storage volume rates of Topçam reservoir are higher compared to that of CNRM-CM5.1. As displayed in Appendix A, average volume of Topçam reservoir is 50% and 71% higher than baseline rate under RCP4.5 and RCP8.5 conditions respectively. Moreover, average volume of Yaylakavak reservoir is 2% and 8% higher than baseline rate under RCP4.5 and RCP8.5 conditions respectively. Therefore, MPI-ESM-MR results show increasing storage volume rates for reservoirs situated in Aydın while CNRM-CM5.1 results indicate decreasing rates for the same reservoirs.

On the other side, reservoirs in Denizli show increasing average storage volume rates under the results of both CNRM-CM5.1 and MPI-ESM-MR. As shown in Appendix A, according to results of CNRM-CM5.1, average storage volume rates of Adıgüzel reservoir are 80% and 75% higher than average baseline rate under RCP4.5 and RCP8.5 respectively. Besides, for Işıklı reservoir, the rates of increase 69% and 66% under RCP4.5 and RCP8.5 respectively. On the other hand, results of MPI-ESM-MR show that the average storage volume of Adıgüzel reservoir is lower compared to that of CNRM-CM5.1. As displayed in Appendix A, average volume of Adıgüzel reservoir is 69% and 64% higher than baseline rate under RCP4.5 and RCP8.5 conditions respectively. Moreover, average volume of Işıklı reservoir is 53% and 49% higher than baseline rate under RCP4.5 and RCP8.5 conditions respectively. These rates are 69% and 66% for Işıklı reservoir under the results of CNRM-CM5.1. Therefore, it reveals that MPI-ESM-MR results show higher increasing storage volume rates for reservoirs situated in Denizli compared to CNRM-CM5.1.

The differential impacts of irrigated land expansion and efficiency improvement on each reservoirs results mainly from two important reasons. Firstly, land expansion rates are not the same for each reservoir. So, the rate of increase in total water demand which is brought with expanded irrigated land size is not the same for reservoirs differing in size. Secondly, since annual water requirement per hectare is not the same for different reservoirs. Consequently, water savings achieved through efficiency improvements are not equal for all reservoirs.

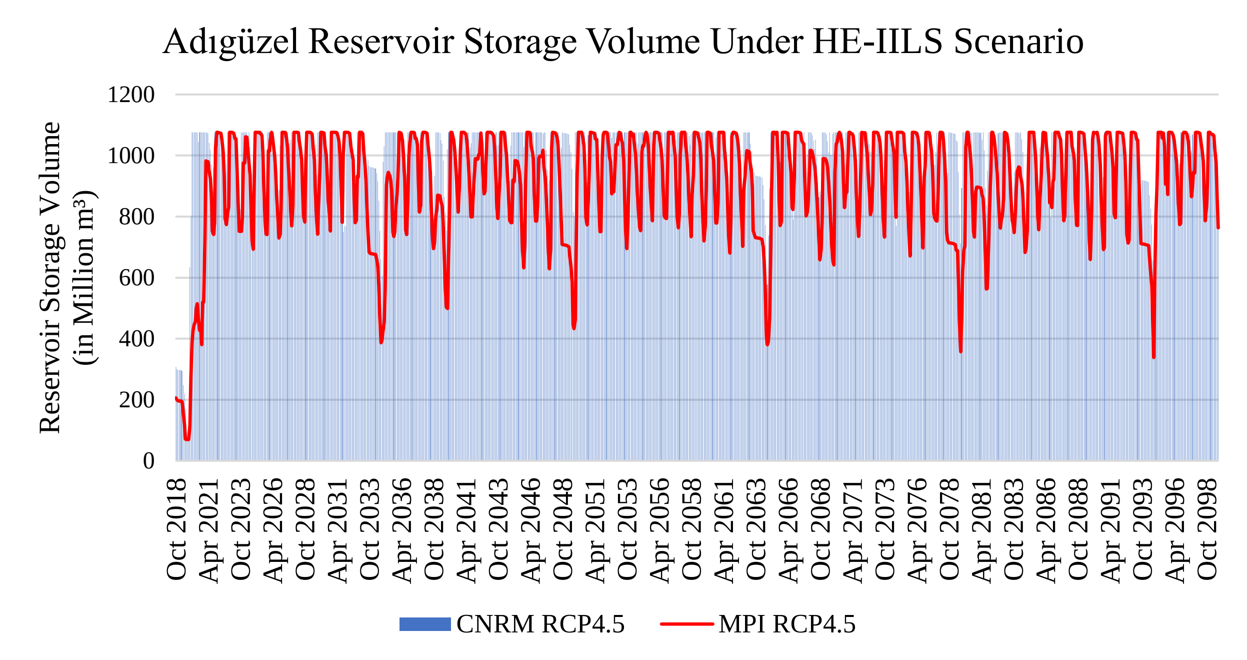

Figure 4.73. Storage volume of Adıgüzel Reservoir under HE-IILS scenario with CNRM RCP4.5 and MPI RCP4.5 climate change scenarios.

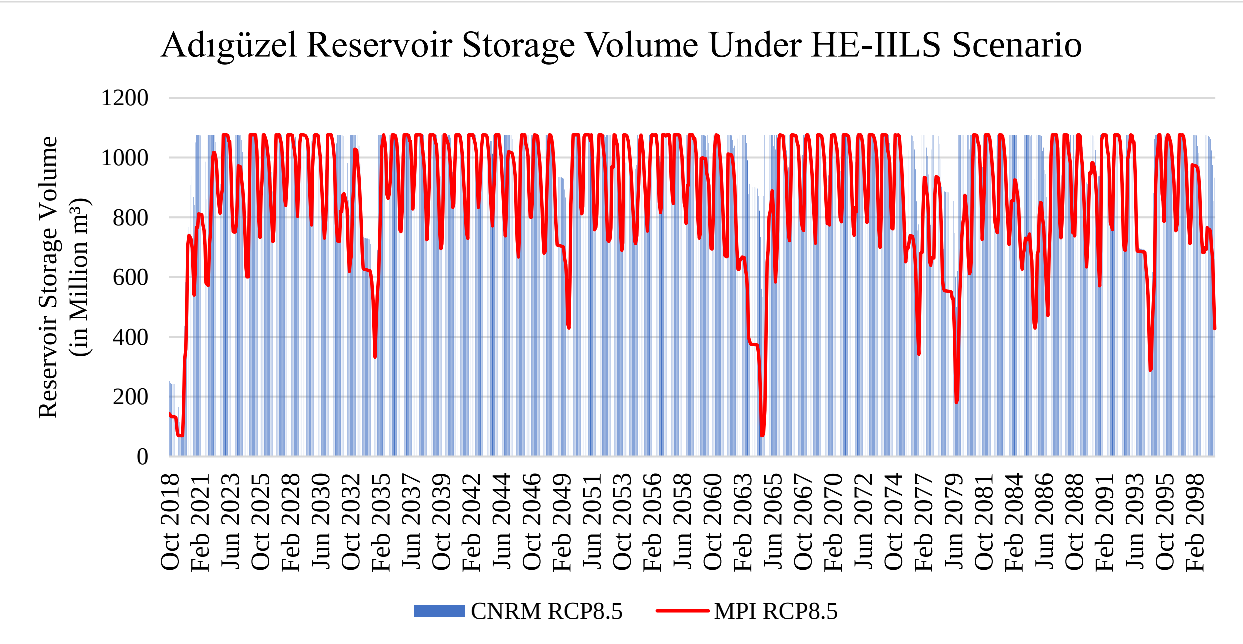

Figure 4.74. Storage volume of Adıgüzel Reservoir under HE-IILS scenario with CNRM RCP8.5 and MPI RCP8.5 climate change scenarios.

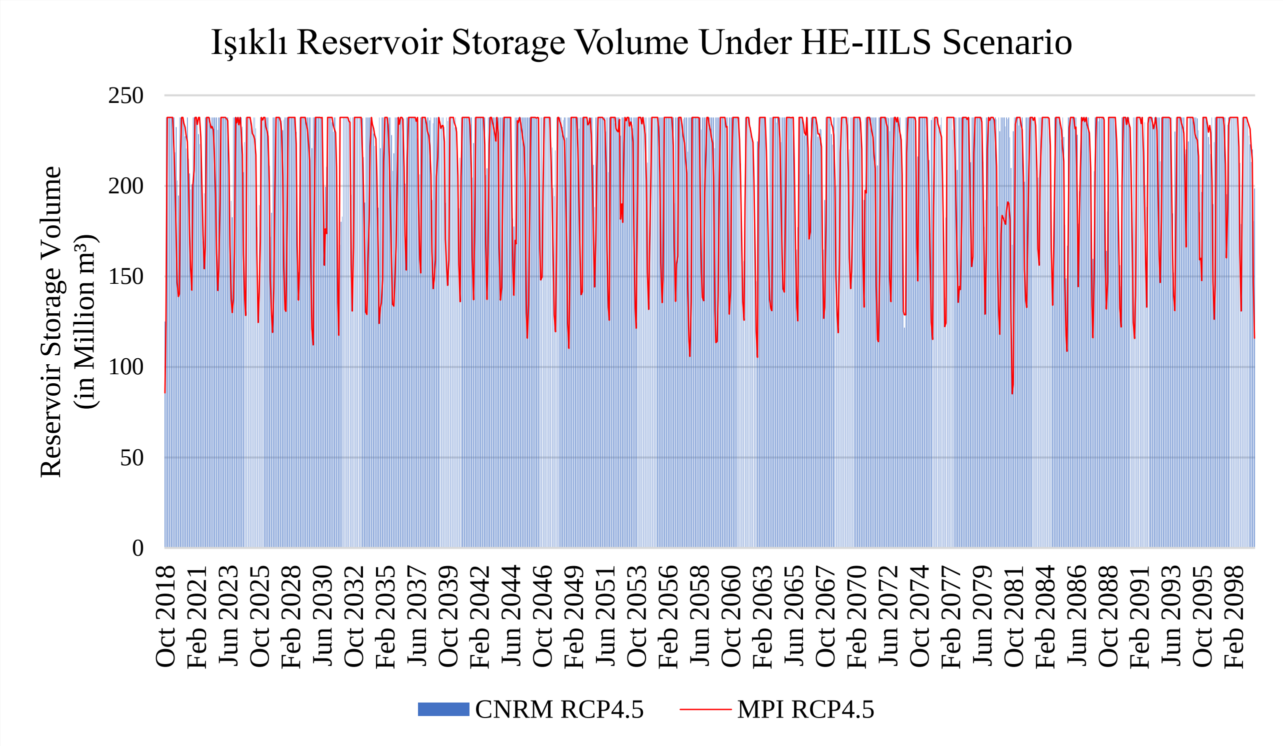

Figure 4.75. Storage volume of Işıklı Reservoir under HE-IILS scenario with CNRM RCP4.5 and MPI RCP4.5 climate change scenarios.

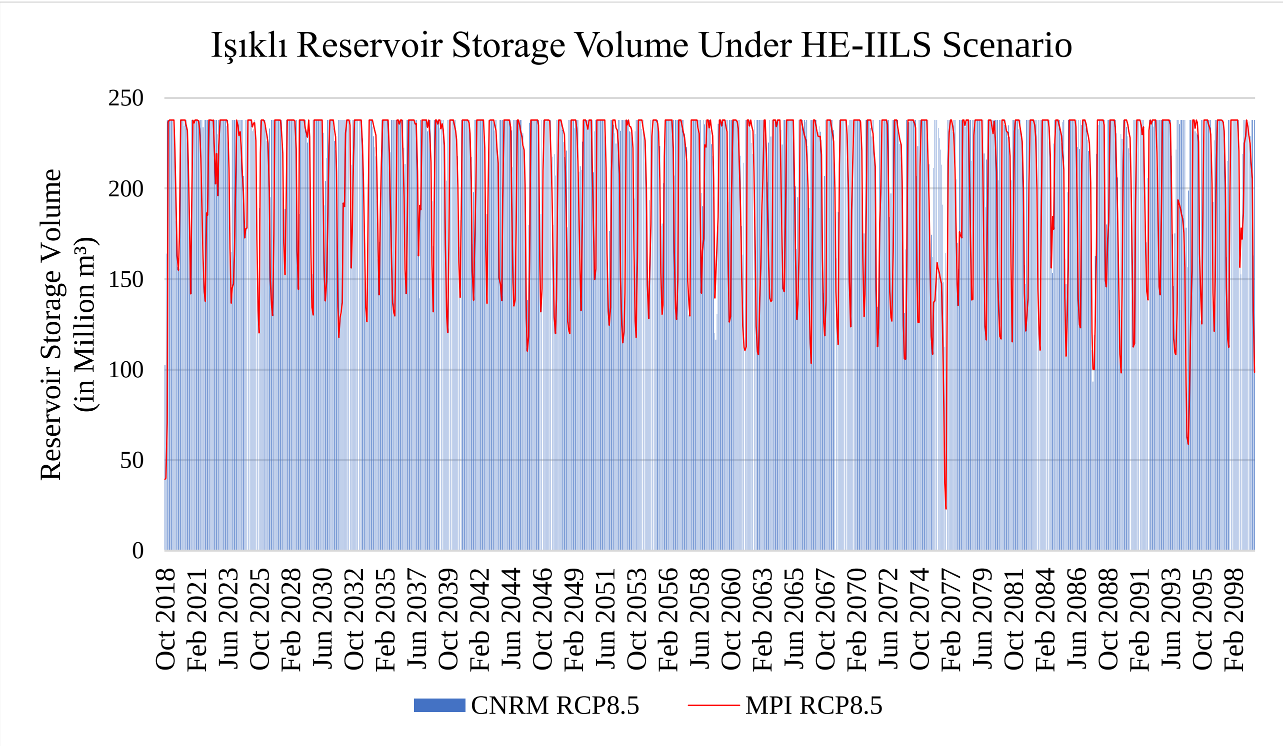

Figure 4.76. Storage volume of Işıklı Reservoir under HE-IILS scenario with CNRM RCP8.5 and MPI RCP8.5 climate change scenarios.

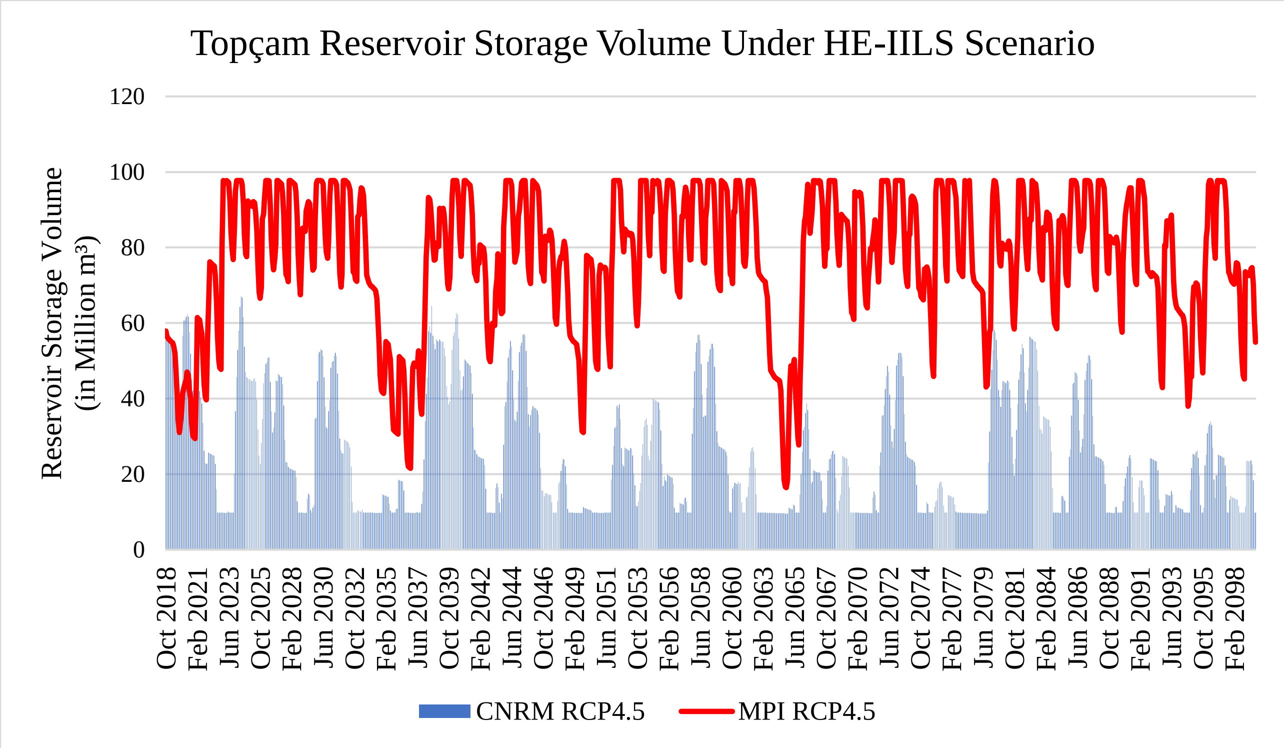

Figure 4.77. Storage volume of Topçam Reservoir under HE-IILS scenario with CNRM RCP4.5 and MPI RCP4.5 climate change scenarios.

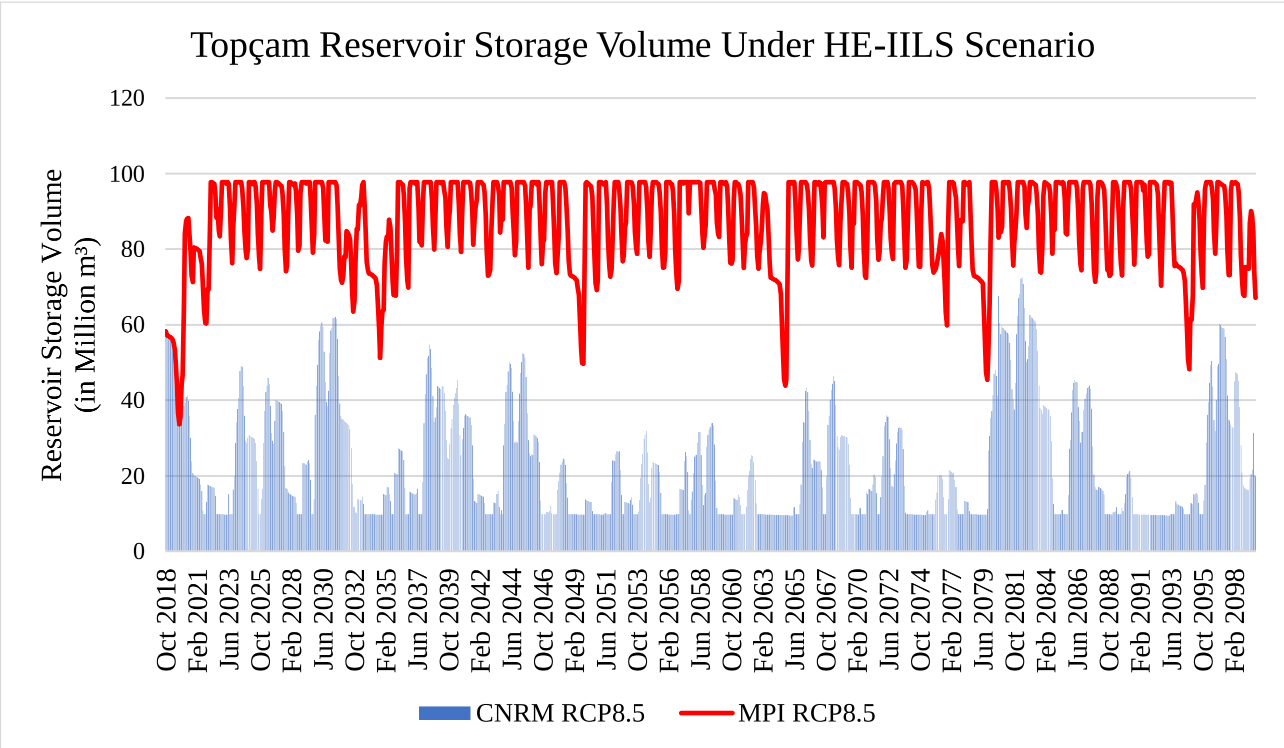

Figure 4.78. Storage volume of Topçam Reservoir under HE-IILS scenario with CNRM RCP8.5 and MPI RCP8.5 climate change scenarios.

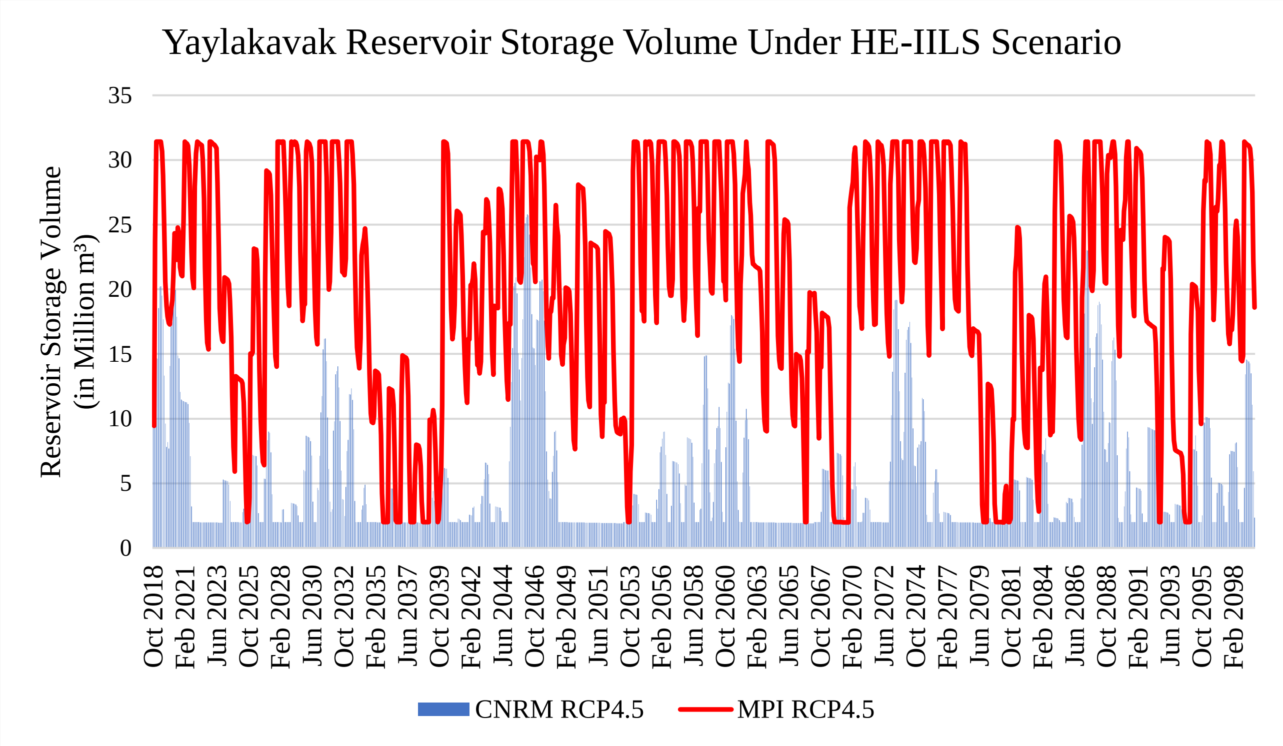

Figure 4.79. Storage volume of Yaylakavak Reservoir under HE-IILS scenario with CNRM RCP4.5 and MPI RCP4.5 climate change scenarios.

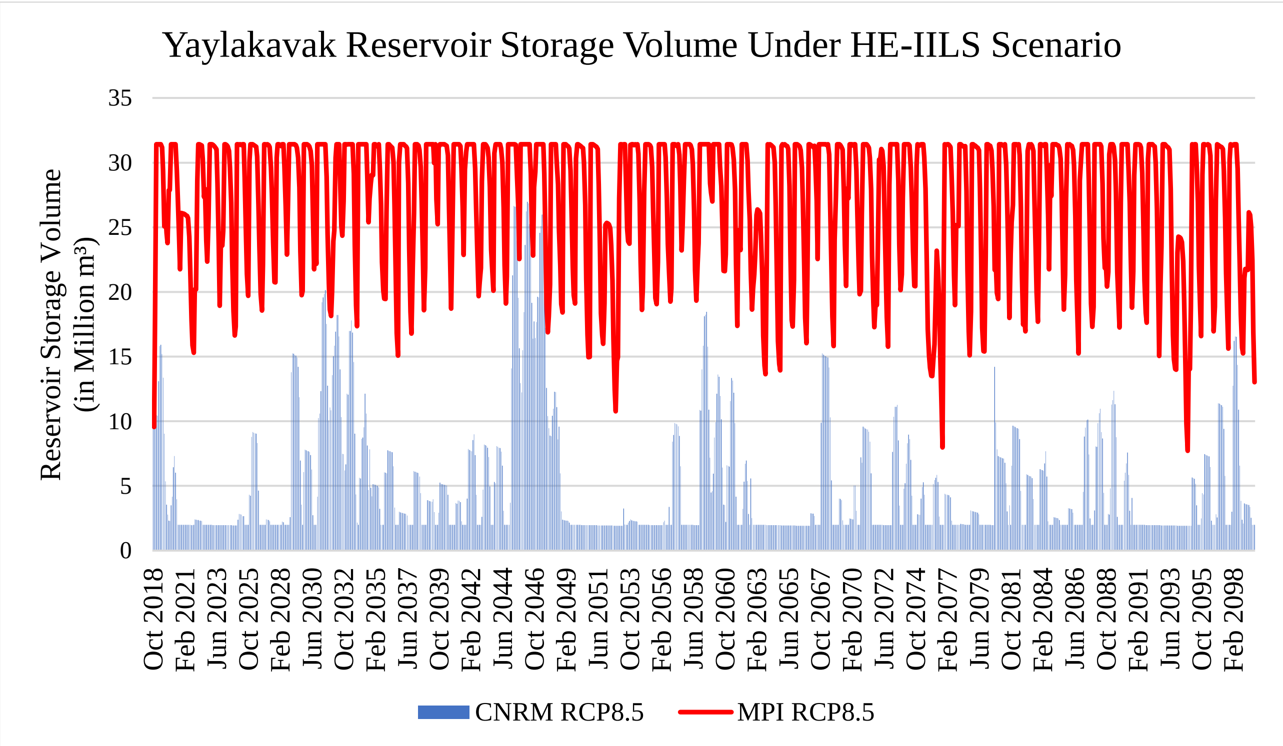

Figure 4.80. Storage volume of Yaylakavak Reservoir under HE-IILS scenario with CNRM RCP8.5 and MPI RCP8.5 climate change scenarios.

5. DISCUSSION

When studying impacts of climate change on ecosystems, the accuracy and precision of climate change models become highly important. As climate models' output becomes another model's input, the uncertainties in the climate models are amplified. In this modeling effort, climatic variables such as the precipitation and temperature parameters are obtained from climate models Max Plank Institute for Meteorology Earth System Model (MPI-ESM-MR) and National Centre for Meteorological Research (CNRM-CM5.1) and used as input parameters in WEAP model to simulate the change in water supply and demand in Büyük Menderes Basin. The choice of which Global Circulation Models (GCM) to utilize is a critical decision as these GCMs are consistent in global future climate patterns however might differ in regional climate patterns and in magnitudes of change. Hence, according to Flato and colleagues (2013) there are five necessary criteria in choosing the right climate change models (i.e. GCM) for studying the impact of climate change in specific ecosystems. The first two of the criteria are compatibility with global projections and with physical laws. The rest are involvement of an adequate number of climatic conditions, representativeness, and accessibility which commonly used GCMs are the most reliable and advanced tools that satisfy these criteria.

However, in 2013 report of IPCC, there are numerous GCMs and it is not plausible and/or practical for climate change impact researchers to use all of these GCMs. Impact researchers need to choose a specific GCM that suits their purpose of studies to the greatest extent possible. IPCC-TGCIA (2007) expresses that researchers should be careful about resolution, validity and release date of GCMs. In this study, only the GCMs (MPI-ESM-MR and CNRM-CM5.1) that are included in the IPCC 2013 report are utilized, therefore the models which do not fulfill validity and recentness criteria are already filtered out. Secondly, in addition to choosing GCMs with proper resolutions, another important point is the uncertainty related to outputs of GCMs. It is important to remark here that results of GCMs are future projections of climatic conditions using stochastic principles (Fajardo et al., 2020). Therefore, there is always uncertainty in GCM results. In order to handle with inherent uncertainty regarding GCMs, at least two or more climate models are recommended to use (Madsen et al., 2012). For all these reasons, this study chooses to utilize from more than one GCM displayed in IPCC 2013 report. The GCMs used in this study are MPI-ESM-MR and CNRM-CM5.1.

There are three important reasons why these two particular GCMs are chosen. The first reason for choosing CNRM-CM5.1 model among many others displayed in 2013 report of IPCC is that this GCM has 50 km resolution while other GCMs such as HadGEM has resolutions of 100 km.

According to Eles and colleagues (2019) climatic parameters especially precipitation, a highly important parameter for this study, is sensitive to the resolution of GCMs. Besides, CNRM-CM5.1 is the only model to extract datasets using the software of “Grid Analysis and Display System” developed by “the Centre for Ocean-Land-Atmosphere Studies”. Lastly, CNRM-CM5.1 is the only GCM whose regional dataset exists for Middle East and North Africa (MENA) region which includes BMB. The second GCM model for this study is MPI-ESM-MR model, downscaled by Boğaziçi University Climate Change and Politics Application and Research Center (IKLIMBU) for the MENA region. The resolution of MPI-ESM-MR model is 10 km.

Nevertheless, there is a critical problem for this study regarding divergent outputs of CNRM-CM5.1 and MPI-ESM-MR extracted for the BMB region. According to Zappa and Shepherd (2017), projections of different GCMs show similar results on average even though considerable variations exist among them. However, the outputs of CNRM-CM5.1 and MPI-ESM-MR do not display similar average results for study area. As seen in Appendix C, CNRM-CM5.1 shows that average precipitation rate for Aydın decline by 100 mm with respect to average baseline rate. On the other hand, MPI-ESM-MR indicate average precipitation rates increase by around 270 mm with respect to average baseline rates for the same cities. Appendix C shows that the same situation exist for Denizli as well. The main reason why significant divergent outputs exist for these two different GCMs is that the data is extracted for a single coordinate within the basin. Due to time and technical limitations, more data points from the MPI-ESM-MR model could not be extracted. Even tough extracting data from numerous coordinates was possible from the CNRM-CM5.1 model, in order to be consistent, using a single data point was preferred. When evaluation model results obtained from this study, the limitation regarding climatic parameters should be considered. Increasing the number of data points within the study area would have increased the precision of climatic parameters obtained from the GCMs.

Another important point to mention regarding the results of this study is calibration and validation results of Tavas and Cindere reservoirs. The calibration and validation results of these two reservoirs are lower than the range of satisfactory results. As shown in Section 4.1, R^2 values for validation period are 0,44 and 0,31 for Tavas and Cindere reservoirs, respectively. There were two challenges in calibration and validation procedures for these two reservoirs. The main reason for unsatisfactorily low R^2 results for these two reservoirs is the inherent algorithms used in WEAP. The WEAP model removes excessive water in reservoirs that would otherwise overflow from reservoirs. However, for these two reservoirs, this mechanism is different than the model representation. Cindere reservoir is used as hydroelectric dam. In Cindere reservoir, inflowing water that sometimes exceed maximum capacity is used for electricity generation. After that, Cindere reservoir releases extra water through its spillways to agricultural areas for irrigation. Therefore, as opposed to WEAP's algorithms, in reality excessive water does not disappear but it is used for irrigation. Consequently, due to the algorithms used in WEAP, there is a significant difference between the observed and simulated reservoir volumes. Since irrigation requirement is not met through excessive water released through spillways, WEAP allocates the stored water to agricultural areas, which results in serious fluctuations in storage volume rates. In order to solve the disparity, another water supply node that provides just as much water that is overflowed in reality is created by setting a monthly limit from this extra supply node to agricultural areas such that is equal to the amount of water that overflow in those particular months. Although R^2 results increase as a result of this improvement (because extreme fluctuations are eliminated), they are still not satisfactory. A similar disparity exists for Tavas reservoir. Even though Tavas is not a hydroelectric dam like Cindere, there are a number of months in that overflowed water is allocated to agricultural lands. Similarly, since WEAP is not capable of transmitting the excessive water to demand nodes, extreme fluctuations take place in reservoir storage volume of Tavas. Consequently, the difference in between observed and simulated reservoir storage volume rates result in unsatisfactory R^2 values. The second reason for low R^2 observed for Cindere and Tavas reservoirs is the observed climate datasets obtained from MGM which are collected in stations near city center. However, the accuracy for reservoirs located away from city centers declines as the distance between stations and reservoirs increase. For example, İkizdere reservoir located close to Aydın city center has the highest R^2 values among all other reservoirs (See Section 4.1) . Therefore, MGM data has secondary effect on the R^2 results for reservoirs and the distance between reservoirs and stations of MGM may affect the difference between observed and simulated results.

The unsatisfactory calibration and validation results for Tavas and Cindere reservoirs show the limitations and suitability of WEAP model. Firstly, the main reason why this study chooses WEAP as the modeling tool is that it allows researchers to carry out IWRM. Besides, its interface is user-friendly and makes modeling process easier. However, the algorithm of WEAP does not cover the possibility that reservoirs may supply inflowing water above their maximum capacity to demand sites. This is especially a critical weakness if reservoirs situated in study area are mainly used for the purposes of hydroelectricity and irrigation (as in the case of Cindere reservoir). This is because, in these kind of reservoirs, irrigation activities are mainly carried out with the help of inflowing water being above the maximum capacity levels. Besides, even if the reservoirs located in study area are not utilized for both irrigation and hydroelectricity, WEAP cannot satisfactorily model the reservoirs where excessive inflowing water is mainly utilized for irrigation (as in the case of Tavas reservoir). Therefore, it is highly important to find out in advance the purposes of reservoirs in study areas.

Total water demand rates during the observation period (2005-2018) displays fluctuations. These fluctuations can be attributed to either an increase in irrigated land area or an increase in water demand per hectare. In the study area, a number of new reservoirs has been constructed during the observation period, such as Çine and İkizdere and addition of these reservoirs consequently increases the irrigated land area. Another possible explanation could be changes in the crop pattern and farmers planting crops that require more irrigation. However, according to the datasets provided by DSI and TUIK, neither the irrigated land area increases, nor the crop patterns change. Yet, for the modeling purposes in order to increase the model efficiency, assumptions parallel to structural changes in the field (i.e., addition of new reservoirs and their impact on irrigated land area) had to be made. Moreover, adjustments to annual water requirement rates per hectare were adjusted to better represent under future emission scenarios such as RCP 4.5 and RCP 8.5 (referencing the values in Gorguner and Kavvas, 2020).

At the end of this study, after coming up with certain insights regarding the future of BMB, it is indispensable to mention additional plausible adaptation strategies and further studies that may be dedicated to water security related problems of BMB. Firstly, as stated in Section 4.3, it is important to note that even the best-case scenario HE-NLUC results in 10% of total water demand being unmet according under future climate scenarios generated by GCM - CNRM-CM5.1. That is, even though HE-NLUC scenario assumes full transition to high-efficiency irrigation systems and assumes no increase in overall irrigated land size, BMB would have water security issues. Therefore, more adaptation strategies must be implemented if we want to eliminate unmet water demand rates totally. These further adaptation strategies can be narrowed down to improvement of overall irrigation water requirements. Crop pattern change, transition to higher efficiency irrigation systems such as subsurface drip irrigation and soil health improvement can be suggested as further adaptation strategies aiming to fully eliminate unmet water demand volumes. As displayed in Figure 3.3 in Section 3.1, farmers in BMB mostly grow crops that require high irrigation water, such as cotton, corn, and sunflower. Therefore, change in dominant crop pattern has a great potential in declining overall irrigation water requirement in the area. Secondly, it is known that water retention capacity of soil and soil health are positively correlated (Lal, 2016). Therefore, any practice that leads to improvement of soil health in BMB has a positive impact on reducing overall irrigation requirement. Zeolite introduction can be one of the possible methods for soil improvement in BMB. Bernardi and colleagues (2012) conducted experiments showing that water retention capacity of soil increases by 10% as a result of addition of zeolite in soil composition. Ippolito and colleagues (2011) reveal also that increasing zeolite amount in soil leads to higher water nutrient, which is again related with water retention capacity of soil. Besides, Jakkula and Wani (2018) shows that zeolite use increases nutrient levels of soil and consequently can be used as an effective fertilizer as well. So, local farmers in BMB can obtain double benefit from zeolite use such that they can reduce water requirement through soil with increased water retention capacity and they can enrich their soil with minerals stored in zeolite.

On the other hand, the unmet water demand problem, as also seen in Section 4.4 to Section 4.8, is observed mostly in reservoirs of Aydın. Therefore, instead of applying the same adaptation strategies to all parts of BMB, strategies for declining agricultural water requirements of agricultural areas situated in Aydın must be prioritized. Therefore, it is important to holistically review impacts of climate change in BMB which vary spatially, to pinpoint where exactly water security related problems are dominant and to act accordingly.

Nevertheless, results of MPI-ESM-MR model, as also stated in Section 4.3, show that unmet water demand barely occurs under scenarios where full transition to high-efficiency irrigation systems takes place throughout BMB. On the other hand, in scenarios where low-efficiency irrigation systems are utilized, considerable total unmet water demand volumes occur under the scenarios of MPI-ESM-MR. This means that, according to MPI-ESM-MR results, irrigation system change in the area should be sufficient to eliminate water security related problems in BMB.

Another significant issue to raise is the possible adoption of the suggested adaptation strategies by local stakeholders and decision makers. First of all, regarding irrigation system change, local farmers are reluctant adoption new technologies with multitude of reasons. Farmers do not think their short term benefits are affected by changes in climatic conditions. In other words, since farmers have not gone through serious drought time periods yet, they tend to believe that they will have not any problems regarding water scarcity. Therefore, they do not have any incentive to spend their revenues on irrigation system changes. Another reason is that drip irrigation systems may sometimes require maintenance because of problems like pipe clogging or deformation and maintenance is extra expense for farmers.

As another issue, as stated in Section 3.3.2, irrigated land expansion has already been going on in Aydın and Denizli. Besides, there are also additional reservoirs in BMB under planning such as the Akbaş reservoir situated in Denizli, suggesting a possible increase in irrigated land expansion and consequently an increase in overall irrigation water requirement in future. Therefore, the most likely scenario is LE-IILS where solely irrigated land expansion occurs during the simulation period. Nevertheless, to demonstrate the impact of irrigation technology improvement, this study evaluates the benefit of using high-efficiency irrigation systems in all BMB by including irrigation system change in two of the scenarios whose results are shown in Section 4.3 to 4.7 (Scenarios HE-IILS, HE-NLUC, and LE-IILS. This way, this study reveals how much water saving is achieved through irrigation system change under changing climatic conditions and under future land-use change trends. Plus, the water saving rates which this study puts forward can be beneficial for further studies.

For further studies, economic analysis of climate change impacts on water budget of BMB could be investigated. The economic impacts of the scenarios generated and evaluated for this study (irrigation system change, irrigated land expansion, and crop pattern change) were not analyzed, however would be valuable for the stakeholders and policy makers as well. An analysis of such can reveal possible financial savings and losses under different scenarios in the following years. Moreover, further studies can also focus on the impact of sowing time on overall agricultural water demand of BMB.

Lastly, the difficulties that I have encountered during formation of this thesis study are in general related with data acquisition and financial issues. Regarding data acquisition necessary for my model, first of all, it takes a lot of energy, time and phone calls to find the right employee to ask for data. That is, as calling a state institution for data demand, they may connect you to wrong employees that have nothing to do with your data request. Even if you find the right person to ask for the datasets you need that person may be on field/in-situ visits and you automatically cannot reach them all that day along. Besides, personnel who are responsible for formation of the datasets that you need may not always be open to sharing the data with you. They sometimes asked me to send written petitions validated by my institute, which takes a lot of time for those petitions to get to the institutions and to get back a response. For these bureaucratic obstacles and inefficiencies, from DSI, it took me around two months to get the annual storage volume of reservoirs located in my study area. Besides, the datasets that DSI provided costs more than 1000 TL and this kind of an extra expense would have been a heavy financial burden for me if the NGO giving me scholarship had not covered my data expenses. Secondly, financial restrictions affected the course of this thesis study in other senses as well. That is because, at the very beginning, this thesis study involved field visits, interview with local farmers and irrigation associations and to make my scenarios based on the results of my interviews on field. However, due to financial limitations, only one field visit was performed and several interviews with farmers. Even small number of interviews provided necessary field notes to build the model to represent the business as usual farmer behavior.

6. CONCLUSION

Water scarcity has always been a problem throughout the history and conflicts resulting from water scarcity related problems are still prevalent today in many different corners of the world. Büyük Menderes Basin (BMB) is one of the most intense agricultural production hubs in Turkey. Therefore, it is a highly water dependent watershed and it is likely to face water scarcity related problems in the future. Previous climate change impact studies carried out for BMB puts forward the high likelihood of future water scarcity problems.

For these reasons, this thesis study evaluates the impacts of climate change on water budget of BMB in the perspective of impacts of adaptation strategies. This way, this study can reveal future water scarcity related problems in Büyük Menderes Basin (BMB), and it can assess in advance the impacts of possible strategies to deal with these problems. In doing so, this study aims to create a model by Water Evaluation and Planning Programme (WEAP) software through which it analyzes the future water budget of BMB under changing climatic conditions, and infrastructural and land use changes.

In the model, there are two different climate change emission scenarios, RCP4.5 and RCP8.5, and four management scenarios which are Business As Usual (BAU), High-Efficiency No Land Use Change (HE-NLUC), High-Efficiency Increased Irrigated Land Size (HE-IILS), and Low-Efficiency Increased Irrigated Land Size (LE-IILS) scenarios. For the WEAP model, climate change scenarios are based on the results of two GCMs, CNRM-CM5.1 and MPI-ESM-MR GCMs. For other scenarios, in BAU scenario, current status observed in the study area is represented with no change in irrigation systems and overall irrigated land size, while HE-NLUC scenario resulting in lowest total water demand and called the best-case scenario assumes that transition to high-efficiency irrigation systems take place and that total irrigated land size remains constant in BMB. On the other hand, In HE-IILS scenario, irrigated land size increases and irrigation systems change. Lastly, in LE-IILS scenario resulting in highest total water demand rates and called the worst-case scenario, assumes that solely total irrigated land size increases in BMB and irrigation systems do not change.

To begin with, model results show that overall water demand in BMB is highly sensitive to changes in efficiency rates of irrigation systems and total irrigated land area (Figure 4.19 and Figure 20). For this study, the effect of changes in efficiency rates is more powerful because irrigated land expansion is limited in BMB and does not have as much impact as efficiency rate changes in irrigation systems (Figure 4.22 and Figure 4.23). With respect to the observation period, overall average water demand rate increases by 24% as a result of increase in irrigated land size while total demand declines by 33% due to transition to high-efficiency irrigation systems in the area. On the other hand, water supply is highly affected by climate change. According to results of both CNRM-CM5.1 and MPI-ESM-MR, surface runoff rates for the simulation period are higher than average baseline rates under RCP4.5 and RCP8.5 (Figure 4.36).

However, unmet water demand rates become concerning during the simulation period despite increasing surface runoff rates. This is firstly because increases in IWR rates in the following year being put forward by Gorguner and Kavvas (2020). According to this study, until the end of 21st century, IWR rates increase by 5% and 12% on average with respect to baseline scenario under RCP4.5 and RCP8.5 respectively (Table 3.6). The study area of Gorguner and Kavvas is Gediz Basin and it is geographically close to BMB, plus the prevalent crop patterns are similar in both basins. Therefore, for this study, it is assumed that similar increases in IWR rates take places in BMB as well. Secondly, due to increased irrigated land size, overall water demand increases during simulation period.

According to results of CNRM-CM5.1, overall unmet water demand rates in the study are highly visible under all management and climate change emission scenarios (Figure 4.28 to Figure 4.31). That is, CNRM-CM5.1 results indicate that positive impacts of adaptation strategies (i.e. efficiency improvements) on water budget of BMB will not be enough to fully eliminate the gap between water supply and water demand. On the other hand, according to MPI-ESM-MR results, overall unmet water demand rates are remarkably lower compared to that of CNRM-CM5.1. Besides, only under LE-IILS scenario, it is shown average annual unmet water demand rates reach out to discernible levels. In other words, based on the results of MPI-ESM-MR, application of adaptation strategies proposed in this study will be adequate to solve water scarcity related problems in the study area. The differences between the results of these two GCMs stand out in one important sense that the GCMs obviously show divergent outcomes regarding the future water budget of BMB under different management and climate change emission scenarios.

Another important point regarding divergent results in this study obtained through CNRM-CM5.1 and MPI-ESM-MR is the regional differences of climate change impacts on reservoir storage volumes. First of all, it is important to distinguish the difference between reservoirs in Aydın and Denizli. Reservoirs in Aydın are Çine, İkizdere, Karacasu, Kemer, Topçam, and Yaylakavak reservoirs and reservoirs in Denizli are Adıgüzel, Cindere, Gökpınar, Işıklı, Tavas reservoirs.

According to outputs of CNRM-CM5.1, Appendix A indicates that average reservoir storage volume rates fall with respect to average baseline rate in reservoirs located in Aydın under RCP4.5 and RCP8.5 conditions. On the other hand, based on the results of the same GCM, reservoirs in Denizli show increasing average storage volume rates. However, according to results of MPI-ESM-MR, reservoir storage volume rates increase in reservoirs located in Denizli and Aydın (Appendix A). The highly divergent results outstand particularly for reservoirs located in Aydın. Appendix A shows average percentage changes of individual reservoirs located Aydın and Denizli with respect to their average baseline rates.

From these takeaway points that different GCMs indicate varying surface runoff rates and consequently varying reservoir storage volumes rates in Denizli and Aydın, I can firstly conclude that coupled models contain high uncertainties in their outputs mainly because projecting future climatic conditions is stochastic process. Therefore, utilizing more than one GCM has critical benefits for researchers. To begin with, it enables researchers to see the range of results achieved through different GCMs. If this study used solely MPI-ESM-MR or CNRM-CM5.1, outcomes regarding future water budget of BMB would depict an entirely different situation. Instead, applying the outputs of these two different GCMs for the study area, this study demonstrates the significance of utilizing from different GCMs. These different climate model results and consequent interpretations affect what adaptation strategies are proposed by researchers in their studies. Besides, as previously stated, the potential impacts of proposed adaptation strategies are also firmly tied to the outputs of GCMs. Therefore, using multiple GCMs increase the reliability of climate change impact studies by providing a wider perspective regarding future climatic conditions of their study areas.

Secondly, field visits could have enhanced the accuracy of the representation of the baseline conditions. Due to lack of financial support, only one field visit was performed, therefore local knowledge and application of irrigation technologies were not fully represented. Interviews with local farmers and irrigation district employees could have provided obstacles for adoption of high-efficiency irrigation systems. As the fundamental objective of this study was to demonstrate the possible impact of climate change on water demand and offering adaptation strategies and modeling their impact on the water budget, field visits and understanding the mechanisms influential on adoption of irrigation technologies were not investigated, which could potentially be the focus of a future study.

REFERENCES

Acreman, M., Tickner, D, 2013. Water Security for Ecosystems, Ecosystems for Water Security. In: Water security: Principles, perspectives, and practices. Lankford B., Bakker K., Zeitoun M., and D. Conway (Eds.), 139-140, Routledge, Taylor & Francis Group, New York, U.S.A.

Ahmadi, A., Ohab-Yazdi, S. A., Zadehvakili, N., Safavi, H. R., 2018. A dynamic model of water resources management using the scenario analysis technique in downstream of the Zayandehroud basin. International Journal of River Basin Management, 17, 451-463.

Allan, C., Xia, J., Pahl-Wostl, C., 2013. Climate change and water security: Challenges for adaptive water management. Current Opinion in Environmental Sustainability, 5, 625-632.

Allen, R. G., Pereira, L. S., Raes, D., Smith, M., 2004. Introduction to Crop Evapotranspiration, 89-103. FAO, Rome, Italy.

Almutairi, B. S., Grossmann, I., Small, M. J., 2019. Climate model projections for future seasonal rainfall cycle statistics in Northwest Costa Rica. International Journal of Climatology, 39, 2933-2946.

Arnold, J. G., Moriasi, D. N., Gassman, P. W., Abbaspour, K. C., White, M. J., Srinivasan, R., Jha, M. K., 2012. SWAT: Model Use, Calibration, and Validation. Transactions of the ASABE, 55, 1491-1508.

Atmaca, D., 2012. Büyük Menderes Havzası’nda Besin Elementleri Taşınım Senaryoları, M.Sc. Thesis, Muğla Adnan Menderes University, Turkey

Asian Development Bank, 2013. Taking Stock: An Objective Framework for Water Security. In: Asian Development Bank, Asian water development outlook 2013: Measuring water security in Asia and the Pacific, 5-6. Asian Development Bank, Mandaluyong, Philippines.

Aydın Çevre ve Şehircilik İl Müdürlüğü, 2007. Aydın İli 2007 Yılı Çevre Durum Raporu. T.C. Çevre ve Şehircilik Bakanlığı, Aydın, Türkiye.

Aydın Çevre ve Şehircilik İl Müdürlüğü, 2014. Aydın İli 2014 Yılı Çevre Durum Raporu. T.C. Çevre ve Şehircilik Bakanlığı, Aydın, Türkiye.

Aydın Çevre ve Şehircilik İl Müdürlüğü, 2018. Aydın İli 2018 Yılı Çevre Durum Raporu. T.C. Çevre ve Şehircilik Bakanlığı, Aydın, Türkiye.

Azgin, S. T., Celik, F. D., 2020. Evaluating Surface Runoff Responses to Land Use Changes in a Data Scarce Basin: A Case Study in Palas Basin, Turkey. Water Resources, 47, 828-834.

Babar, S., Ramesh, H, 2015. Streamflow Response to Land Use–Land Cover Change over the Nethravathi River Basin, India. Journal of Hydrologic Engineering, 20, 1-10.

Balyuk, S. A., Nosonenko, A. A., Drozd, E. N., 2018. Technical support for the conservation and use of salt-affected soils. In: Handbook for saline soil management, Rojas, R. V., Pankova, E. I., Balyuk, S. A., Krasilʹnikov, P. K., Khasankhanova, G. M. (Eds.), 42-48. Food and Agriculture Organization of the United Nations, Rome, Italy.

Bernardi, A., Oliviera, P., Monte, M., Souza-Barros, F., 2012. Brazilian sedimentary zeolite use in agriculture. Microporous and Mesoporous Materials, 16-21.

Brath, A., Montanari, A., Moretti, G., 2006. Assessing the effect on flood frequency of land use change via hydrological simulation (with uncertainty). Journal of Hydrology, 324, 141-153.

Bell, A. R., Ward, P. S., Ashfaq, M., Davies, S., 2020. Valuation and Aspirations for Drip Irrigation in Punjab, Pakistan. Journal of Water Resources Planning and Management, 146, 04020035-1-04020035-12.

Brouwer, C., Prins, K., Heibloem, M., 1991. Irrigation efficiencies. In: Irrigation Water Management: Irrigation Scheduling, 30-35, FAO, Rome, Italy.

Büke, A., Gültekin, M., Aksoy, M., Dıvrak, A., Göcek, B. B., Berke, Ç, Çeşmeci, H., 2013. Büyük Menderes Havza Atlası.

Chen, D., Gao, G., Xu, C., Guo, J., Ren, G., 2005. Comparison of the Thornthwaite method and pan data with the standard Penman-Monteith estimates of reference evapotranspiration in China. Climate Research, 28, 123-132.

Copernicus, 2019. CORINE Land Cover, https://land.copernicus.eu/pan-european/corine-land-cover. Data accessed September 2020.

Costa, M. H., Botta, A., Cardille, J. A., 2003. Effects of large-scale changes in land cover on the discharge of the Tocantins River, Southeastern Amazonia. Journal of Hydrology, 283, 206-217.

Daly, H. E., 1991. Steady-state economics. Island Press, Washington DC, U.S.A.

Demircan, M., Gürkan, H., Eskioğlu, O., Arabacı, H., Coşkun, M., 2017. Climate Change Projections for Turkey: Three Models and Two Scenarios. Turkish Journal of Water Science and Management, 1, 22-43.

Denizli Çevre ve Şehircilik Müdürlüğü, 2015. Denizli İli 2015 Yılı Çevre Durum Raporu. T.C. Çevre ve Şehircilik Bakanlığı, Denizli, Türkiye.

Denizli Çevre ve Şehircilik Müdürlüğü, 2017. Denizli İli 2017 Yılı Çevre Durum Raporu. T.C. Çevre ve Şehircilik Bakanlığı, Denizli, Türkiye.

Denizli Çevre ve Şehircilik Müdürlüğü, 2019. Denizli İli 2019 Yılı Çevre Durum Raporu. T.C. Çevre ve Şehircilik Bakanlığı, Denizli, Türkiye.

Devak, M., Dhanya, C. T., 2017. Sensitivity analysis of hydrological models: Review and way forward. Journal of Water and Climate Change, 8, 557-575.

Dong, C., Schoups, G., Giesen, N. V., 2013. Scenario development for water resource planning and management: A review. Technological Forecasting and Social Change, 80, 749-761.

DSI, 2010. Toprak ve Su Kaynakları. http://www.dsi.gov.tr/topraksu.htm. Data accessed July 2020.

DSI, 2011. Tarım: Sulamanın Önemi. http://www.dsi.gov.tr/docs/hizmet-alanlari/tarim-sulama.pdf?sfvrsn=2. Date accessed July 2020.

Döll, P., 2002. Impact of Climate Change and Variability on Irrigation Requirements: A Global Perspective. Climatic Change, 54, 269-293.

Elliott, J., Deryng, D., Müller, C., Frieler, K., Konzmann, M., Gerten, D., . . . Wisser, D., 2013. Constraints and potentials of future irrigation water availability on agricultural production under climate change. Proceedings of the National Academy of Sciences, 111, 3239-3244.

Ent, R. J., Savenije, H. H., Schaefli, B., Steele-Dunne, S. C., 2010. Origin and fate of atmospheric moisture over continents. Water Resources Research, 46, 1-12.

European Commission, 2017. Nature-Based Solutions, https://ec.europa.eu/research/environment/index.cfm?pg=nbs. Date accessed July 2020.

Evett, S. R., Colaizzi, P. D., Howell, T. A., 2005. Drip and evaporation, https://mountainscholar.org/handle/10217/205462. Date accessed October 2020,

Fajardo, J., Corcoran, D., Roehrdanz, P. R., Hannah, L., Marquet, P. A., 2020. GCM compareR: A web application to assess differences and assist in the selection of general circulation models for climate change research. Methods in Ecology and Evolution, 11, 656-663.

FAO, 2012. Status and Trends in Land and Water Resources. In: State of the World's Land and Water Resources for Food and Agriculture: Managing systems at risk, 19-63. FAO, New York, U.S.A.

FAO, 2014. Did you know...?, http://www.fao.org/nr/water/aquastat/didyouknow/index3.stm. Data accessed October 2020.

FAO, 2015. AQUASTAT - FAO's Global Information System on Water and Agriculture, http://www.fao.org/aquastat/en/overview/methodology/water-use. Data accessed July 2020.

FAO, 2015. Irrigation area visualizations, http://www.fao.org/nr/water/aquastat/irrigationdrainage/treemap/print1.stm. Data accessed July 2020.

FAO, 2015. Water withdrawal ratios by continent, http://www.fao.org/aquastat/en/overview/methodology/water-use. Data accessed June 2020.

FAO, 2017. Water for sustainable food and agriculture: A report produced for the G20 Presidency of Germany. FAO, Rome, Italy.

Flato, G., J. Marotzke, B. Abiodun, P. Braconnot, S.C. Chou, W. Collins, P. Cox, F. Driouech, S. Emori, V. Eyring, C. Forest, P. Gleckler, E. Guilyardi, C. Jakob, V. Kattsov, C. Reason and M. Rummukainen, 2013. Evaluation of Climate Models. In: Climate Change 2013: The Physical Science Basis. Contribution of Working Group I to the Fifth Assessment Report of the Intergovernmental Panel on Climate Change, Stocker, T.F., D. Qin, G.-K. Plattner, M. Tignor, S.K. Allen, J. Boschung, A. Nauels, Y. Xia, V. Bex and P.M. Midgley (Eds.), Cambridge University Press, Cambridge, United Kingdom and New York, NY, USA.

Flörke, M., Schneider, C., Mcdonald, R. I., 2018. Water competition between cities and agriculture driven by climate change and urban growth. Nature Sustainability, 1, 51-58.

Girgin, A., Kayam, Y., 2002. Denizli-Sarayköy ve Aydın-Söke Ovalarında Bazı Toprak Sorunları, Tav Suyu Ve Yıkama Suyu Uygulamaları, https://atilagirgin.weebly.com/den304zl304-saraykoumly-ve-aydin-soumlke-ovalarinda-bazi-toprak-sorunlari-tav-suyu-ve-yikama-suyu-uygulamalari.html. Date accessed July 2020.

Goldewijk, K. K., Beusen, A., Janssen, P., 2010. Long-term dynamic modeling of global population and built-up area in a spatially explicit way: HYDE 3.1. The Holocene, 20, 565-573.

Gorguner, M., Kavvas, M. L., 2020. Modeling impacts of future climate change on reservoir storages and irrigation water demands in a Mediterranean basin. Science of the Total Environment, 748, 1-19.

Guerrero, R. A., Acha, E. M., Framiñan, M. B., Lasta, C. A., 1997. Physical oceanography of the Río de la Plata Estuary, Argentina. Continental Shelf Research, 17, 727-742.

Grid Analysis and Display System (GrADS). (n.d.), http://cola.gmu.edu/grads/. Date accessed December 2020.

Grafton, R. Q., Williams, J., Perry, C. J., Molle, F., Ringler, C., Steduto, P., . . . Allen, R. G., 2018. The paradox of irrigation efficiency. Science, 361, 748-750.

Grantham, T. E., Figueroa, R., Prat, N., 2012. Water management in Mediterranean river basins: A comparison of management frameworks, physical impacts, and ecological responses. Hydrobiologia, 719, 451-482.

Grey, D., Sadoff, C. W., 2007. Sink or Swim? Water security for growth and development. Water Policy, 9, 545-571.

Griewank, A., Walther, A., 2008. Evaluating derivatives: Principles and techniques of algorithmic differentiation. Society for Industrial and Applied Mathematics, Philadelphia, U.S.A.

Hannah, L., 2014. The Climate System and Climate Change. In: Climate Change Biology, 13-52, Elsevier Academic Press, Oxford, UK.

Hanson, B., May, D., 2011. Drip Irrigation Salinity Management for Row Crops, https://anrcatalog.ucanr.edu/pdf/8447.pdf. Data accessed July 2020.

He, C., Liu, Z., Gou, S., Zhang, Q., Zhang, J., Xu, L., 2019. Detecting global urban expansion over the last three decades using a fully convolutional network. Environmental Research Letters, 14, 1-16.

Heermann, D. F., Wallender, W. W., Bos, G. M., 1992. Irrigation Efficiency and Uniformity. In: Management of farm irrigation systems, Hoffmann G. J., Howell T. A., Solomon K. H. (Eds.), 125-149. American Society of Agricultural Engineers. St. Joseph, MI, U.S.A.

Hejazi, M., Edmonds, J., Clarke, L., Kyle, P., Davies, E., Chaturvedi, V., Kim, S., 2014. Long-term global water projections using six socioeconomic scenarios in an integrated assessment modeling framework. Technological Forecasting and Social Change, 81, 205-226.

Hillel, D., 2008. Soil and Water Management. Soil in the Environment, 175-195.

Hirschi, M., Leopold, D. E., Schwingshackl, C., Wartenburger, R., Meier, R., Gudmundsson, L., Seneviratne, S. I., 2020. Soil moisture and evapotranspiration, https://www.research-collection.ethz.ch/bitstream/handle/20.500.11850/389455/HydroCH2018_SM_ET.pdf?sequence=2&isAllowed=y. Data accessed July 2020.

Howell, T. A., 2003. Irrigation Efficiency, https://www.researchgate.net/publication/43256707_Irrigation_Efficiency. Data accessed July 2020.

Huang, Z., Hejazi, M., Tang, Q., Vernon, C. R., Liu, Y., Chen, M., Calvin, K., 2019. Global agricultural green and blue water consumption under future climate and land use changes. Journal of Hydrology, 574, 242-256.

Ikeno, J., 2018. Intra- and Inter-Sectorial Competition for Water Resources around Mwanga Town in Kilimanjaro Region, Tanzania. African Study Monographs, 55, 101-118.

Iles, C. E., Vautard, R., Strachan, J., Joussaume S., Eggen, B. R., Hewitt, C. D.,2019. The benefits of increasing resolution in global and regional climate simulations for European climate extremes. Geoscientific Model Development, 13, 5583–5607.

IPCC-TGICA, 2007. General Guidelines on the Use of Scenario Data for Climate Impact and Adaptation Assessment, Version 2. In: Climate Data and Scenarios, 15-49.

Irmak, S., Odhiambo, L. O., Kranz, W. L., Eisenhauer, D. E., 2011. Irrigation Efficiency and Uniformity, and Crop Water Use Efficiency, https://digitalcommons.unl.edu/cgi/viewcontent.cgi?article=1455&context=biosysengfacpub. Data accessed July 2020.

Jakkula, V. S. and Wani, S. P., 2018. Zeolites: Potential soil amendments for improving nutrient and water use efficiency and agriculture productivity. Scientific Reviews & Chemical Communications, 8, 1-15.

Gregorio, A.D., Jansen, L. J., 1998. Land Cover Classification System (LCCS): Classification Concepts and User Manual. In: Land cover classification system, 3-4. FAO, Rome, Italy.

Jensen, M. E., 2007. Beyond irrigation efficiency. Irrigation Science, 25, 233-245.

Jones, J. A. A., Vardanian, T. G., Hakopian, C., 2009. Threats to Global Water Security: Population Growth, Terrorism, Climate Change, or Commercialization? In: Jones, J. A. A, Threats to global water security, 3-15. Springer, Dordrecht, Netherlands.

Khalil, A., Rittima, A., Phankamolsil, Y., 2018. The projected changes in water status of the Mae Klong Basin, Thailand, using WEAP model. Paddy and Water Environment, 16, 439-455.

Koch, H., Biewald, A., Liersch, S., Azevedo, J. R., Silva, G. N., Kölling, K., . . . Hattermann, F. F., 2015. Scenarios of climate and land-use change,water demand and water availability for the São Francisco River basin. Revista Brasileira De Ciências Ambientais (Online), 36, 96-114.

Lal, R., 2016. Soil health and carbon management. Food and Energy Security, 5, 212-222.

Le Treut, H., R. Somerville, U. Cubasch, Y. Ding, C. Mauritzen, A. Mokssit, T. Peterson and M. Prather, 2007: Historical Overview of Climate Change. In: Solomon, S., D. Qin, M. Manning, Z. Chen, M. Marquis, K.B. Averyt, M. Tignor and H.L. Miller (Eds.), Climate Change 2007: The Physical Science Basis. Contribution of Working Group I to the Fourth Assessment Report of the Intergovernmental Panel on Climate Change Cambridge University Press, Cambridge, United Kingdom and New York, NY, USA.

Li, Z., Deng, X., Wu, F., Hasan, S., 2015. Scenario Analysis for Water Resources in Response to Land Use Change in the Middle and Upper Reaches of the Heihe River Basin. Sustainability, 7, 3086-3108.

Liang, S., Wang, J., 2020. Land Cover and Land Use Changes. In: Advanced remote sensing: Terrestrial information extraction and applications, 704-763. Academic Press, London, United Kingdom.

Liew, M. W., Arnold, J. G., Bosch, D. D., 2005. Problems and Potential of Autocalibrating a Hydrologic Model. Transactions of the ASAE, 48, 1025-1040.

Liu, J., Zhang, C., Kou, L., Zhou, Q., 2017. Effects of Climate and Land Use Changes on Water Resources in the Taoer River. Advances in Meteorology, 2017, 1-13.

López-Moreno, J., Zabalza, J., Vicente-Serrano, S., Revuelto, J., Gilaberte, M., Azorin-Molina, C., Tague, C., 2014. Impact of climate and land use change on water availability and reservoir management: Scenarios in the Upper Aragón River, Spanish Pyrenees. Science of The Total Environment, 493, 1222-1231.

Maddocks, A., Young, R., Reig, P., 2019. Ranking the World's Most Water-Stressed Countries in 2040, https://www.wri.org/blog/2015/08/ranking-world-s-most-water-stressed-countrtübiies-2040. Data accessed July 2020.

Madsen, M. S., Maule, C. F., Mackellar, N., Olesen, J., Christensen, J. H., 2012. Selection of climate change scenario data for impact modelling. Food Additives & Contaminants: Part A, 29, 1502-1513.

Mahmood, R., Hubbard, K., 2002. Anthropogenic land-use change in the North American tall grass-short grass transition and modification of near-surface hydrologic cycle. Climate Research, 21, 83-90.

Mallakpour, I., Villarini, G., 2015. The changing nature of flooding across the central United States. Nature Climate Change, 5, 250-254.

Marx, K., 2014. The Labour-Process and the Process of Producing Surplus-Value. In: Das Capital 127-128, CreateSpace Independent Publishing Platform, North Charleston, U.S.A.

McCartney, M., Arranz, R., 2009. Evaluation of water demand Scenarios for the Olifants River catchment, South Africa. International Journal of River Basin Management, 7, 379-390.

Myhre, G., D. Shindell, F.-M. Bréon, W. Collins, J. Fuglestvedt, J. Huang, D. Koch, J.-F. Lamarque, D. Lee, B. Mendoza, T. Nakajima, A. Robock, G. Stephens, T. Takemura and H. Zhang, 2013: Anthropogenic and Natural Radiative Forcing. In: Climate Change 2013: The Physical Science Basis. Contribution of Working Group I to the Fifth Assessment Report of the Intergovernmental Panel on Climate Change, Stocker, T.F., D. Qin, G.-K. Plattner, M. Tignor, S.K. Allen, J. Boschung, A. Nauels, Y. Xia, V. Bex and P.M. Midgley (Eds.), Cambridge University Press, Cambridge, United Kingdom and New York, NY, USA.

Moriasi, D. N., Arnold, J. G., Liew, M. W., Bingner, R. L., Harmel, R. D., Veith, T. L., 2007. Model Evaluation Guidelines for Systematic Quantification of Accuracy in Watershed Simulations. Transactions of the ASABE, 50, 885-900.

Nagabhatla, N., Springgay, E., Dudley, N., 2018. Forests as Nature-Based Solutions for Ensuring Urban Water Security. Unaslyva, 69, 43-52.

Nakicenovic, N., Davidson, O., Davis, G., Grübler, A., Kram, T., La Rovere, E. L., . . . Dadi, Z., 2000. Summary for Policymakers. In: Nakićenović, N., Alcamo J., Davis G., Vries B., Fenhann, J., Gaffin S.,. (Eds.), Special report on emissions scenarios, 1-21. Cambridge University Press, Cambridge, UK.

Ning, L., Bradley, R. S., 2015. NAO and PNA influences on winter temperature and precipitation over the eastern United States in CMIP5 GCMs. Climate Dynamics, 46, 1257-1276.

NASA, 2020. The Effects of Climate Change, https://climate.nasa.gov/effects/. Data accessed June 2020.

Nash, J., Sutcliffe, J., 1970. River flow forecasting through conceptual models part I — A discussion of principles. Journal of Hydrology, 10, 282-290.

National Drought Mitigation Centre, 2020. https://droughtmonitor.unl.edu/Data/Timeseries.aspx. Data accessed June 2020.

Ning, L., Bradley, R. S., 2015. NAO and PNA influences on winter temperature and precipitation over the eastern United States in CMIP5 GCMs. Climate Dynamics, 46, 1257-1276.

Ndulue, E. L., Mbajiorgu, C. C., Ugwu, S. N., Ogwo, V., Ogbu, K. N., 2015. Assessment of land use/cover impacts on runoff and sediment yield using hydrologic models: A review. Journal of Ecology and The Natural Environment, 7, 46-55.

Oftadeh, E., Shourian, M., Saghafian, B., 2017. An Ultimatum Game Theory Based Approach for Basin Scale Water Allocation Conflict Resolution. Water Resources Management, 31, 4293-4308.

Orman ve Su İşleri Bakanlığı, 2016. İklim Değişikliğinin Su Kaynaklarına Etkisi Projesi, http://iklim.ormansu.gov.tr/ckfinder/userfiles/files/Iklim_NihaiRapor.pdf. Data accessed September 2020.

Page, M. L., Fakir, Y., Aouissi, J., 2020. Modeling for integrated water resources management in the Mediterranean region. Water Resources in the Mediterranean Region, 157-190.

Pahl-Wostl, C., 2009. A conceptual framework for analysing adaptive capacity and multi-level learning processes in resource governance regimes. Global Environmental Change, 19, 354-365.

Peña-Arancibia, J. L., Bruijnzeel, L. A., Mulligan, M., Dijk, A. I., 2019. Forests as ‘sponges’ and ‘pumps’: Assessing the impact of deforestation on dry-season flows across the tropics. Journal of Hydrology, 574, 946-963.

Pianosi, F., Beven, K., Freer, J., Hall, J. W., Rougier, J., Stephenson, D. B., Wagener, T., 2016. Sensitivity analysis of environmental models: A systematic review with practical workflow. Environmental Modelling & Software, 79, 214-232.

Pouyat, R. V., Pataki, D. E., Belt, K. T., Groffman, P. M., Hom, J., Band, L. E., 2007. Effects of Urban Land-Use Change on Biogeochemical Cycles. Terrestrial Ecosystems in a Changing World Global Change — The IGBP Series, 45-58.

Purkey, D. R., Joyce, B., Vicuna, S., Hanemann, M. W., Dale, L. L., Yates, D., Dracup, J. A., 2007. Robust analysis of future climate change impacts on water for agriculture and other sectors: A case study in the Sacramento Valley. Climatic Change, 87, 109-122.

Pushpalatha, R., Perrin, C., Moine, N. L., Mathevet, T., Andréassian, V., 2011. A downward structural sensitivity analysis of hydrological models to improve low-flow simulation. Journal of Hydrology, 411, 66-76.

Ramankutty, N., Foley, J. A., 1999. Estimating historical changes in global land cover: Croplands from 1700 to 1992. Global Biogeochemical Cycles, 13, 997-1027.

Singh, V. P., Frevert, D. K. (Eds), 2002. Mathematical models of large watershed hydrology, Water Resources Publications, Denver, U.S.A.

Ramirez, V. H., Harmsen, E. W., 2014. Water Vapor Flux Models for Agriculture. In: Evapotranspiration: Principles and applications for water management, Goyal, M. R., Harmsen, E. W. (Eds.), 20-65. Apple Academic Press., Toronto, Canada.

Randall, D.A., R.A. Wood, S. Bony, R. Colman, T. Fichefet, J. Fyfe, V. Kattsov, A. Pitman, J. Shukla, J. Srinivasan, R.J. Stouffer, A. Sumi and K.E. Taylor, 2007: Climate Models and Their Evaluation. In: Climate Change 2007: The Physical Science Basis. Contribution of Working Group I to the Fourth Assessment Report of the Intergovernmental Panel on Climate Change, Solomon, S., D. Qin, M. Manning, Z. Chen, M. Marquis, K.B. Averyt, M. Tignor and H.L. Miller (Eds.), Cambridge University Press, Cambridge, United Kingdom and New York, NY, USA.

Ravar, Z., Zahraie, B., Sharifinejad, A., Gozini, H., Jafari, S., 2020. System dynamics modeling for assessment of water–food–energy resources security and nexus in Gavkhuni basin in Iran. Ecological Indicators, 108, 105682.

Reicosky, D. C., Wilts, A. R., 2004. Crop Water Requirements. In: Hillel, D., Hatfield, J. L., Scow, K. M., Powlson, D. S., Singer, M. J., Rosenzweig C. (Eds.), Encyclopedia of soils in the environment, 322-334, Academic Press, Oxford, UK.

Rival, 1989. In The New Merriam-Webster dictionary. Springfield, MA: Merriam-Webster.

Rockström, J., Falkenmark, M., Karlberg, L., Hoff, H., Rost, S., Gerten, D., 2009. Future water availability for global food production: The potential of green water for increasing resilience to global change. Water Resources Research, 45, 1-16.

Rogelj, J., Meinshausen, M., Knutti, R., 2012. Global warming under old and new scenarios using IPCC climate sensitivity range estimates. Nature Climate Change, 2, 248-253.

Ruben, G. B., Zhang, K., Dong, Z., Xia, J., 2020. Analysis and Projection of Land-Use/Land-Cover Dynamics through Scenario-Based Simulations Using the CA-Markov Model: A Case Study in Guanting Reservoir Basin, China. Sustainability, 12, 3747-3768.

Sade, R., Rimmer, A., Samuels, R., Salingar, Y., Denisyuk, M., Alpert, P., 2016. Water Management in a Complex Hydrological Basin—Application of Water Evaluation and Planning Tool (WEAP) to the Lake Kinneret Watershed, Israel. In: Integrated Water Resources Management: Concept, Research and Implementation, Borchardt D., Bogardi J., Ibisch R. (Eds.), 35-57. Springer.

Schultz, B., Uhlenbrook, S., 2008. Water security. Water for a Changing World - Developing Local Knowledge and Capacity.

Schyns, J. F., Hoekstra, A. Y., Booij, M. J., Hogeboom, R. J., Mekonnen, M. M., 2019). Limits to the world's green water resources for food, feed, fiber, timber, and bioenergy. Proceedings of the National Academy of Sciences, 116, 4893-4898.

SEI US, 2020. WEAP: Water Evaluation and Planning system, https://www.sei.org/projects-and-tools/tools/weap/. Data accessed July 2020.

Sieber, J., Purkey, D., 2015. Water Evaluation and Planning System - User Guide, https://www.weap21.org/downloads/WEAP_User_Guide.pdf. Data accessed July 2020.

Siebert, S., Doell, P., 2007. Irrigation water use – A global perspective. In Lozán J. L., Global change: Enough water for all?: Scientific facts, 104-107, Wissenschaftliche Auswertungen, Hamburg, Germany.

Siebert, S., Kummu, M., Porkka, M., Döll, P., Ramankutty, N., Scanlon, B. R., 2014 . Hydrology and Earth System Sciences Discussions, 11, 13207-13258.

Smith, J. B., Klein, R. J., Huq, S., 2003. Introduction. In: Climate change, adaptive capacity and development, Smith, J. B., Klein, R. J., Huq, S., 1-9, Imperial College Press, London, UK.

Spring, Ú O., Brauch, H. G., 2009. Securitizing Water. In: Facing Global Environmental Change, 175-176, Springer, Berlin, Germany

Sun, Z., Wang, Q., Batkhishig, O., Ouyang, Z., 2016. Relationship between Evapotranspiration and Land Surface Temperature under Energy- and Water-Limited Conditions in Dry and Cold Climates. Advances in Meteorology, 2016, 1-9.

TAGEM, DSI., 2016. Türkiye'de Sulanan Bitkilerin Bitki Su Tüketimi Rehberi, https://www.tarimorman.gov.tr/TAGEM/Belgeler/T%C3%BCrkiyede%20Sulanan%20Bitkilerin%20Su%20T%C3%BCketimi%20Rehberi%205-9-2016.pdf. Data accessed August 2020.

Tarantola, S., Campolongo, F., Ratto, M. 2007). Test Cases. In: Saltelli, A., Sensitivity analysis in practice: A guide to assessing scientific models, 63-90. John Wiley & Sons, Chichester, England.

Tilman, D., 1999. Global environmental impacts of agricultural expansion: The need for sustainable and efficient practices. Proceedings of the National Academy of Sciences, 96, 5995-6000.

Tarım ve Orman Bakanlığı, 2018. Havza Koruma Eylem Planlarının Nehir Havzası Yönetim Planlarına Dönüştürülmesi için Teknik Yardım. Retrieved June 20, 2020, from http://ribamap.ormansu.gov.tr/shared/files/en_1546426129.pdf

Tübitak, 2010. Büyük Menderes Havzası Eylem Plan Raporu, https://www.tarimorman.gov.tr/SYGM/Belgeler/havza%20koruma%20eylem%20planlar%C4%B1/B.Menderes_Havzas%C4%B1.pdf. Data accessed July 2020.

TUIK, 2019. Bitkisel Üretim İstatistikleri, https://data.tuik.gov.tr/Search/Search?text=tarim. Data accessed August 2020.

Valentín, F., Nortes, P. A., Domínguez, A., Sánchez, J. M., Intrigliolo, D. S., Alarcón, J. J., López-Urrea, R., 2019. Comparing evapotranspiration and yield performance of maize under sprinkler, superficial and subsurface drip irrigation in a semi-arid environment. Irrigation Science, 38, 105-115.

Vörösmarty, C. J., Mcintyre, P. B., Gessner, M. O., Dudgeon, D., Prusevich, A., Green, P., . . . Davies, P. M., 2010. Erratum: Global threats to human water security and river biodiversity. Nature, 468, 334-334.

Wang, Y., Li, S., Qin, S., Guo, H., Yang, D., Lam, H., 2020. How can drip irrigation save water and reduce evapotranspiration compared to border irrigation in arid regions in northwest China. Agricultural Water Management, 239, 106256.

WaterAid, 2012. Water security framework, https://washmatters.wateraid.org/sites/g/files/jkxoof256/files/download-our-water-security-framework.pdf. Data accessed July 2020.

WEAP, n.d. Schematic View, https://www.weap21.org/WebHelp/Schematic_View.htm. November 2020.

Wilson, T. S., Schmidt, N. D., Langridge, R., 2020. Land-Use Change and Future Water Demand in California's Central Coast. Land, 9, 1-21.

World Bank, 2014. Agricultural irrigated land (% of total agricultural land)–Turkey, https://data.worldbank.org/indicator/AG.LND.IRIG.AG.ZS?locations=TR. Data accessed September 2020.

World Water, 2020. Water Conflict Chronology, http://www.worldwater.org/conflict/list/. Data accessed July 2020.

Xie, M., Küffner, U., Moigne, G. L., 1993. Measures To Improve Efficiency: Technological Option. In: Using water efficiently: Technological options, 19-26, The World Bank, Washington DC, U.S.A.

Yang, L., Hao, M., Cao, Q., Liu, K., Xiao, L., Pei, L., Wu, X., 2020. Quantitative Impact and Research on Water Supply Management and Demand in Beijing under the WEAP Model. IOP Conference Series: Earth and Environmental Science, 514, 022055.

Yates, D., Sieber, J., Purkey, D., Huber-Lee, A., 2005. WEAP21—A Demand-, Priority-, and Preference-Driven Water Planning Model. Water International, 30, 487-500.

Yıldız, M., Özkaya, M., Gürbüz, A., Uçar, G, 2007. Turkey Surface Water Potential and Its Change in Time, International Congress on River Basin Management, 127-139, Antalya, 22-24 June 2007, Turkey.

Yilmaz, B., Harmancioglu, N. B., 2010. An Indicator Based Assessment for Water Resources Management in Gediz River Basin, Turkey. Water Resources Management, 24, 4359-4379.

Zappa, G., Shepherd, T., 2017. Storylines of Atmospheric Circulation Change for European Regional Climate Impact Assessment. Journal of Climate, 30, 6561-6577.

Zeitoun, M., Bakker, K., Conway, D., 2013. Introduction: A Battle of Ideas for Water Security. In: Lankford, B. A., Water security: Principles, perspectives, and practices, 3-4, Routledge, Taylor & Francis Group, New York, U.S.A.

Çakmak, Ö, Baran, T., 2015. Büyük Menderes Havzası Yağışlarında Eğilim Analizi, Su Yapıları Sempozyumu, 419-428, 19-21 November 2015, Turkey.

Çevre ve Orman Bakanlığı, 2007. Birleşmiş Milletler İklim Değişikliği Çerçeve Sözleşmesi Kapsamında Birinci Ulusal Bildirimi, https://www.mgm.gov.tr/FILES/iklim/birinci-Ulusal-Bildirimi.pdf. Data accessed June 2020.

Çevre ve Şehircilik Bakanlığı, 2015. Gediz Havzası Kirlilik Önleme Eylem Planı, https://webdosya.csb.gov.tr/db/cygm/editordosya/Gediz_KOEP_2015_04_14.pdf. Data accessed July 2020.

Çevre ve Şehircilik Bakanlığı, 2016. Büyük Menderes Nehir Havzası Taslak Yönetim Planı, https://webdosya.csb.gov.tr/db/scd/menu/buyuk-menderes-nehir-havzasi-scd-raporu_final_tr_20181108013851.pdf. Data accessed July 2020.

APPENDICES

APPENDIX A: ANNUAL AVERAGE BASELINE RESERVOIR STORAGE VOLUME RATES AND DECADAL AVERAGE DIFFERENCE OF RESERVOIR STORAGE VOLUMES WITH RESPECT BASELINE SCENARIO

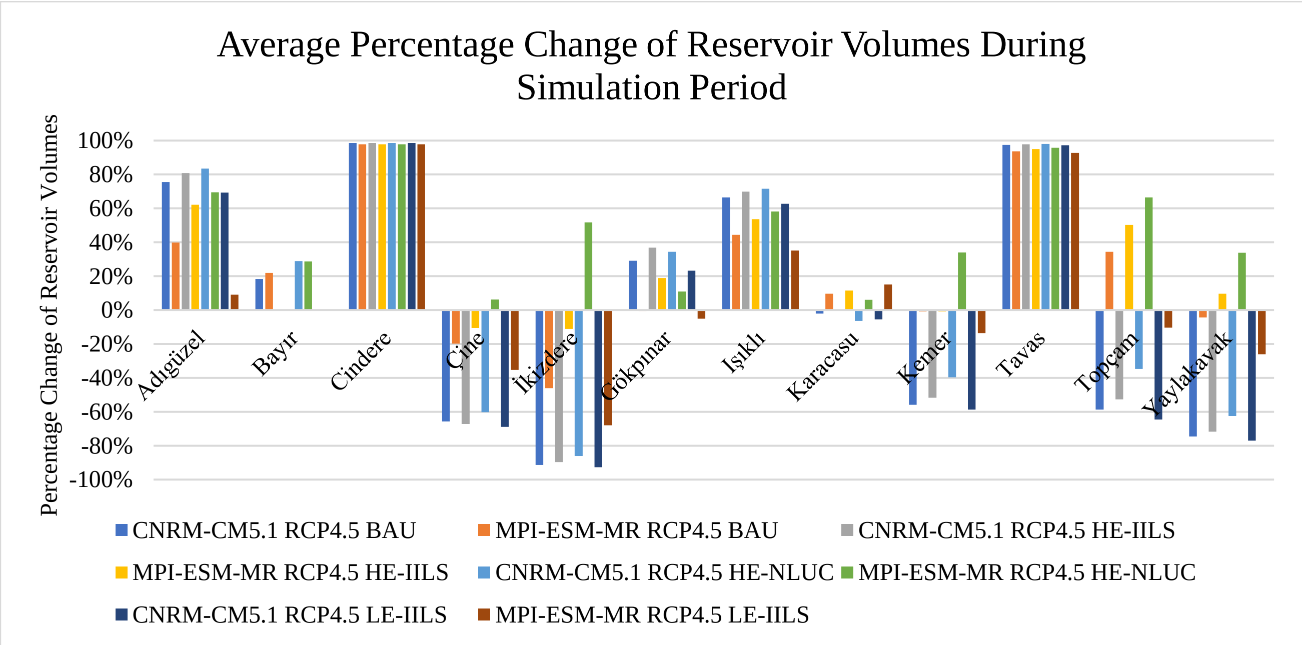

Figure 1.1. Average percentage change of reservoir volumes during simulation period with respect to average reservoir volume under the results of CNRM and MPI and RCP4.5 conditions.

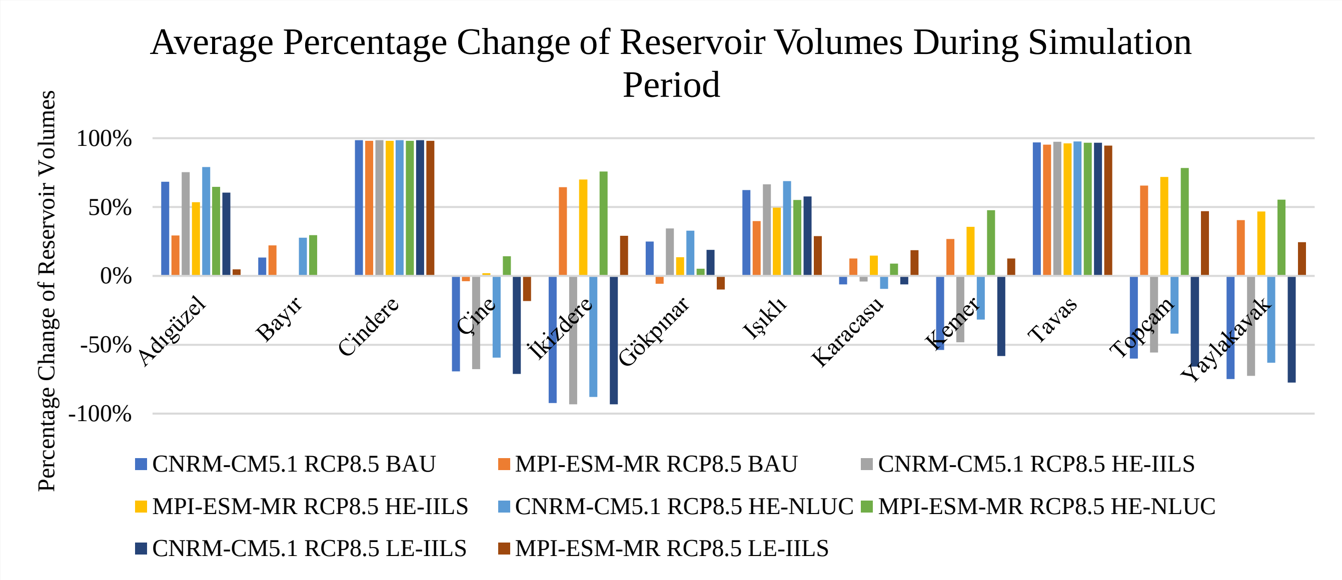

Figure 1.2. Average percentage change of reservoir volumes during simulation period with respect to average reservoir volume under the results of CNRM and MPI and RCP8.5 conditions.

Table 1. Annual average baseline reservoir storage volume rates (in million m^3).

	Adıgüzel	Bayır	Cindere	Çine	Gökpınar	İkizdere	Işıklı	Karacasu	Kemer	Tavas	Topçam	Yaylakava
2005	496,49	0,00	0,00	0,00	18,53	0,00	109,99	0,00	154,58	0,00	43,35	14,19
2006	396,33	0,00	0,00	0,00	19,91	0,00	137,52	0,00	196,60	0,00	50,28	16,92
2007	185,47	0,00	0,00	0,00	13,03	0,00	111,32	0,00	99,19	0,00	33,38	12,31
2008	272,42	0,00	0,00	0,00	15,90	0,00	101,02	0,00	262,94	0,00	45,80	22,96
2009	390,09	5,48	0,00	0,00	18,19	0,00	154,52	0,00	296,07	0,00	65,29	19,33
2010	558,08	6,73	0,00	0,00	19,96	0,00	180,25	0,00	253,15	0,00	68,92	20,25
2011	793,46	5,89	72,77	0,00	23,06	0,00	172,23	0,00	269,13	0,00	62,98	20,20
2012	796,09	6,67	83,02	0,00	20,02	0,00	154,84	0,00	288,61	0,00	58,06	19,99
2013	814,15	5,13	82,24	0,00	20,94	127,95	132,17	12,40	342,85	52,76	62,61	21,68
2014	650,13	5,17	77,39	306,03	20,12	126,54	133,43	11,55	286,15	42,41	40,59	18,94
2015	810,86	4,94	82,14	180,86	24,84	138,76	186,17	14,66	304,74	51,06	55,36	20,02
2016	696,00	3,59	82,86	237,54	18,19	122,32	113,82	14,63	337,10	38,24	46,95	19,13
2017	561,03	3,41	81,58	283,10	21,12	59,79	108,59	13,01	191,92	41,95	38,10	13,91
2018	419,15	4,61	81,90	247,84	19,30	59,92	90,56	13,35	163,18	38,71	41,46	17,25
Average	559,98	5,16	80,49	251,07	19,51	105,88	134,74	13,27	246,16	44,19	50,94	18,36

Table 2. Decadal average reservoir storage difference of Adıgüzel Reservoir under different scenarios with respect to average baseline volume rate (in million m^3).

	2019-2030	2031-2040	2041-2050	2051-2060	2061-2070	2071-2080	2081-2090	2091-2100
CNRM-CM5.1 RCP4.5 BAU	365,5	387,1	480,9	500,1	407,3	427,2	422,8	393,3
CNRM-CM5.1 RCP8.5 BAU	323,5	389,6	404,3	400,2	401,7	373,4	436,9	333,4
MPI-ESM-MR RCP4.5 BAU	190,1	178,4	213,0	346,2	186,6	270,1	82,8	315,4
MPI-ESM-MR RCP8.5 BAU	149,3	196,2	285,1	323,6	125,6	90,2	68,7	81,7
CNRM-CM5.1 RCP4.5 HE-IILS	394,2	439,0	494,0	508,1	444,9	464,7	453,4	437,4
CNRM-CM5.1 RCP8.5 HE-IILS	358,8	427,6	445,3	446,8	440,8	421,3	466,4	389,1
MPI-ESM-MR RCP4.5 HE-IILS	270,2	327,7	356,4	409,8	345,6	365,8	371,3	379,9
MPI-ESM-MR RCP8.5 HE-IILS	263,7	330,0	368,0	396,3	250,7	253,2	303,5	298,4
CNRM-CM5.1 RCP4.5 HE-NLUC	402,5	463,5	500,3	511,2	464,9	478,1	468,8	460,1
CNRM-CM5.1 RCP8.5 HE-NLUC	369,4	446,6	466,4	466,9	461,7	445,0	480,0	418,6
MPI-ESM-MR RCP4.5 HE-NLUC	288,9	382,2	402,3	436,1	404,2	399,0	413,4	410,6
MPI-ESM-MR RCP8.5 HE-NLUC	285,6	382,9	405,5	427,3	333,2	354,9	385,3	361,7
CNRM-CM5.1 RCP4.5 LE-IILS	347,3	323,9	462,3	490,0	364,8	379,9	390,3	346,0
CNRM-CM5.1 RCP8.5 LE-IILS	301,8	349,1	360,4	336,8	359,1	310,5	407,3	285,7
MPI-ESM-MR RCP4.5 LE-IILS	29,7	4,0	-68,1	269,3	73,1	-24,2	-74,4	196,9
MPI-ESM-MR RCP8.5 LE-IILS	19,9	112,7	189,9	133,1	-3,4	-26,1	-103,1	-109,4

Table 3. Decadal average reservoir storage difference of Bayır Reservoir under different scenarios with respect to average baseline volume rate (in million m^3).

	2019-2030	2031-2040	2041-2050	2051-2060	2061-2070	2071-2080	2081-2090	2091-2100
CNRM-CM5.1 RCP4.5 BAU	0,54	1,21	1,09	0,81	0,83	1,15	1,03	0,95
CNRM-CM5.1 RCP8.5 BAU	0,37	1,26	1,07	0,40	0,96	0,29	0,94	0,22
MPI-ESM-MR RCP4.5 BAU	0,69	1,41	1,18	0,96	1,16	1,13	1,21	1,27
MPI-ESM-MR RCP8.5 BAU	0,83	1,52	1,49	1,26	0,99	1,04	1,18	0,83
CNRM-CM5.1 RCP4.5 HE-NLUC	1,14	1,68	1,58	1,45	1,50	1,63	1,54	1,51
CNRM-CM5.1 RCP8.5 HE-NLUC	0,98	1,67	1,53	1,38	1,49	1,48	1,52	1,52
MPI-ESM-MR RCP4.5 HE-NLUC	1,05	1,68	1,55	1,42	1,51	1,54	1,64	1,58
MPI-ESM-MR RCP8.5 HE-NLUC	1,17	1,73	1,76	1,58	1,45	1,56	1,61	1,45

Table 4. Decadal average reservoir storage difference of Cindere Reservoir under different scenarios with respect to average baseline volume rate (in million m^3).

	2019-2030	2031-2040	2041-2050	2051-2060	2061-2070	2071-2080	2081-2090	2091-2100
CNRM-CM5.1 RCP4.5 BAU	2,98	3,73	3,77	3,76	3,72	3,72	3,68	3,68
CNRM-CM5.1 RCP8.5 BAU	3,03	3,72	3,69	3,69	3,74	3,72	3,67	3,67
MPI-ESM-MR RCP4.5 BAU	2,94	3,68	3,67	3,67	3,68	3,69	3,67	3,66
MPI-ESM-MR RCP8.5 BAU	3,10	3,66	3,60	3,64	3,60	3,65	3,65	3,64
CNRM-CM5.1 RCP4.5 HE-IILS	2,98	3,73	3,77	3,76	3,72	3,72	3,68	3,68
CNRM-CM5.1 RCP8.5 HE-IILS	3,03	3,72	3,69	3,69	3,74	3,72	3,67	3,67
MPI-ESM-MR RCP4.5 HE-IILS	2,94	3,68	3,67	3,67	3,68	3,69	3,67	3,66
MPI-ESM-MR RCP8.5 HE-IILS	3,10	3,66	3,60	3,64	3,60	3,65	3,65	3,64
CNRM-CM5.1 RCP4.5 HE-NLUC	2,98	3,73	3,77	3,76	3,72	3,72	3,68	3,69
CNRM-CM5.1 RCP8.5 HE-NLUC	3,03	3,72	3,69	3,69	3,74	3,72	3,67	3,67
MPI-ESM-MR RCP4.5 HE-NLUC	2,94	3,68	3,67	3,67	3,68	3,69	3,67	3,66
MPI-ESM-MR RCP8.5 HE-NLUC	3,10	3,66	3,60	3,64	3,60	3,65	3,65	3,64
CNRM-CM5.1 RCP4.5 LE-IILS	2,98	3,73	3,77	3,76	3,72	3,72	3,68	3,69
CNRM-CM5.1 RCP8.5 LE-IILS	3,03	3,72	3,69	3,69	3,74	3,72	3,67	3,67
MPI-ESM-MR RCP4.5 LE-IILS	2,94	3,68	3,67	3,67	3,68	3,69	3,67	3,66
MPI-ESM-MR RCP8.5 LE-IILS	3,10	3,66	3,60	3,64	3,60	3,65	3,65	3,64

Table 5. Decadal average reservoir storage difference of Çine Reservoir under different scenarios with respect to average baseline volume rate (in million m^3).

	2019-2030	2031-2040	2041-2050	2051-2060	2061-2070	2071-2080	2081-2090	2091-2100
CNRM-CM5.1 RCP4.5 BAU	-148,54	-175,22	-159,35	-148,66	-149,05	-154,84	-184,96	-87,79
CNRM-CM5.1 RCP8.5 BAU	-170,49	-152,59	-177,94	-191,19	-177,08	-175,68	-177,18	-171,15
MPI-ESM-MR RCP4.5 BAU	-48,46	-64,12	-75,51	-16,27	-47,56	-10,55	-88,55	-46,17
MPI-ESM-MR RCP8.5 BAU	-12,54	-10,63	18,47	3,04	0,3	-4,19	-24,41	-47,34
CNRM-CM5.1 RCP4.5 HE-HLUC	-161,54	-182,19	-168,83	-170,37	-166,51	-178,37	-187,06	-136,03
CNRM-CM5.1 RCP8.5 HE-HLUC	-167,21	-138,66	-176,42	-189,55	-173,75	-173,8	-173,22	-165,74
MPI-ESM-MR RCP4.5 HE-HLUC	-28,06	-30,14	-42,13	-2,25	-31,78	7,72	-65,26	-20,81
MPI-ESM-MR RCP8.5 HE-HLUC	-0,31	7,49	31,51	16,8	15,68	8,84	-9,11	-29,12
CNRM-CM5.1 RCP4.5 HE-NLUC	-148,54	-175,22	-159,35	-148,66	-149,05	-154,84	-184,96	-87,79
CNRM-CM5.1 RCP8.5 HE-NLUC	-159,56	-62,5	-163,86	-184,47	-159,29	-160,13	-160,08	-140,36
MPI-ESM-MR RCP4.5 HE-NLUC	-2,68	26,03	3,99	27,58	5,99	41,47	-3,55	26,51
MPI-ESM-MR RCP8.5 HE-NLUC	17,12	51,94	61	46,79	44,38	34,41	25,2	6,53
CNRM-CM5.1 RCP4.5 LE-HLUC	-170,21	-184,12	-171,33	-175,39	-172,44	-180,33	-188,16	-143,09
CNRM-CM5.1 RCP8.5 LE-HLUC	-173,77	-162,37	-180,26	-194,42	-182,88	-179,01	-183,28	-175,89
MPI-ESM-MR RCP4.5 LE-HLUC	-76,49	-99,65	-106,87	-48,82	-82,84	-73,33	-125,23	-94,35
MPI-ESM-MR RCP8.5 LE-HLUC	-31,61	-52,14	-9,41	-28,81	-40,02	-40,56	-77,39	-84,05

Table 6. Decadal average reservoir storage difference of Gökpınar Reservoir under different scenarios with respect to average baseline volume rate (in million m^3).

	2019-2030	2031-2040	2041-2050	2051-2060	2061-2070	2071-2080	2081-2090	2091-2100
CNRM-CM5.1 RCP4.5 BAU	5,06	5,38	6,44	7,27	4,92	5,77	4,63	5,79
CNRM-CM5.1 RCP8.5 BAU	4,51	5,12	5,18	4,88	5,41	4,78	4,86	4,25
MPI-ESM-MR RCP4.5 BAU	-0,45	-1,94	0,71	0,24	0,52	-0,01	-0,99	0,96
MPI-ESM-MR RCP8.5 BAU	-1,36	0,12	-0,10	-0,50	-1,34	-1,65	-1,60	-2,51
CNRM-CM5.1 RCP4.5 HE-IILS	6,56	6,52	7,22	7,79	6,19	6,83	6,09	6,85
CNRM-CM5.1 RCP8.5 HE-IILS	6,12	6,19	6,42	6,14	6,61	6,08	6,10	5,87
MPI-ESM-MR RCP4.5 HE-IILS	2,34	1,04	2,96	2,78	2,69	1,90	1,29	3,72
MPI-ESM-MR RCP8.5 HE-IILS	2,11	2,63	2,33	1,83	0,10	0,22	0,65	0,00
CNRM-CM5.1 RCP4.5 HE-NLUC	6,93	7,10	7,55	7,96	6,84	7,33	6,72	7,34
CNRM-CM5.1 RCP8.5 HE-NLUC	6,51	6,74	7,03	6,77	7,16	6,66	6,76	6,70
MPI-ESM-MR RCP4.5 HE-NLUC	3,31	2,98	4,26	4,17	4,13	3,74	3,26	4,91
MPI-ESM-MR RCP8.5 HE-NLUC	3,25	4,08	3,83	3,74	1,72	1,89	2,53	1,62
CNRM-CM5.1 RCP4.5 LE-IILS	4,21	4,11	5,58	6,57	3,66	4,22	3,42	4,39
CNRM-CM5.1 RCP8.5 LE-IILS	3,65	4,24	3,79	3,49	4,15	3,77	3,86	2,62
MPI-ESM-MR RCP4.5 LE-IILS	-0,88	-2,56	-0,57	-1,06	-0,19	-0,78	-1,74	-0,21
MPI-ESM-MR RCP8.5 LE-IILS	-1,83	-0,93	-1,13	-1,52	-1,93	-2,38	-2,45	-3,24

Table 7. Decadal average reservoir storage difference of İkizdere Reservoir under different scenarios with respect to average baseline volume rate (in million m^3).

	2019-2030	2031-2040	2041-2050	2051-2060	2061-2070	2071-2080	2081-2090	2091-2100
CNRM-CM5.1 RCP4.5 BAU	-90,1	-99,8	-96,7	-101,6	-98,0	-98,8	-101,1	-87,4
CNRM-CM5.1 RCP8.5 BAU	-93,0	-97,3	-95,9	-101,4	-98,9	-98,3	-98,6	-97,8
MPI-ESM-MR RCP4.5 BAU	-56,8	-13,4	-68,6	-27,0	-28,3	-57,2	-68,8	-69,9
MPI-ESM-MR RCP8.5 BAU	59,4	77,3	77,3	71,4	78,9	61,3	65,7	54,3
CNRM-CM5.1 RCP4.5 HE-IILS	-83,8	-99,1	-94,8	-101,3	-96,6	-97,8	-101,0	-82,6
CNRM-CM5.1 RCP8.5 HE-IILS	-88,5	-96,1	-94,1	-101,3	-98,7	-97,4	-96,0	-96,7
MPI-ESM-MR RCP4.5 HE-IILS	0,1	69,2	61,2	74,8	67,4	60,8	55,6	61,4
MPI-ESM-MR RCP8.5 HE-IILS	68,2	80,4	79,9	77,2	81,3	69,6	73,0	69,4
CNRM-CM5.1 RCP4.5 HE-NLUC	-79,9	-97,5	-89,4	-99,5	-93,0	-95,5	-99,3	-72,5
CNRM-CM5.1 RCP8.5 HE-NLUC	-84,8	-91,1	-89,3	-100,6	-96,9	-95,7	-89,8	-93,0
MPI-ESM-MR RCP4.5 HE-NLUC	-2,1	68,1	59,2	74,3	66,3	58,6	54,0	59,8
MPI-ESM-MR RCP8.5 HE-NLUC	71,6	83,8	83,4	82,8	84,0	77,8	80,1	80,7
CNRM-CM5.1 RCP4.5 LE-IILS	-91,2	-100,3	-98,4	-101,9	-99,6	-99,5	-101,3	-92,6
CNRM-CM5.1 RCP8.5 LE-IILS	-94,4	-98,1	-98,2	-101,5	-99,4	-98,9	-100,5	-99,0
MPI-ESM-MR RCP4.5 LE-IILS	-71,8	-46,4	-85,4	-53,4	-78,7	-74,7	-84,5	-81,7
MPI-ESM-MR RCP8.5 LE-IILS	48,7	57,3	67,8	53,8	70,0	15,3	-23,9	-42,4

Table 8. Decadal average reservoir storage difference of Işıklı Reservoir under different scenarios with respect to average baseline volume rate (in million m^3).

	2019-2030	2031-2040	2041-2050	2051-2060	2061-2070	2071-2080	2081-2090	2091-2100
CNRM-CM5.1 RCP4.5 BAU	85,9	88,4	95,5	99,3	86,0	90,0	81,9	89,4
CNRM-CM5.1 RCP8.5 BAU	83,7	84,7	86,4	81,8	88,3	82,0	80,6	84,0
MPI-ESM-MR RCP4.5 BAU	55,2	55,4	62,3	60,6	61,2	61,6	53,2	69,6
MPI-ESM-MR RCP8.5 BAU	58,9	60,4	61,0	57,5	50,3	43,6	52,1	44,5
CNRM-CM5.1 RCP4.5 HE-IILS	92,5	94,0	98,6	101,0	91,0	94,9	88,8	94,7
CNRM-CM5.1 RCP8.5 HE-IILS	90,2	90,4	92,6	88,4	93,3	87,8	87,4	90,7
MPI-ESM-MR RCP4.5 HE-IILS	70,2	72,1	73,7	72,5	72,6	73,5	69,7	79,1
MPI-ESM-MR RCP8.5 HE-IILS	74,3	73,0	72,3	70,3	64,4	58,6	66,3	62,3
CNRM-CM5.1 RCP4.5 HE-NLUC	94,2	96,5	100,1	101,7	93,6	96,8	92,4	97,0
CNRM-CM5.1 RCP8.5 HE-NLUC	91,8	93,1	95,2	91,4	95,7	90,8	90,4	93,6
MPI-ESM-MR RCP4.5 HE-NLUC	74,3	78,8	79,6	78,7	78,8	79,7	78,4	83,9
MPI-ESM-MR RCP8.5 HE-NLUC	77,9	79,7	78,4	77,0	72,0	68,3	73,7	72,7
CNRM-CM5.1 RCP4.5 LE-IILS	82,4	81,8	91,8	96,6	80,8	84,9	74,4	83,8
CNRM-CM5.1 RCP8.5 LE-IILS	79,5	78,5	80,0	74,8	82,8	75,4	73,3	76,9
MPI-ESM-MR RCP4.5 LE-IILS	47,4	37,2	48,7	48,0	49,6	49,4	39,3	59,7
MPI-ESM-MR RCP8.5 LE-IILS	49,6	47,2	47,1	43,1	32,5	29,9	34,4	27,8

Table 9. Decadal average reservoir storage difference of Karacasu Reservoir under different scenarios with respect to average baseline volume rate (in million m^3).

	2019-2030	2031-2040	2041-2050	2051-2060	2061-2070	2071-2080	2081-2090	2091-2100
CNRM-CM5.1 RCP4.5 BAU	-0,16	0,03	-0,8	-0,26	-0,97	-0,59	-0,58	1,06
CNRM-CM5.1 RCP8.5 BAU	-0,04	0,48	-1,24	-1,77	-0,42	-1,56	-0,47	-1,54
MPI-ESM-MR RCP4.5 BAU	1,05	1,51	0,74	1,75	1,35	0,78	1,64	1,36
MPI-ESM-MR RCP8.5 BAU	1,93	2,01	1,8	2,05	1,63	1,31	1,9	0,87
CNRM-CM5.1 RCP4.5 HE-HLUC	0,8	0,23	-0,57	0,02	-0,8	-0,3	-0,34	1,36
CNRM-CM5.1 RCP8.5 HE-HLUC	0,4	0,64	-0,81	-1,56	-0,23	-1,3	-0,29	-1,21
MPI-ESM-MR RCP4.5 HE-HLUC	1,37	1,72	1,02	2,01	1,7	1,06	1,83	1,62
MPI-ESM-MR RCP8.5 HE-HLUC	2,31	2,25	2,08	2,34	1,93	1,58	2,12	1,09
CNRM-CM5.1 RCP4.5 HE-NLUC	-0,99	-0,29	-1,24	-0,75	-1,23	-1,14	-0,93	-0,15
CNRM-CM5.1 RCP8.5 HE-NLUC	-0,48	0,15	-1,66	-2,22	-0,71	-2,11	-0,84	-2,15
MPI-ESM-MR RCP4.5 HE-NLUC	0,65	1,16	0,26	1,25	0,72	0,34	1,26	0,8
MPI-ESM-MR RCP8.5 HE-NLUC	1,4	1,61	1,27	1,46	0,97	0,79	1,57	0,49
CNRM-CM5.1 RCP4.5 LE-HLUC	1,64	0,73	0,2	0,72	-0,3	0,38	0,56	1,98
CNRM-CM5.1 RCP8.5 LE-HLUC	-0,04	0,48	-1,24	-1,77	-0,42	-1,56	-0,47	-1,54
MPI-ESM-MR RCP4.5 LE-HLUC	1,93	2,08	1,4	2,43	2,2	1,71	2,24	2,1
MPI-ESM-MR RCP8.5 LE-HLUC	1,95	2,08	1,8	2,05	1,86	1,61	1,94	0,89

Table 10. Decadal average reservoir storage difference of Kemer Reservoir under different scenarios with respect to average baseline volume rate (in million m^3).

	2019-2030	2031-2040	2041-2050	2051-2060	2061-2070	2071-2080	2081-2090	2091-2100
CNRM-CM5.1 RCP4.5 BAU	-131,8	-139,2	-145,1	-158,7	-145,2	-138,3	-131,6	-111,0
CNRM-CM5.1 RCP8.5 BAU	-135,8	-93,7	-139,8	-176,2	-133,8	-127,8	-127,1	-123,4
MPI-ESM-MR RCP4.5 BAU	12,2	-32,2	-27,4	33,6	22,3	22,3	-34,0	-10,6
MPI-ESM-MR RCP8.5 BAU	74,0	78,0	93,2	74,9	67,9	28,7	68,8	41,3
CNRM-CM5.1 RCP4.5 HE-IILS	-103,9	-146,2	-161,6	-149,8	-149,4	-168,4	-157,8	-125,2
CNRM-CM5.1 RCP8.5 HE-IILS	-119,5	-58,9	-127,4	-174,0	-116,1	-116,8	-111,3	-107,9
MPI-ESM-MR RCP4.5 HE-IILS	56,8	4,5	22,3	59,3	57,1	51,2	-8,5	17,9
MPI-ESM-MR RCP8.5 HE-IILS	103,0	99,2	110,9	97,4	93,1	54,6	91,0	68,8
CNRM-CM5.1 RCP4.5 HE-NLUC	-80,3	-120,0	-134,4	-113,3	-114,5	-158,7	-135,9	-96,3
CNRM-CM5.1 RCP8.5 HE-NLUC	-99,6	-7,7	-78,7	-161,5	-70,0	-97,6	-77,5	-33,5
MPI-ESM-MR RCP4.5 HE-NLUC	95,9	93,0	97,6	95,4	94,8	81,2	59,4	71,6
MPI-ESM-MR RCP8.5 HE-NLUC	120,8	126,4	132,9	125,7	121,4	94,3	120,0	110,5
CNRM-CM5.1 RCP4.5 LE-IILS	-138,0	-145,8	-150,7	-166,7	-150,9	-144,7	-139,4	-120,8
CNRM-CM5.1 RCP8.5 LE-IILS	-142,4	-109,5	-149,1	-179,4	-145,6	-137,2	-143,1	-140,8
MPI-ESM-MR RCP4.5 LE-IILS	-14,6	-51,8	-55,2	-9,2	-20,1	-19,3	-53,4	-44,5
MPI-ESM-MR RCP8.5 LE-IILS	43,7	41,2	52,0	40,1	27,9	2,0	25,8	14,8

Table 11. Decadal average reservoir storage difference of Tavas Reservoir under different scenarios with respect to average baseline volume rate (in million m^3).

	2019-2030	2031-2040	2041-2050	2051-2060	2061-2070	2071-2080	2081-2090	2091-2100
CNRM-CM5.1 RCP4.5 BAU	17,2	20,4	20,5	20,4	20,2	20,2	19,2	20,3
CNRM-CM5.1 RCP8.5 BAU	16,5	20,3	19,7	19,5	20,3	20,2	19,3	20,1
MPI-ESM-MR RCP4.5 BAU	14,7	19,8	18,7	18,6	19,3	18,5	18,7	19,7
MPI-ESM-MR RCP8.5 BAU	15,4	19,8	18,4	18,2	19,1	18,1	18,4	19,2
CNRM-CM5.1 RCP4.5 HE-IILS	17,5	20,5	20,6	20,5	20,3	20,3	19,5	20,4
CNRM-CM5.1 RCP8.5 HE-IILS	16,9	20,4	19,9	19,8	20,4	20,3	19,6	20,2
MPI-ESM-MR RCP4.5 HE-IILS	15,5	20,0	19,2	19,1	19,6	19,1	19,2	19,9
MPI-ESM-MR RCP8.5 HE-IILS	15,9	19,9	18,9	18,8	19,5	18,6	19,0	19,5
CNRM-CM5.1 RCP4.5 HE-NLUC	17,6	20,5	20,6	20,5	20,3	20,4	19,7	20,4
CNRM-CM5.1 RCP8.5 HE-NLUC	17,0	20,4	20,0	20,0	20,4	20,4	19,8	20,3
MPI-ESM-MR RCP4.5 HE-NLUC	15,7	20,2	19,4	19,4	19,7	19,4	19,4	20,0
MPI-ESM-MR RCP8.5 HE-NLUC	16,1	20,0	19,2	19,2	19,6	19,0	19,3	19,7
CNRM-CM5.1 RCP4.5 LE-IILS	17,0	20,4	20,5	20,3	20,2	20,2	18,9	20,2
CNRM-CM5.1 RCP8.5 LE-IILS	16,3	20,3	19,6	19,1	20,3	20,0	19,0	20,0
MPI-ESM-MR RCP4.5 LE-IILS	14,3	19,5	18,3	18,1	19,0	18,0	18,2	19,6
MPI-ESM-MR RCP8.5 LE-IILS	15,0	19,5	17,8	17,5	18,5	17,5	17,9	18,9

Table 12. Decadal average reservoir storage difference of Topçam Reservoir under different scenarios with respect to average baseline volume rate (in million m^3).

	2019 - 2030	2031 - 2040	2041 - 2050	2051 - 2060	2061 - 2070	2071 - 2080	2081 - 2090	2091-2100
CNRM-CM5.1 RCP4.5 BAU	-23,5	-27,1	-30,7	-28,1	-35,9	-31,6	-27,2	-34,8
CNRM-CM5.1 RCP8.5 BAU	-26,1	-27,2	-32,7	-35,0	-33,9	-33,7	-24,3	-31,9
MPI-ESM-MR RCP4.5 BAU	13,9	8,2	17,6	29,0	18,1	24,9	27,1	1,1
MPI-ESM-MR RCP8.5 BAU	28,1	29,3	35,9	39,1	33,3	32,3	38,3	31,2
CNRM-CM5.1 RCP4.5 HE-IILS	-16,2	-23,8	-25,8	-24,8	-35,3	-29,9	-21,3	-34,2
CNRM-CM5.1 RCP8.5 HE-IILS	-22,7	-24,1	-29,8	-34,1	-32,8	-32,9	-18,2	-29,3
MPI-ESM-MR RCP4.5 HE-IILS	24,5	18,9	24,9	34,3	23,7	30,6	32,8	22,3
MPI-ESM-MR RCP8.5 HE-IILS	34,2	34,9	38,0	40,6	36,6	35,3	40,4	35,3
CNRM-CM5.1 RCP4.5 HE-NLUC	-7,3	-12,6	-6,6	-14,2	-31,1	-26,5	-1,3	-32,1
CNRM-CM5.1 RCP8.5 HE-NLUC	-16,4	-15,6	-18,5	-30,6	-29,0	-30,9	2,3	-24,1
MPI-ESM-MR RCP4.5 HE-NLUC	28,2	30,6	34,8	40,4	31,3	36,4	38,9	33,1
MPI-ESM-MR RCP8.5 HE-NLUC	36,2	39,8	40,8	42,6	40,2	39,2	42,6	39,5
CNRM-CM5.1 RCP4.5 LE-IILS	-26,5	-32,3	-35,1	-31,9	-36,6	-33,7	-31,7	-35,3
CNRM-CM5.1 RCP8.5 LE-IILS	-28,6	-31,7	-35,0	-35,6	-35,8	-34,5	-32,0	-35,1
MPI-ESM-MR RCP4.5 LE-IILS	-4,8	-4,7	-14,9	19,0	-1,0	-5,1	-11,2	-19,7
MPI-ESM-MR RCP8.5 LE-IILS	23,7	15,6	29,2	34,3	24,6	18,2	30,0	15,6

Table 13. Decadal average reservoir storage difference of Yaylakavak Reservoir under different scenarios with respect to average baseline volume rate with respect to average baseline volume rate (in million m^3).

	2019-2030	2031-2040	2041-2050	2051-2060	2061-2070	2071-2080	2081-2090	2091-2100
CNRM-CM5.1 RCP4.5 BAU	-13,8	-14,2	-12,3	-14,4	-14,4	-14,1	-12,9	-13,4
CNRM-CM5.1 RCP8.5 BAU	-14,2	-12,5	-11,1	-14,5	-14,7	-14,6	-13,8	-14,6
MPI-ESM-MR RCP4.5 BAU	0,3	-3,9	-1,8	1,8	-2,4	3,8	-1,9	-2,5
MPI-ESM-MR RCP8.5 BAU	7,4	8,9	9,2	7,6	7,4	5,9	8,0	5,1
CNRM-CM5.1 RCP4.5 HE-IILS	-12,5	-14,0	-11,4	-14,2	-14,3	-13,6	-12,2	-13,2
CNRM-CM5.1 RCP8.5 HE-IILS	-14,0	-11,5	-9,7	-14,3	-14,6	-14,5	-13,6	-14,5
MPI-ESM-MR RCP4.5 HE-IILS	3,9	-2,8	2,8	4,2	-0,3	4,9	0,5	0,9
MPI-ESM-MR RCP8.5 HE-IILS	9,0	9,7	9,9	8,7	8,5	7,4	9,0	6,7
CNRM-CM5.1 RCP4.5 HE-NLUC	-12,0	-11,9	-8,3	-13,3	-12,1	-11,7	-9,9	-12,5
CNRM-CM5.1 RCP8.5 HE-NLUC	-13,6	-6,6	-5,7	-13,5	-12,7	-14,3	-12,6	-13,8
MPI-ESM-MR RCP4.5 HE-NLUC	6,9	2,3	8,5	8,5	6,3	7,4	4,6	5,2
MPI-ESM-MR RCP8.5 HE-NLUC	10,0	10,8	10,9	10,4	10,2	9,4	10,4	9,2
CNRM-CM5.1 RCP4.5 LE-IILS	-13,9	-14,4	-13,8	-14,7	-14,6	-14,5	-13,6	-13,7
CNRM-CM5.1 RCP8.5 LE-IILS	-14,3	-13,4	-12,9	-14,7	-14,8	-14,9	-14,2	-14,8
MPI-ESM-MR RCP4.5 LE-IILS	-3,0	-5,9	-6,1	-1,2	-6,4	-1,5	-5,6	-8,4
MPI-ESM-MR RCP8.5 LE-IILS	5,4	5,9	6,9	5,0	4,4	2,4	4,7	1,3

APPENDIX B: ANNUAL AVERAGE CLIMATIC CONDITIONS IN AYDIN, DENIZLI, AND MUĞLA DURING OBSERVATION PERIOD

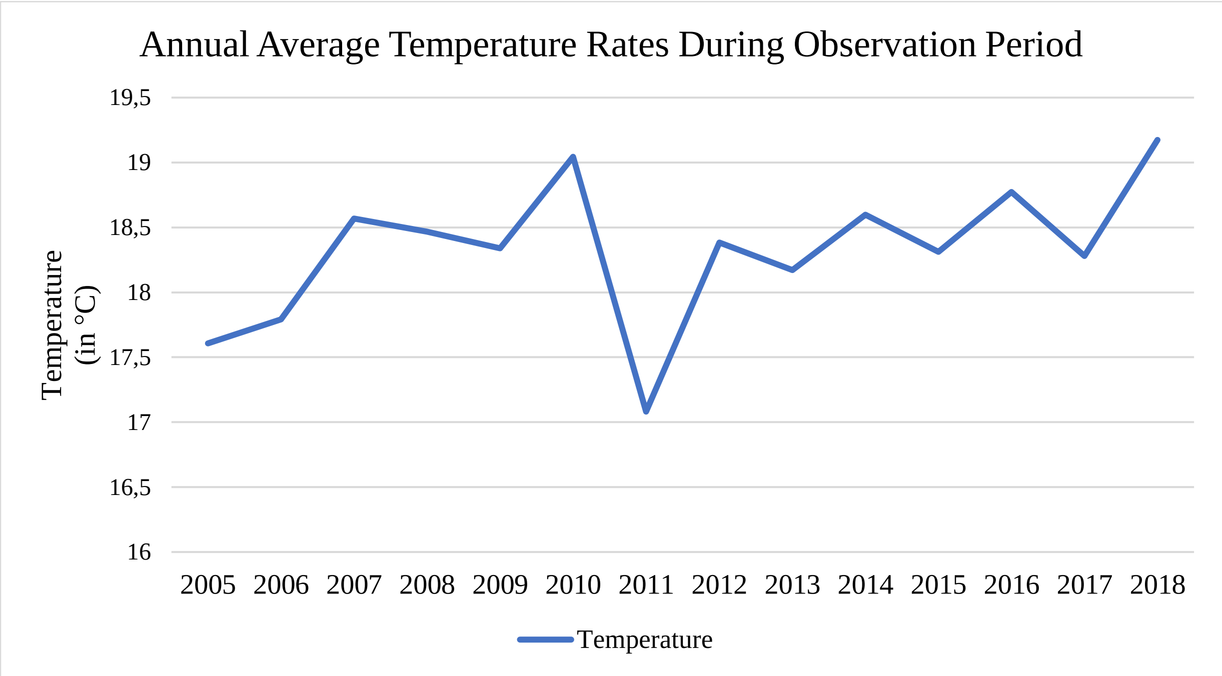

Figure 1.1. Annual average temperature rates of Aydın between 2005 and 2018 (Source: MGM).

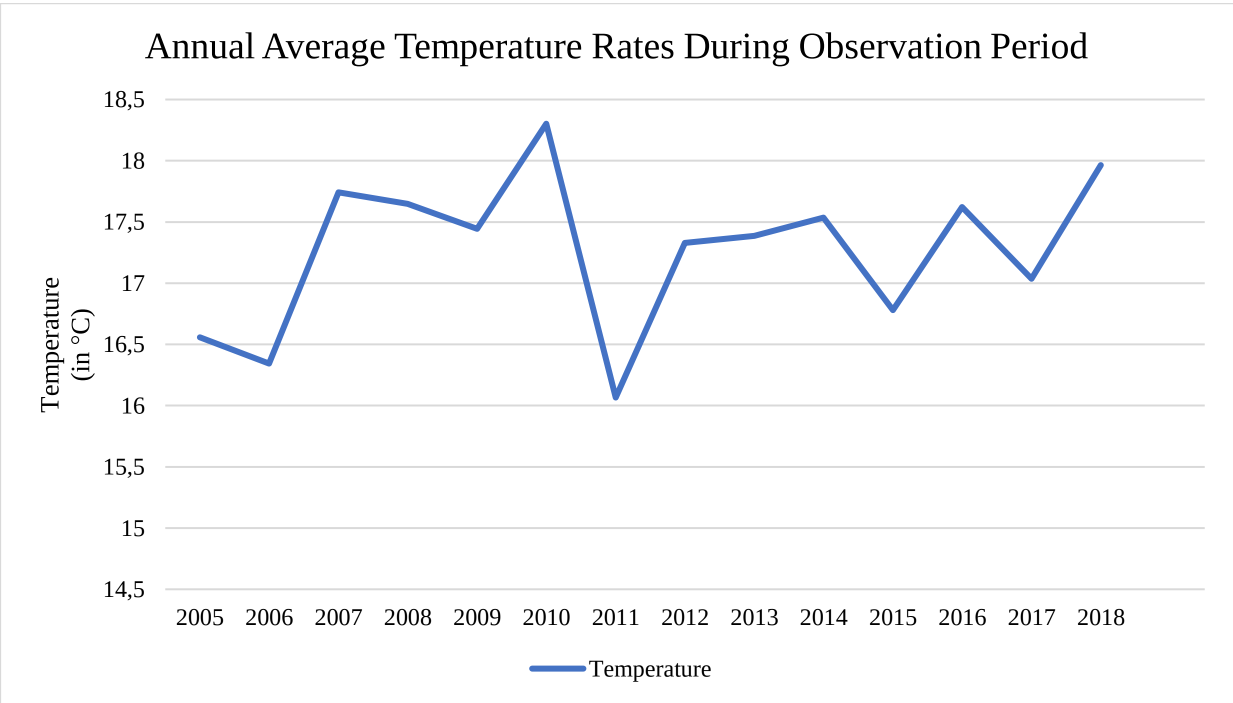

Figure 1.2. Annual average temperature rates of Denizli between 2005 and 2018 (Source: MGM).

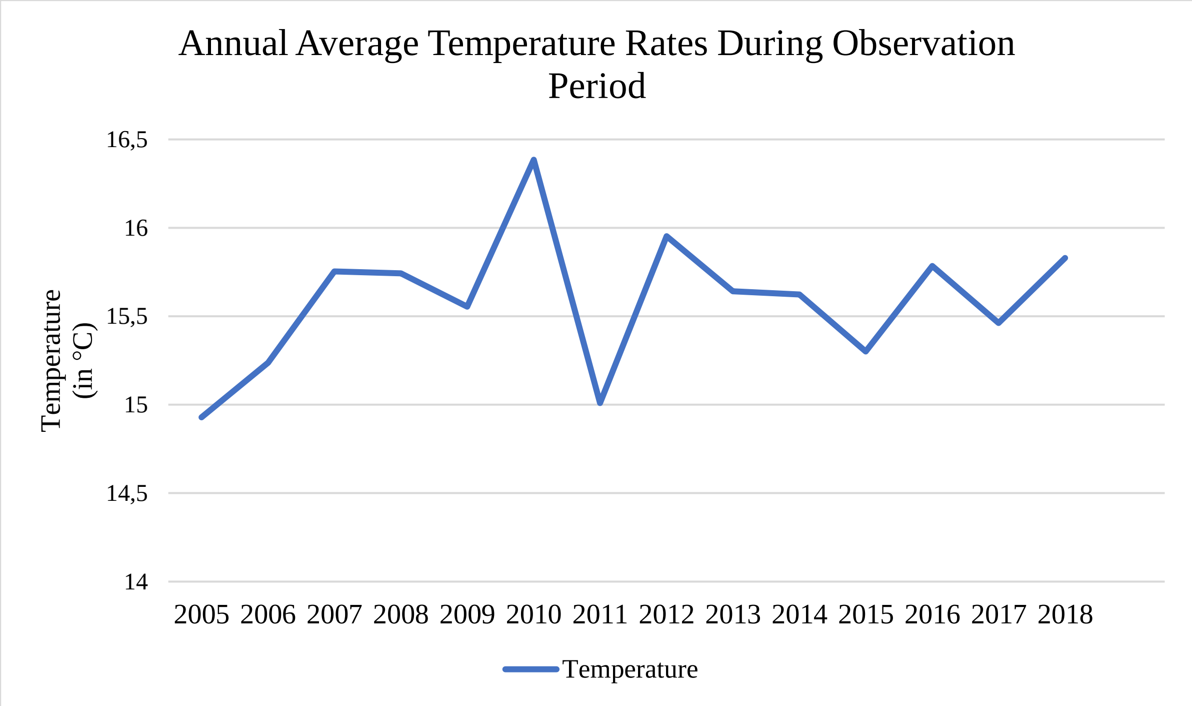

Figure 1.3. Annual average temperature rates of Muğla between 2005 and 2018 (Source: MGM).

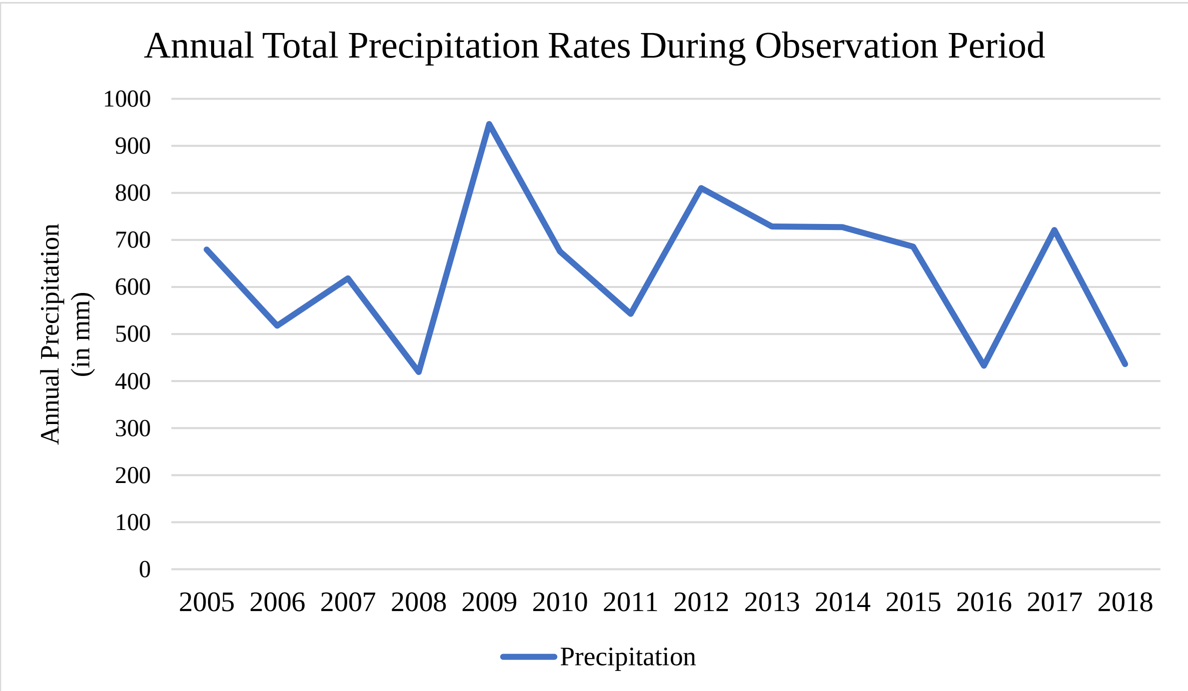

Figure 1.4. Annual total precipitation rates of Aydın between 2005 and 2018 (Source: MGM).

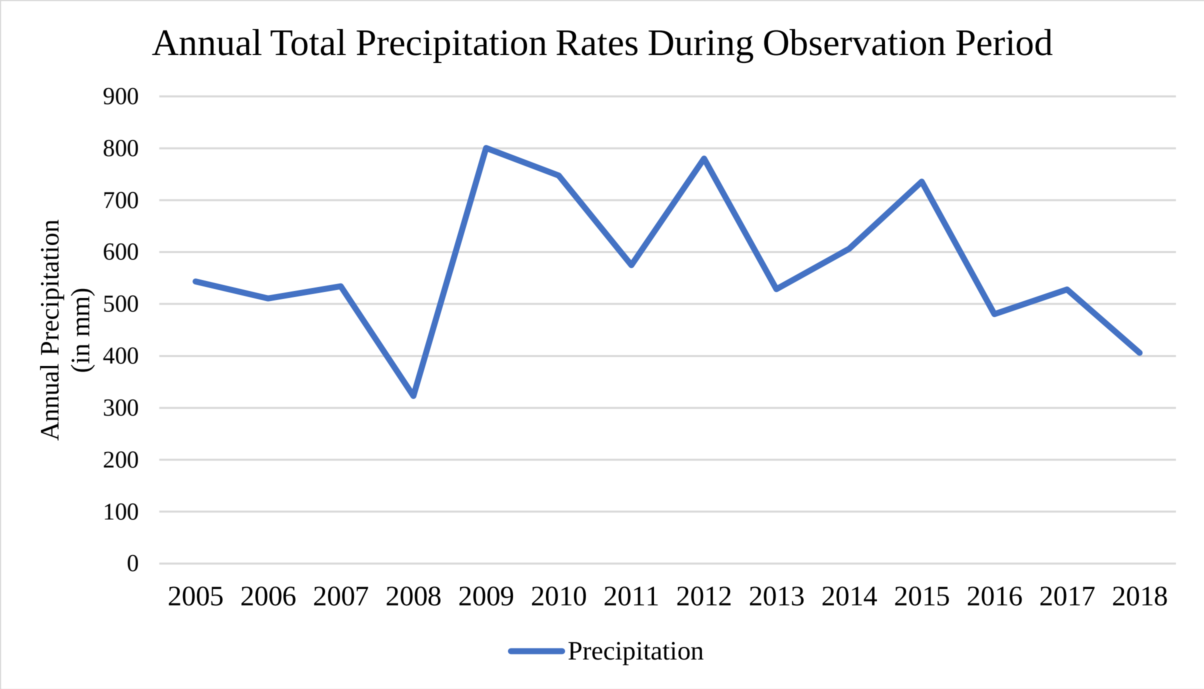

Figure 1.5. Annual total precipitation rates of Denizli between 2005 and 2018 (Source: MGM).

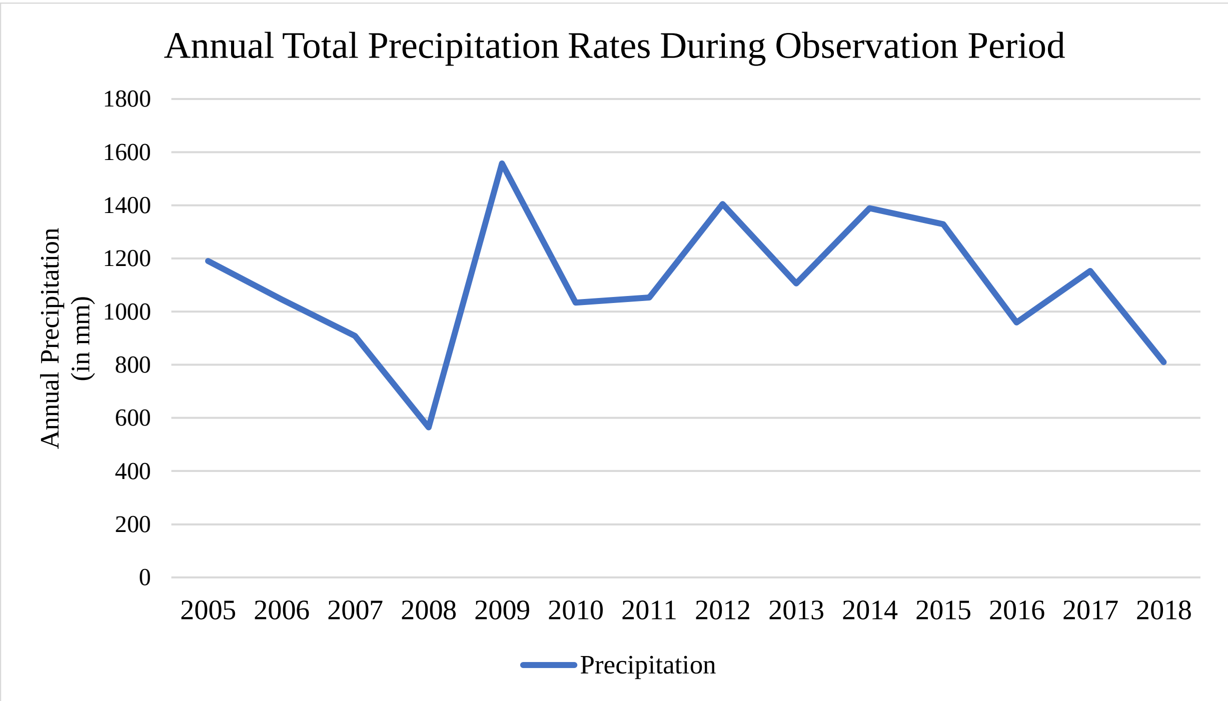

Figure 1.6. Annual total precipitation rates of Muğla between 2005 and 2018 (Source: MGM).

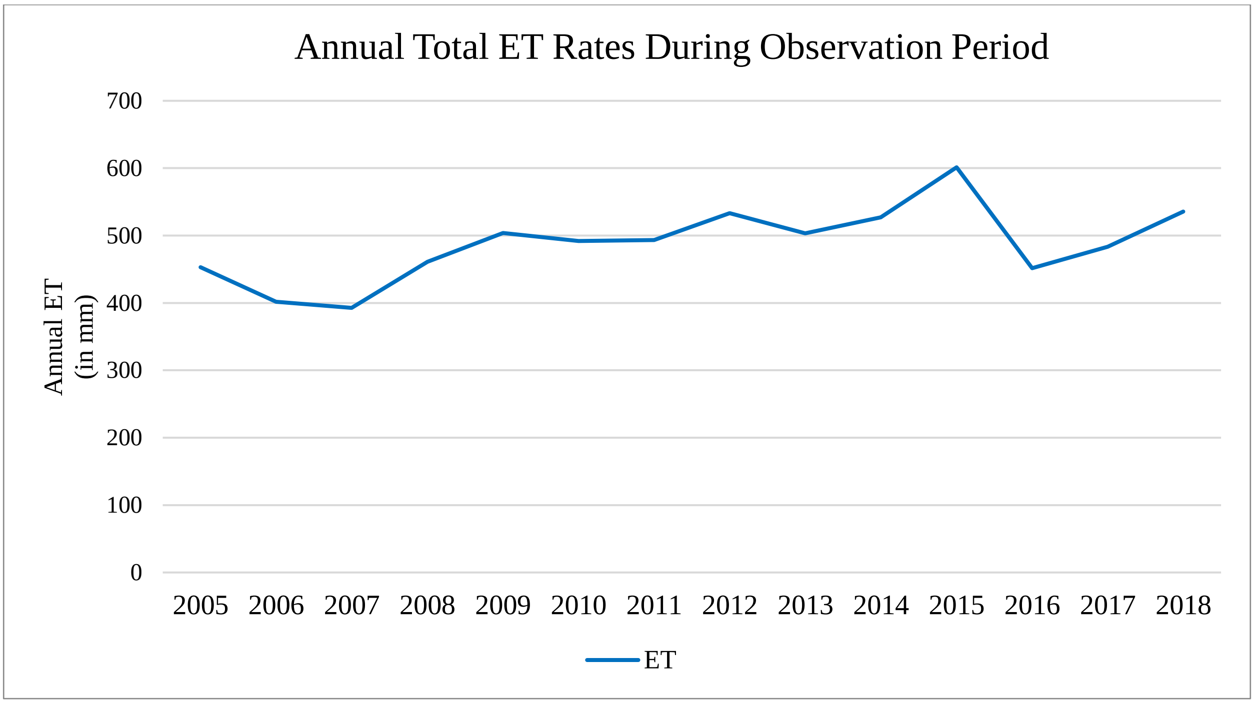

Figure 1.7. Annual total ET rates of Aydın between 2005 and 2018 (Source: GLEAM).

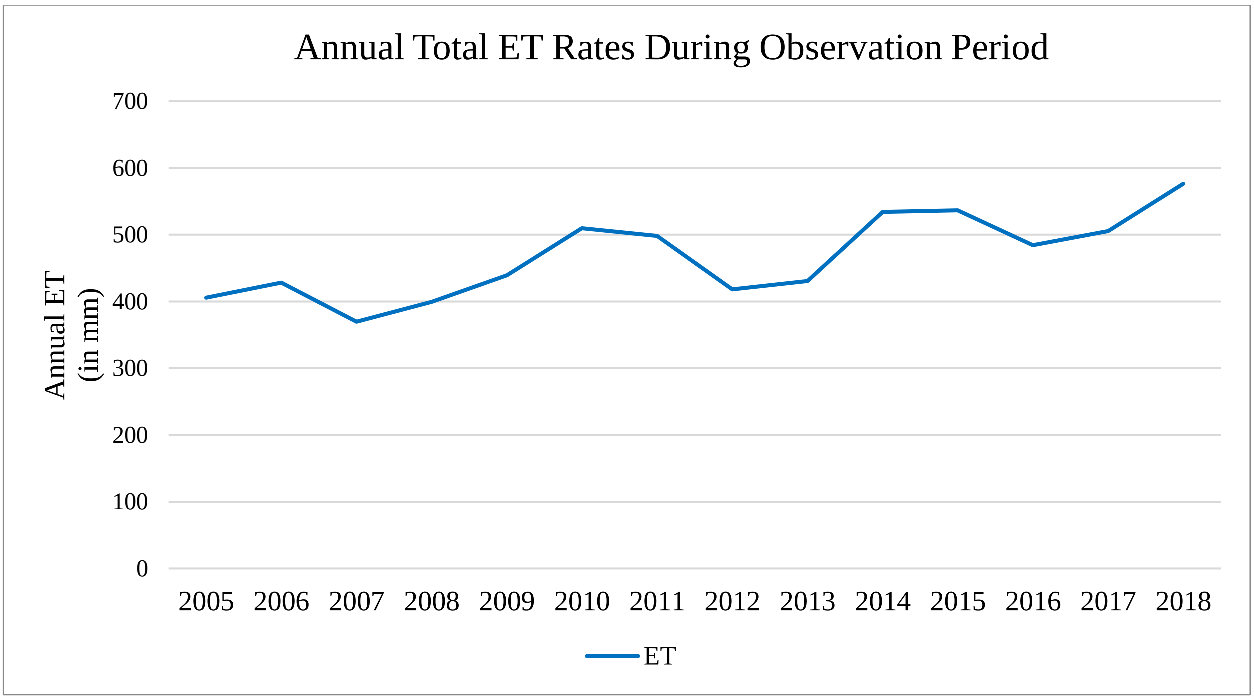

Figure 1.8. Annual total ET rates of Denizli between 2005 and 2018 (Source: GLEAM).

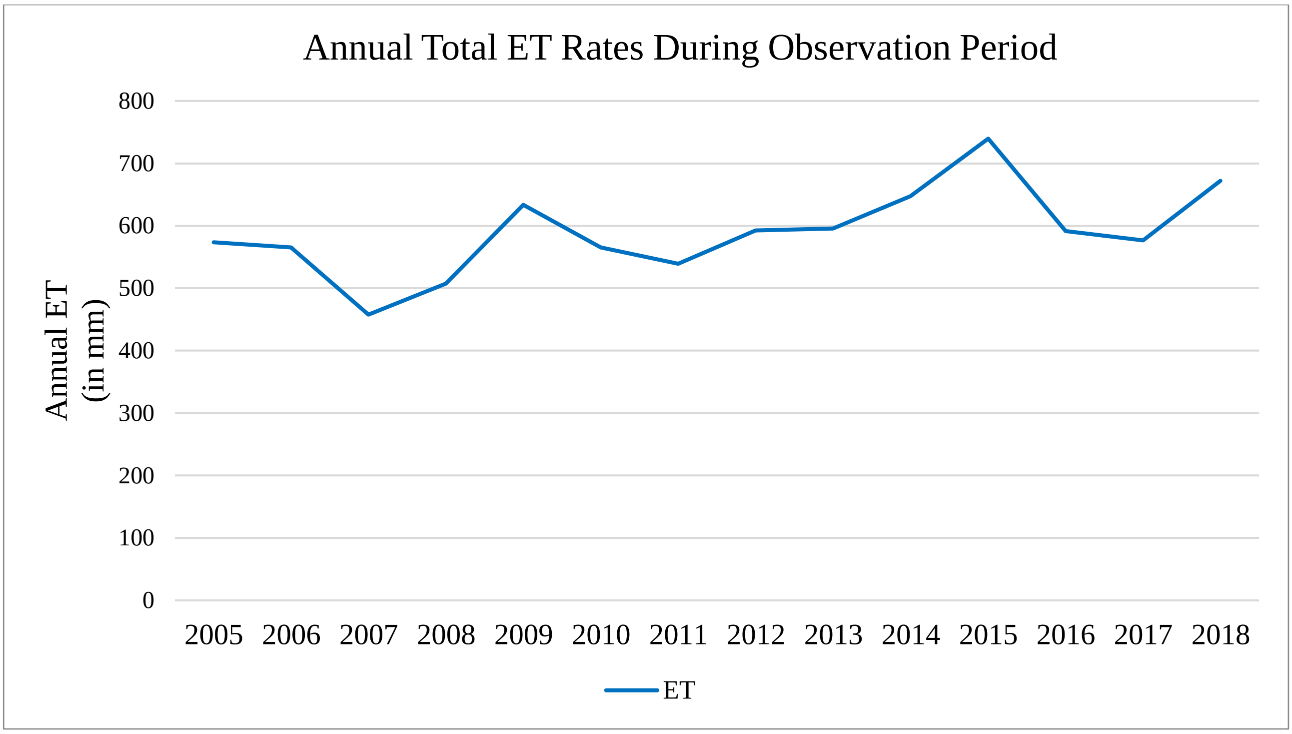

Figure 1.9. Annual total ET rates of Muğla between 2005 and 2018 (Source: GLEAM).

APPENDIX C: DECADAL AVERAGE DIFFERENCE OF CLIMATIC CONDITIONS IN AYDIN, DENIZLI, MUĞLA, AND UŞAK WITH RESPECT TO BASELINE SCENARIO

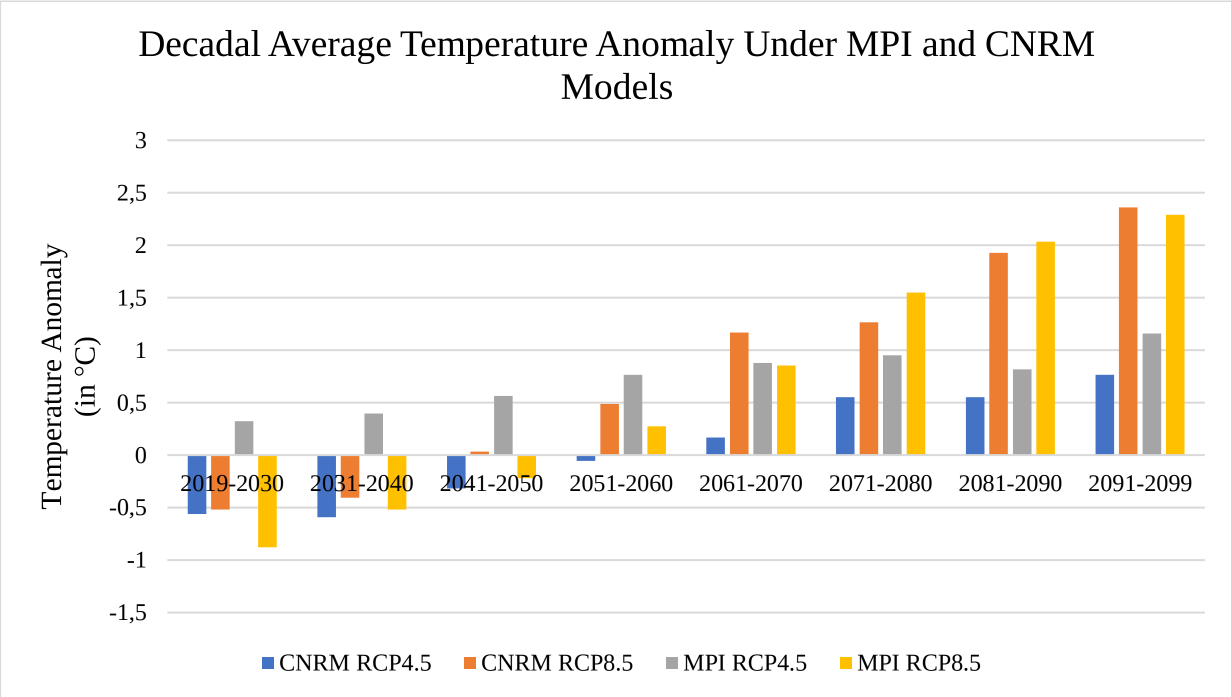

Figure 1.1. Decadal average temperature difference of Aydın under MPI-ESM-MR and CNRM-CM5.1 models between 2019 and 2100.

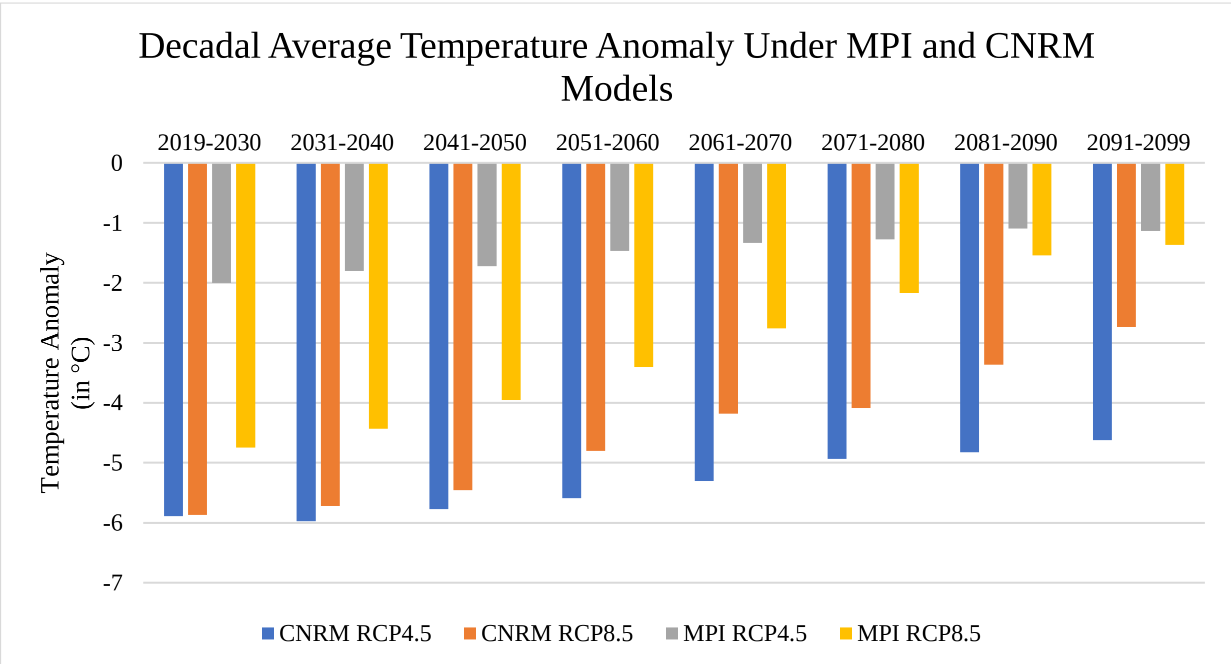

Figure 1.2. Decadal average temperature difference of Denizli under MPI-ESM-MR and CNRM-CM5.1 models between 2019 and 2100.

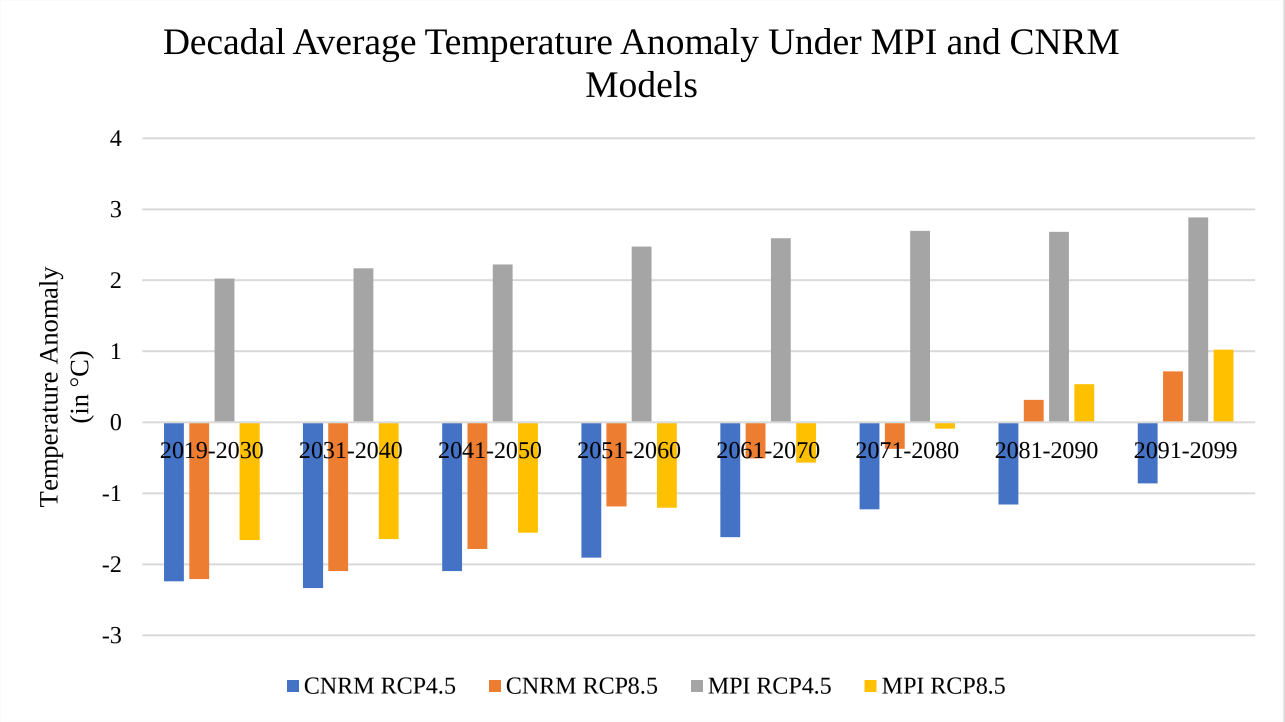

Figure 1.3. Decadal average temperature difference of Muğla under MPI-ESM-MR and CNRM-CM5.1 models between 2019 and 2100.

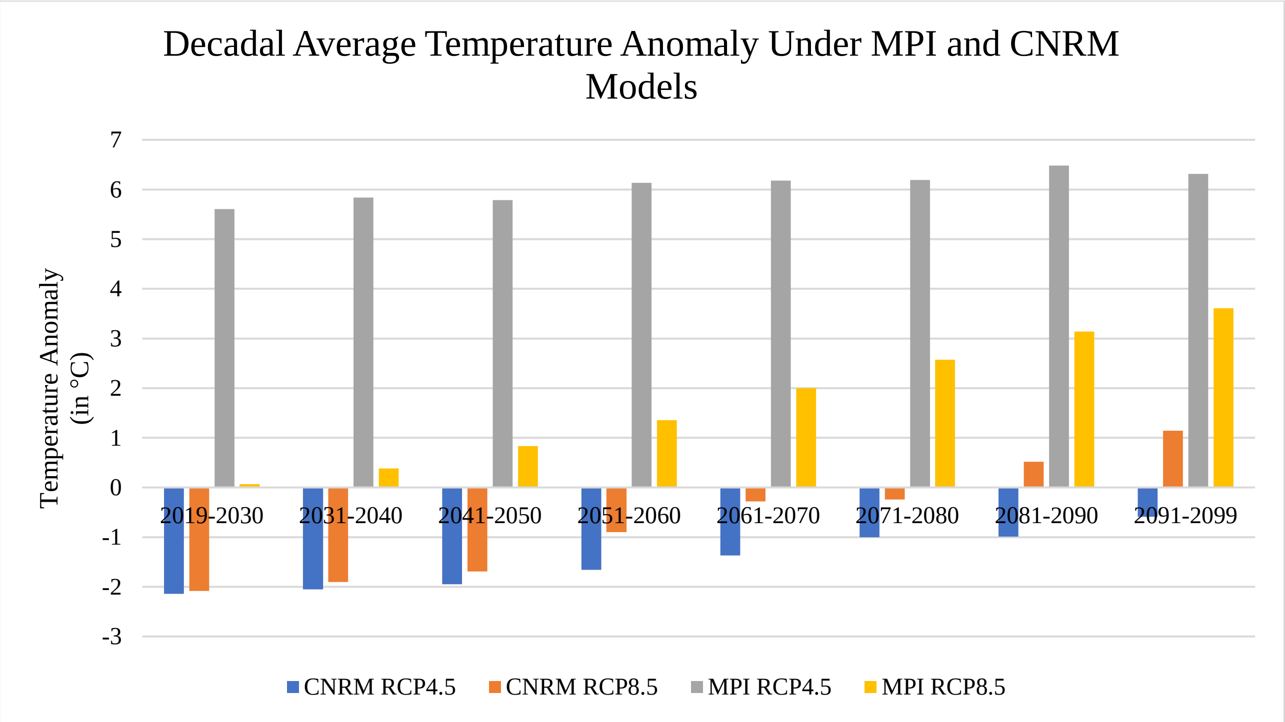

Figure 1.4. Decadal average temperature difference of Uşak under MPI-ESM-MR and CNRM-CM5.1 models between 2019 and 2100.

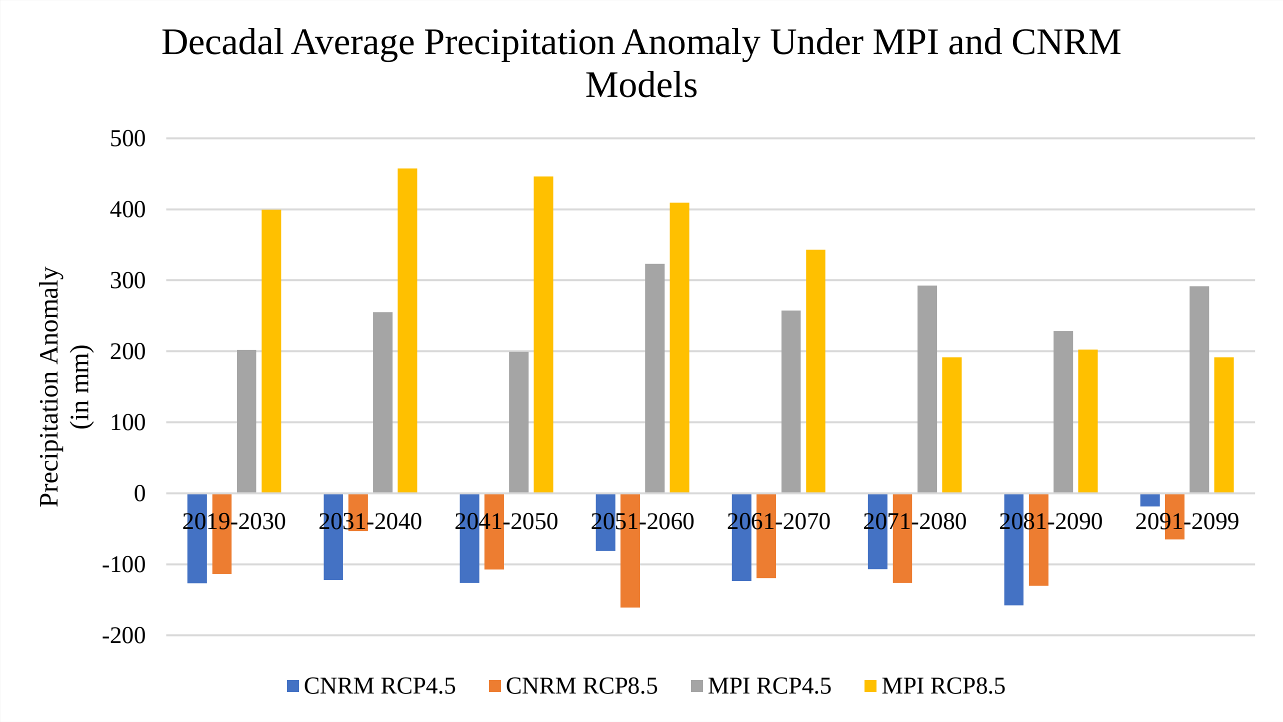

Figure 1.5. Decadal average precipitation difference of Aydın under MPI-ESM-MR and CNRM-CM5.1 models between 2019 and 2100.

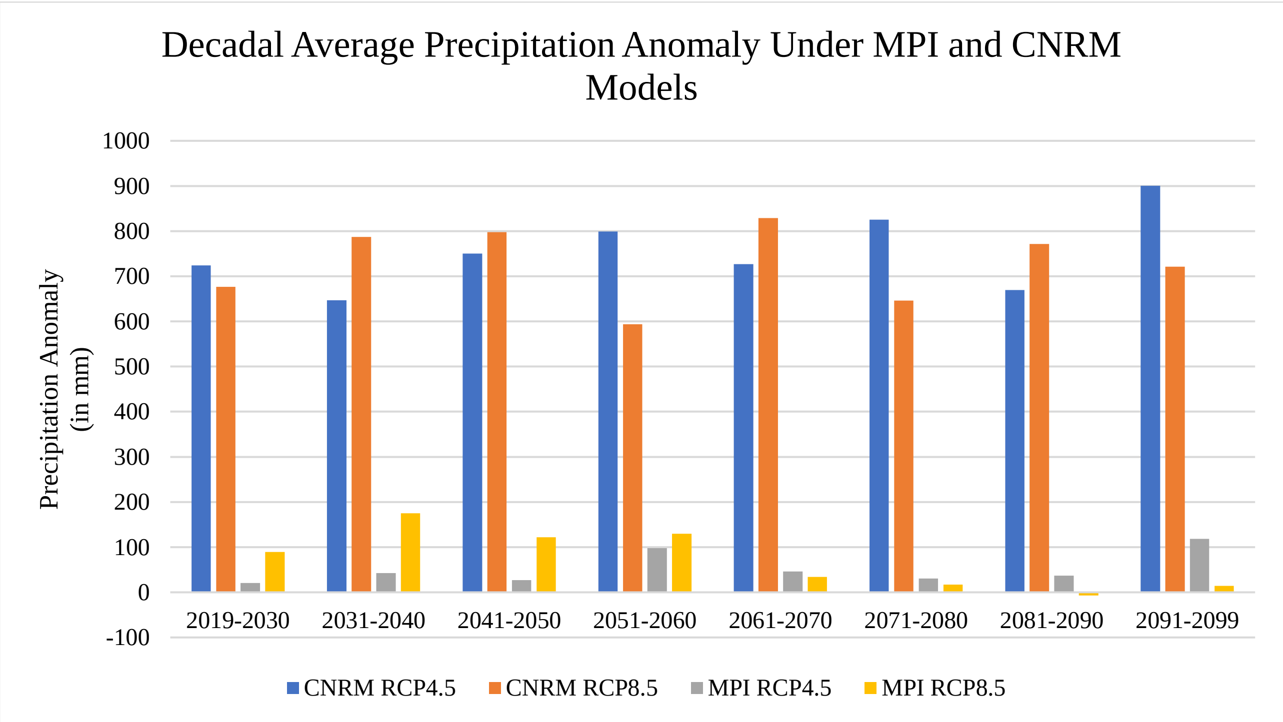

Figure 1.6. Decadal average precipitation difference of Denizli under MPI-ESM-MR and CNRM-CM5.1 models between 2019 and 2100.

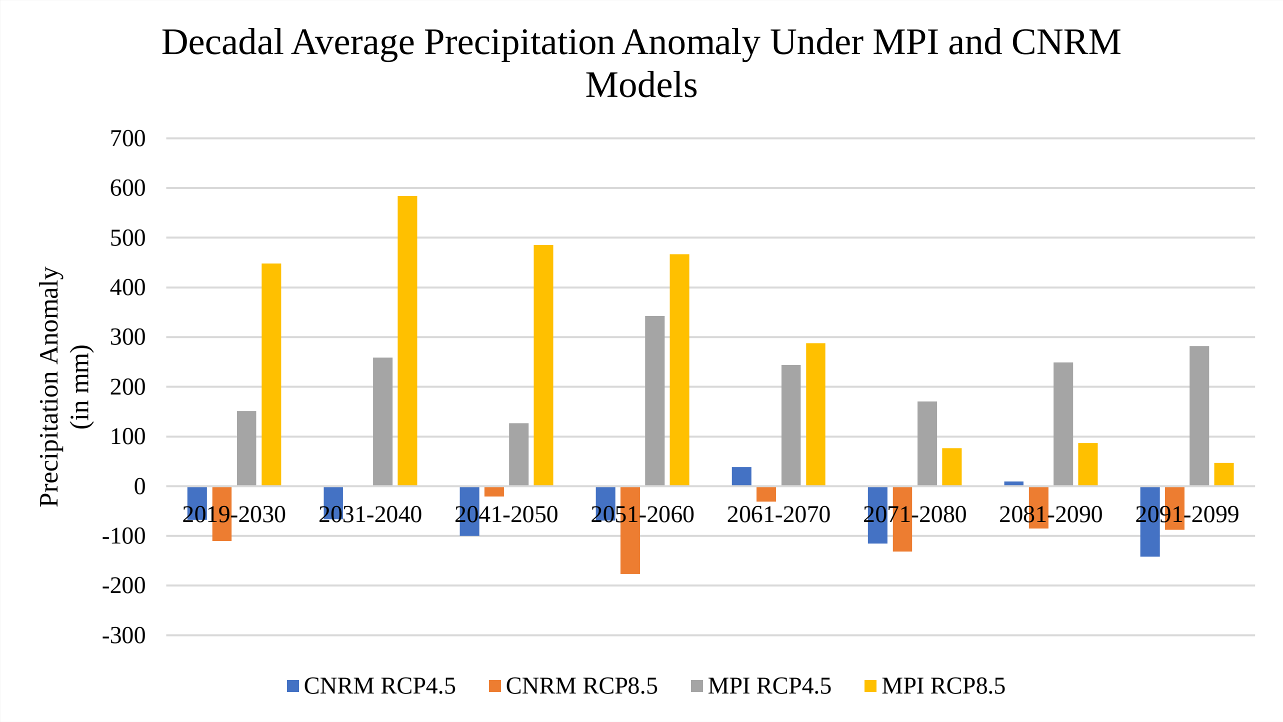

Figure 1.7. Decadal average precipitation difference of Muğla under MPI-ESM-MR and CNRM-CM5.1 models between 2019 and 2100.

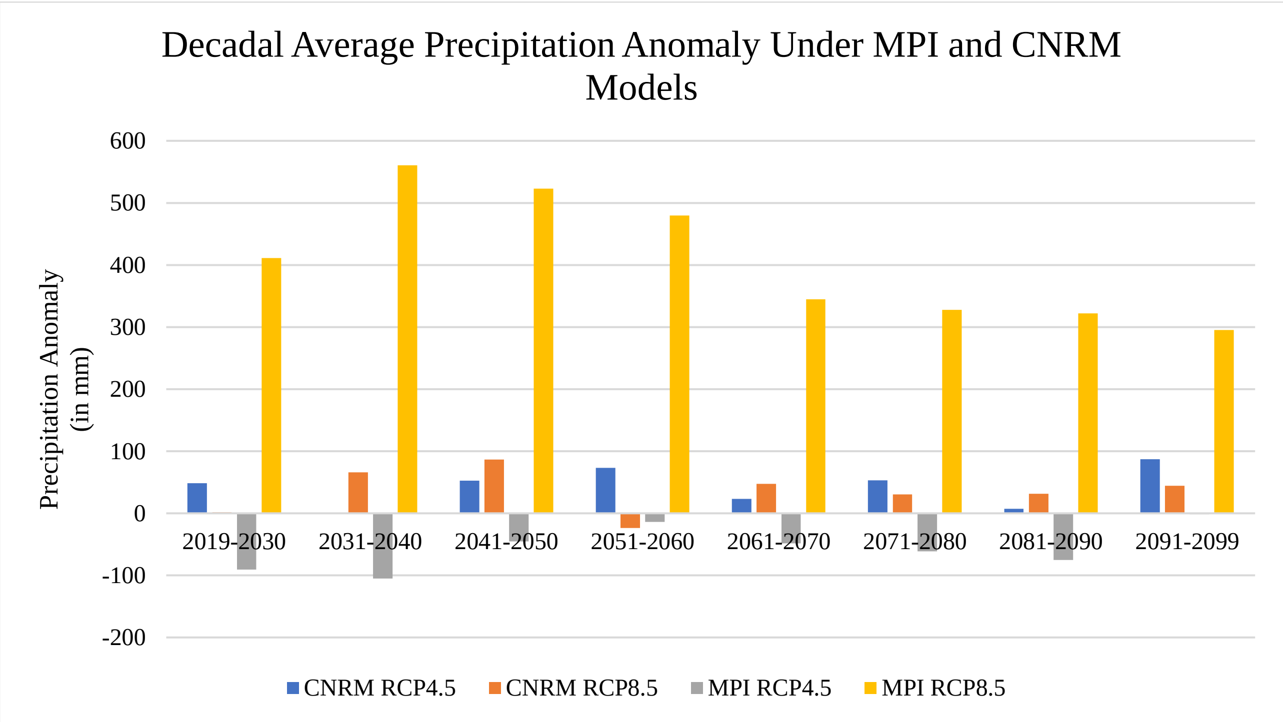

Figure 1.8. Decadal average precipitation difference of Uşak under MPI-ESM-MR and CNRM-CM5.1 models between 2019 and 2100.

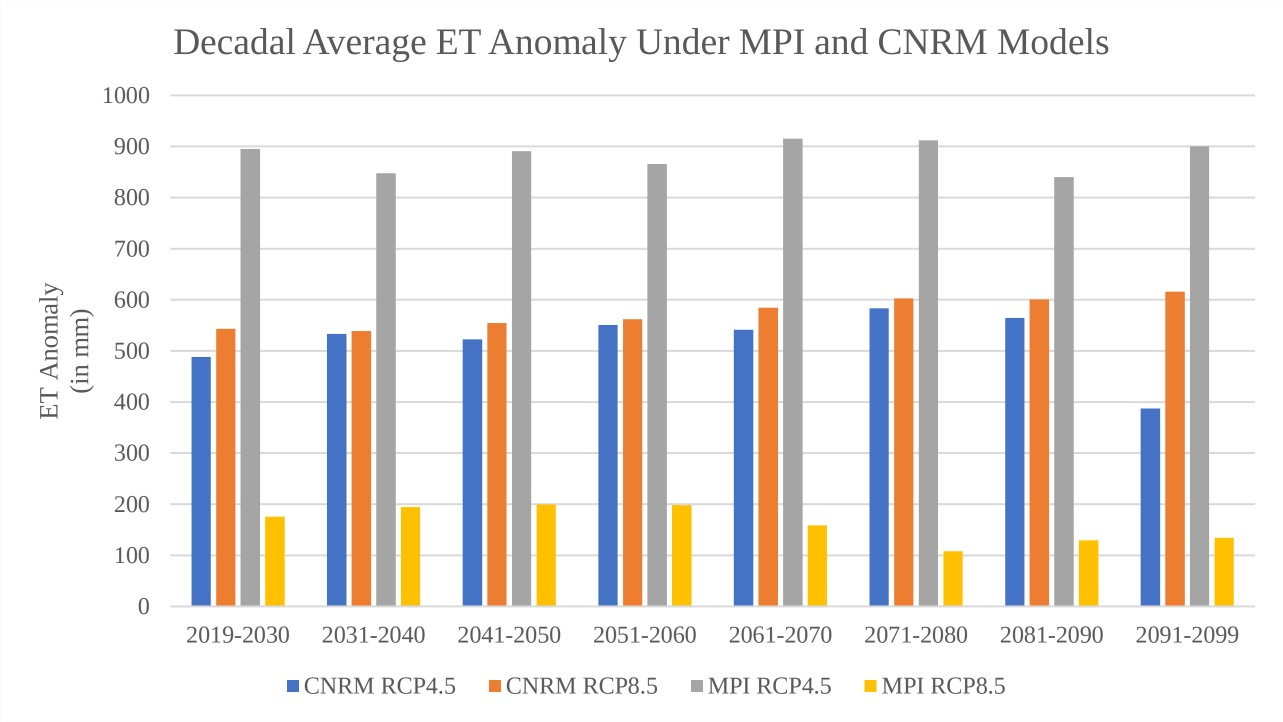

Figure 1.9. Decadal average ET difference of Aydın under MPI-ESM-MR and CNRM-CM5.1 models between 2019 and 2100.

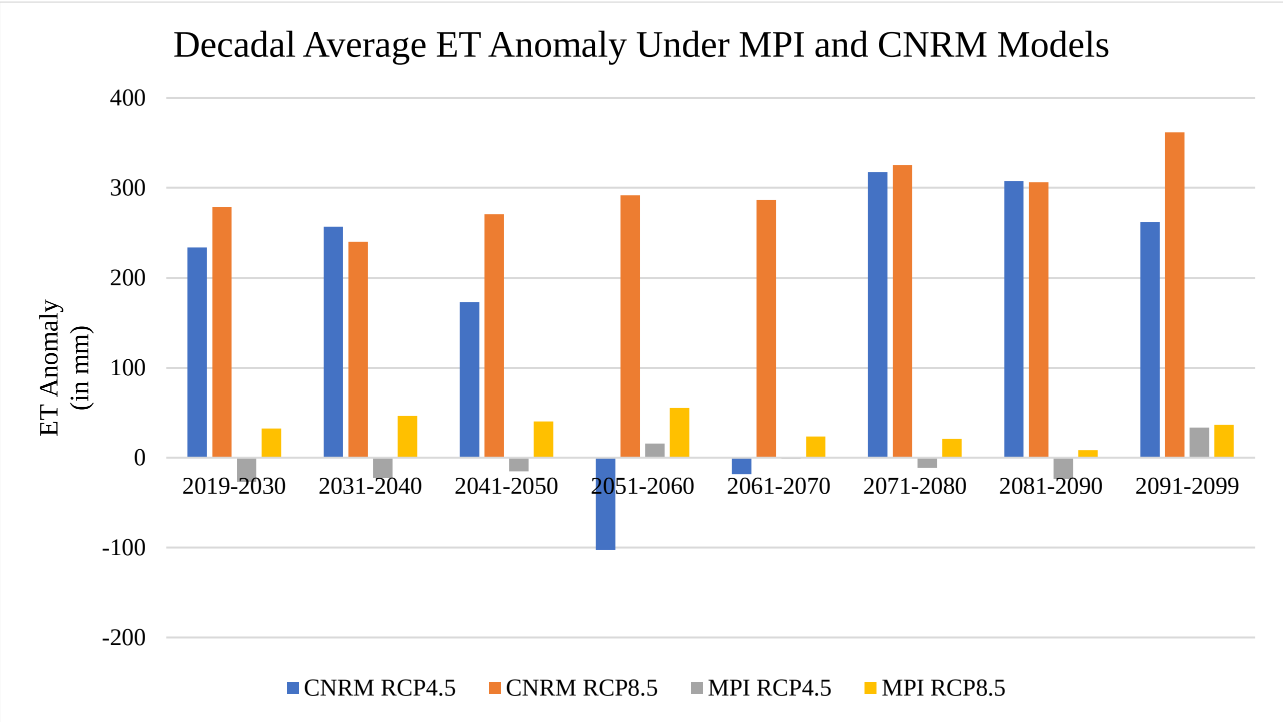

Table 1.10. Decadal average ET difference of Denizli under MPI-ESM-MR and CNRM-CM5.1 models between 2019 and 2100.

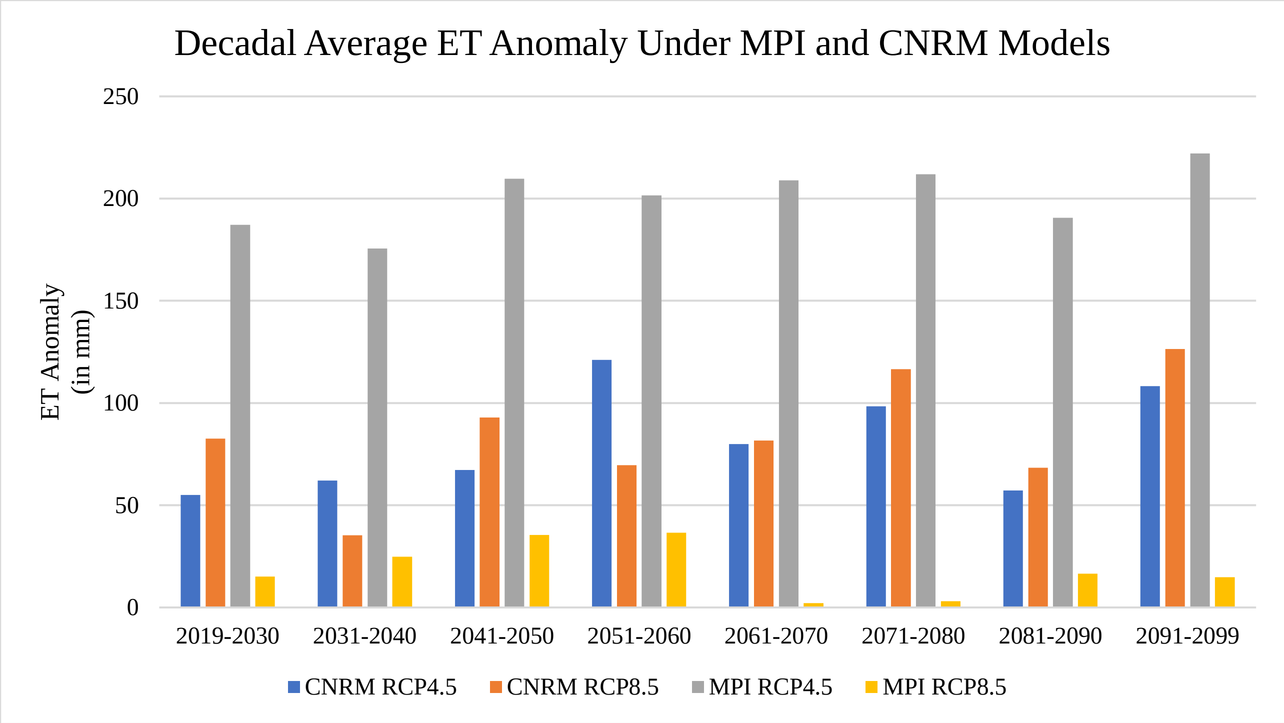

Figure 1.11. Decadal average ET difference of Muğla under MPI-ESM-MR and CNRM-CM5.1 models between 2019 and 2100.

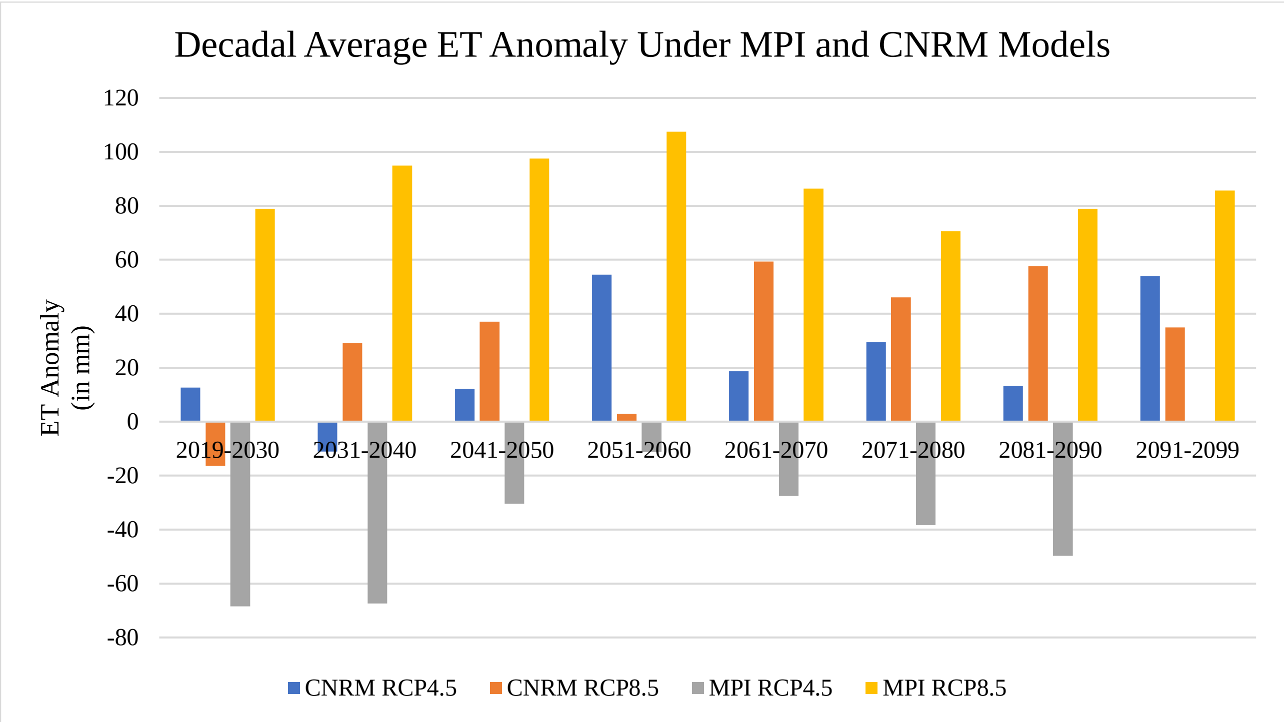

Figure 1.12. Decadal average ET difference of Uşak under MPI-ESM-MR and CNRM-CM5.1 models between 2019 and 2100.

APPENDIX D: STORAGE VOLUME OF RESERVOIRS IN AYDIN, DENIZLI, AND MUĞLA DURING SIMULATION PERIODS UNDER DIFFERENT SCENARIOS

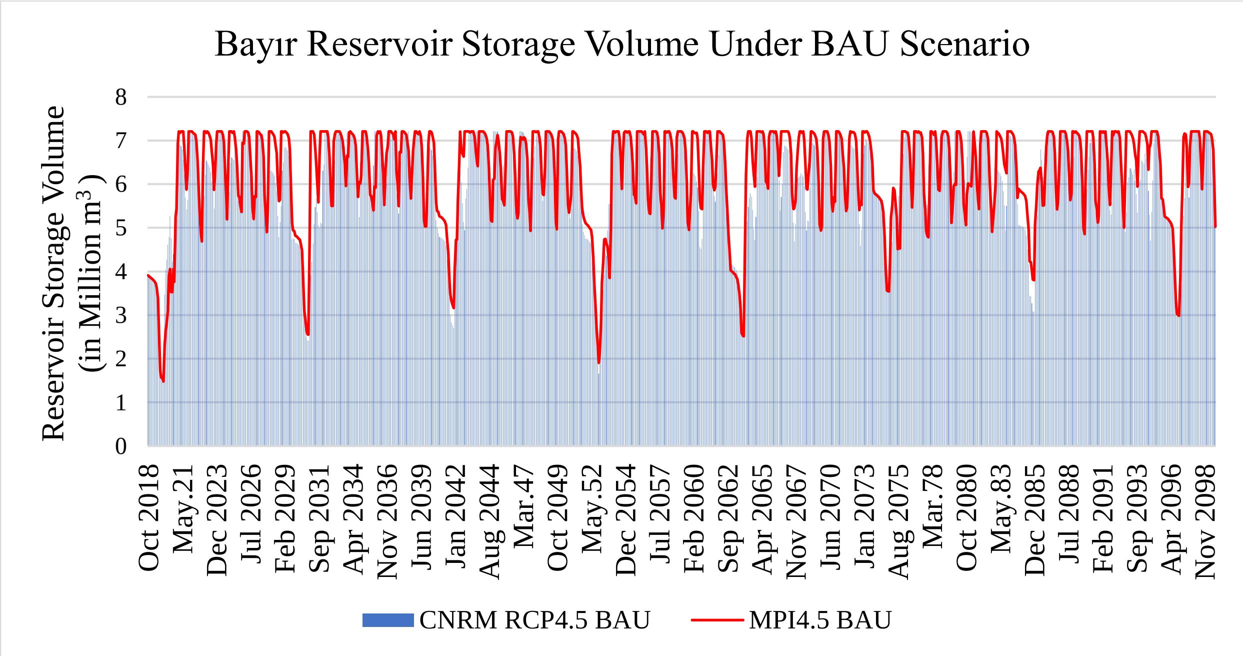

Figure 1.1. Storage volume of Bayır Reservoir under BAU scenario with CNRM RCP4.5 and MPI RCP4.5 climate change scenarios.

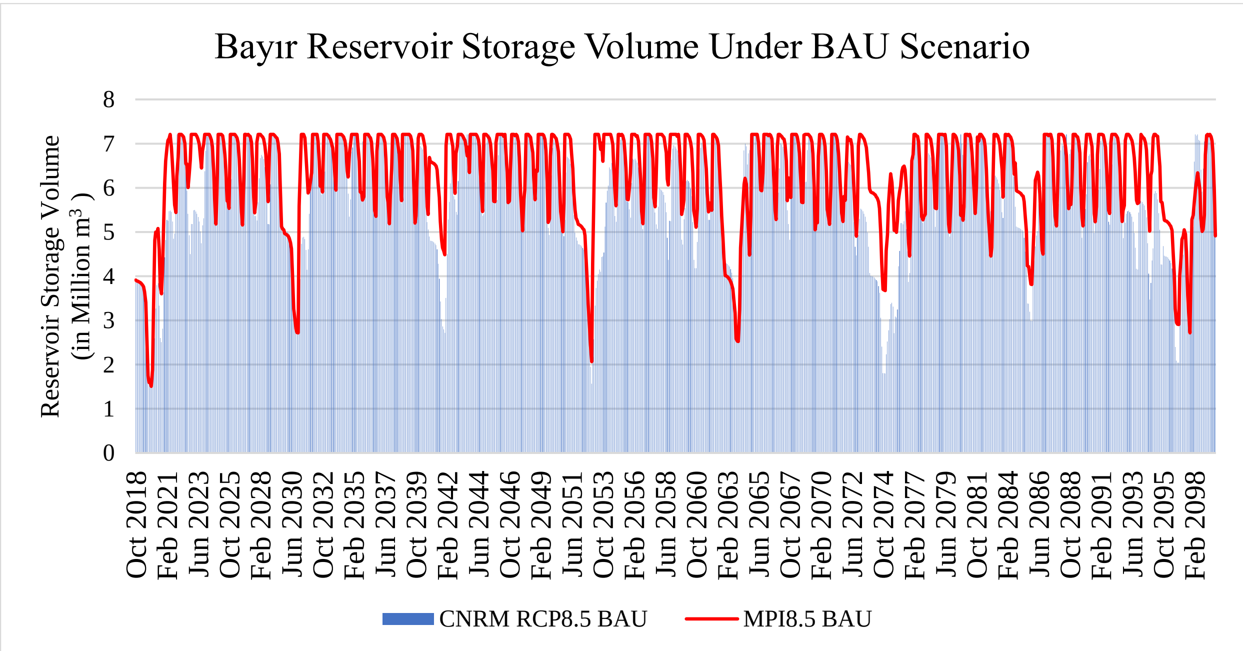

Figure 1.2. Storage volume of Bayır Reservoir under BAU scenario with CNRM RCP8.5 and MPI RCP8.5 climate change scenarios.

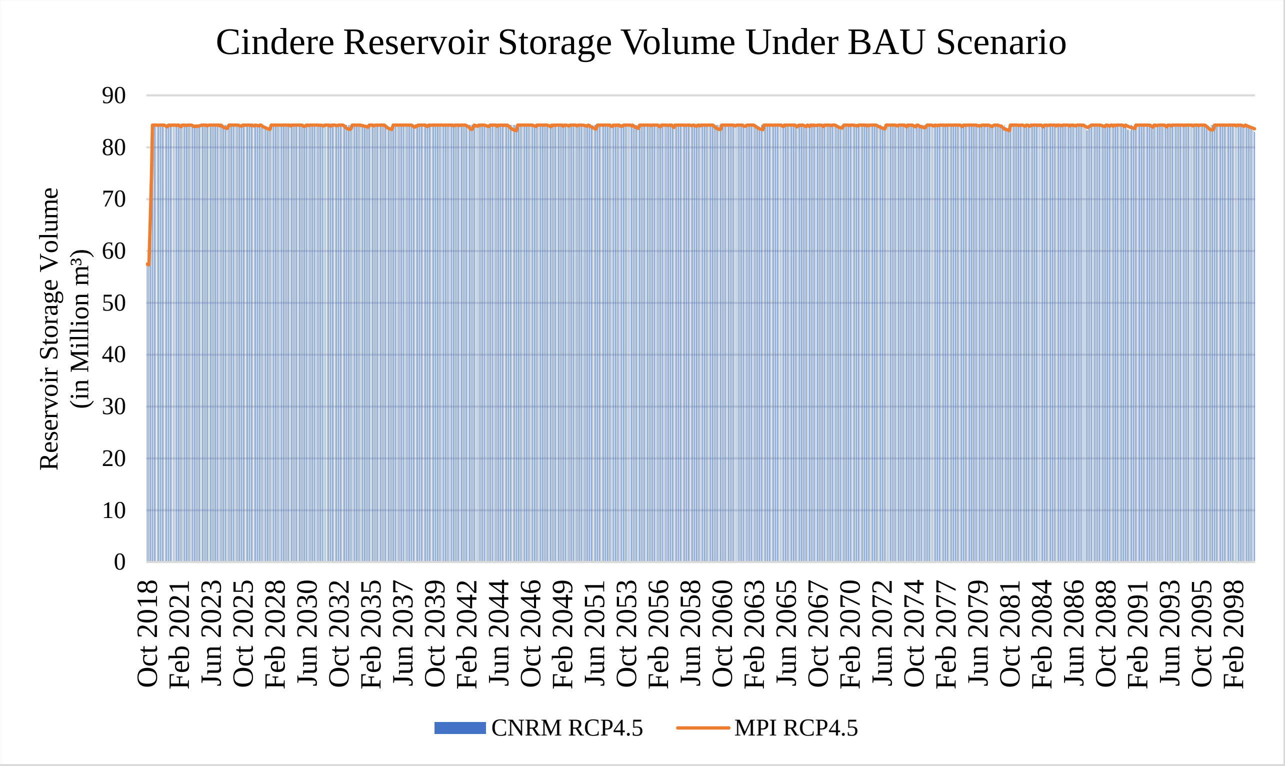

Figure 1.3. Storage volume of Cindere Reservoir under BAU scenario with CNRM RCP4.5 and MPI RCP4.5 climate change scenarios.

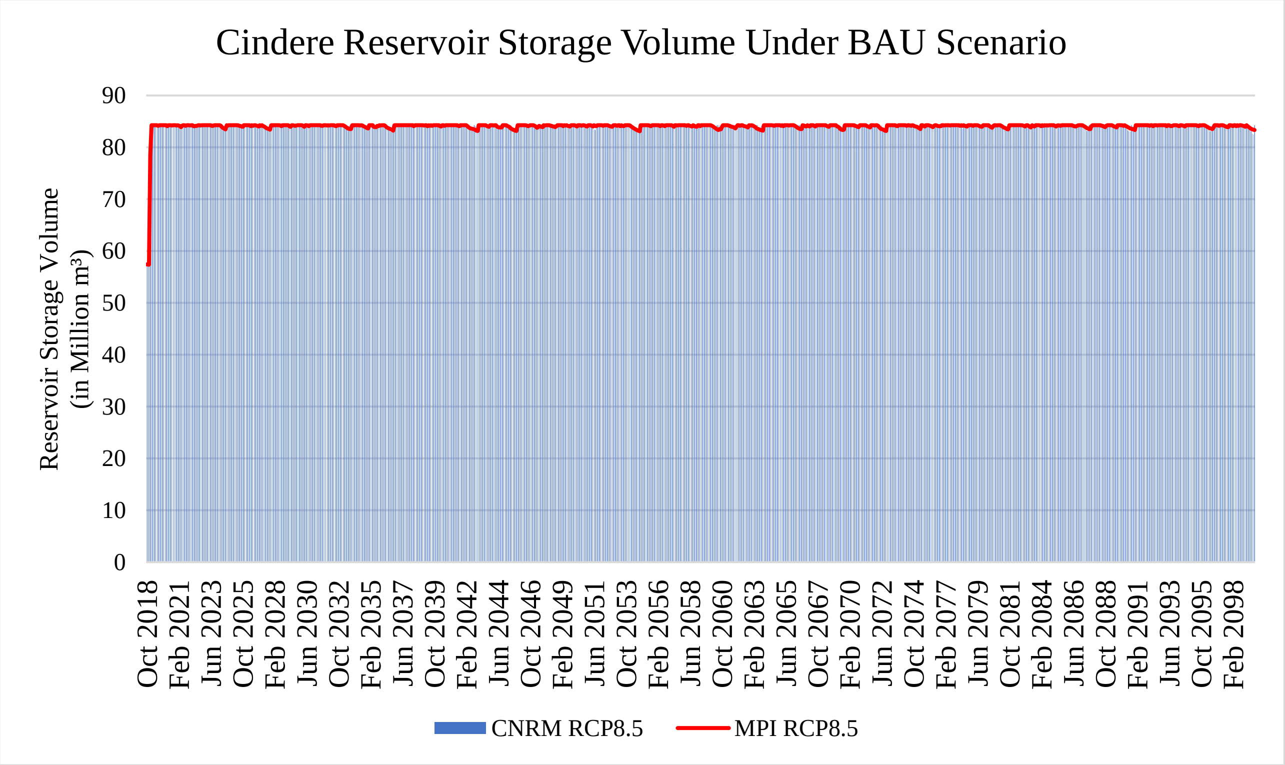

Figure 1.4. Storage volume of Cindere Reservoir under BAU scenario with CNRM RCP8.5 and MPI RCP8.5 climate change scenarios.

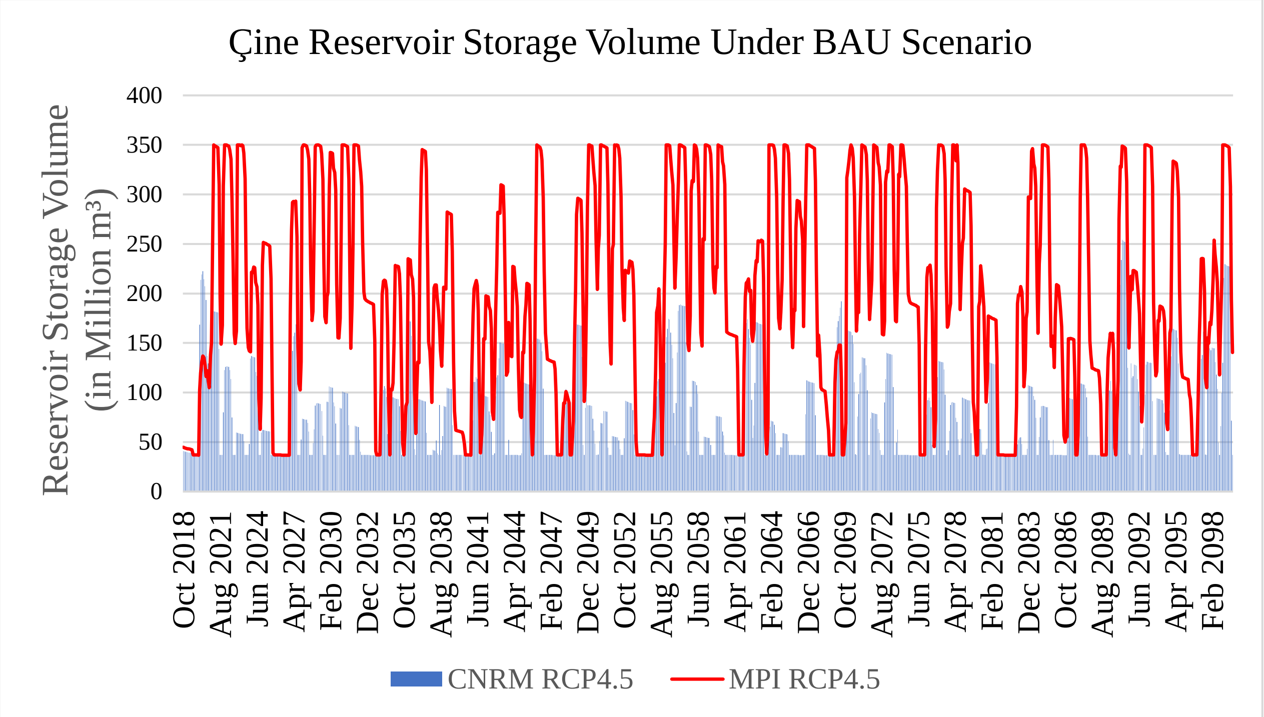

Figure 1.5. Storage volume of Çine Reservoir under BAU scenario with CNRM RCP4.5 and MPI RCP4.5 climate change scenarios.

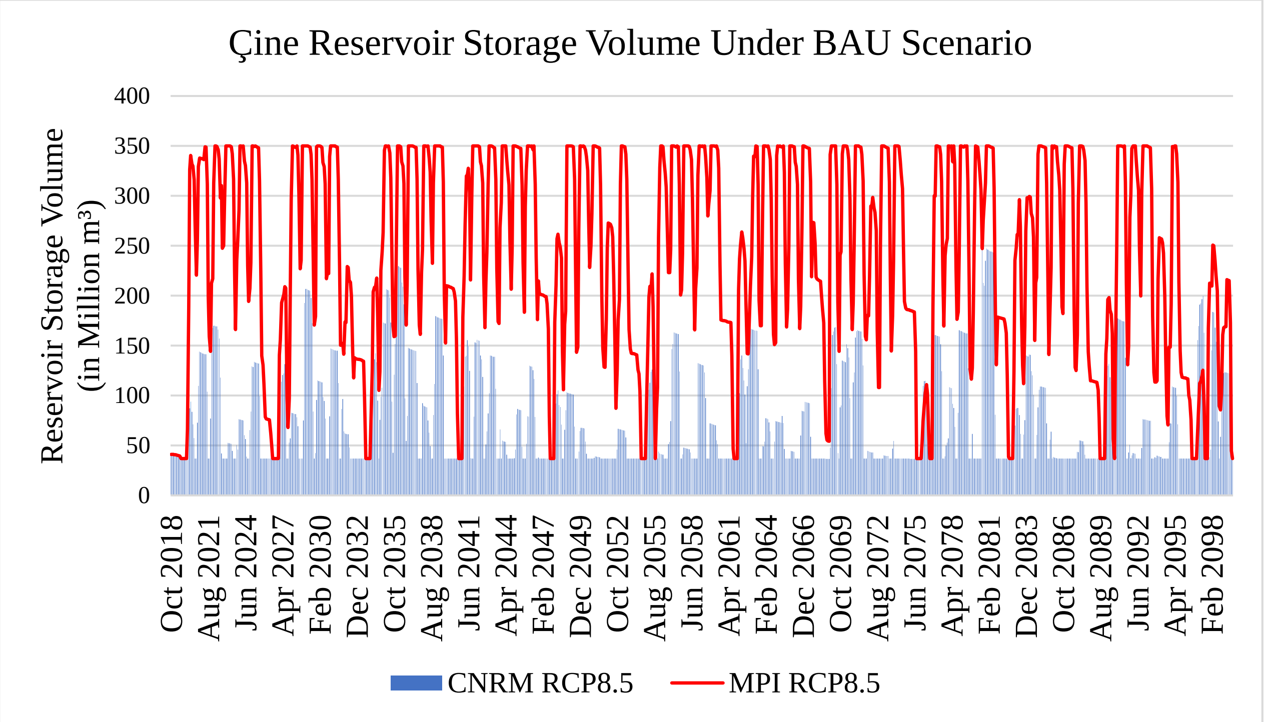

Figure 1.6. Storage volume of Çine Reservoir under BAU scenario with CNRM RCP8.5 and MPI RCP8.5 climate change scenarios.

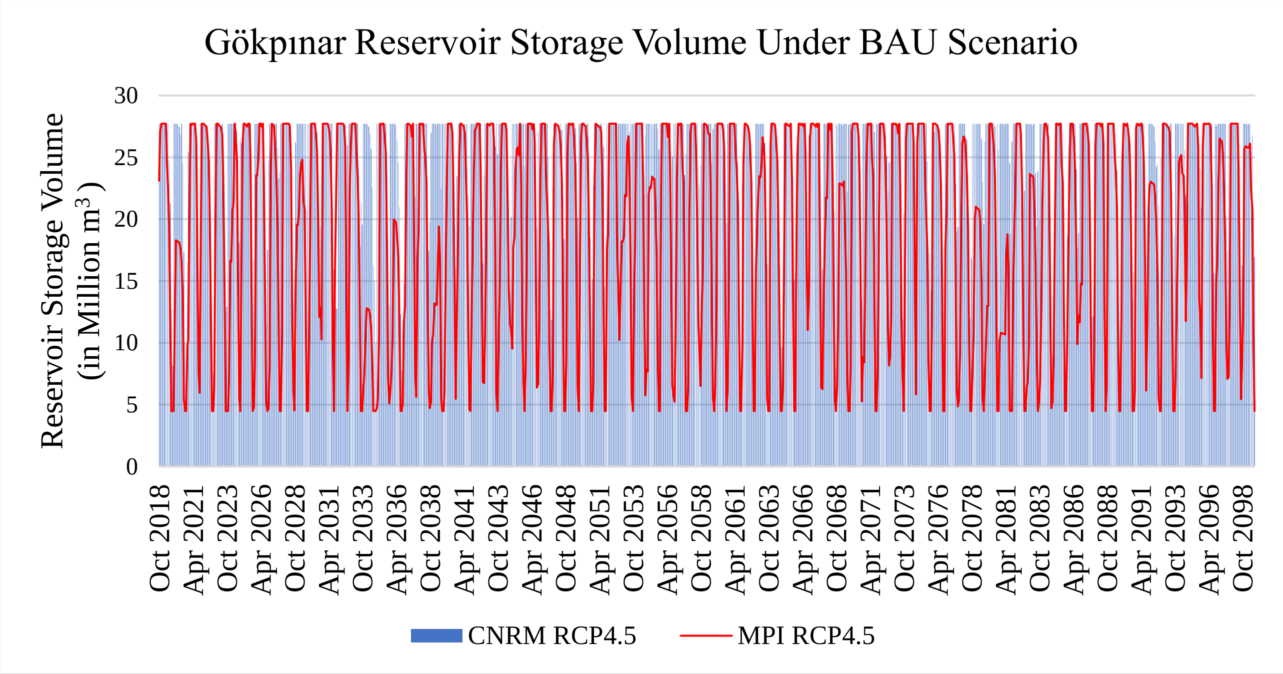

Figure 1.7. Storage volume of Gökpınar Reservoir under BAU scenario with CNRM RCP8.5 and MPI RCP8.5 climate change scenarios.

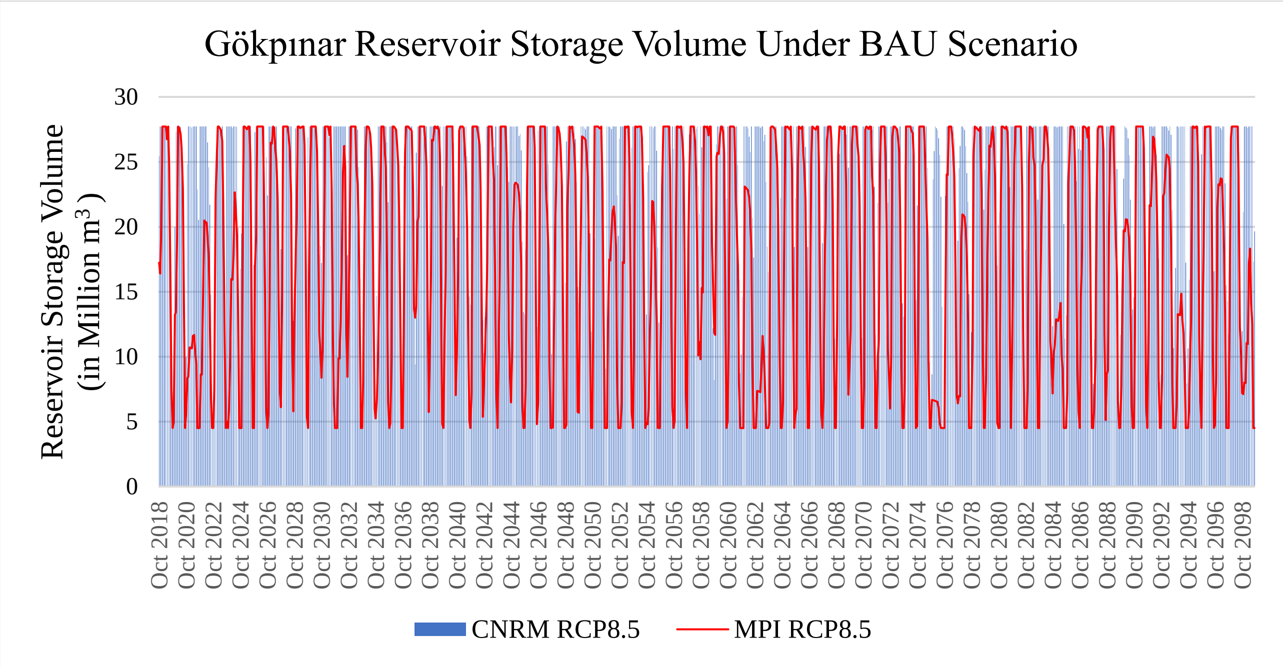

Figure 1.8. Storage volume of Gökpınar Reservoir under BAU scenario with CNRM RCP8.5 and MPI RCP8.5 climate change scenarios.

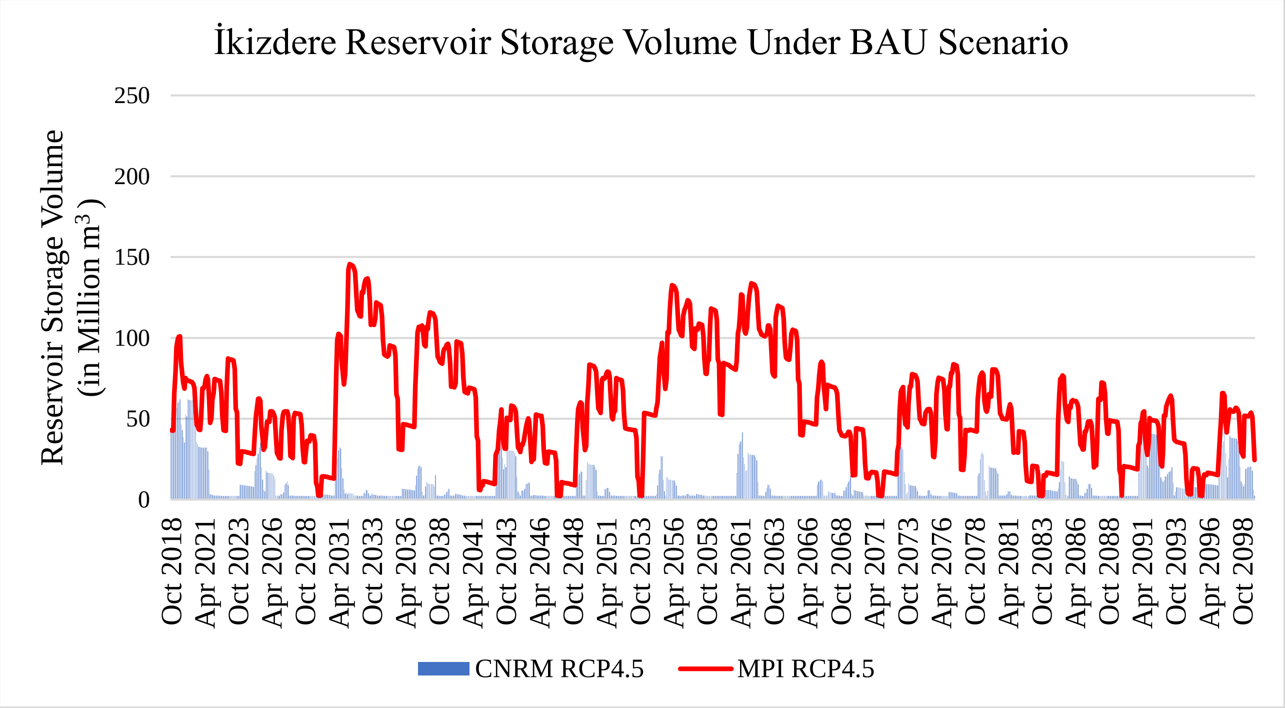

Figure 1.9. Storage volume of İkizdere Reservoir under BAU scenario with CNRM RCP4.5 and MPI RCP4.5 climate change scenarios.

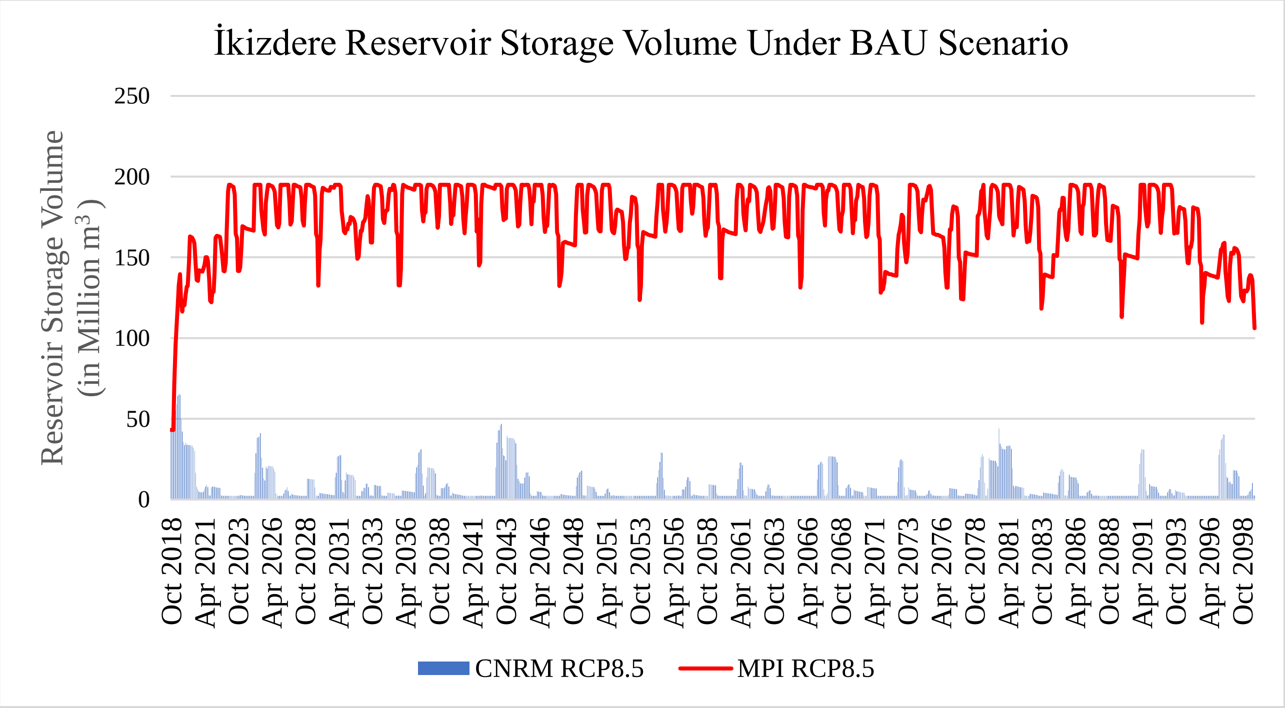

Figure 1.10. Storage volume of İkizdere Reservoir under BAU scenario with CNRM RCP4.5 and MPI RCP4.5 climate change scenarios.

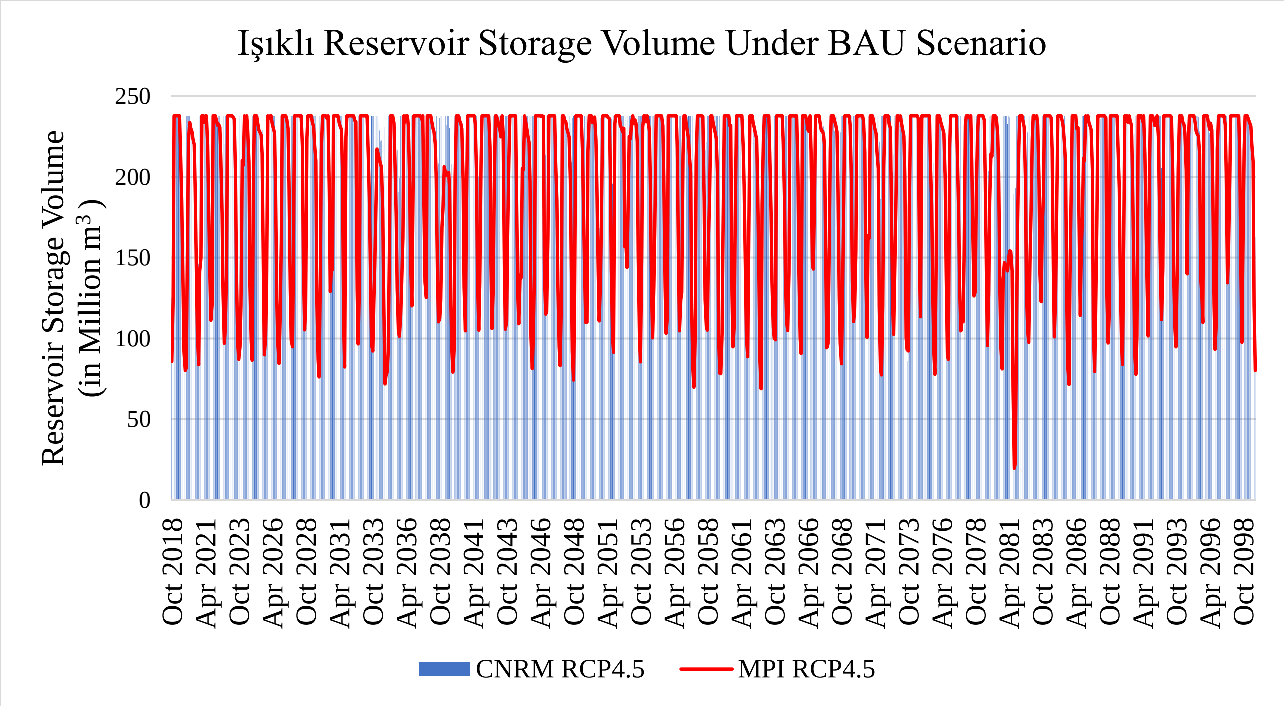

Figure 1.11. Storage volume of Işıklı Reservoir under BAU scenario with CNRM RCP4.5 and MPI RCP4.5 climate change scenarios.

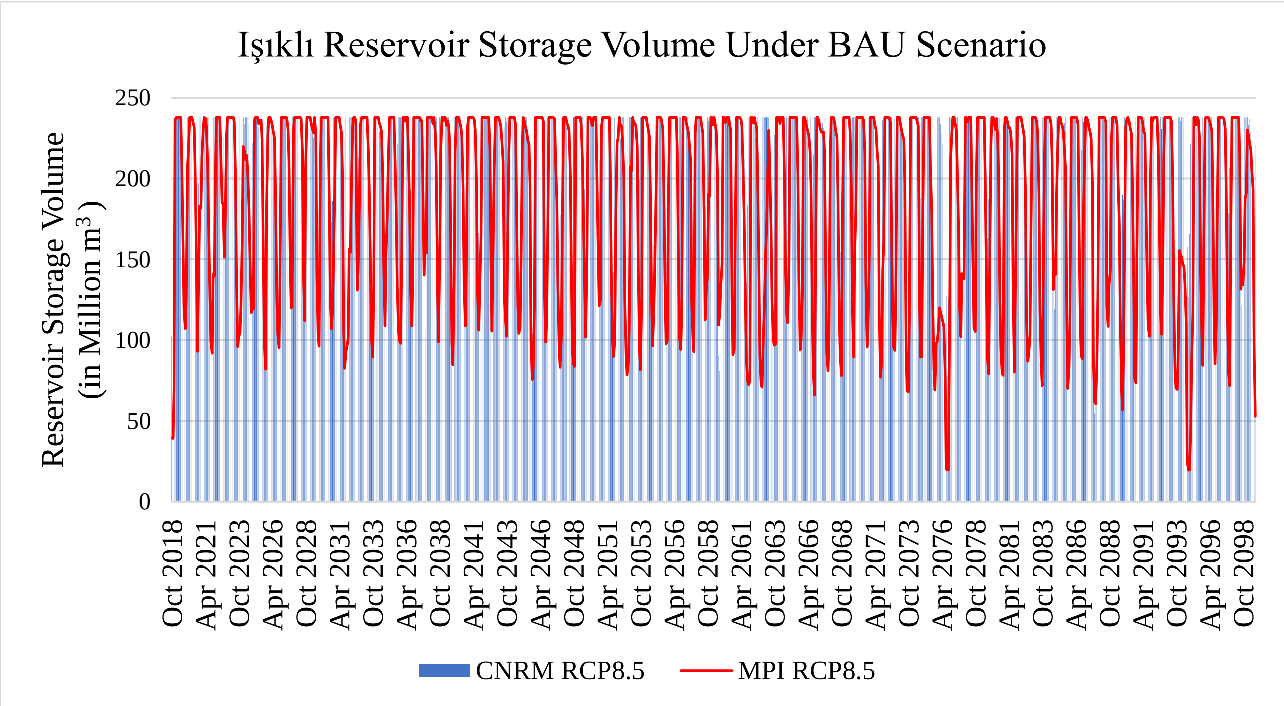

Figure 1.12. Storage volume of Işıklı Reservoir under BAU scenario with CNRM RCP8.5 and MPI RCP8.5 climate change scenarios.

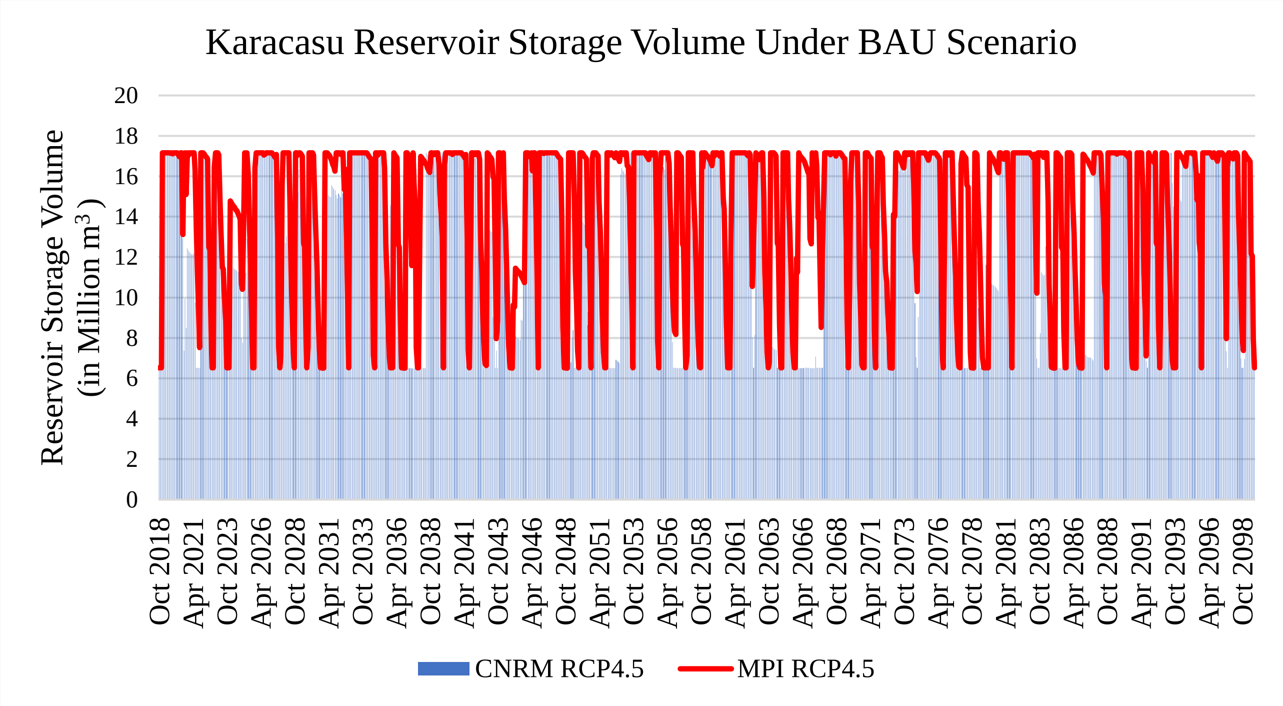

Figure 1.13. Storage volume of Karacasu Reservoir under BAU scenario with CNRM RCP4.5 and MPI RCP4.5 climate change scenarios.

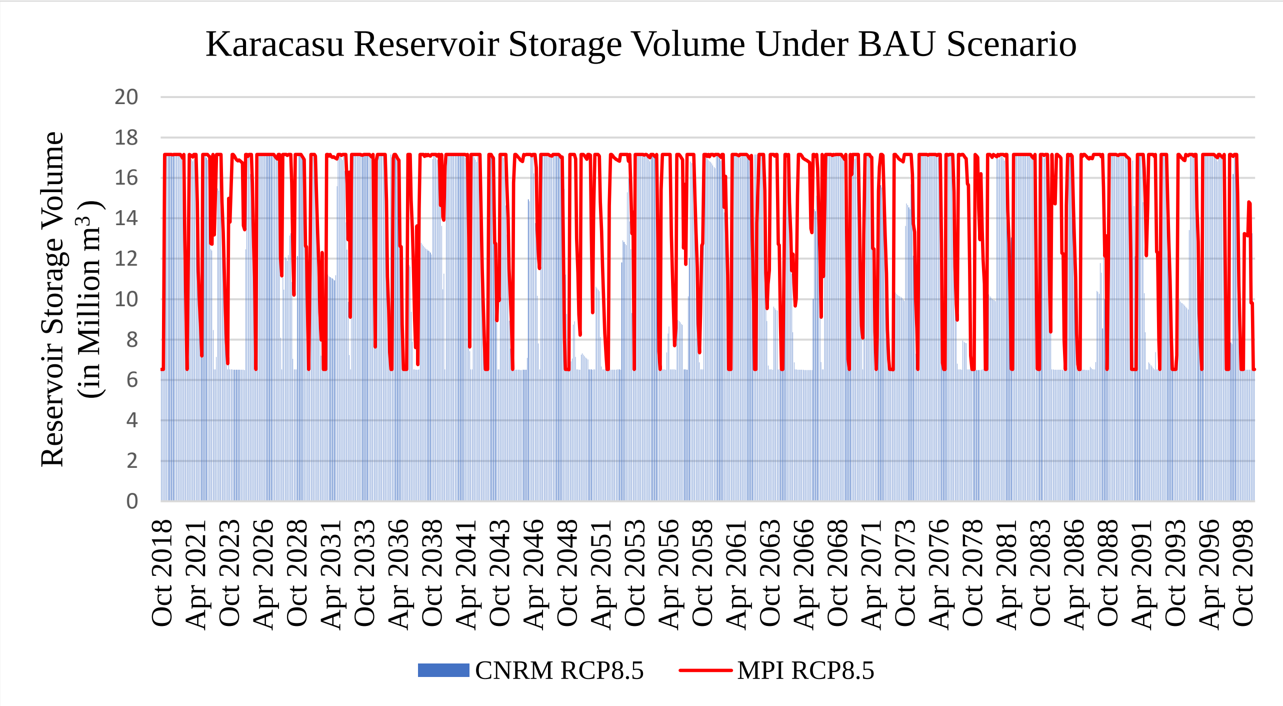

Figure 1.14. Storage volume of Karacasu Reservoir under BAU scenario with CNRM RCP8.5 and MPI RCP8.5 climate change scenarios.

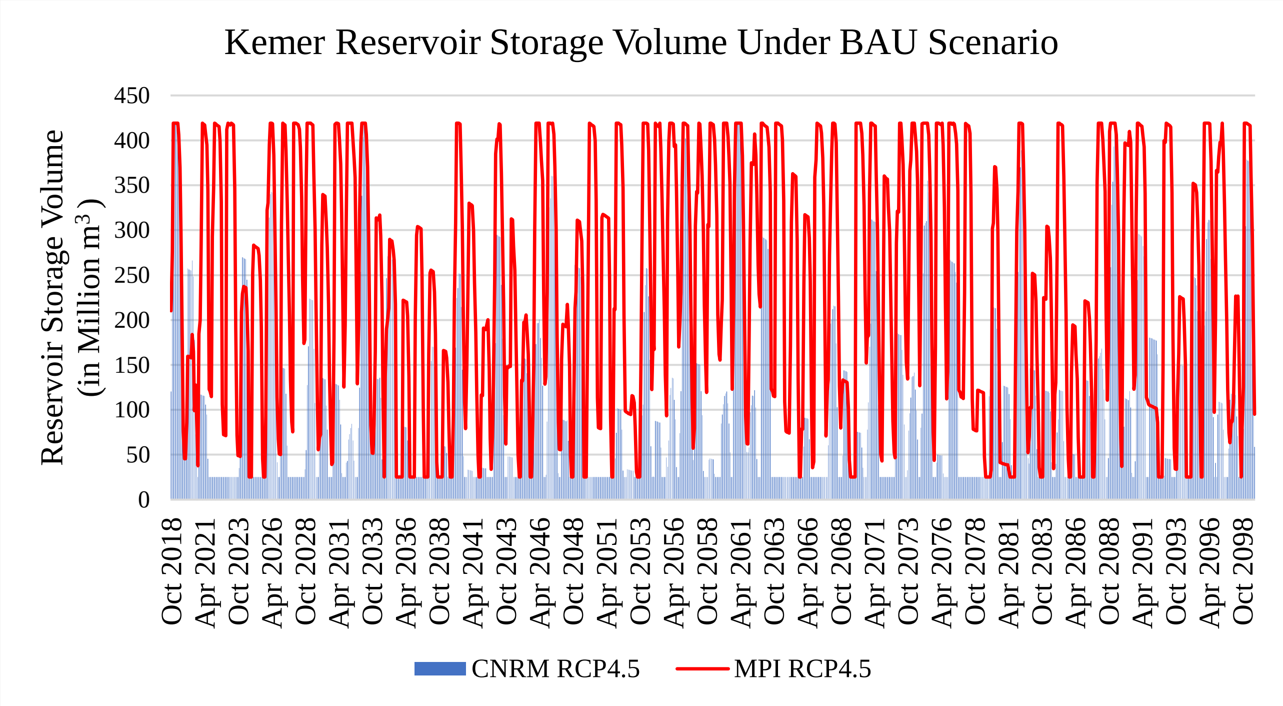

Figure 1.15. Storage volume of Kemer Reservoir under BAU scenario with CNRM RCP4.5 and MPI RCP4.5 climate change scenarios.

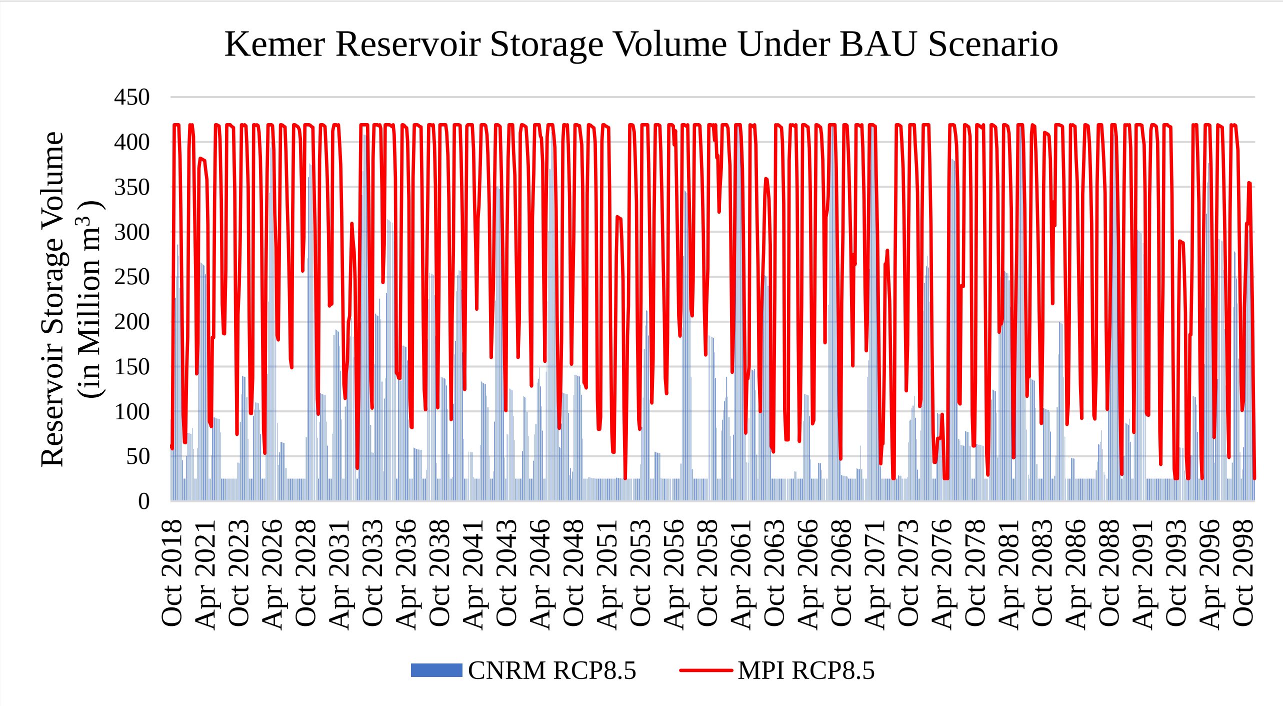

Figure 1.16. Storage volume of Kemer Reservoir under BAU scenario with CNRM RCP8.5 and MPI RCP8.5 climate change scenarios.

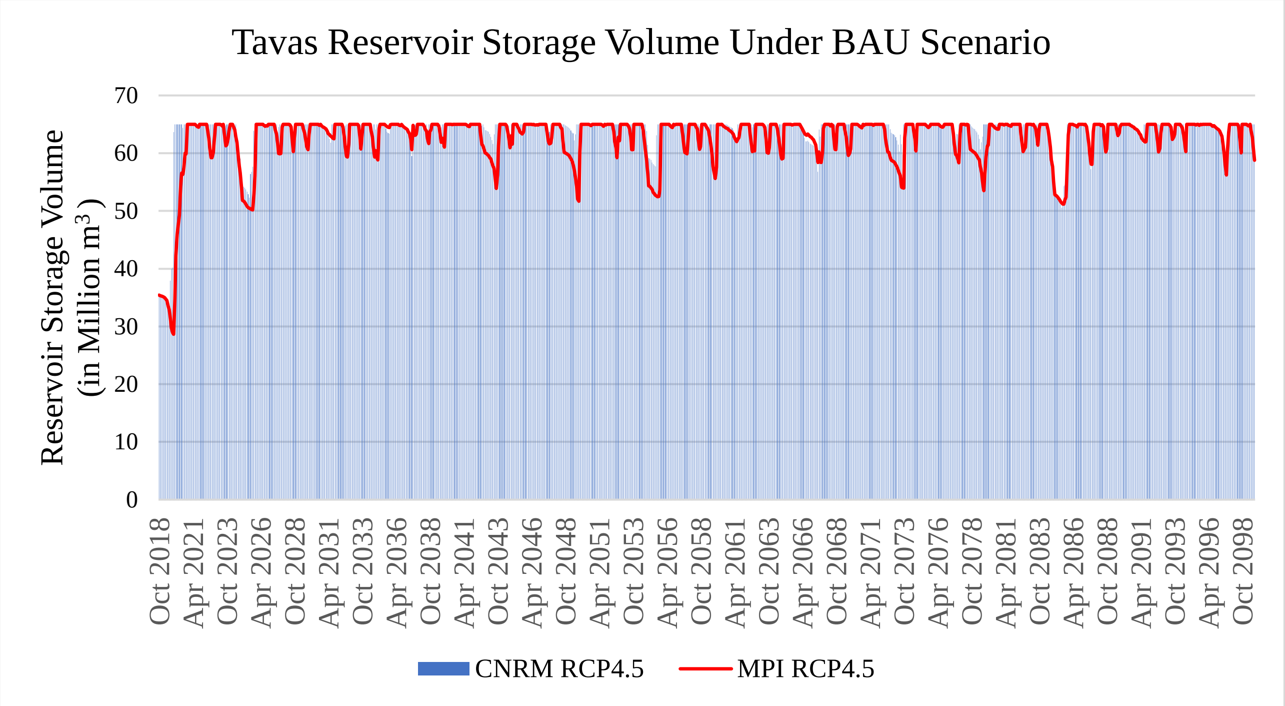

Figure 1.17. Storage volume of Tavas Reservoir under BAU scenario with CNRM RCP4.5 and MPI RCP4.5 climate.

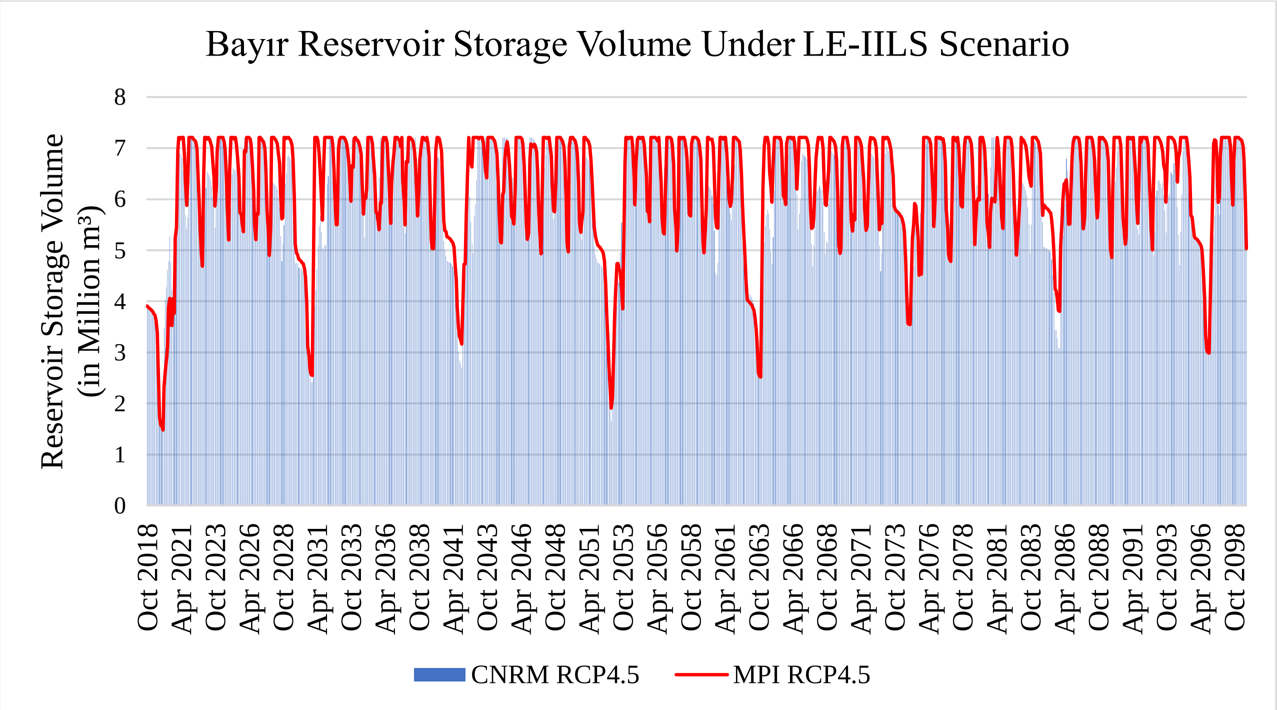

Figure 1.18. Storage volume of Bayır Reservoir under LE-IILS scenario with CNRM RCP4.5 and MPI RCP4.5 climate change scenarios.

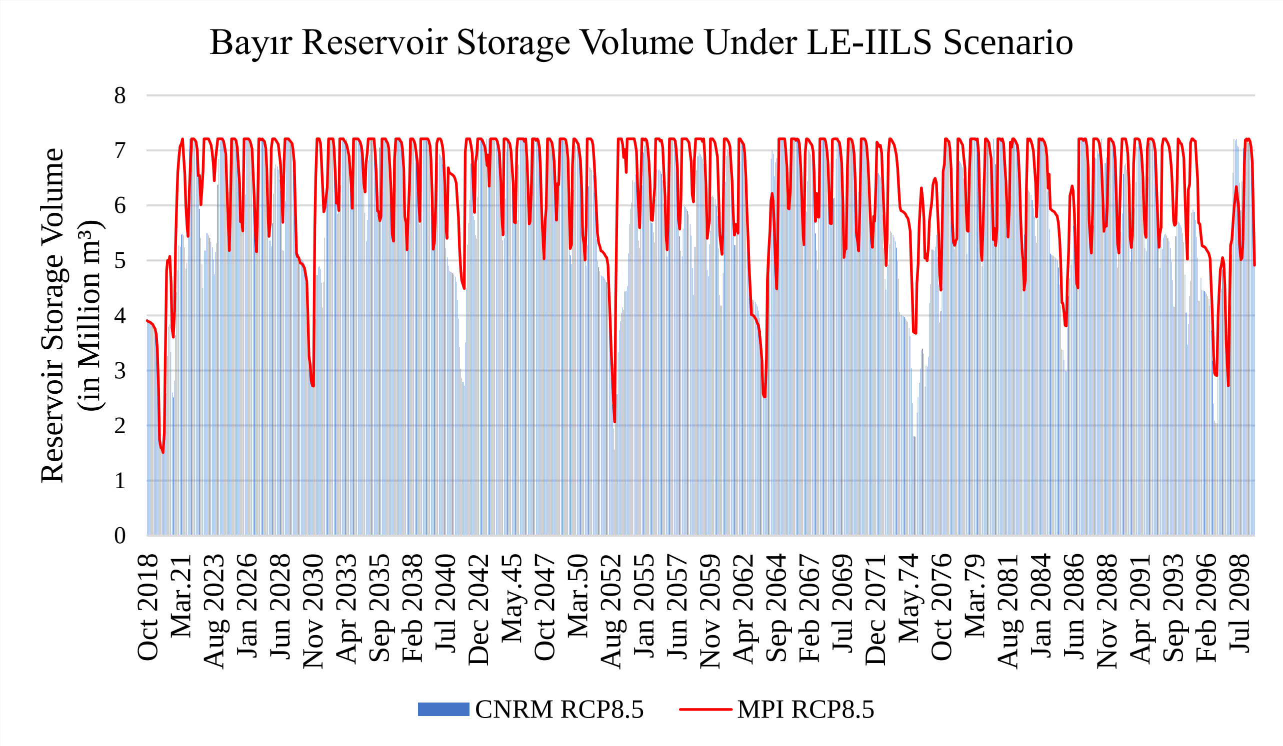

Figure 1.19. Storage volume of Bayır Reservoir under LE-IILS scenario with CNRM RCP4.5 and MPI RCP4.5 climate change scenarios.

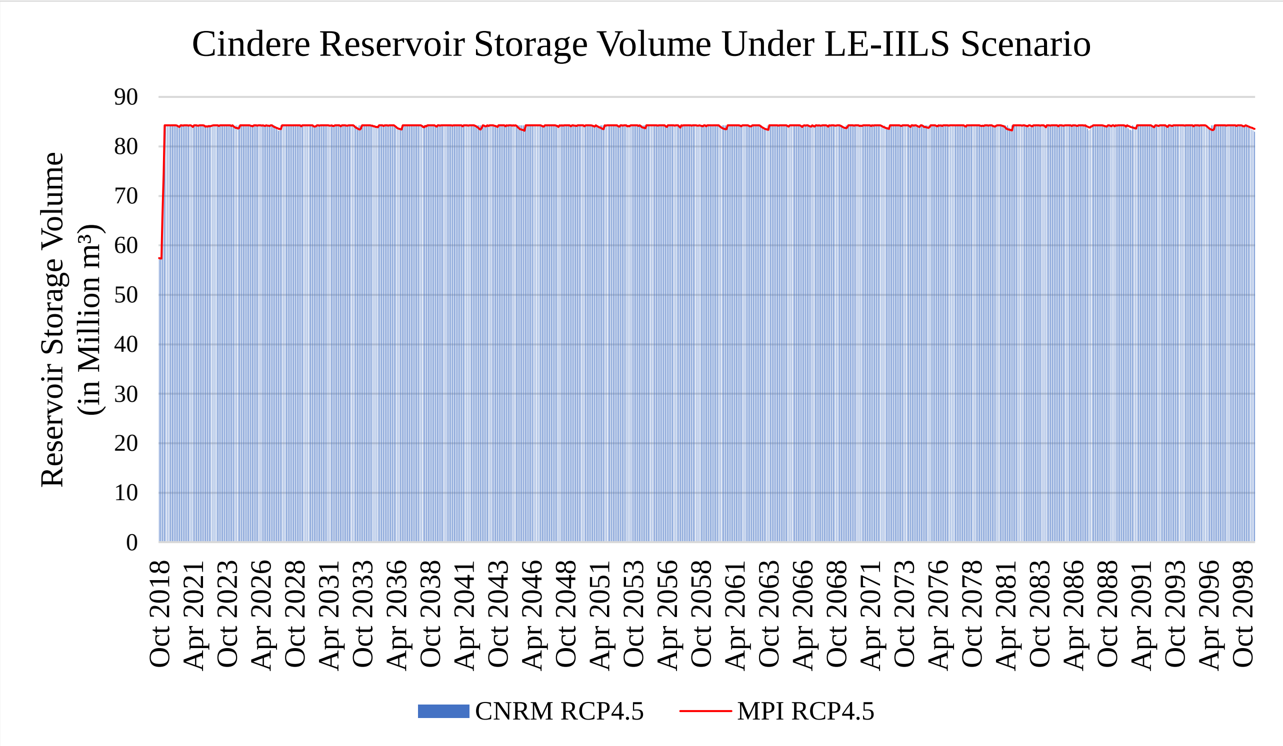

Figure 1.20. Storage volume of Cindere Reservoir under LE-IILS scenario with CNRM RCP4.5 and MPI RCP4.5 climate change scenarios.

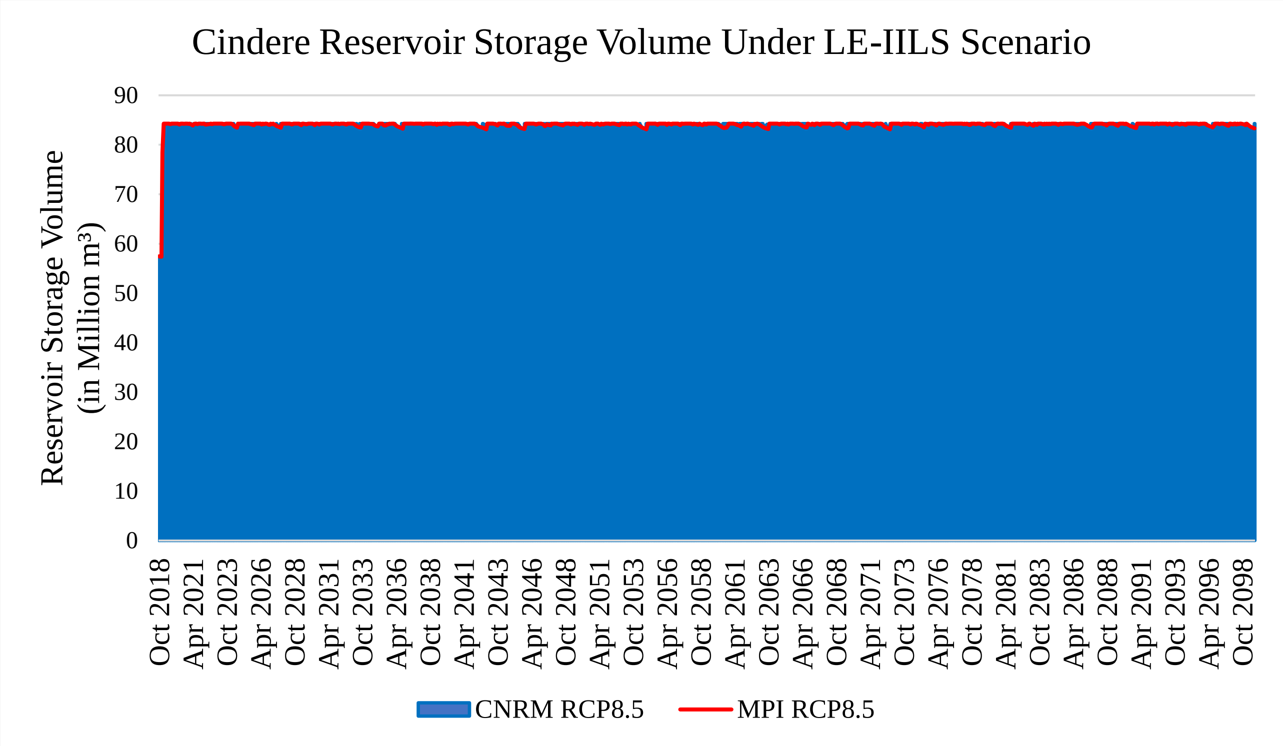

Figure 1.21. Storage volume of Cindere Reservoir under LE-IILS scenario with CNRM RCP8.5 and MPI RCP8.5 climate change scenarios.

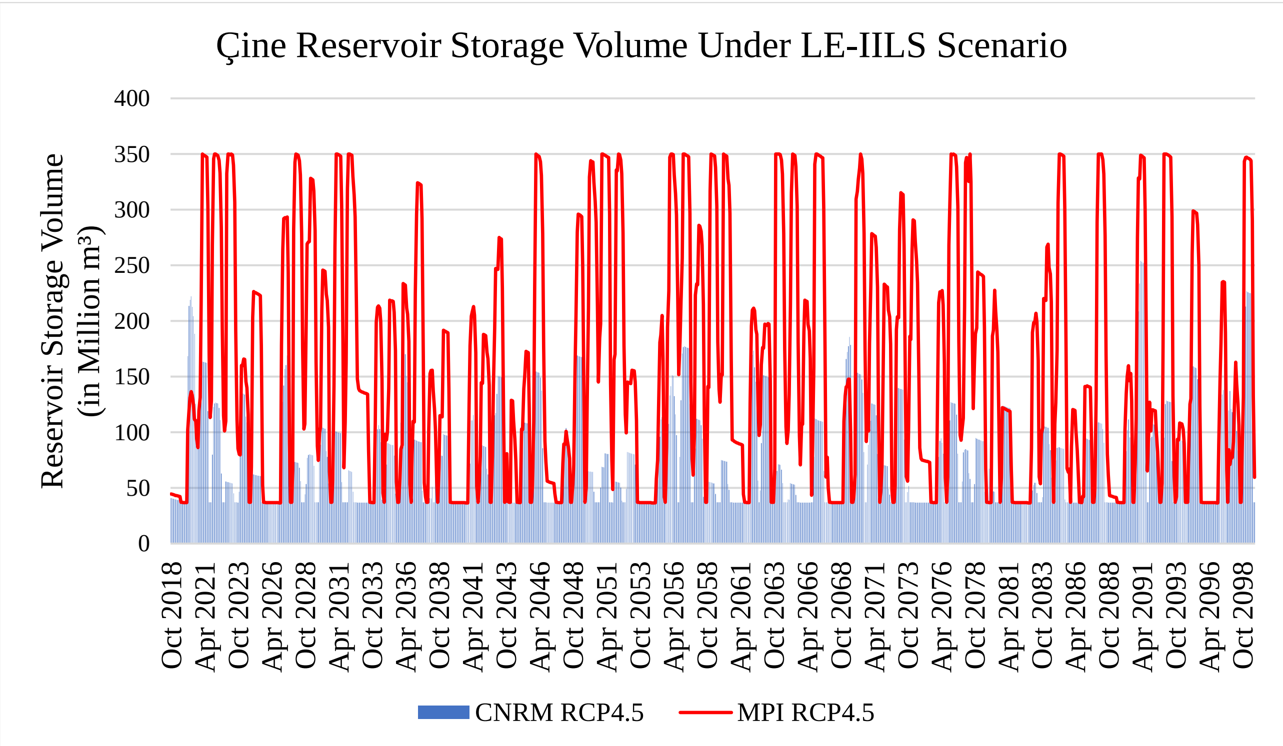

Figure 1.22. Storage volume of Çine Reservoir under LE-IILS scenario with CNRM RCP4.5 and MPI RCP4.5 climate change scenarios.

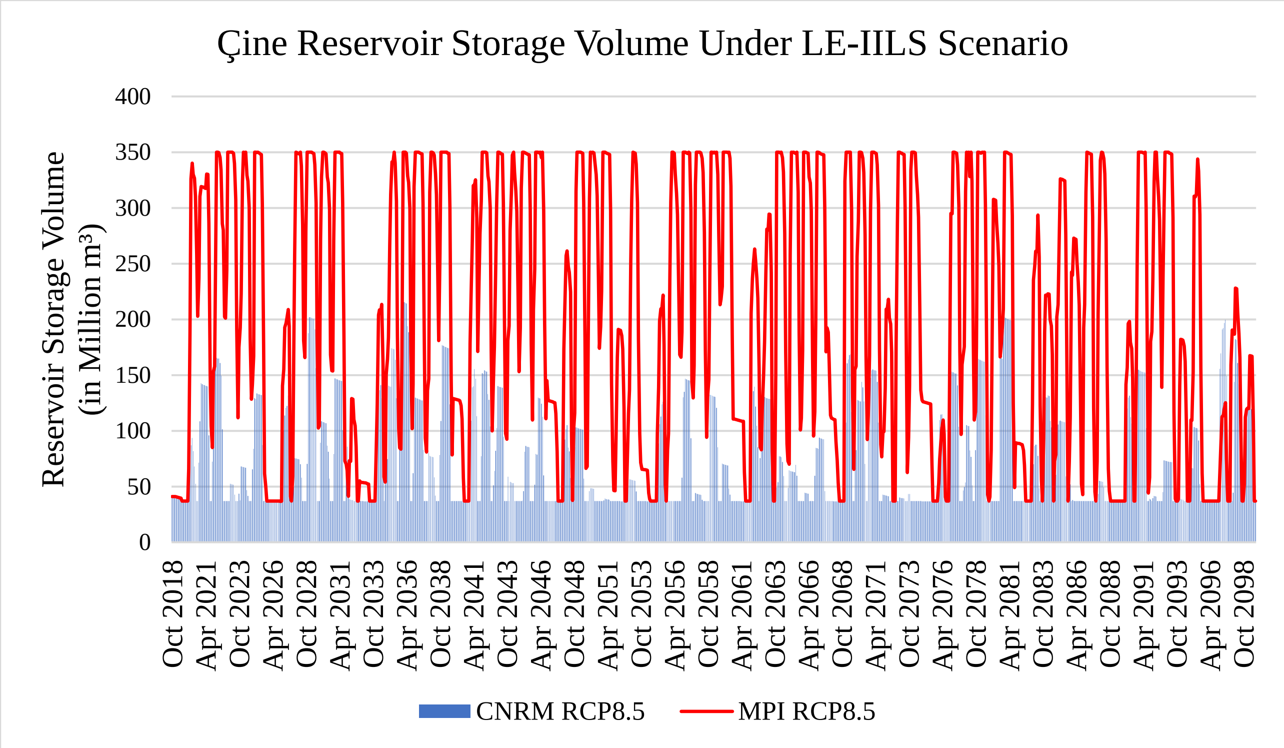

Figure 1.23. Storage volume of Çine Reservoir under LE-IILS scenario with CNRM RCP8.5 and MPI RCP8.5 climate change scenarios.

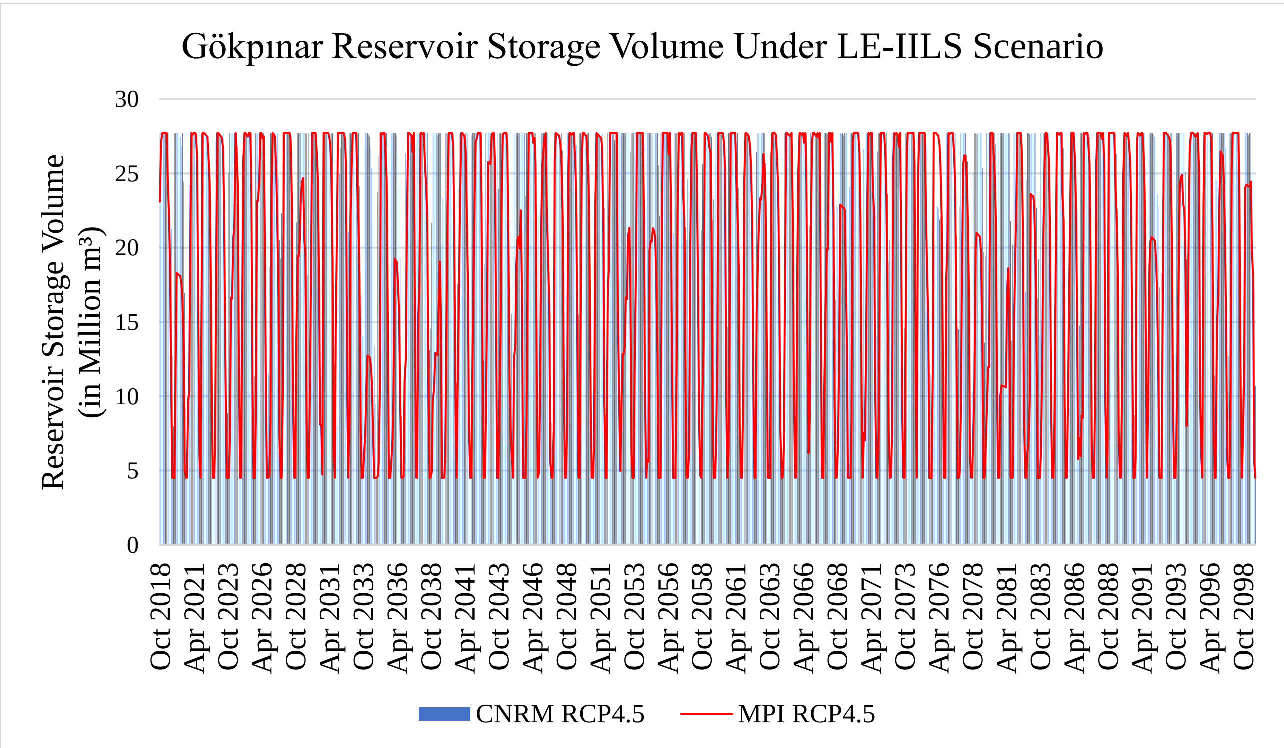

Figure 1.24. Storage volume of Gökpınar Reservoir under LE-IILS scenario with CNRM RCP4.5 and MPI RCP4.5 climate change scenarios.

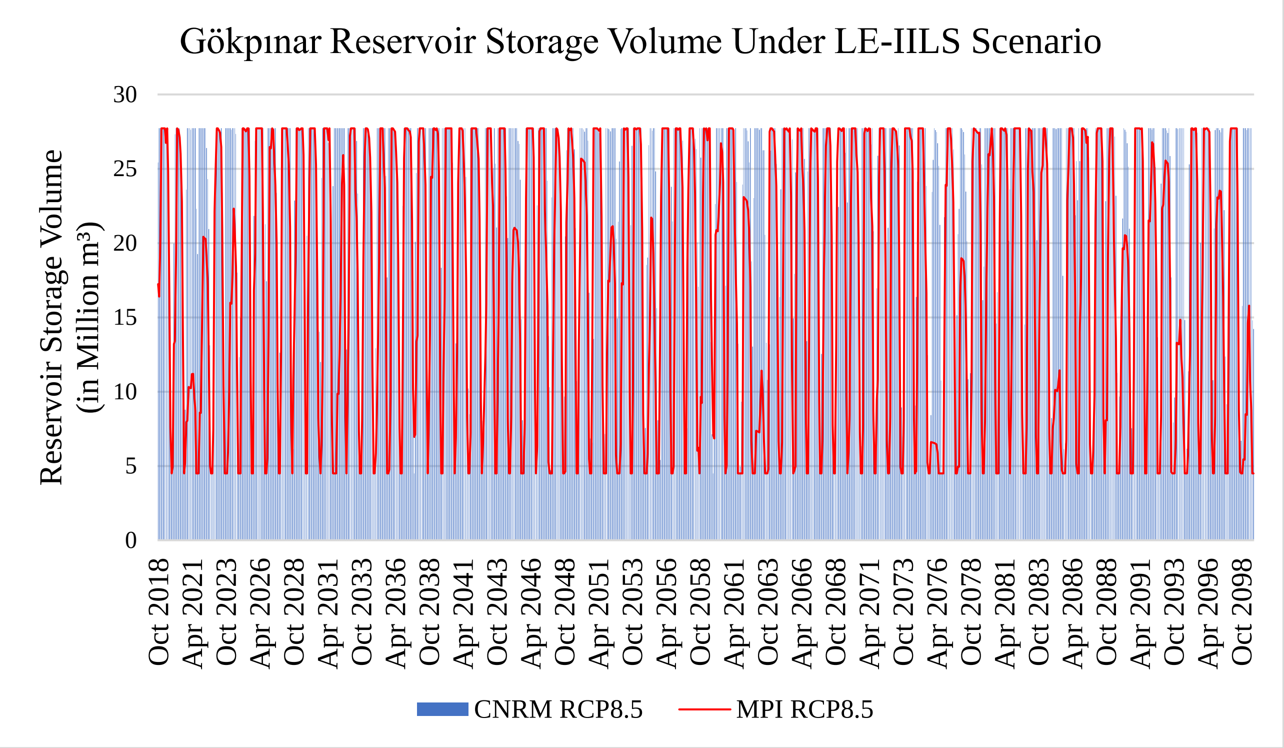

Figure 1.25. Storage volume of Gökpınar Reservoir under LE-IILS scenario with CNRM RCP8.5 and MPI RCP8.5 climate change scenarios.

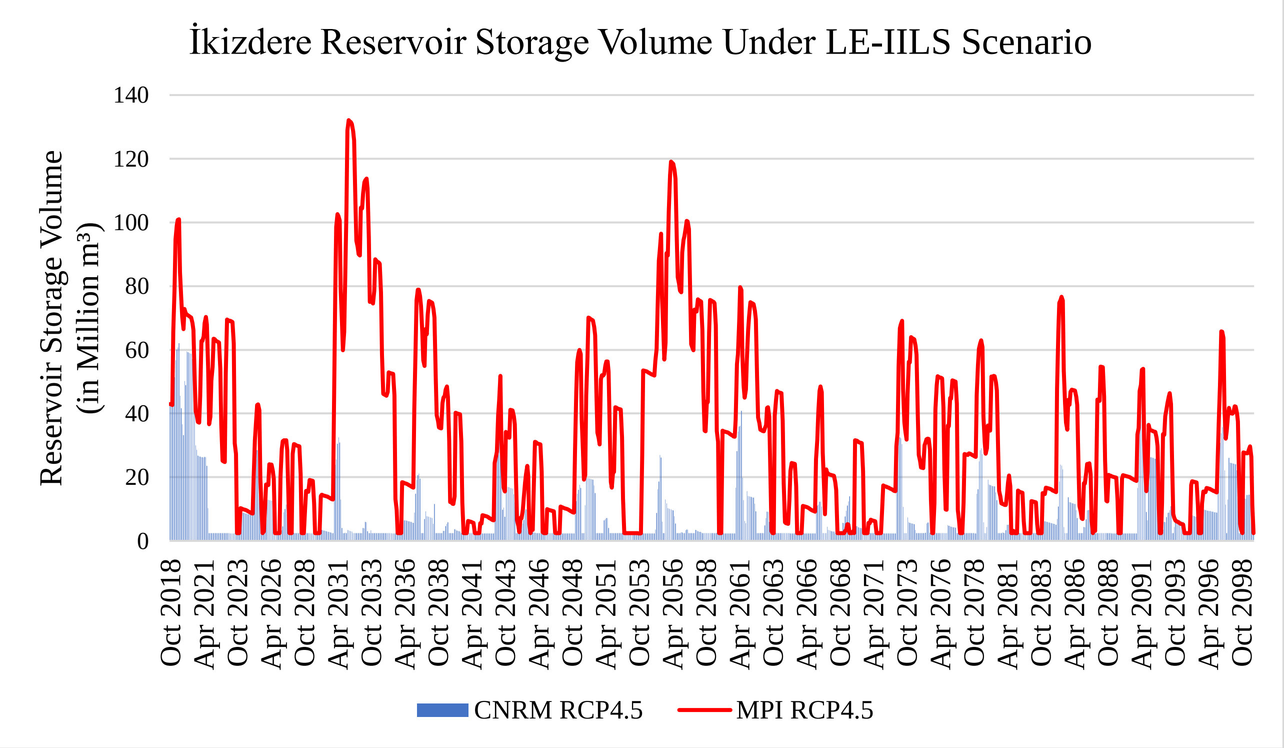

Figure 1.26. Storage volume of İkizdere Reservoir under LE-IILS scenario with CNRM RCP4.5 and MPI RCP4.5 climate change scenarios.

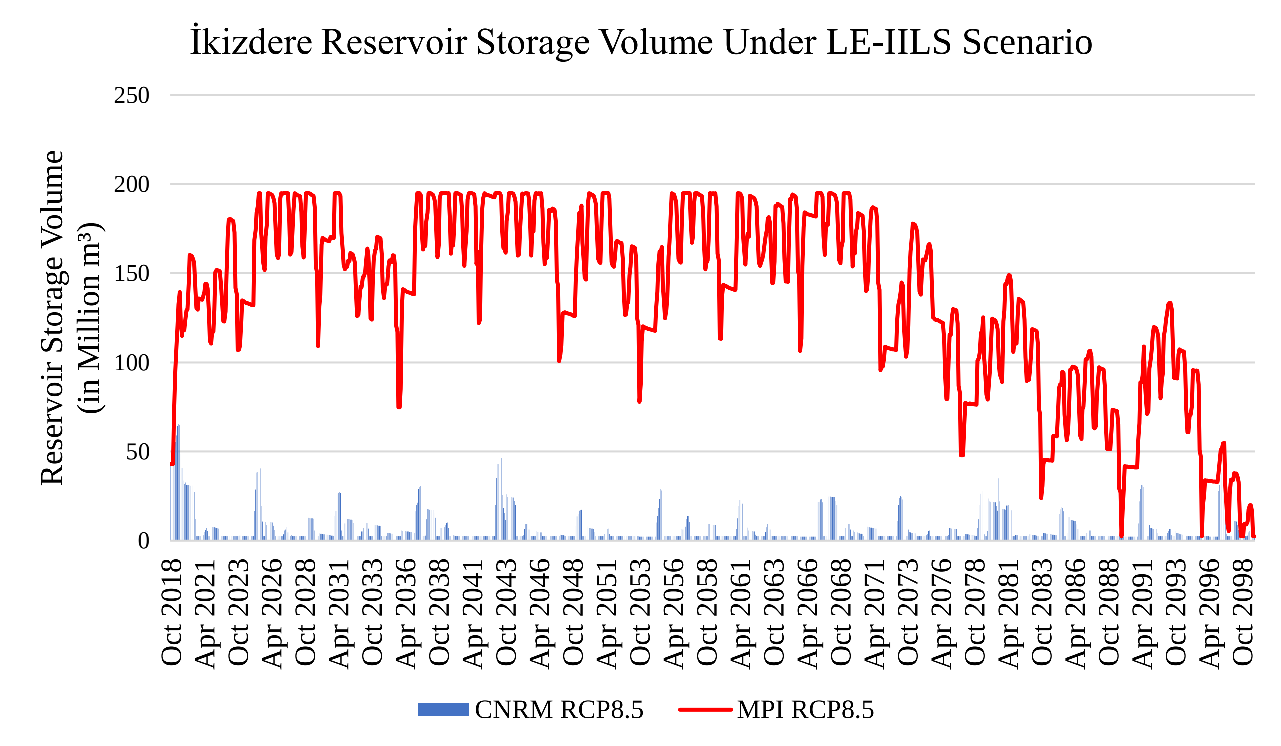

Figure 1.27. Storage volume of İkizdere Reservoir under LE-IILS scenario with CNRM RCP8.5 and MPI RCP8.5 climate change scenarios.

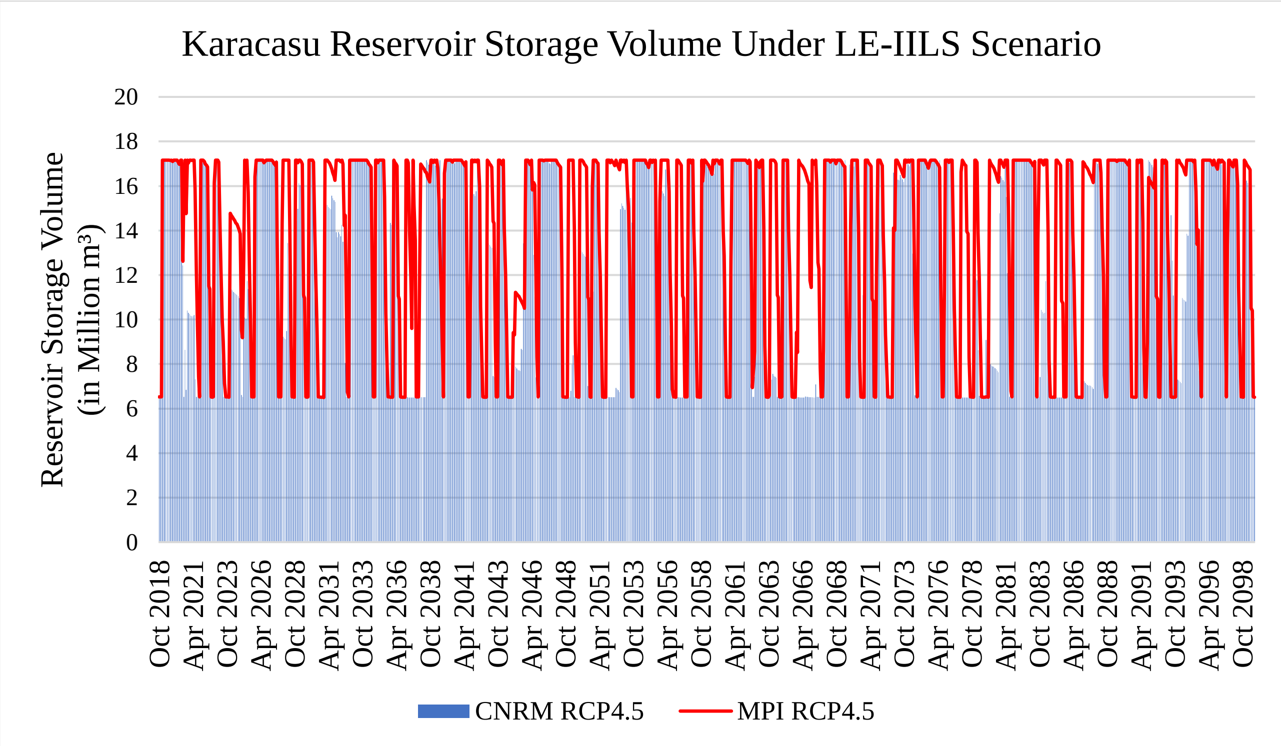

Figure 1.28. Storage volume of Karacasu Reservoir under LE-IILS scenario with CNRM RCP4.5 and MPI RCP4.5 climate change scenarios.

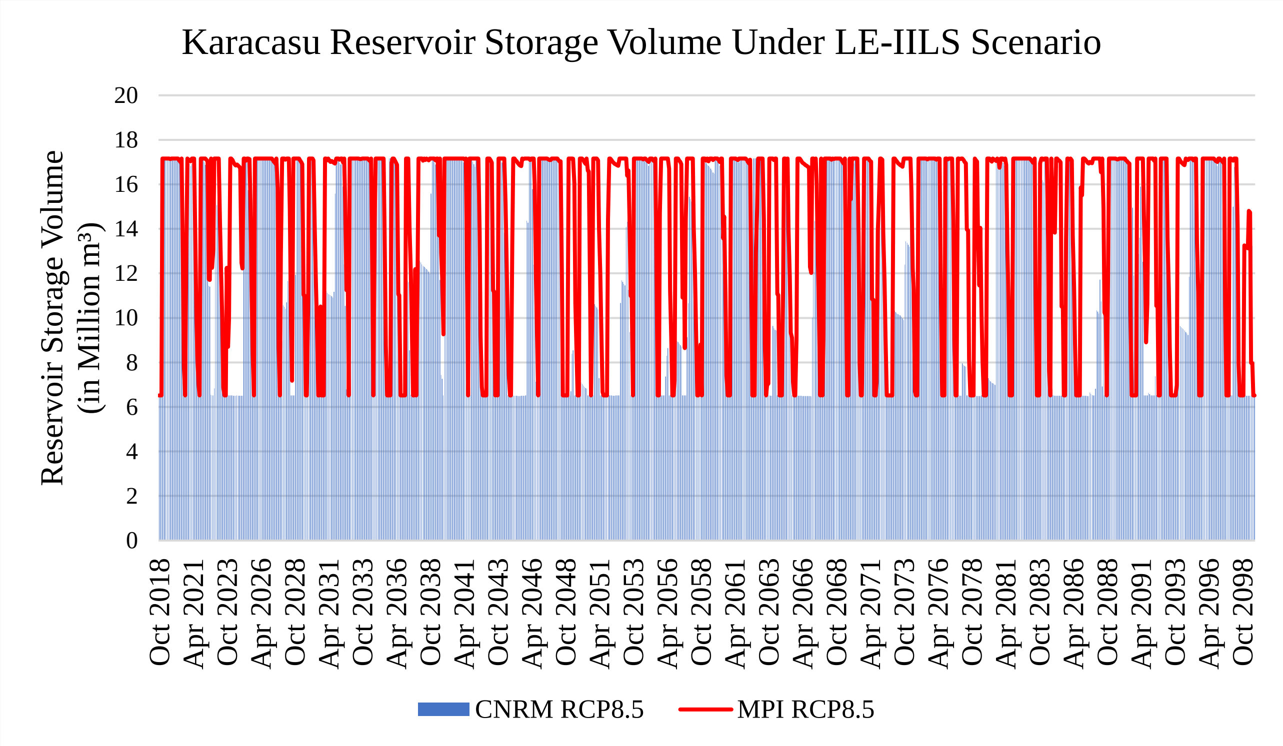

Figure 1.29. Storage volume of Karacasu Reservoir under LE-IILS scenario with CNRM RCP8.5 and MPI RCP8.5 climate change scenarios.

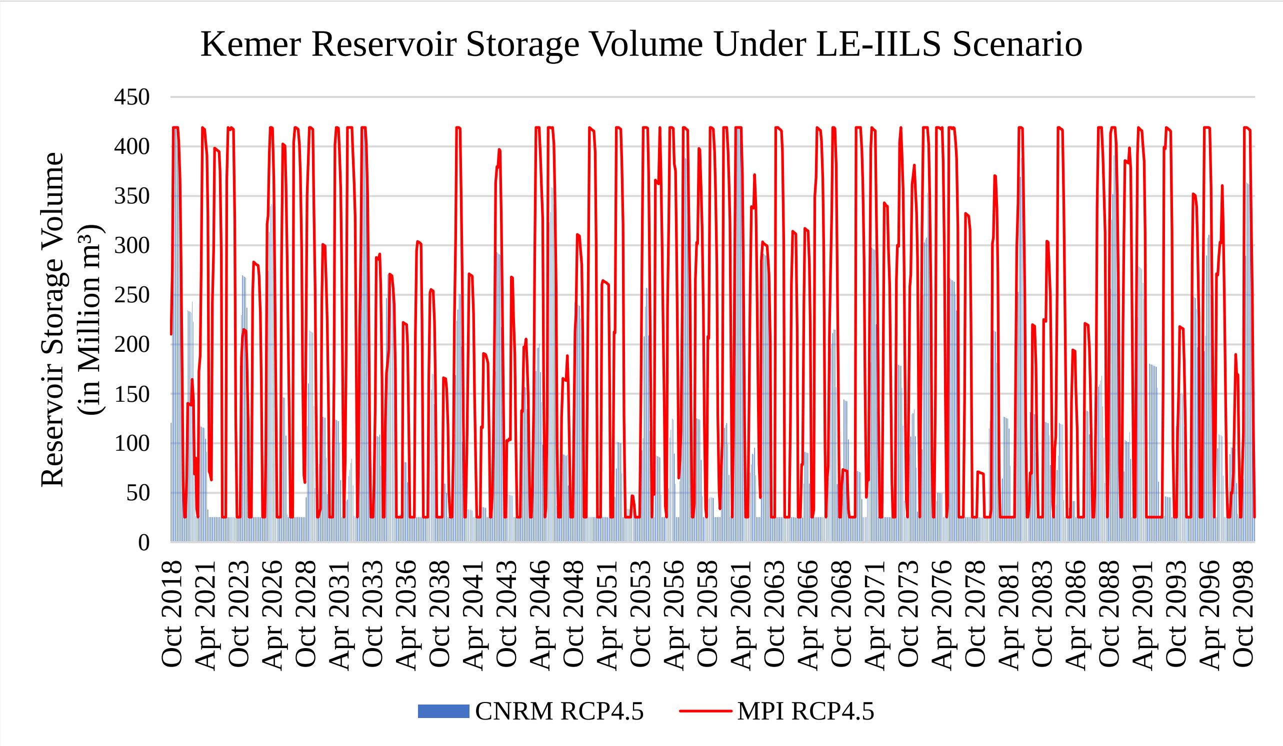

Figure 1.30. Storage volume of Kemer Reservoir under LE-IILS scenario with CNRM RCP4.5 and MPI RCP4.5 climate change scenarios.

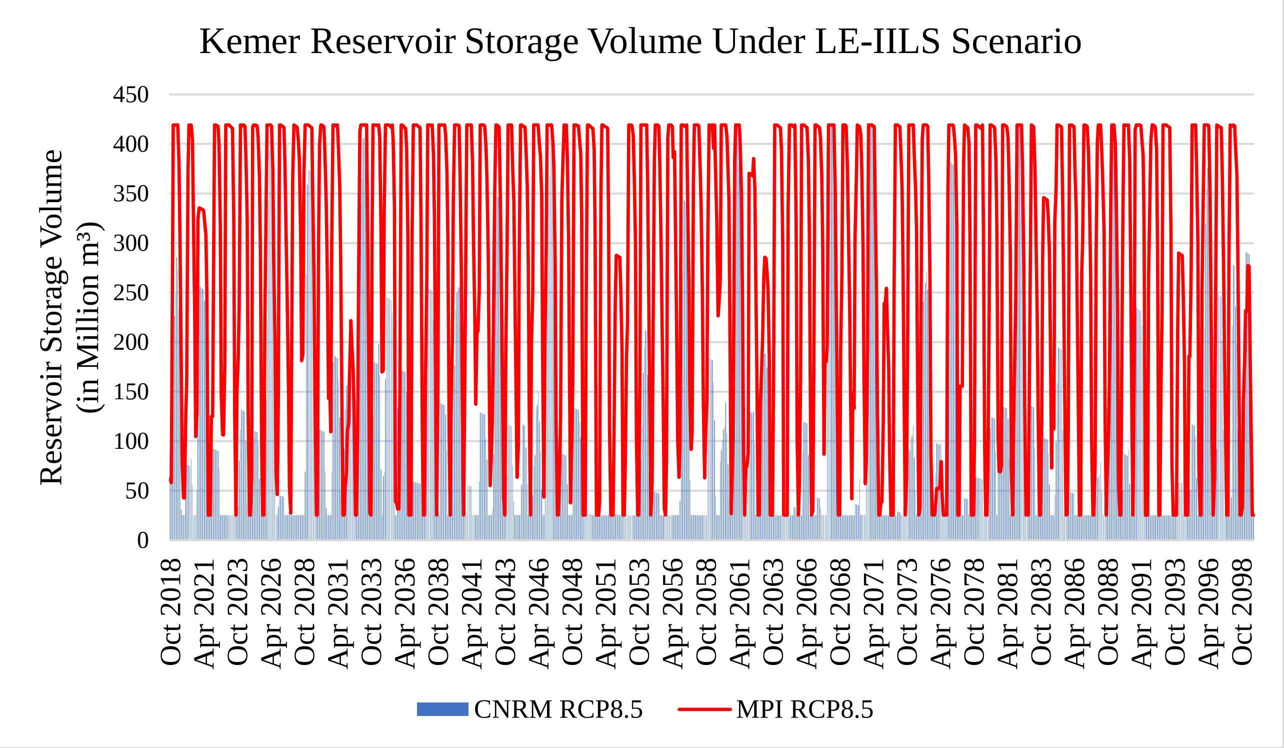

Figure 1.31. Storage volume of Kemer Reservoir under LE-IILS scenario with CNRM RCP4.5 and MPI RCP4.5 climate change scenarios.

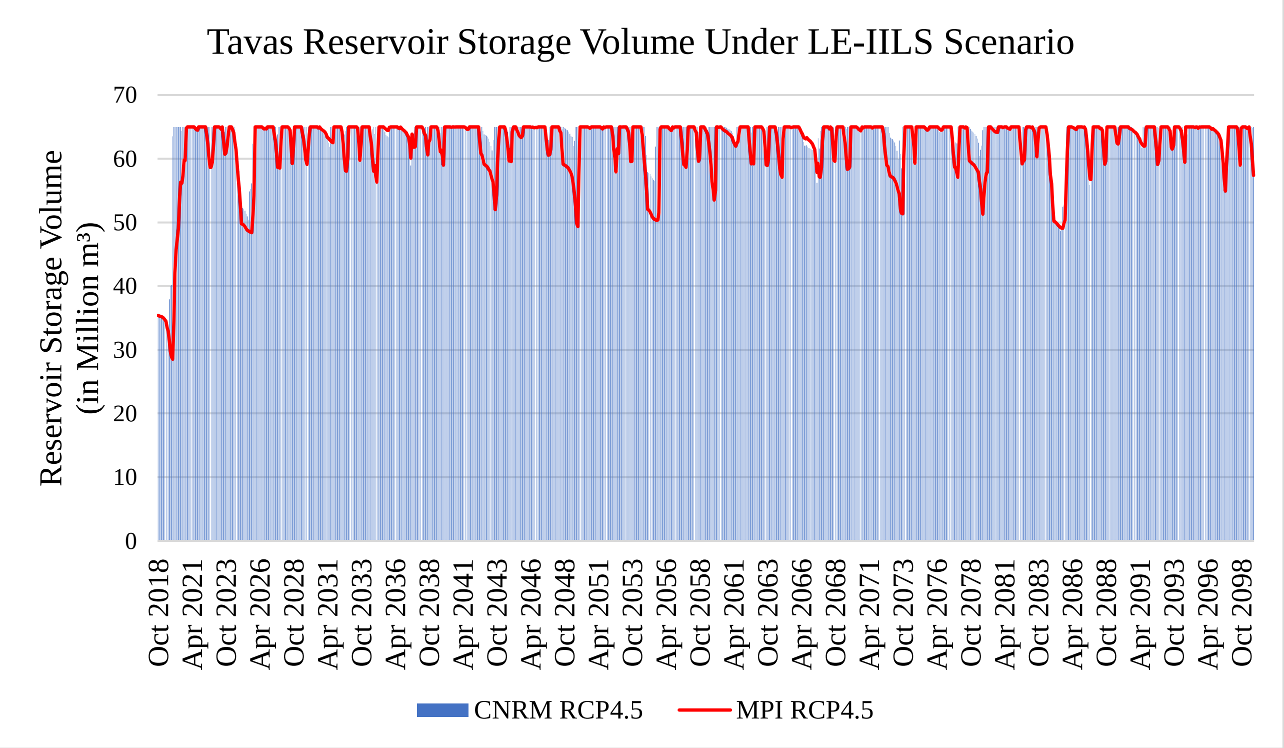

Figure 1.32. Storage volume of Tavas Reservoir under LE-IILS scenario with CNRM RCP4.5 and MPI RCP4.5 climate change scenarios.

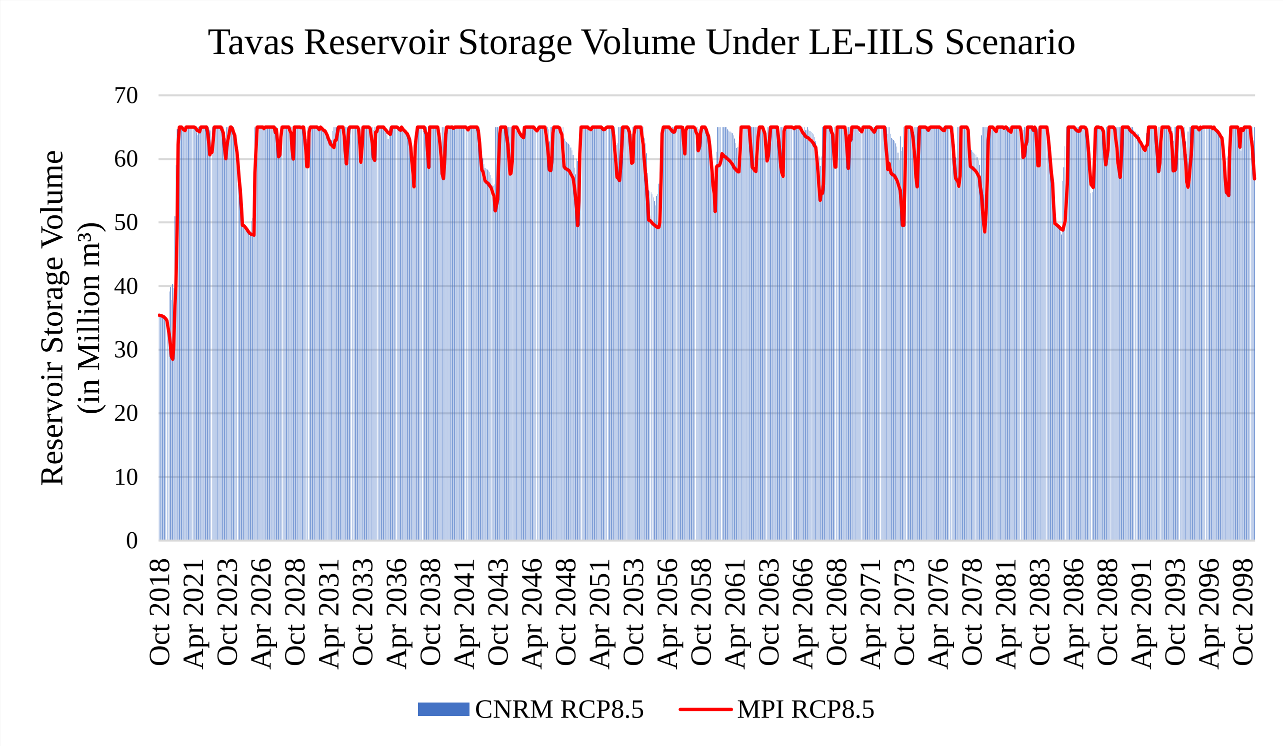

Figure 1.33. Storage volume of Tavas Reservoir under LE-IILS scenario with CNRM RCP8.5 and MPI RCP8.5 climate change scenarios.

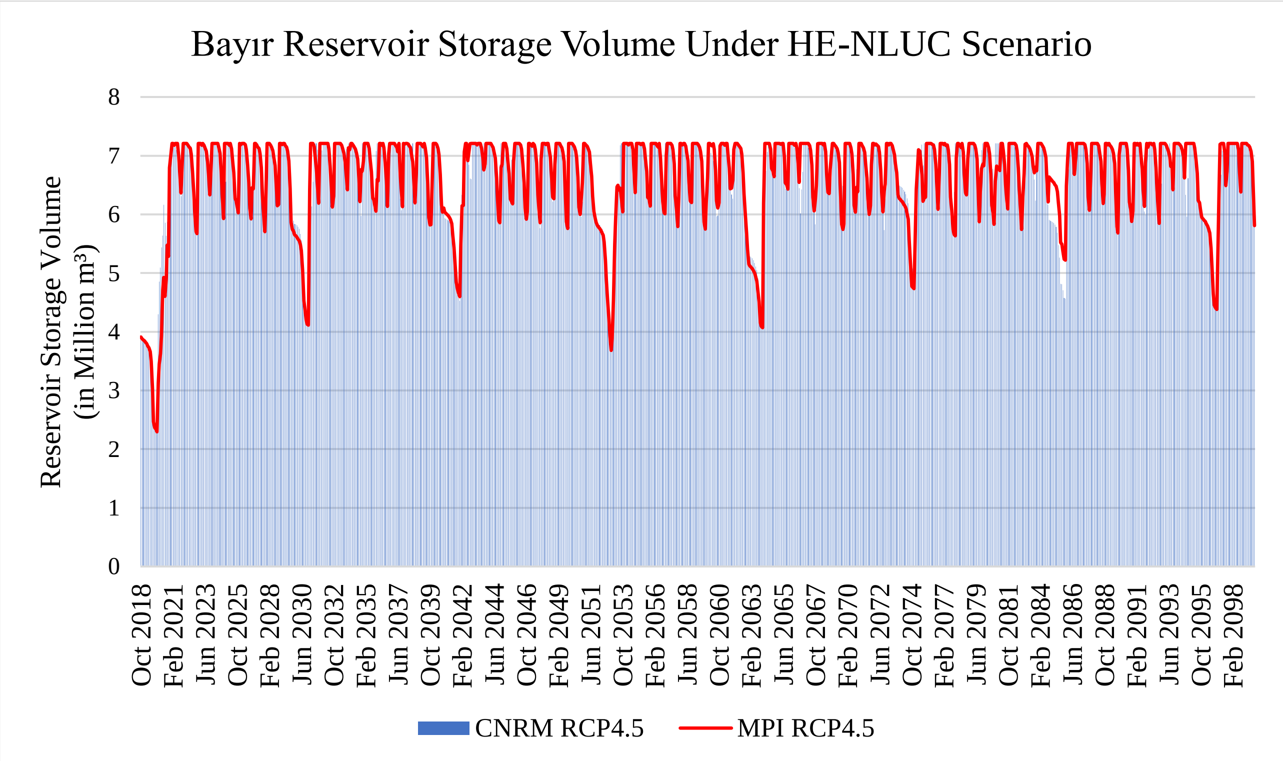

Figure 1.34. Storage volume of Bayır Reservoir under HE-NLUC scenario with CNRM RCP4.5 and MPI RCP4.5 climate change scenarios.

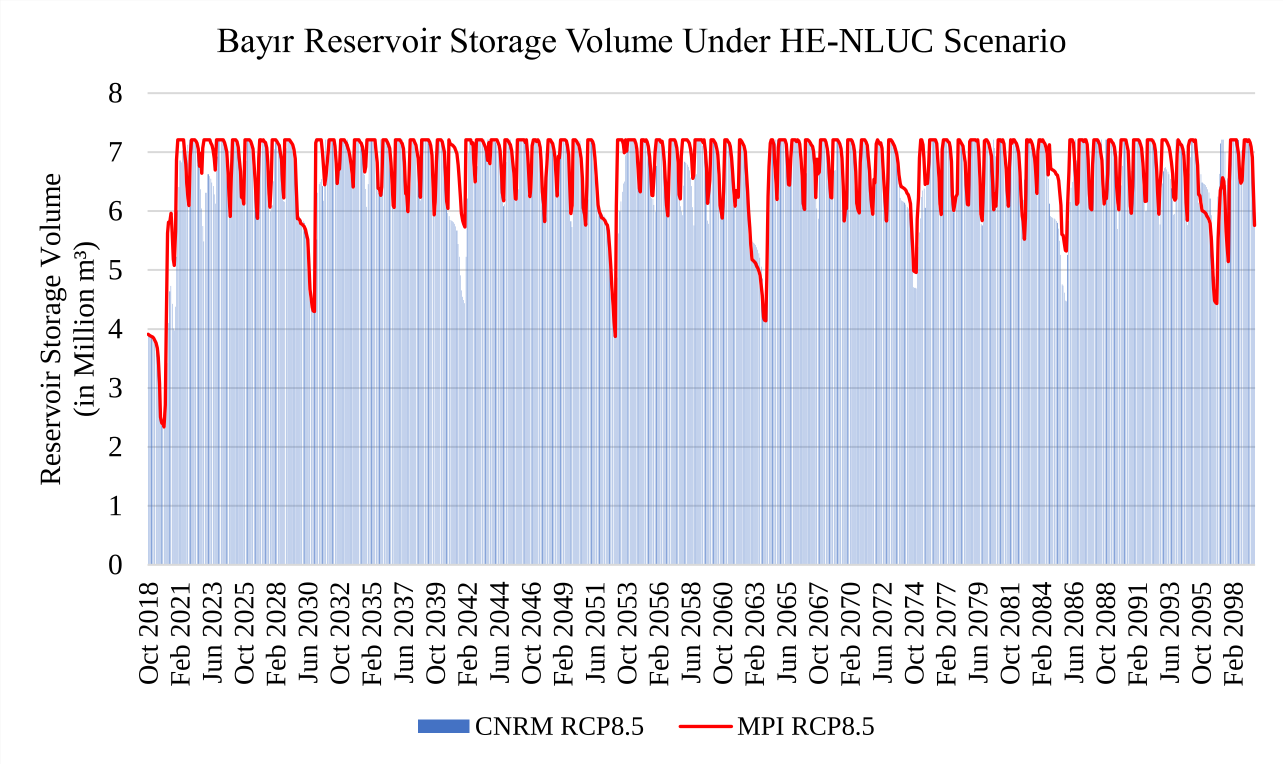

Figure 1.35. Storage volume of Bayır Reservoir under HE-NLUC scenario with CNRM RCP8.5 and MPI RCP8.5 climate change scenarios.

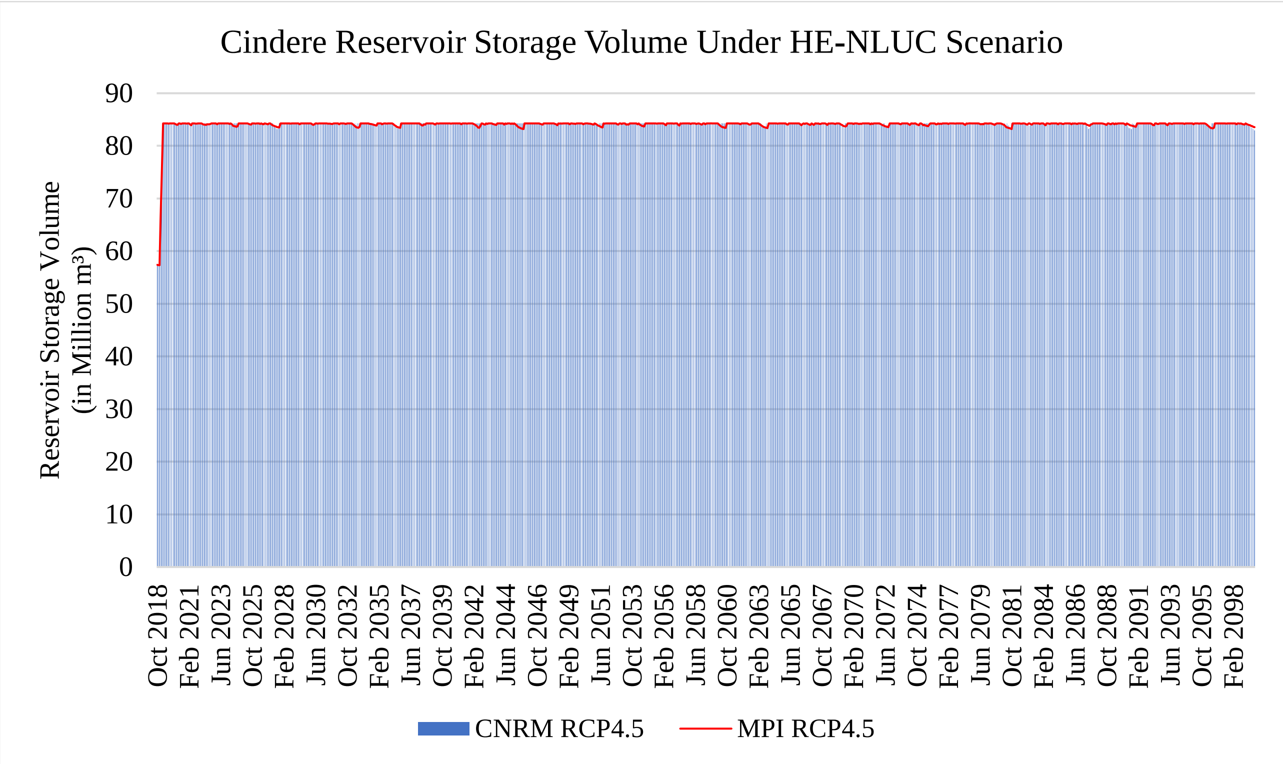

Figure 1.36. Storage volume of Cindere Reservoir under HE-NLUC scenario with CNRM RCP4.5 and MPI RCP4.5 climate change scenarios.

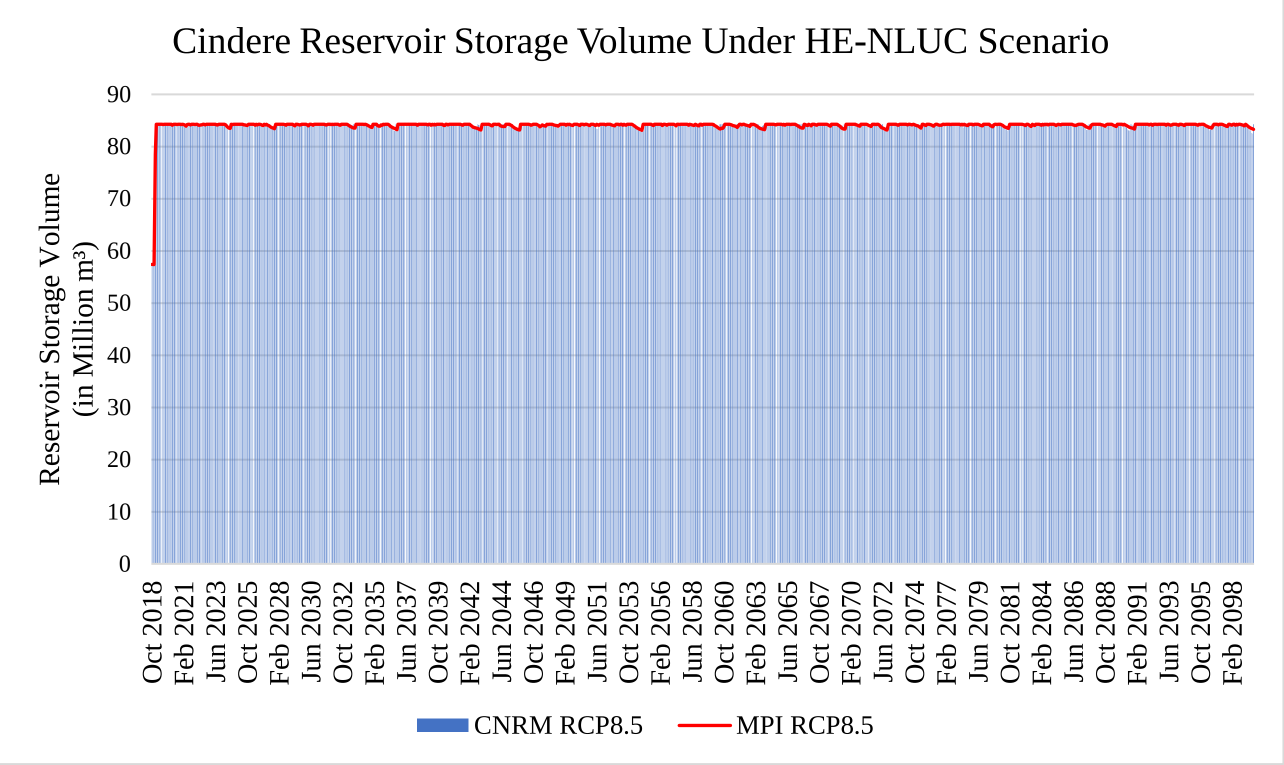

Figure 1.37. Storage volume of Cindere Reservoir under HE-NLUC scenario with CNRM RCP8.5 and MPI RCP8.5 climate change scenarios.

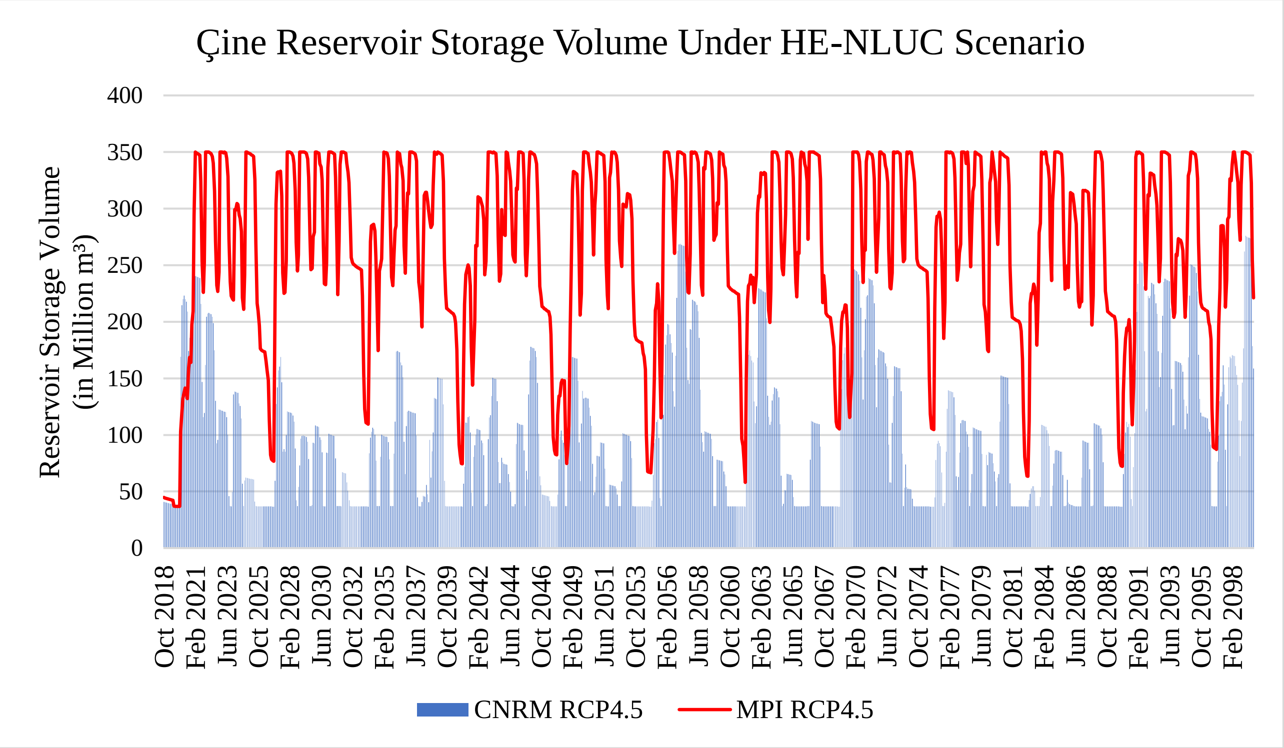

Figure 1.38. Storage volume of Çine Reservoir under HE-NLUC scenario with CNRM RCP4.5 and MPI RCP4.5 climate change scenarios.

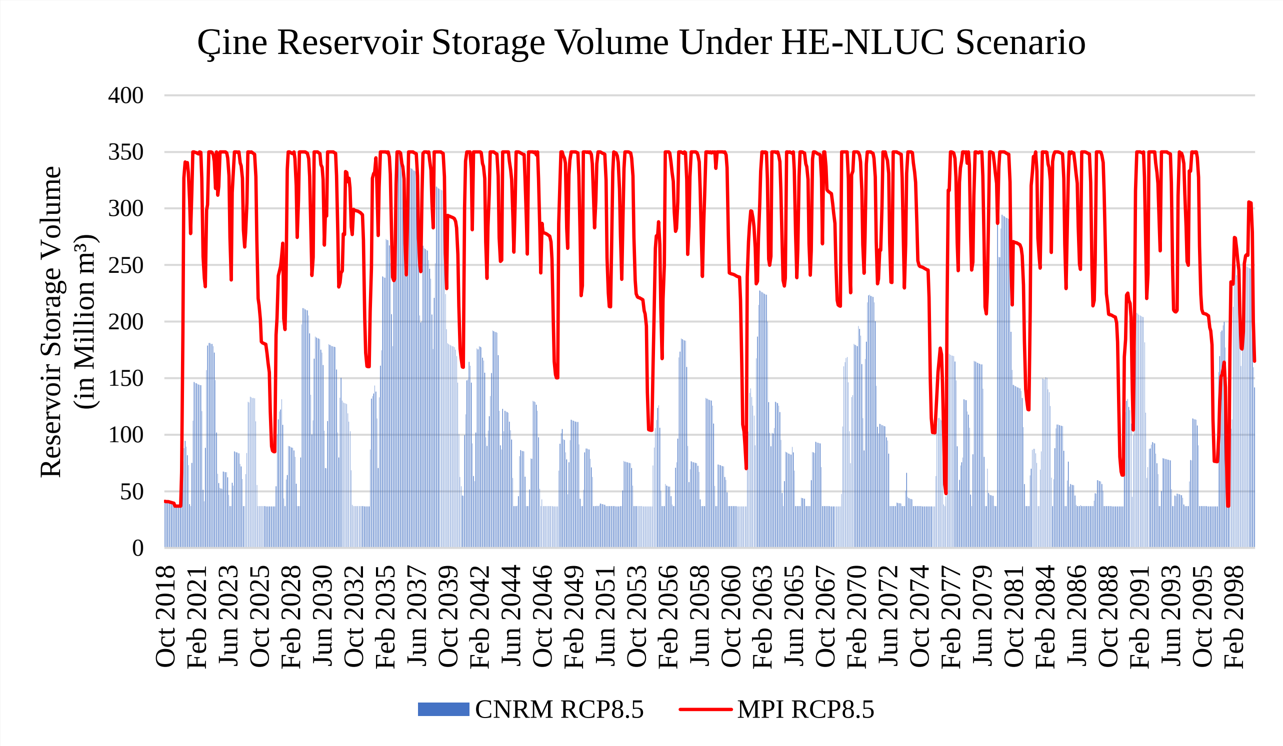

Figure 1.39. Storage volume of Çine Reservoir under HE-NLUC scenario with CNRM RCP8.5 and MPI RCP8.5 climate change scenarios.

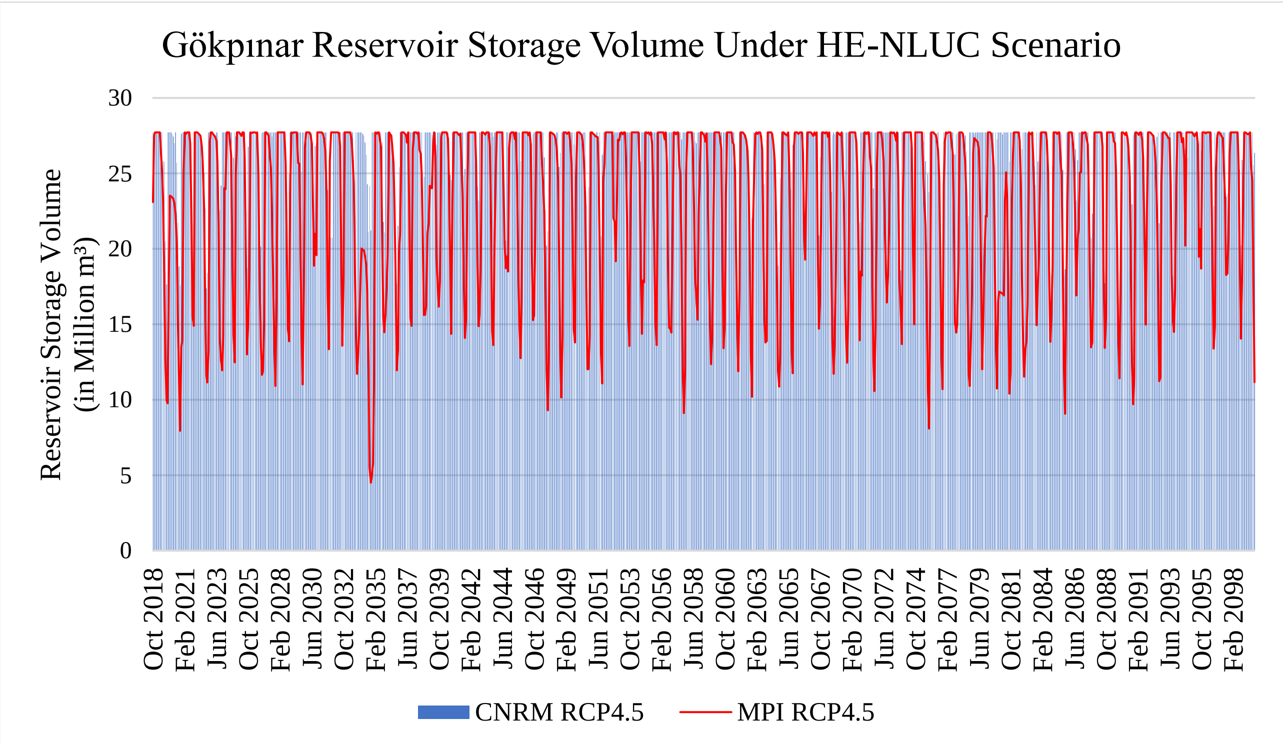

Figure 1.40. Storage volume of Gökpınar Reservoir under HE-NLUC scenario with CNRM RCP4.5 and MPI RCP4.5 climate change scenarios.

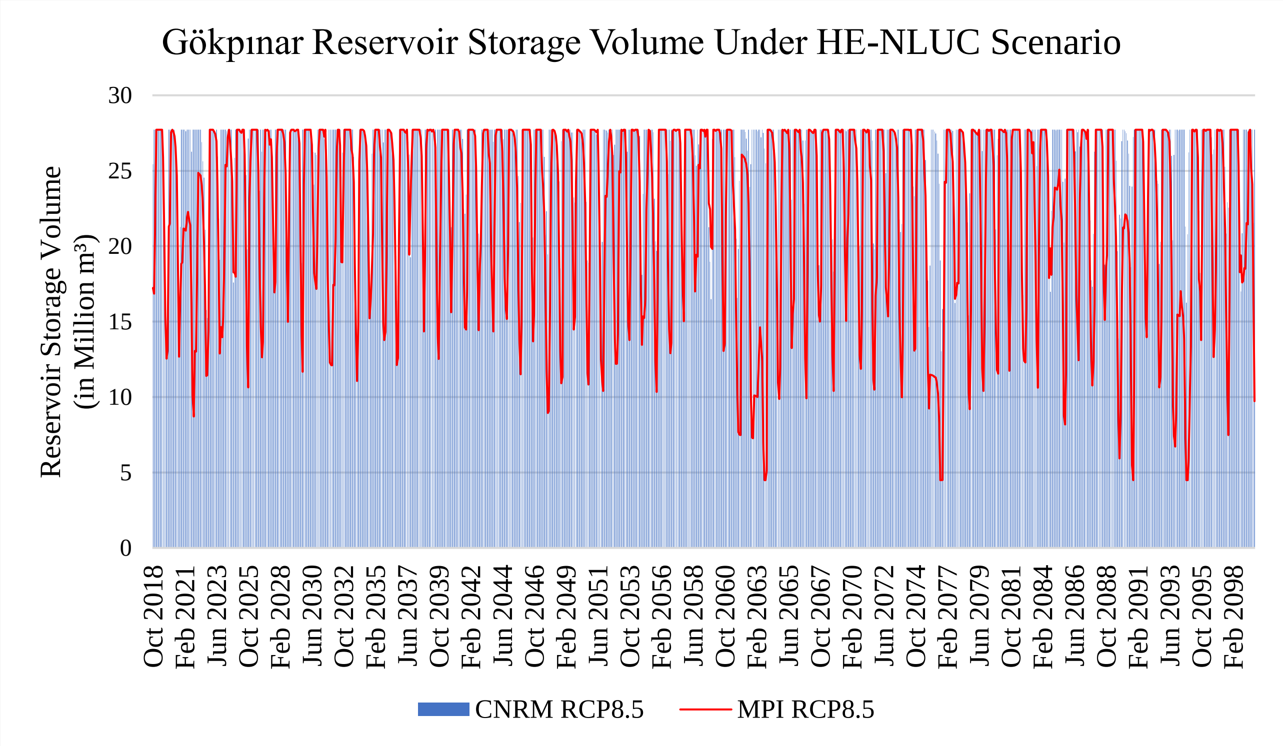

Figure 1.41. Storage volume of Gökpınar Reservoir under HE-NLUC scenario with CNRM RCP8.5 and MPI RCP8.5 climate change scenarios.

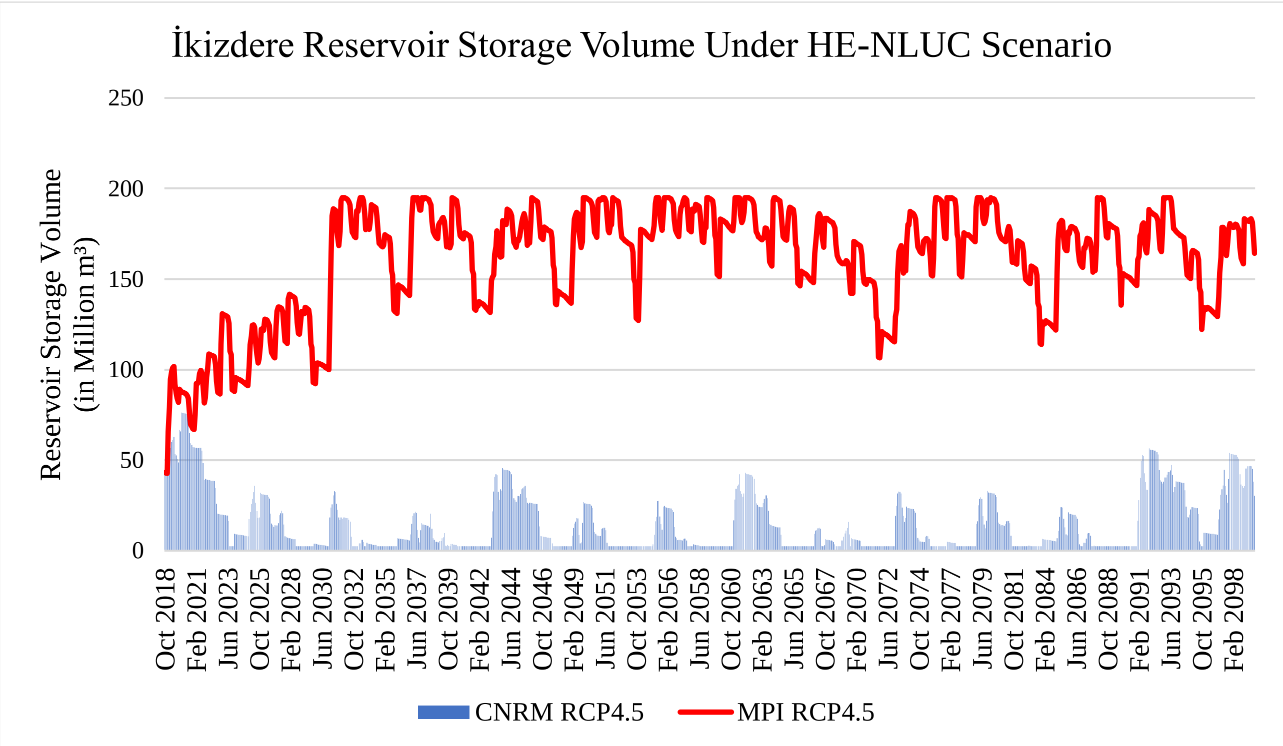

Figure 1.42. Storage volume of İkizdere Reservoir under HE-NLUC scenario with CNRM RCP4.5 and MPI RCP4.5 climate change scenarios.

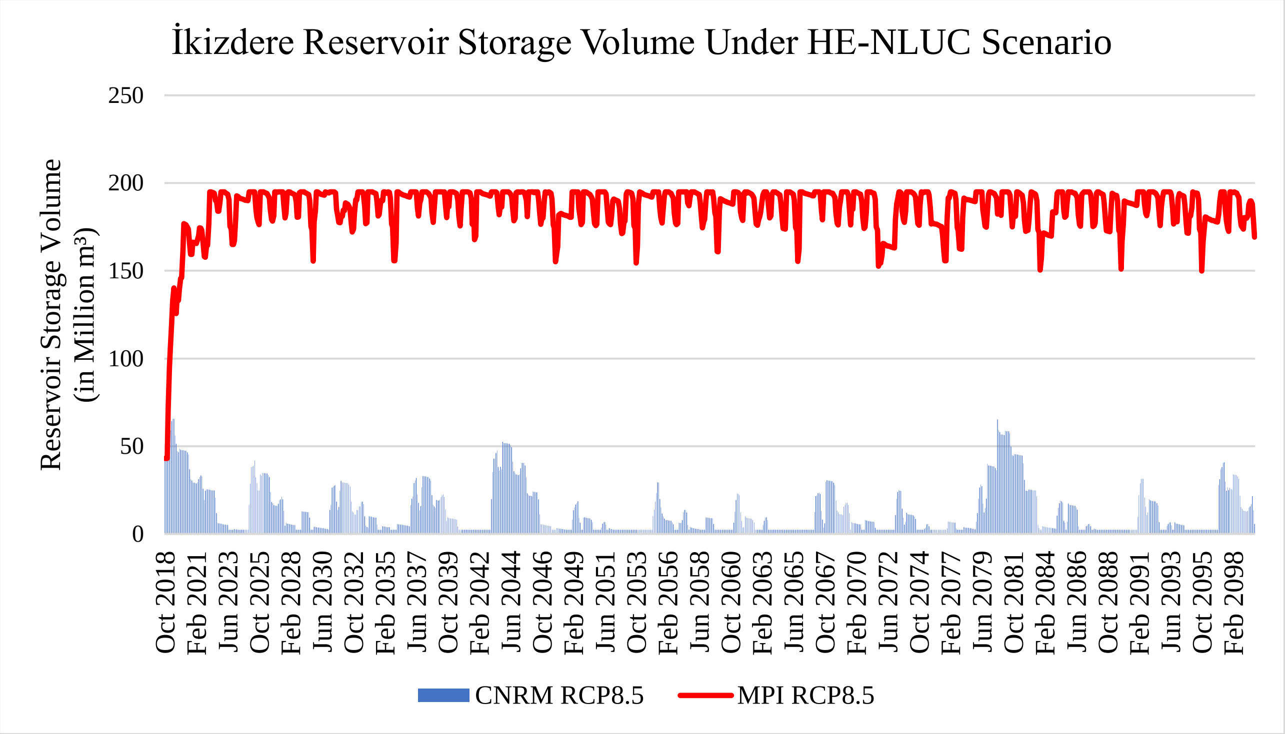

Figure 1.43. Storage volume of İkizdere Reservoir under HE-NLUC scenario with CNRM RCP8.5 and MPI RCP8.5 climate change scenarios.

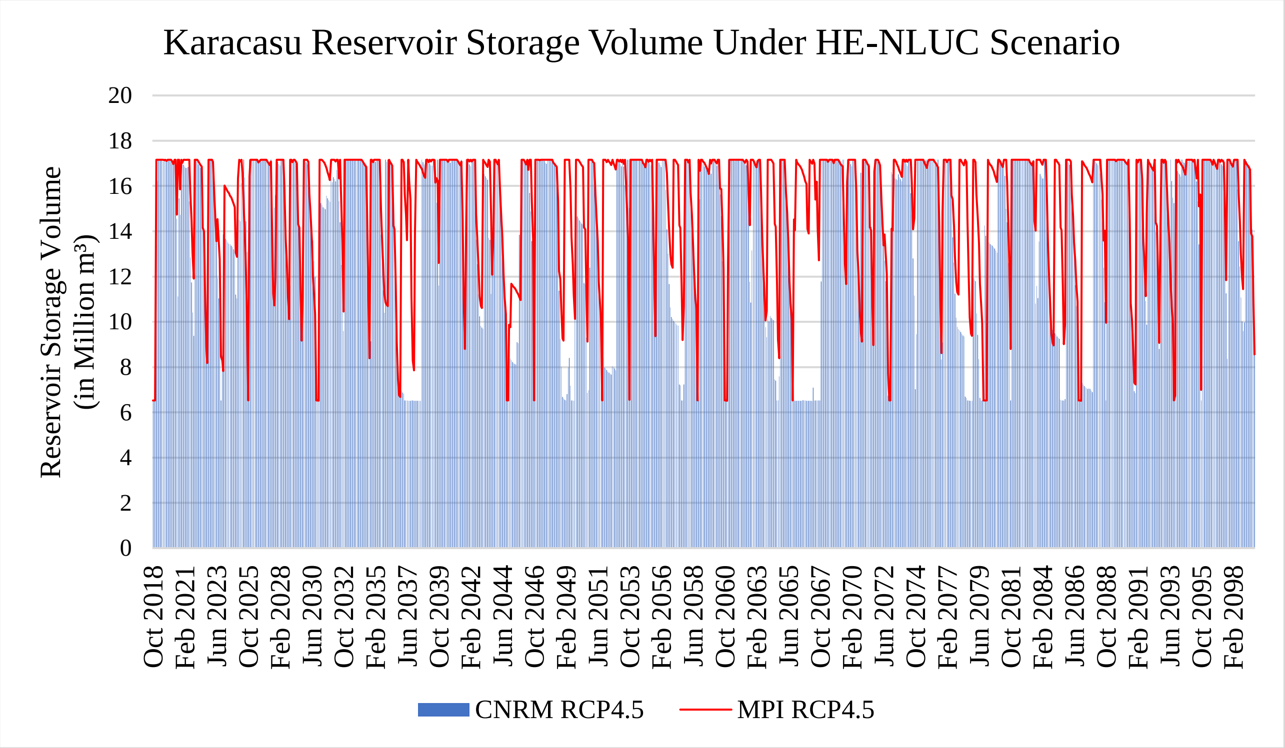

Figure 1.44. Storage volume of Karacasu Reservoir under HE-NLUC scenario with CNRM RCP4.5 and MPI RCP4.5 climate change scenarios.

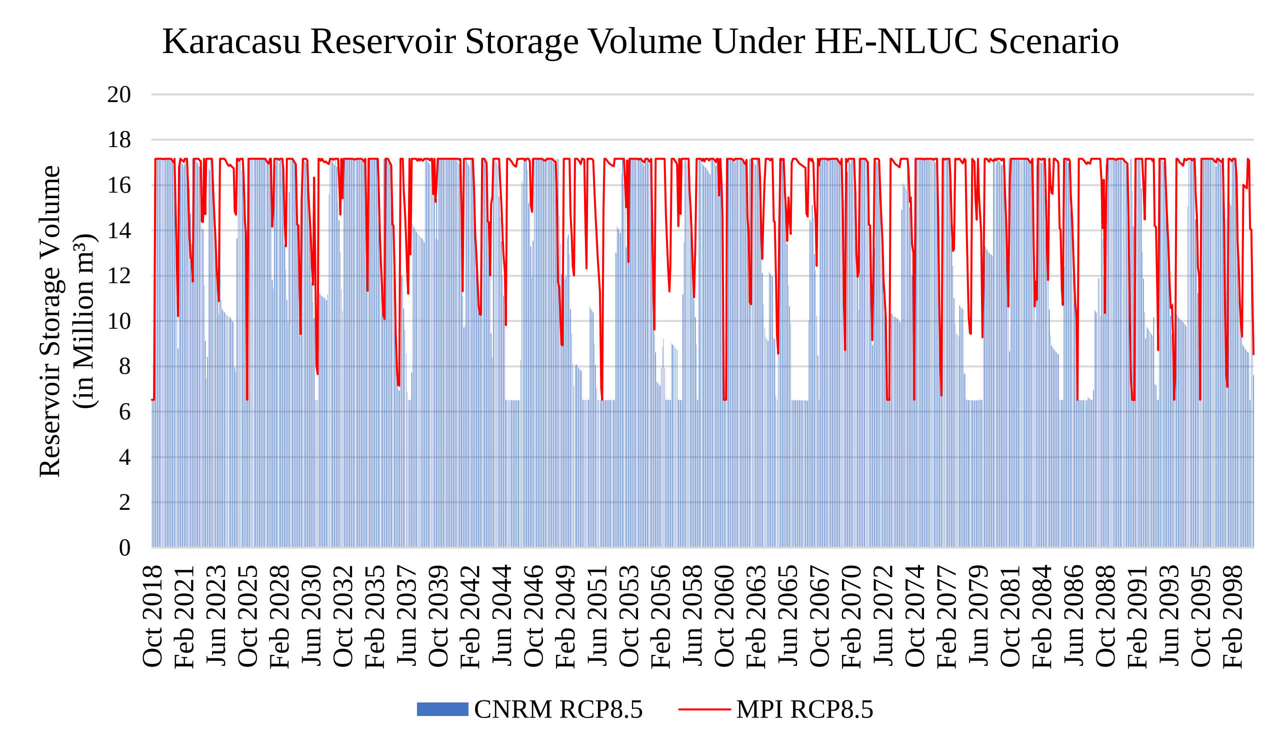

Figure 1.45. Storage volume of Karacasu Reservoir under HE-NLUC scenario with CNRM RCP8.5 and MPI RCP8.5 climate change scenarios.

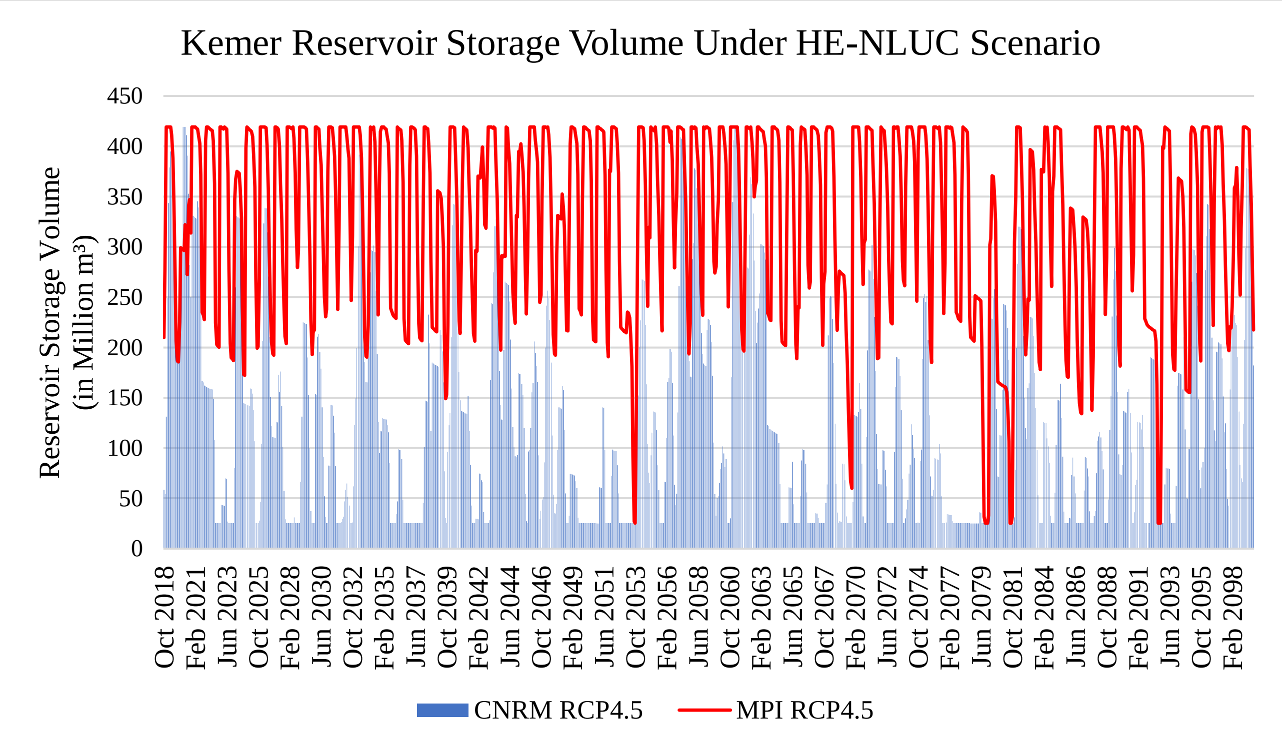

Figure 1.46. Storage volume of Kemer Reservoir under HE-NLUC scenario with CNRM RCP4.5 and MPI RCP4.5 climate change scenarios.

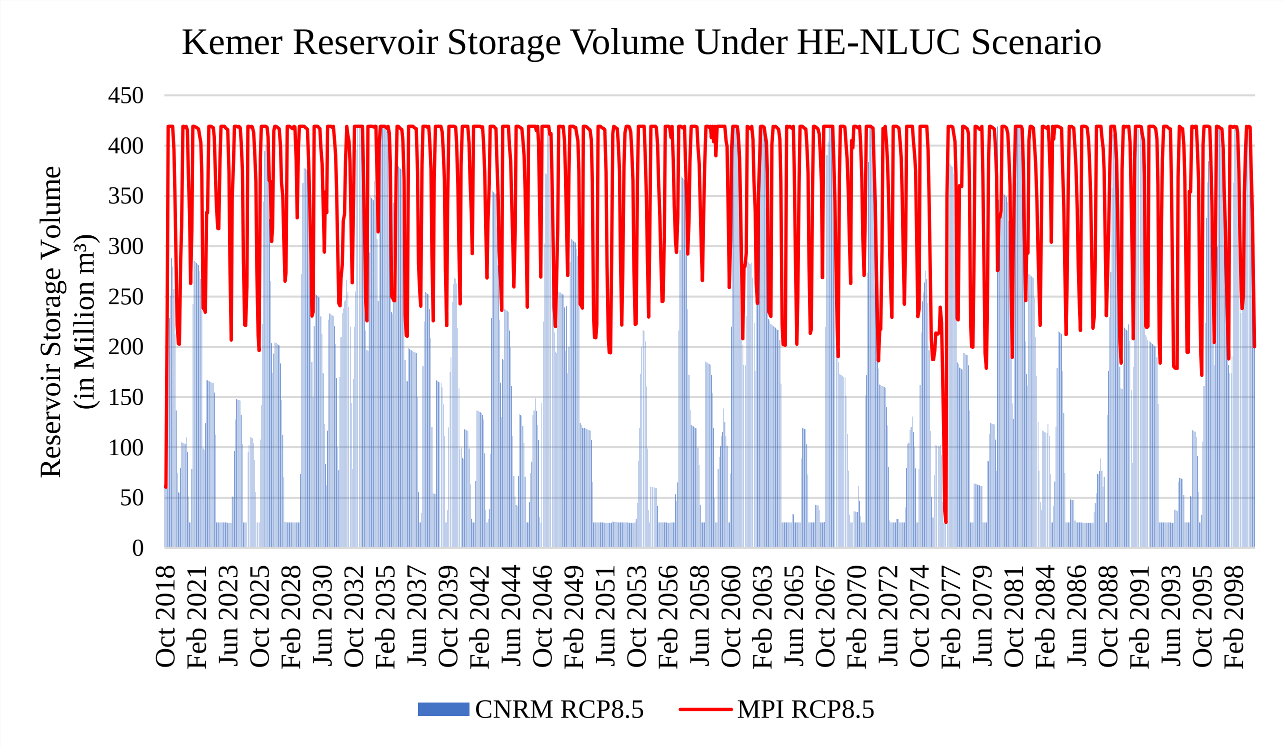

Figure 1.47. Storage volume of Kemer Reservoir under HE-NLUC scenario with CNRM RCP8.5 and MPI RCP8.5 climate change scenarios.

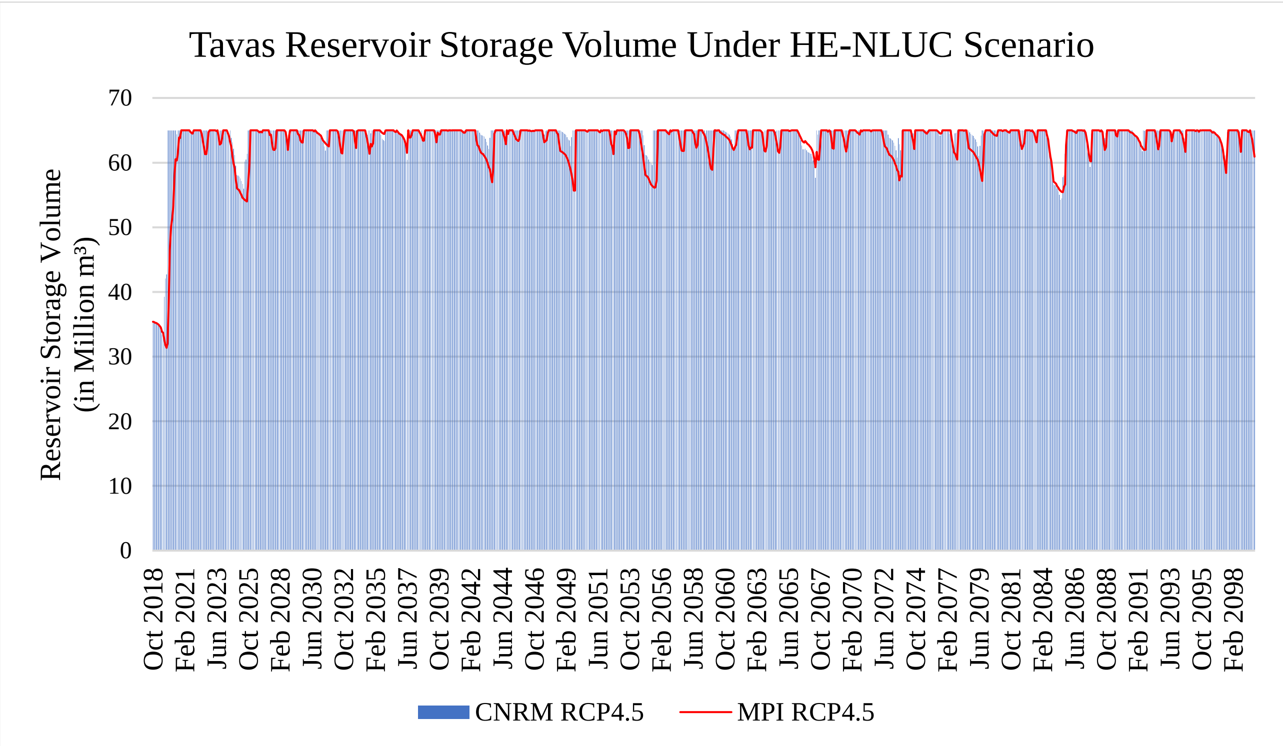

Figure 1.48. Storage volume of Tavas Reservoir under HE-NLUC scenario with CNRM RCP4.5 and MPI RCP4.5 climate change scenarios.

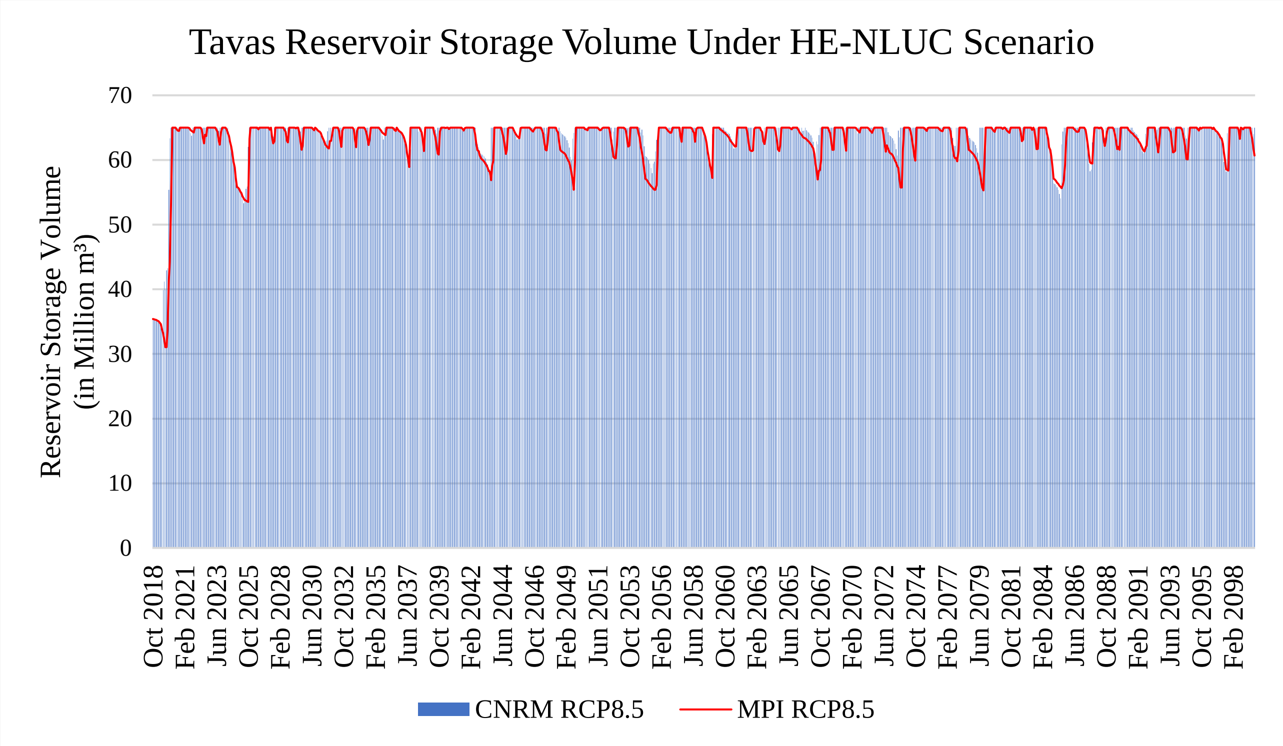

Figure 1.49. Storage volume of Tavas Reservoir under HE-NLUC scenario with CNRM RCP8.5 and MPI RCP8.5 climate change scenarios.

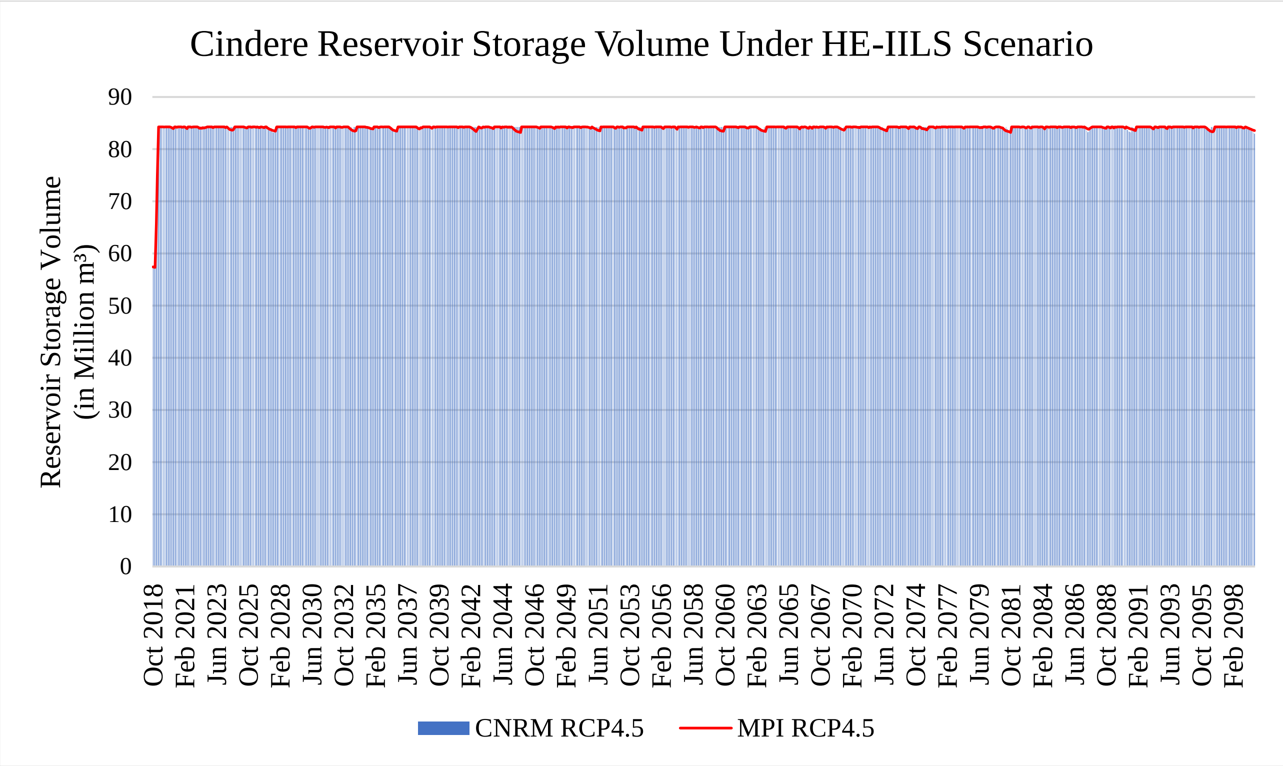

Figure 1.50. Storage volume of Cindere Reservoir under HE-IILS scenario with CNRM RCP4.5 and MPI RCP4.5 climate change scenarios.

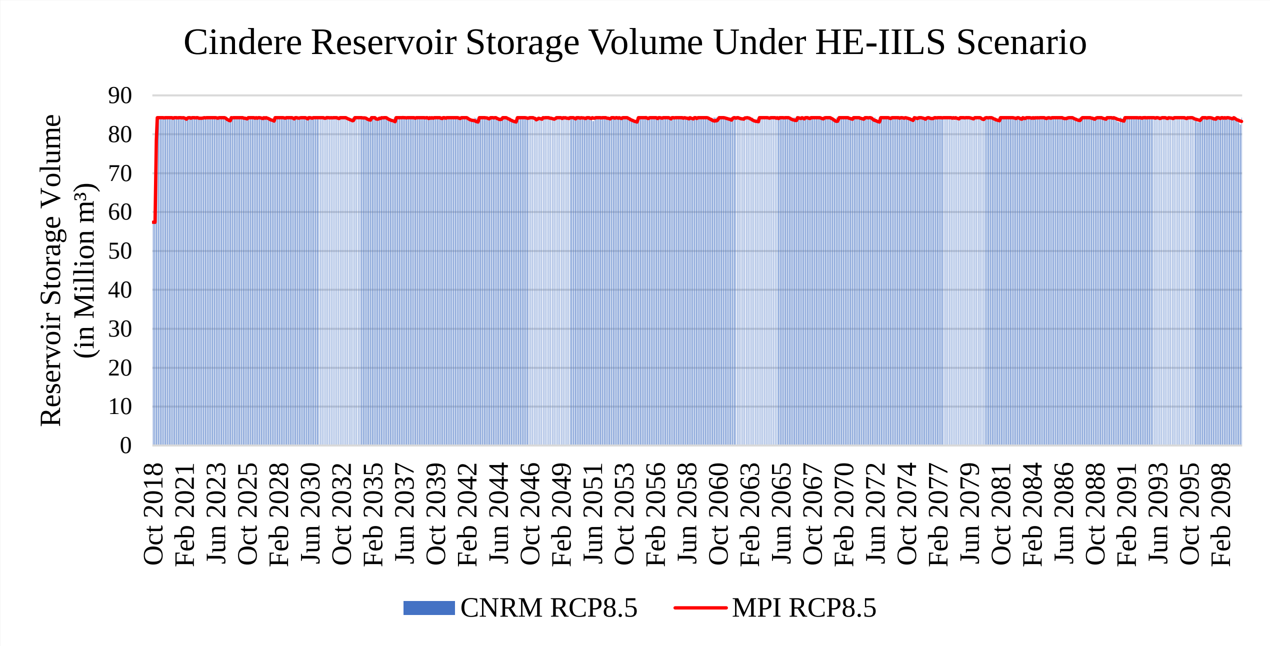

Figure 1.51. Storage volume of Cindere Reservoir under HE-IILS scenario with CNRM RCP8.5 and MPI RCP8.5 climate change scenarios.

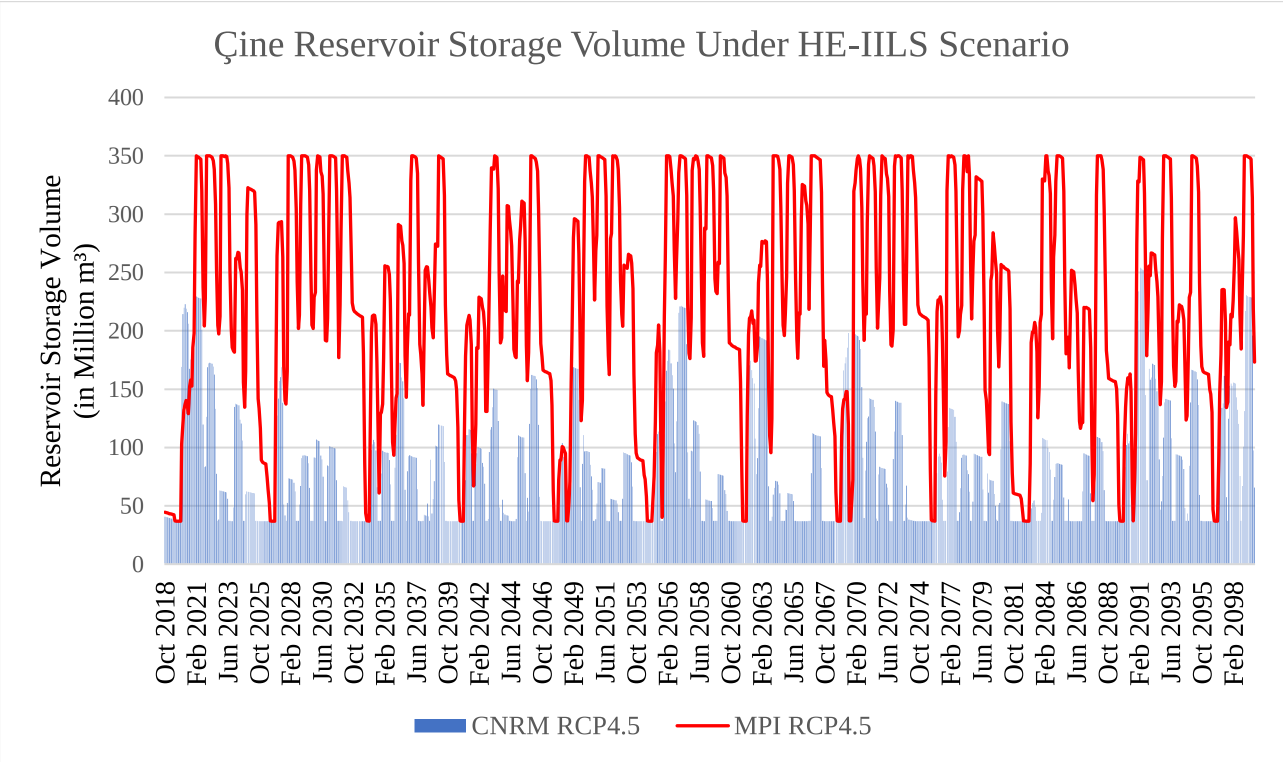

Figure 1.52. Storage volume of Çine Reservoir under HE-IILS scenario with CNRM RCP4.5 and MPI RCP4.5 climate change scenarios.

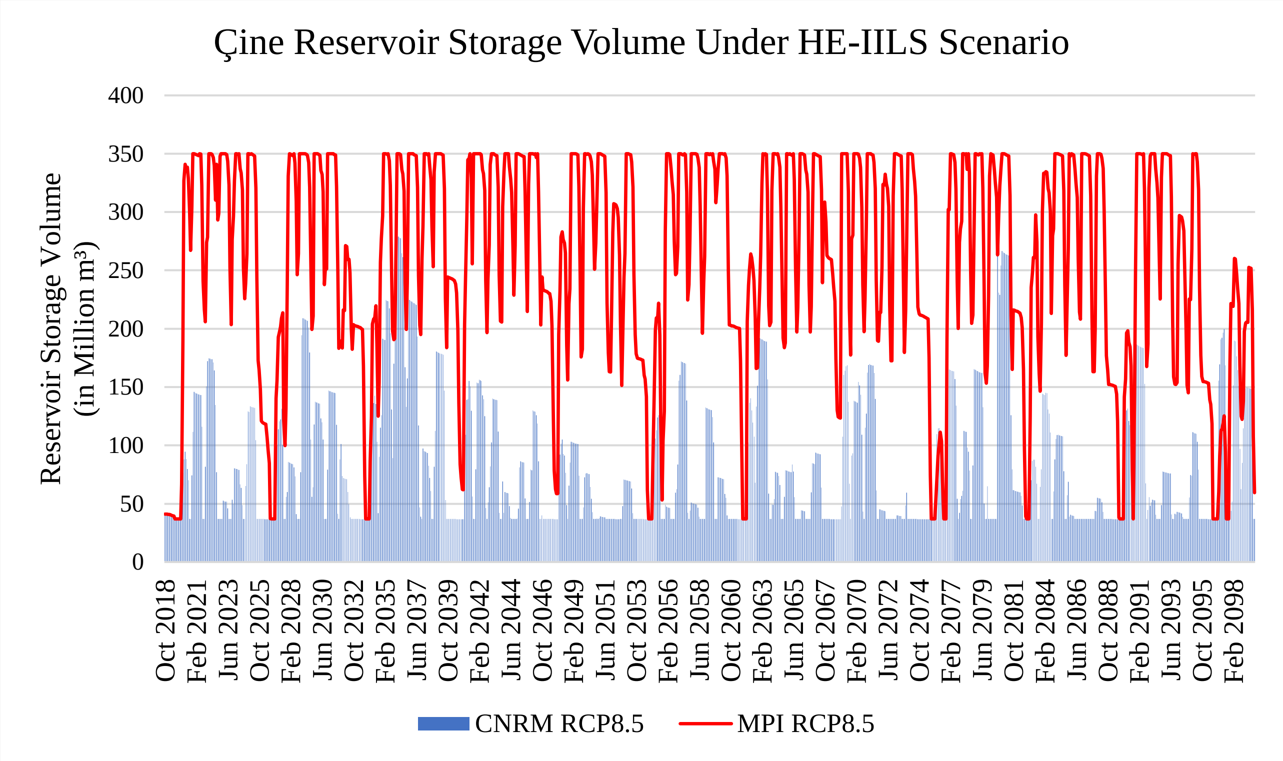

Figure 1.53. Storage volume of Çine Reservoir under HE-IILS scenario with CNRM RCP8.5 and MPI RCP8.5 climate change scenarios.

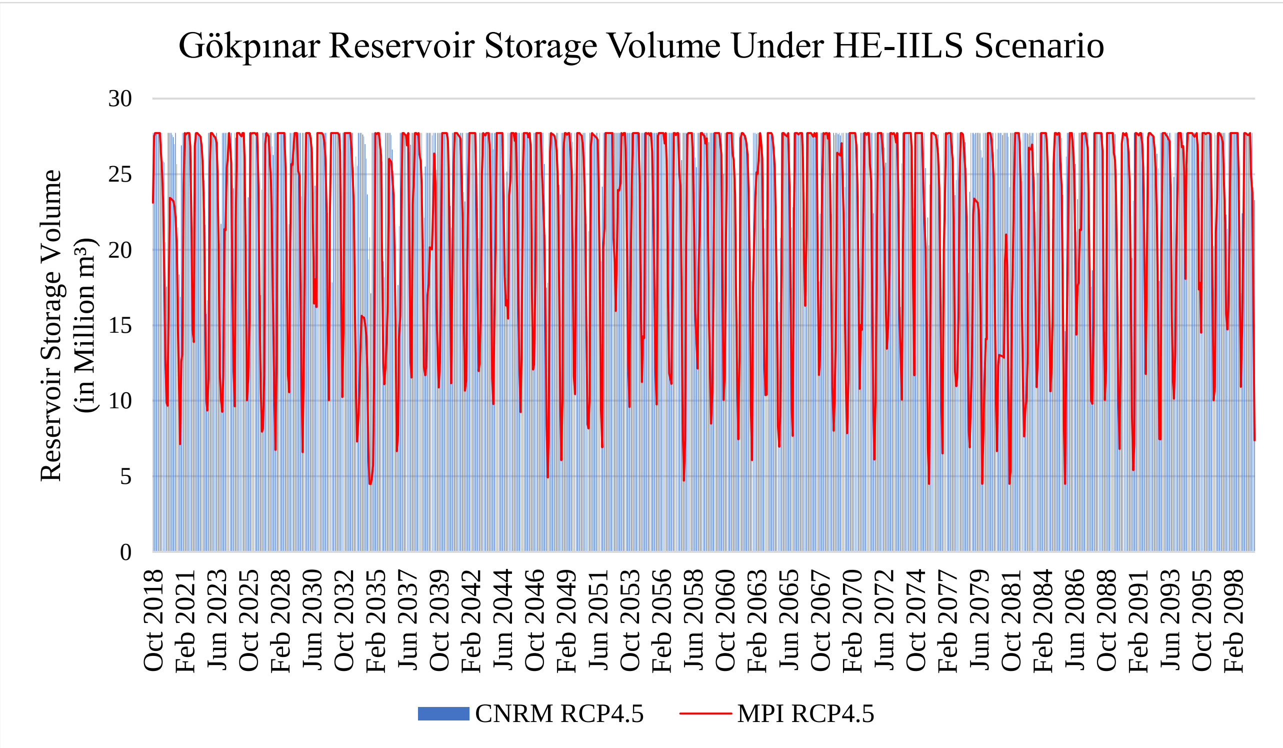

Figure 1.54. Storage volume of Gökpınar Reservoir under HE-IILS scenario with CNRM RCP4.5 and MPI RCP4.5 climate change scenarios.

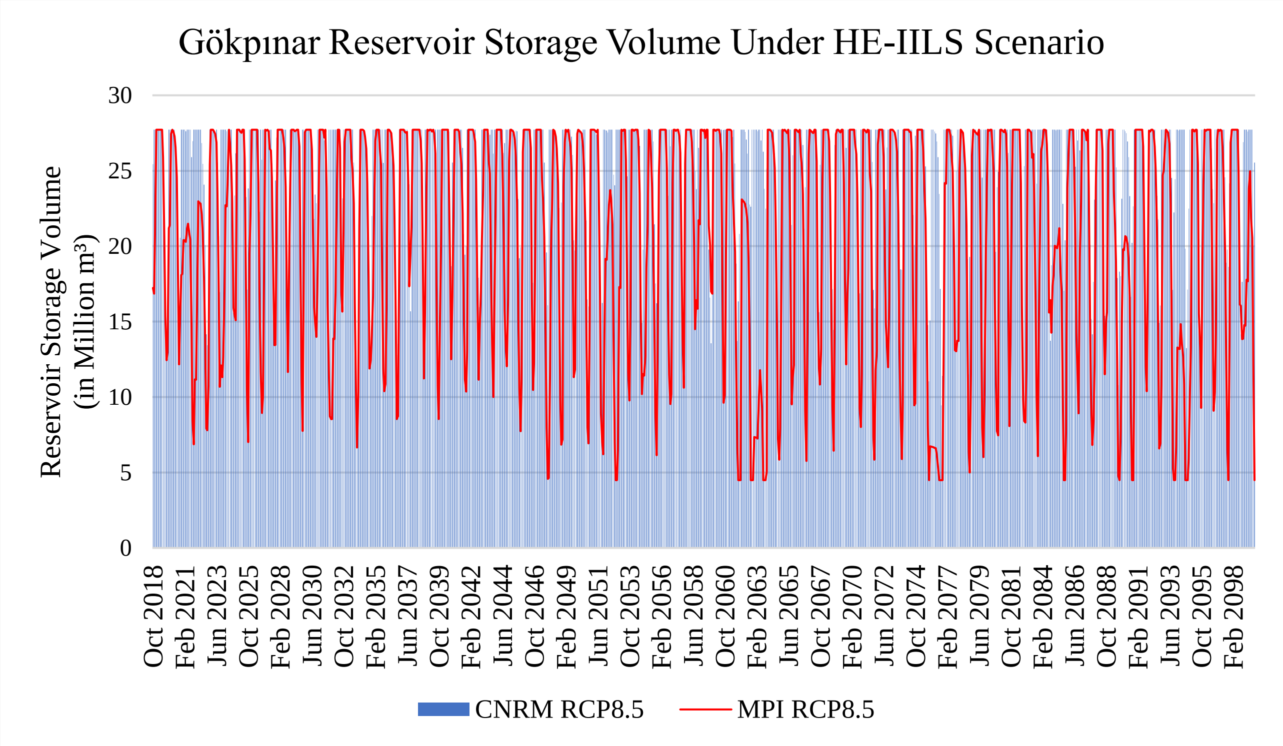

Figure 1.55. Storage volume of Gökpınar Reservoir under HE-IILS scenario with CNRM RCP8.5 and MPI RCP8.5 climate change scenarios.

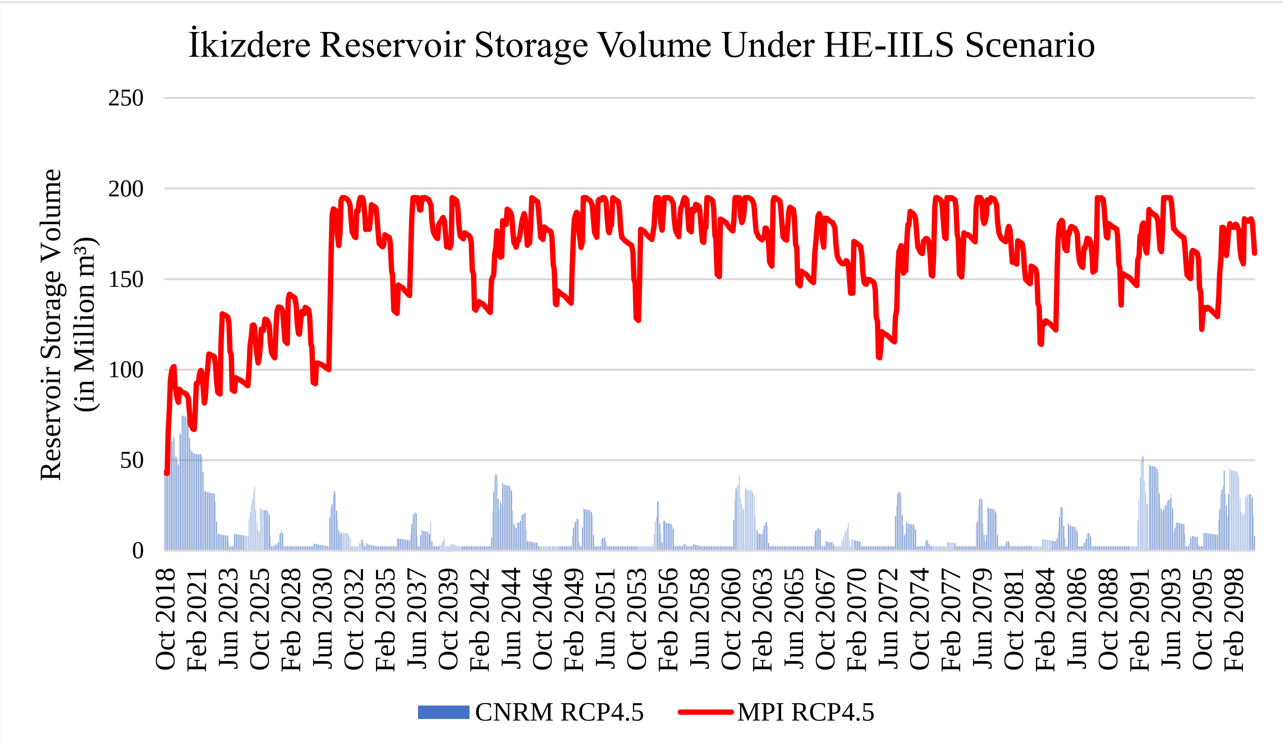

Figure 1.56. Storage volume of İkizdere Reservoir under HE-IILS scenario with CNRM RCP4.5 and MPI RCP4.5 climate change scenarios.

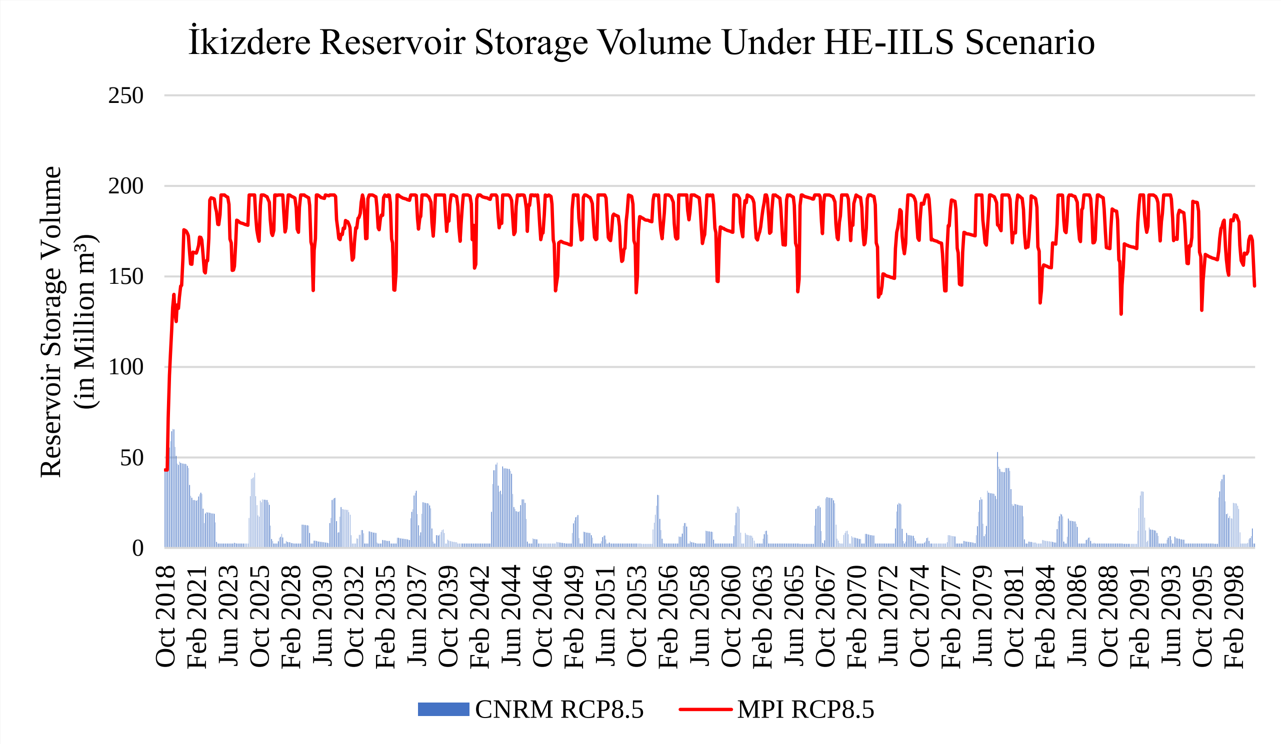

Figure 1.57. Storage volume of İkizdere Reservoir under HE-IILS scenario with CNRM RCP8.5 and MPI RCP8.5 climate change scenarios.

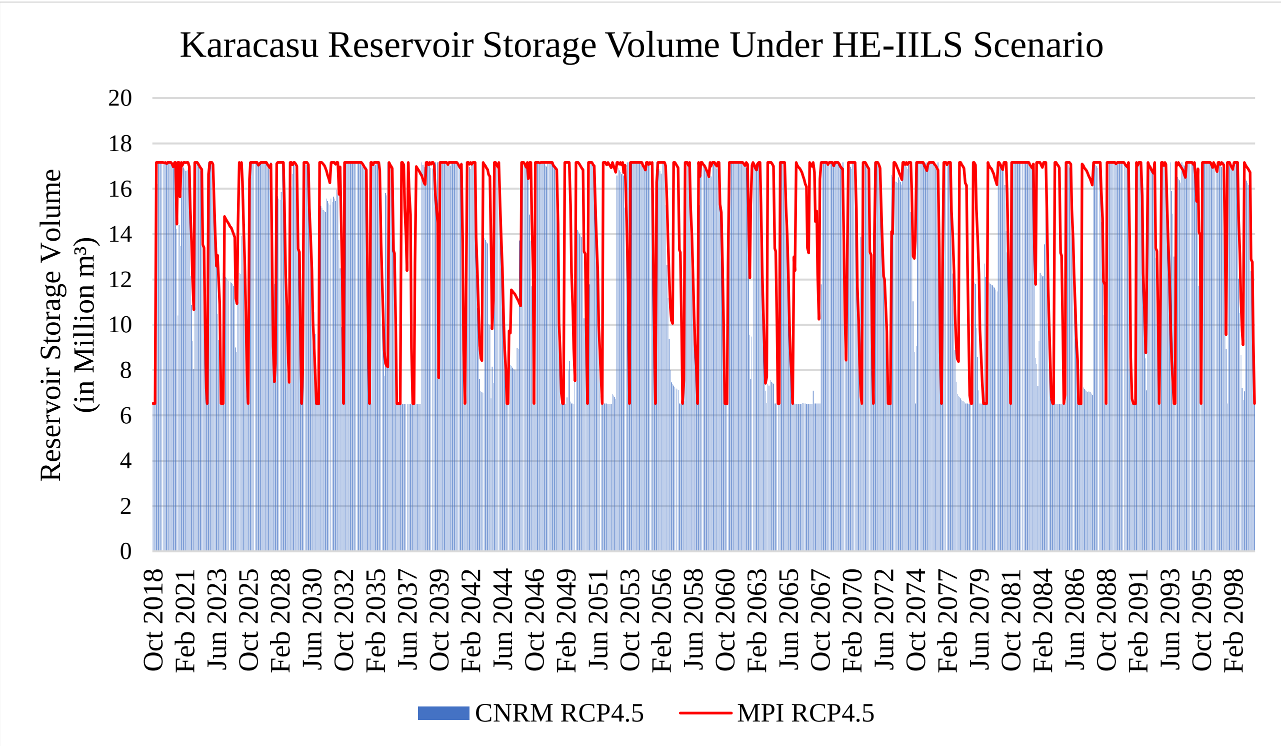

Figure 1.58. Storage volume of Karacasu Reservoir under HE-IILS scenario with CNRM RCP4.5 and MPI RCP4.5 climate change scenarios.

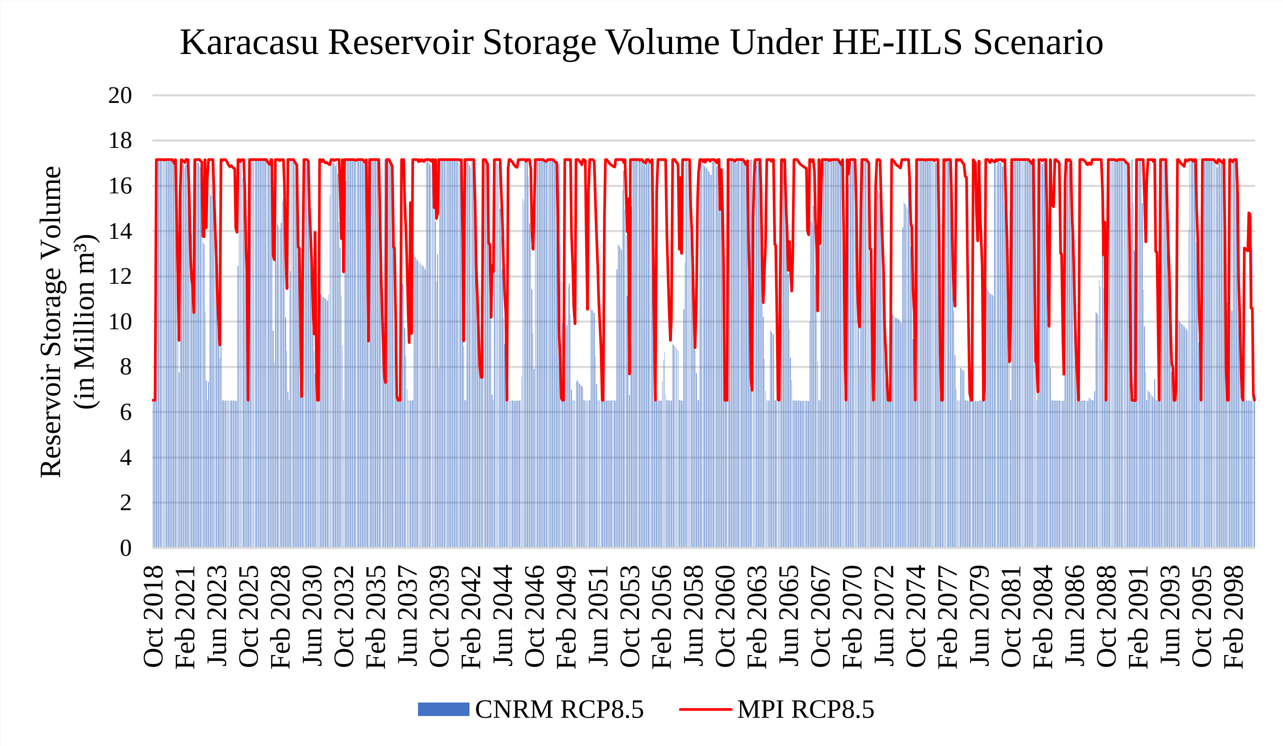

Figure 1.59. Storage volume of Karacasu Reservoir under HE-IILS scenario with CNRM RCP8.5 and MPI RCP8.5 climate change scenarios.

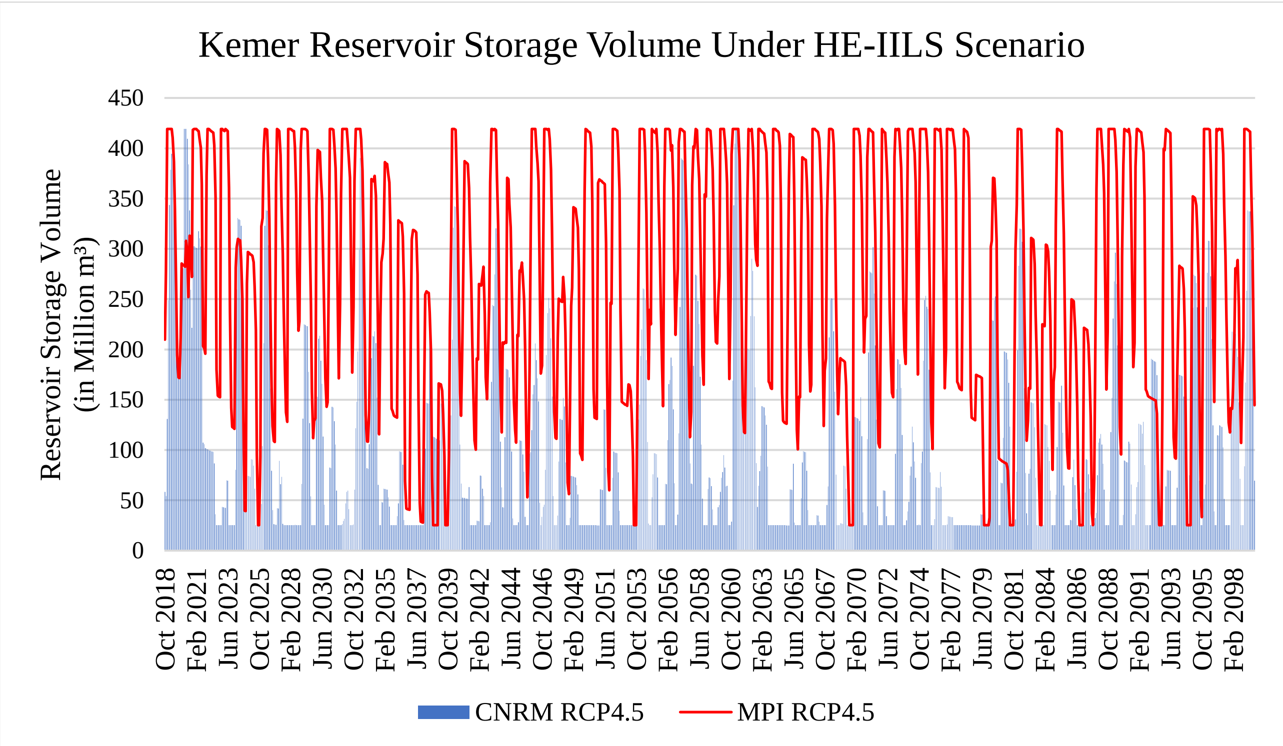

Figure 1.60. Storage volume of Kemer Reservoir under HE-IILS scenario with CNRM RCP4.5 and MPI RCP4.5 climate change scenarios.

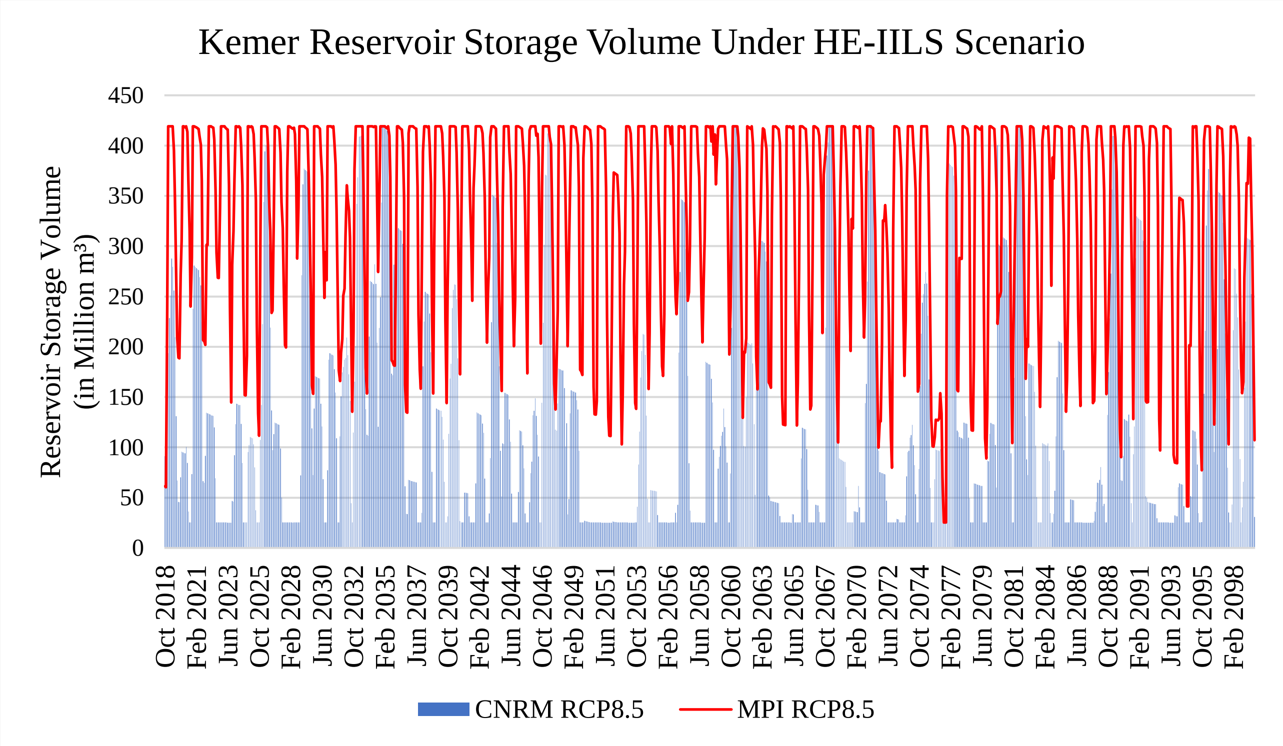

Figure 1.61. Storage volume of Kemer Reservoir under HE-IILS scenario with CNRM RCP8.5 and MPI RCP8.5 climate change scenarios.

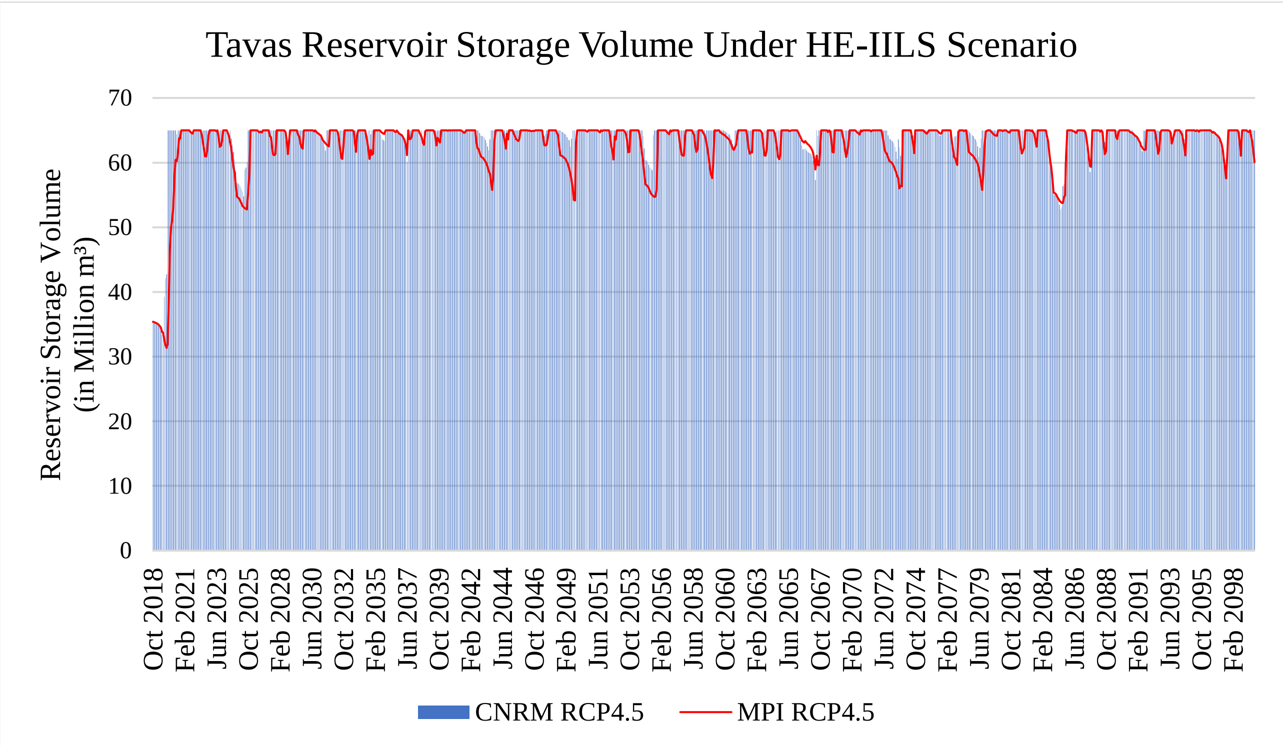

Figure 1.62. Storage volume of Tavas Reservoir under HE-IILS scenario with CNRM RCP4.5 and MPI RCP4.5 climate change scenarios.

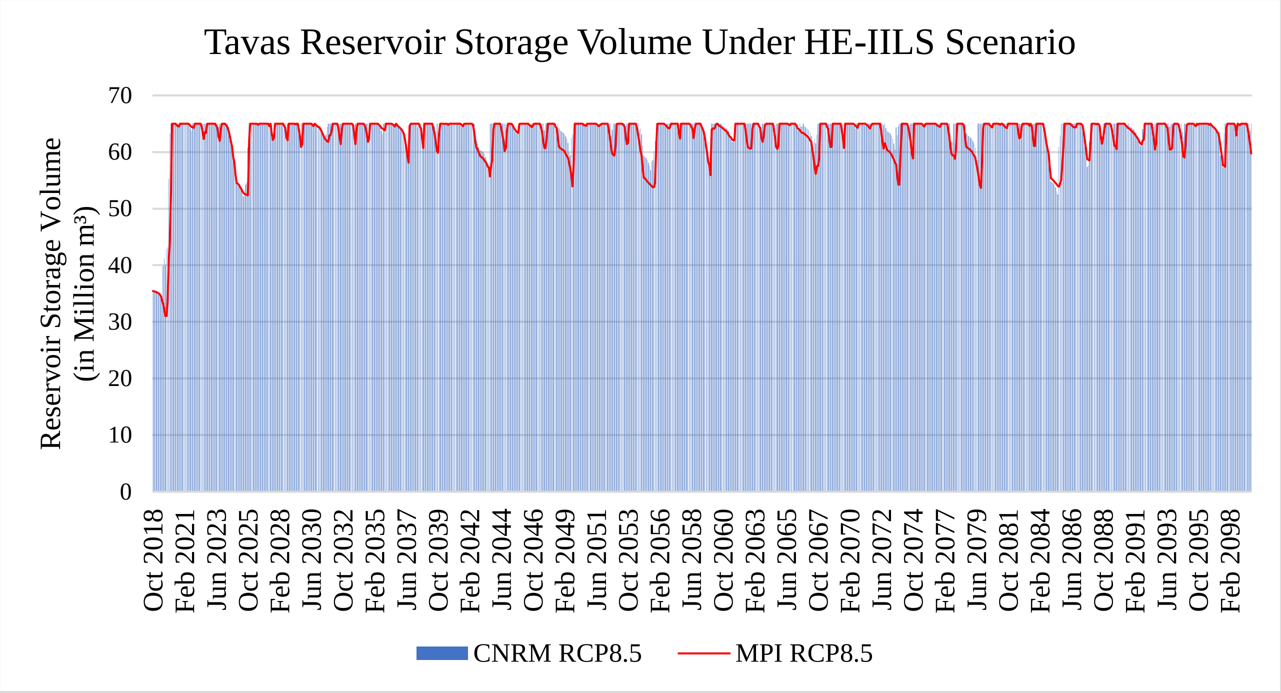

Figure 1.63. Storage volume of Tavas Reservoir under HE-IILS scenario with CNRM RCP8.5 and MPI RCP8.5 climate change scenarios.